UNIVERSITY OF SOUTHAMPTON

# Modelling sedimentary biogeochemical processes in a high nitrate, UK estuary (the Gt. Ouse) with emphasis on the nitrogen cycle

by

Boris A. Kelly-Gerreyn B.Sc., M.Sc.

Thesis submitted to the University of Southampton for the degree of

Doctor of Philosophy

School of Ocean and Earth Science

Faculty of Science

January 2003

# Graduate School of the Southampton Oceanography Centre

This PhD dissertation by

*Boris Kelly-Gerreyn*

has been produced under the supervision of the following persons

Supervisor/s

Dr. David J Hydes

Chair of Advisory Panel

Dr. Rachel Mills

Member/s of Advisory Panel

Dr. Rachel Mills
Dr. David J Hydes
Dr. Duncan A Purdie

*For my sublime brother, Philip.*
*You are always with me*

UNIVERSITY OF SOUTHAMPTON

ABSTRACT

FACULTY OF SCIENCE
SCHOOL OF OCEAN AND EARTH SCIENCE

Doctor of Philosophy

# MODELLING SEDIMENTARY BIOGEOCHEMICAL PROCESSES IN A HIGH NITRATE, UK ESTUARY (THE GT. OUSE) WITH EMPHASIS ON THE NITROGEN CYCLE

by Boris A. Kelly-Gerreyn

The description, calibration and application of a reaction-diffusion model of early diagenesis is presented. Unlike previous models it has been developed for a temperate latitude estuary (upper and lower Gt. Ouse, UK) impacted by high nitrate concentrations (annual mean 700μM). Five variables, $O_2$, $NO_3^-$, $NH_4^+$, $SO_4^=$ and $S^=$, are modelled from the steady state distributions of bulk total organic carbon (TOC).

Different representations of the first order rate constant, k, for TOC mineralisation are tested. Use of separate k values for individual mineralisation pathways is the only way to reproduce the data but at the cost of 1) increasing the degrees of freedom in the model and 2) conceptual simplicity. This casts doubt over the universal applicability of diagenetic models in high $NO_3^-$ environments. Underestimation of the observed ammonium fluxes leads to the inclusion of dissimilatory nitrate reduction to ammonium (DNRA) into a diagenetic model for the first time. Use of an empirical temperature function successfully simulates rates of denitrification and DNRA. It is concluded that temperature is an important control in partitioning nitrate reduction into DNRA and denitrification in the Gt. Ouse sediments. This temperature effect implies that during an extended warm summer in temperate estuaries receiving high nitrate inputs, nitrate reduction may contribute to, rather than counteract a eutrophication event. A literature review showing that DNRA can account for up to 100% of the nitrate reduction in different locations around the world, means that diagenetic models of the nitrogen cycle in coastal areas should include DNRA.

A parameter sensitivity analysis (PSA) reveals a highly non linear model response to parameter changes of ± 50%. The variability in model response among the sites in the Gt. Ouse highlights the importance of accounting for differences in 1) the relative contributions of oxic, suboxic and anoxic mineralization to total organic carbon mineralization; 2) rates of oxygen consumption and 3) oxygen penetration depths. Organic carbon mineralization rates are most sensitive to porosity and diffusion related parameters and to literature ranges of half saturation constants which influence the rate of sulphate reduction. Variations in these parameters suggest that it is unwise to consider parameters as constant in space highlighting a possible barrier to the development of a universally robust model.

The response of the model to changes in the thickness of the diffusive boundary layer (DBL, 0.0001-0.1cm) is examined. Neglecting the presence of the DBL in core incubations may result in erroneous measurements of solute fluxes: higher oxygen (13-63%) and ammonium (13-40%) fluxes and lower nitrate (5-20%) and sulphate (20-980%) fluxes than might be occurring *in situ*. Thicker DBLs decrease organic carbon degradation rates (8-42%) implicating the DBL as a factor in organic carbon preservation. This contrasts with previous findings based on assumptions about oxygen consumption which do not apply in the Gt. Ouse sediments.

The model is used to investigate the variability in the observed intra-annual changes in solute fluxes across the sediment-water interface (SWI). Variations in temperature and overlying concentrations of nitrate, ammonium and sulphate are insufficient to explain the measured variability. This casts doubt on a data-based assumption that concentrations of organic carbon were in steady state at all sites. It is concluded that organic carbon should be dynamically modeled in these sediments. Higher measured than predicted fluxes of oxygen and nitrate across the SWI, indicate the presence of porewater advection or enhanced transport by turbulent diffusion induced by the stirring rates in the core incubations. Inclusion of such transport processes is a recommended area for future work.

**Contents list**


| | | |
|---|---|---|
| List of figures | | iv |
| List of tables | | vii |
| Preface | | xii |
| Acknowledgments | | xiii |
| **Chapter 1** | **Introduction** | **1** |
| 1.1 | Global perspective | 1 |
| 1.2 | Sediments as biogeochemical reactors | 2 |
| 1.3 | Early diagenesis | 3 |
| 1.4 | The early diagenesis of organic matter | 4 |
| 1.5 | Flux of solutes across the sediment-water interface | 9 |
| 1.6 | Nitrogen and its cycling in estuarine sediments | 10 |
| 1.7 | Organic nitrogen mineralisation (ammonification) | 13 |
| 1.8 | Nitrification | 15 |
| 1.8.1 | Factors regulating nitrification | 16 |
| 1.9 | Nitrate reduction - denitrification and DNRA | 20 |
| 1.9.1 | Factors regulating nitrate reduction | 24 |
| 1.10 | Diagenetic modelling philosophy | 28 |
| 1.11 | The history and development of models of early diagenesis | 30 |
| 1.11.1 | The reaction terms of diagenesis | 32 |
| 1.12 | Modelling strategy | 36 |
| 1.12.1 | Overall aim and objective | 36 |
| 1.12.2 | Structure of the thesis and justification of the objectives | 37 |
| **Chapter 2** | **Description of the data: the Gt. Ouse estuary** | **41** |
| 2.1 | The upper estuary (sites 1-4) | 43 |
| 2.2 | The lower estuary (sites 4-9) | 47 |
| **Chapter 3** | **Development and calibration of an early diagenesis model for high nitrate, low reactive sediments in a temperate latitude estuary (Great Ouse, UK)** | **50** |
| 3.1 | The Model | 50 |
| 3.1.1 | Model description | 50 |
| 3.1.2 | Model assumptions | 52 |
| 3.1.3 | Model formulation | 54 |
| 3.1.4 | Initialisation and boundary conditions | 57 |
| 3.1.5 | The numerical scheme and its solution | 58 |
| 3.1.6 | Parameterisation | 60 |
| 3.1.6.1 | The first order rate constant for organic decay, $k$ | 60 |
| 3.2 | Results | 62 |
| 3.3.1 | Values of $k$ | 62 |
| 3.3.2 | SWI Fluxes | 63 |
| 3.3.3 | Mineralisation Rates | 65 |
| 3.3 | Discussion | 67 |
| 3.3.1 | $k$, the first order rate constant | 67 |

| | | |
|---|---|---|
| 3.3.2 | Model Runs | 70 |
| 3.3.3 | Parameter sensitivity analysis (PSA) | 77 |
| 3.3.3.1 | Oxygen processes | 87 |
| 3.3.3.2 | Nitrate processes | 91 |
| 3.3.3.3 | Ammonium processes | 94 |
| 3.3.3.4 | Sulphate and sulphide processes | 97 |
| 3.3.3.5 | Carbon mineralisation | 97 |
| 3.3.3.6 | Porosity | 98 |
| 3.3.3.7 | PSA and model robustness | 103 |
| 3.4 | Conclusions | 108 |
| **Chapter 4** | **The diffusive boundary layer and its impact on early diagenetic processes** | **110** |
| 4.1 | Introduction | 110 |
| 4.2 | Structure of the interfacial region | 111 |
| 4.3 | Model setup | 113 |
| 4.4 | Results | 115 |
| 4.4.1 | Porewater profiles | 115 |
| 4.4.2 | SWI fluxes | 121 |
| 4.4.3 | Sedimentary processes | 123 |
| 4.5 | Discussion | 129 |
| 4.6 | Conclusions | 135 |
| **Chapter 5** | **Modelling observed seasonality in the upper Gt. Ouse sediments** | **138** |
| 5.1 | Introduction | 138 |
| 5.2 | Changes to the model in Chapter 3 required to account for seasonality | 139 |
| 5.3.1 | Temperature | 139 |
| 5.3.2 | Boundary conditions | 140 |
| 5.3.3 | Initial conditions | 140 |
| 5.3 | Porewater data and location of the concentration in top 1cm of sediment | 141 |
| 5.4 | Model runs | 143 |
| 5.5 | Results | 144 |
| 5.5.1 | Porewater profiles | 144 |
| 5.5.2 | Solute fluxes across the sediment-water interface | 149 |
| 5.5.3 | C, N, S and O budgets | 153 |
| 5.6 | Discussion | 160 |
| 5.6.1 | Porewater profiles | 161 |
| 5.6.2 | Solute fluxes across the SWI: explaining the seasonality in the model | 164 |
| 5.6.2.1 | Oxygen fluxes | 165 |
| 5.6.2.2 | Nitrate fluxes | 168 |
| 5.6.2.3 | Ammonium fluxes | 170 |
| 5.6.2.4 | Sulphate fluxes (and sulphate reduction) | 173 |
| 5.6.3 | Solute fluxes across the SWI : explaining the seasonality in the observations with reference to the model predictions | 175 |
| 5.6.4 | Differences in model performance: porewater profiles vs. SWI | 179 |

| | | |
|---|---|---|
| | fluxes | |
| 5.6.5 | C, N, S and O budgets | 180 |
| 5.6.6 | Annually integrated rates of mineralization: comparisons with Mfit | 181 |
| 5.7 | Conclusions | 184 |
| **Chapter 6** | **Pathways of dissimilatory nitrate reduction in the lower Gt. Ouse: a diagenetic model discriminating denitrification and dissimilatory nitrate reduction to ammonium on the basis of temperature** | **186** |
| 6.1 | Introduction | 186 |
| 6.2 | Model description, equations and assumptions | 186 |
| 6.3 | Boundary conditions, initialisation and imposed data | 187 |
| 6.4 | Temperature and proportioning of nitrate reduction into denitrification and DNRA | 188 |
| 6.5 | Implementation of equation 6.3 into the model | 192 |
| 6.6 | Results | 195 |
| 6.6.1 | Nitrate reduction | 196 |
| 6.6.2 | DNRA and total ammonium production | 200 |
| 6.6.3 | SWI Fluxes | 201 |
| 6.6.3.1 | Nitrate | 201 |
| 6.6.3.2 | Ammonium | 202 |
| 6.6.3.3 | Oxygen | 205 |
| 6.7 | Discussion | 206 |
| 6.7.1 | Nitrate reduction | 206 |
| 6.7.2 | DNRA and total ammonium production | 211 |
| 6.7.3 | First order rate constants | 213 |
| 6.7.4 | SWI Fluxes | 213 |
| 6.7.4.1 | Nitrate | 213 |
| 6.7.4.2 | Ammonium | 215 |
| 6.7.4.3 | Oxygen | 216 |
| 6.8 | Conclusions | 217 |
| **Chapter 7** | **Summary and final conclusions** | **219** |
| | **Appendices** | **225** |
| | **References** | **234** |

**List of Figures**


| | | |
|---|---|---|
| Figure 1.1 | The sedimentary nitrogen cycle (DNRA = dissimilatory nitrate reduction to ammonium) | 12 |
| Figure 2.1 | Map showing study area and site locations in the Great Ouse estuary | 42 |
| Figure 2.2 | Intra-annual changes in determinands at 4 sites in the upper Gt. Ouse | 48 |
| Figure 3.1 | 1-dimensional numerical grid scheme of the model | 51 |
| Figure 3.2 | Biogeochemical reactions of the diagenetic model(TOC = total organic carbon) | 52 |
| Figure 3.3a-c | Modeled and measured (Nedwell and Trimmer, 1996) solute exchange across the sediment water interface at 4 sites in the upper Gt. Ouse ($M_{fit}$ = separate k fitted to each mineralization pathway; $M_{exp}$ = k defined by $k_z = k_0 e^{-\alpha z}$; $M_{calc}$ = k calculated from data, see Table 3.5. Note that observed data are annual integrals from 7 monthly measurements) | 64 |
| Figure 3.4a-c | Modeled and stoichiometric (Nedwell and Trimmer (1996) calculations of oxic, suboxic and anoxic mineralization rates at each site in the upper Gt. Ouse ($M_{fit}$ = separate $k$ fitted to each mineralization pathway; $M_{exp}$ = $k$ defined by $k_z = k_0 e^{-\alpha z}$; $M_{calc}$ = $k$ calculated from data, see Table 3.5. Note that observed data are annual integrals from 7 monthly measurements) | 66 |
| Figure 3.5 | Comparison of profiles of first order rate constants for denitrification, $k_z$ and $k_{no3}$, at site 3. (Both constants are modified by oxygen inhibition and nitrate limitation, see equation 2 .8 in Table 3.1. For comparison, the maximum value of both rate constants is also profiled) | 72 |
| Figure 4.1 | Schematic diagram of the vertical structure of the benthic boundary layer (BBL). Adapted from Dade *et al.* (2001). z = depth, \|u\| = flow magnitude. | 112 |
| Figure 4.2 | Numerical grid incorporating the diffusive boundary layer (DBL). See text for details and refer to Figure 3.1 | 114 |
| Figure 4.3 | The effect of changing DBL thicknesses on oxygen porewater profiles | 117 |
| Figure 4.4 | The effect of changing DBL thicknesses on nitrate porewater profiles | 118 |
| Figure 4.5 | The effect of changing DBL thicknesses on sulphate porewater profiles | 119 |
| Figure 4.6 | The effect of changing DBL thicknesses on ammonium porewater profiles | 120 |
| Figure 4.7 | The effect of changing DBL thicknesses on solute fluxes across the SWI at 4 sites in the Gt. Ouse. | 122 |
| Figure 4.8 | The effect of changing DBL thicknesses on modeled sedimentary processes | 123 |
| Figure 4.9 | Effect of increasing the diffusion distance between two fixed end point concentrations of an idealized conservative tracer | 128 |

| | | |
|---|---|---|
| | in a model sediment ($C_0$, $C_1$ = fixed concentration at the surface and bottom where $C_0 < C_1$; $dz_{1,2}$ = diffusion distance between $C_0$ and $C_1$) | |
| Figure 5.1 | Converting sediment core measurements into porewater concentration profiles. | 142 |
| Figure 5.2 | Modeled and measured porewater profiles of nitrate at 4 sites in the upper Gt. Ouse | 145 |
| Figure 5.3 | Modeled and measured porewater profiles of ammonium at 4 sites in the upper Gt. Ouse | 146 |
| Figure 5.5. | Modeled and measured porewater profiles of sulphate at 4 sites in the upper Gt. Ouse | 147 |
| Figure 5.5 | Modeled and measured porewater profiles of oxygen at 4 sites in the upper Gt. Ouse | 148 |
| Figure 5.6 | Modeled and measured oxygen fluxes across the SWI at 4 sites in the upper Gt. Ouse | 150 |
| Figure 5.7 | Modeled and measured nitrate fluxes across the SWI at 4 sites in the upper Gt. Ouse | 151 |
| Figure 5.8 | Modeled and measured ammonium fluxes across the SWI at 4 sites in the upper Gt. Ouse | 152 |
| Figure 5.9 | Predicted percentage contributions of the different pathways of organic carbon mineralization to total organic carbon mineralization at 4 sites in the upper Gt. Ouse | 154 |
| Figure 5.10 | Modeled oxygen budget at 4 sites in the upper Gt. Ouse | 155 |
| Figure 5.11 | Modeled nitrate budget at 4 sites in the upper Gt. Ouse | 156 |
| Figure 5.12 | Modeled ammonium budget at 4 sites in the upper Gt. Ouse | 157 |
| Figure 5.13 | Modeled sulphur budget at 4 sites in the upper Gt. Ouse | 158 |
| Figure 5.14 | Modeled and measured porewater profiles of nitrate at site 2 in the upper Gt. Ouse with $k_{no3} = 0.09\ y^{-1}$ | 163 |
| Figure 5.15 | Effect of runs 1 to 4 (see Table 5.1) on oxygen fluxes (mmol $m^{-2}\ d^{-1}$) across the SWI at 4 sites in the upper Gt. Ouse | 166 |
| Figure 5.16 | Effect of runs 1 and 3 (see Table 5.1) on nitrate fluxes (mmol $m^{-2}\ d^{-1}$) across the SWI at 4 sites in the upper Gt. Ouse | 169 |
| Figure 5.17 | Effect of runs 1, 3, 4 and 5 (see Table 5.1) on ammonium fluxes (mmol $m^{-2}\ d^{-1}$) across the SWI at 4 sites in the upper Gt. Ouse | 171 |
| Figure 5.18 | Effect of runs 1, 3 and 4 (see Table 5.1) on sulphate fluxes (mmol $m^{-2}\ d^{-1}$) across the SWI at 4 sites in the upper Gt. Ouse | 174 |
| Figure 5.19 | Modeled seasonal rates of oxic, suboxic and anoxic mineralization at 4 sites in the upper Gt. Ouse | 182 |
| Figure 6.1 | Relationship of $P_D$ (temperature selection in nitrate reduction, see text) with temperature at six sites in the lower Gt. Ouse sediments. | 191 |
| Figure 6.2 | Plot of $FitP_D$ and mean $P_D$ (from Figure 6.1) versus temperature | 193 |
| Figure 6.3 | Modeled ($M+FitP_D$ and $M-FitP_D$, see text) and observed rates of uncoupled denitrification at 6 sites in the lower Gt. Ouse; error bars = ±SE; nitrate in the overlying water is also plotted. Data from Trimmer *et al.*, 1998) | 197 |

| | | |
|---|---|---|
| Figure 6.4 | Modelled and calculated rates of sedimentary $DNRA_w$ (see text for details) at six sites in the lower Gt. Ouse (calculated rates = measured nitrate flux to sediment - measured rate of denitrification ($D_w$); error bars = ±SE; Data from Trimmer *et al.*, 1998). | 198 |
| Figure 6.5 | Percentage contribution of DNRA to total ammonium production at each temperature at 6 sites in the lower Gt. Ouse sediments. The remaining percentage is due to TOC mineralization. | 201 |
| Figure 6.6 | Modeled and observed fluxes of nitrate across the SWI at 6 sites in the lower Gt. Ouse (error bars are ±SE from triplicate samples; Trimmer *et al.*, 1998) | 203 |
| Figure 6.7 | Modeled and observed fluxes of ammonium across the SWI at 6 sites in the lower Gt. Ouse (error bars are ±SE from triplicate samples; Trimmer *et al.*, 1998) | 204 |
| Figure 6.8 | Modeled and observed fluxes of oxygen across the SWI at sites 5. and 7 in the lower Gt. Ouse (error bars are ±SE from triplicate samples; Trimmer *et al.*, 1998) | 205 |
| Figure 6.9 | Comparison of $FitP_D$ and data from King and Nedwell (1985.) vs temperature. (King and Nedwell data calculated from their Figure 5.). | 207 |

**List of Tables**


| | | |
|---|---|---|
| Table 1.1 | Sequence of diagenetic redox reactions for the major pathways of organic matter degradation (OM = $(CH_2O)_x$ $(NH_3)_y$ ; x = 106 and y = 16 for all reactions; # in $kJmol^{-1}$ of $CH_2O$; adapted from Tromp *et al.*, 1995) | 6 |
| Table 1.2 | Percentage contribution of dissimilatory nitrate reduction to ammonium (DNRA) in sedimentary nitrate reduction at different locations around the world (ABT = Acetylene Blockage Technique; est.nit = estimate of nitrification). | 22 |
| Table 1.3 | Factors controlling the pathway of nitrate reduction (DEN = denitrification, DNRA = dissimilatory nitrate reduction to ammonium) | 27 |
| Table 2.1a | Sediment characteristics for the 4 sites in the upper Gt. Ouse investigated between December 1992 and November 1993. (Adapted from Nedwell and Trimmer, 1996). | 45 |
| Table 2.1b | Sediment characteristics of the 6 sites in the lower Gt. Ouse investigated between April 1991 and April 1995 (taken from Trimmer et al., 1998) | 45 |
| Table 2.2 | Annual budget of sedimentary organic carbon in the upper Gt. Ouse (adapted from Nedwell and Trimmer, 1996) | 46 |
| Table 3.1 | Model equations for each variable (D is the diffusion term in equation 3.1. The remaining terms represent the sum of R reactions in equation 3.1; TOC = total organic carbon; $k$ = first order rate constant for organic decay; $\phi$ = porosity. All other parameters are defined in Table 3.2). | 57 |
| Table 3.2 | Parameter values and their sources | 58 |
| Table 3.3 | Boundary conditions and values (7 visit mean; units: μM) at the 4 sites | 59 |
| Table 3.4 | Calculation of $k_{calc}$ for each site in the upper Great Ouse estuary (see text for further details) | 61 |
| Table 3.5 | Values of k for model runs $M_{fit}$ and $M_{exp}$ derived by fitting the model to stoichiometrically determined mineralisation rates (Nedwell and Trimmer, 1996). Units: $y^{-1}$ ($k_{o2} = k$ for oxic mineralisation; $k_{no3} = k$ for suboxic mineralisation; $k_{so4} = k$ for anoxic mineralisation; $k_0 = k$ in top sediment model box (box i = 1, Figure 3.1); $\alpha$ = coefficient of decrease; z = depth. See text for further details) | 62 |
| Table 3.6a | Parameter sensitivity analysis at site 1 (each parameter decreased by 50%;values represent percentage change in rate/flux associated with each variable; swi = SWI flux; o2r = oxygen respiration; nit = nitrification; s-ox = sulphide oxidation; nr = nitrate reduction; bflx = bottom boundary flux; oxamm = oxic ammonification; subamm = suboxic ammonification; anamm = anoxic ammonification; totamm = total ammonification; sr = sulphate reduction; ox, sub, an = oxic, suboxic, anoxic mineralization; parameters defined in Table 3.2) | 80 |
| Table 3.6b | Parameter sensitivity analysis at site 1 (each parameter | 81 |

| | | |
|---|---|---|
| | increased by 50%;values represent percentage change in rate/flux associated with each variable; swi = SWI flux; o2r = oxygen respiration; nit = nitrification; s-ox = sulphide oxidation; nr = nitrate reduction; bflx = bottom boundary flux; oxamm = oxic ammonification; subamm = suboxic ammonification; anamm = anoxic ammonification; totamm = total ammonification; sr = sulphate reduction; ox, sub, an = oxic, suboxic, anoxic mineralization; parameters defined in Table 3.2) | |
| Table 3.7a | Parameter sensitivity analysis at site 2 (each parameter decreased by 50%;values represent percentage change in rate/flux associated with each variable; swi = SWI flux; o2r = oxygen respiration; nit = nitrification; s-ox = sulphide oxidation; nr = nitrate reduction; bflx = bottom boundary flux; oxamm = oxic ammonification; subamm = suboxic ammonification; anamm = anoxic ammonification; totamm = total ammonification; sr = sulphate reduction; ox, sub, an = oxic, suboxic, anoxic mineralization; parameters defined in Table 3.2 | 82 |
| Table 3.7b | Parameter sensitivity analysis at site 2 (each parameter increased by 50%;values represent percentage change in rate/flux associated with each variable; swi = SWI flux; o2r = oxygen respiration; nit = nitrification; s-ox = sulphide oxidation; nr = nitrate reduction; bflx = bottom boundary flux; oxamm = oxic ammonification; subamm = suboxic ammonification; anamm = anoxic ammonification; totamm = total ammonification; sr = sulphate reduction; ox, sub, an = oxic, suboxic, anoxic mineralization; parameters defined in Table 3.2) | 83 |
| Table 3.8a | Parameter sensitivity analysis at site 3 (each parameter decreased by 50%;values represent percentage change in rate/flux associated with each variable; swi = SWI flux; o2r = oxygen respiration; nit = nitrification; s-ox = sulphide oxidation; nr = nitrate reduction; bflx = bottom boundary flux; oxamm = oxic ammonification; subamm = suboxic ammonification; anamm = anoxic ammonification; totamm = total ammonification; sr = sulphate reduction; ox, sub, an = oxic, suboxic, anoxic mineralization; parameters defined in Table 3.2) | 84 |
| Table 3.8b | Parameter sensitivity analysis at site 3 (each parameter increased by 50%;values represent percentage change in rate/flux associated with each variable; swi = SWI flux; o2r = oxygen respiration; nit = nitrification; s-ox = sulphide oxidation; nr = nitrate reduction; bflx = bottom boundary flux; oxamm = oxic ammonification; subamm = suboxic ammonification; anamm = anoxic ammonification; totamm = total ammonification; sr = sulphate reduction; ox, sub, an = oxic, suboxic, anoxic mineralization; parameters defined in Table 3.2) | 85 |
| Table 3.9a | Parameter sensitivity analysis at site 4 (each parameter | 86 |

| | | |
|---|---|---|
| | decreased by 50%;values represent percentage change in rate/flux associated with each variable; swi = SWI flux; o2r = oxygen respiration; nit = nitrification; s-ox = sulphide oxidation; nr = nitrate reduction; bflx = bottom boundary flux; oxamm = oxic ammonification; subamm = suboxic ammonification; anamm = anoxic ammonification; totamm = total ammonification; sr = sulphate reduction; ox, sub, an = oxic, suboxic, anoxic mineralization; parameters defined in Table 3.2) | |
| Table 3.9b | Parameter sensitivity analysis at site 4 (each parameter increased by 50%;values represent percentage change in rate/flux associated with each variable; swi = SWI flux; o2r = oxygen respiration; nit = nitrification; s-ox = sulphide oxidation; nr = nitrate reduction; bflx = bottom boundary flux; oxamm = oxic ammonification; subamm = suboxic ammonification; anamm = anoxic ammonification; totamm = total ammonification; sr = sulphate reduction; ox, sub, an = oxic, suboxic, anoxic mineralization; parameters defined in Table 3.2) | 87 |
| Table 3.10 | The effect of ±50% changes in porosity on the percentage contribution of oxic, suboxic and anoxic mineralization to total organic carbon mineralization | 102 |
| Table 3.11 | Model sensitivity to ±50% changes in the bulk diffusion coefficient ( equation 3.3) for all variables. ( swi = SWI flux; o2r = oxygen respiration; nit = nitrification; s-ox = sulphide oxidation; nr = nitrate reduction; bflx = bottom boundary flux; oxamm = oxic ammonification; subamm = suboxic ammonification; anamm = anoxic ammonification; totamm = total ammonification; sr = sulphate reduction; ox, sub,an = oxic, suboxic, anoxic mineralization) | 105 |
| Table 3.12 | The effect of changes in $k_{sAnoxInhNO3}$ on the percentage contribution of oxic, suboxic and anoxic mineralization to total organic carbon mineralization | 107 |
| Table 4.1 | Response of oxygen concentrations (μM) at 0.05 cm in the sediment to changes in the DBL thickness (see also Figure 3.3a) | 116 |
| Table 5.1 | Model sensitivity runs ($O2_{bw}$, $NO3_{bw}$, $SO4_{bw}$ = oxygen, nitrate, sulphate concentration in the overlying water; $NH4_{bbc}$ = ammonium concentration in the sediment bottom boundary; values used are the mean across all sites and sample dates) | 165 |
| Table 5.2 | Summary of controls on seasonality in the model (T = temperature; $SO4_{bw}$, $NO3_{bw}$ = overlying concentrations of sulphate and nitrate, respectively; $NH4_{bbc}$ = bottom boundary concentration of ammonium) | 175 |
| Table 5.3 | Comparison of annual rates of carbon mineralization (mol C $m^{-2} y^{-1}$) at the 4 sites in the Gt. Ouse derived from the annual model in chapter 2 ($M_{fit}$) and the seasonal model | 183 |
| Table 6.1 | Rates of uncoupled denitrification (Dw), fluxes of nitrate (Nf) across the sediment water interface and values for PD ( = Dw/Nf, see text) at the six sites in the lower Gt. Ouse. (cnp = | 189 |

| | | |
|---|---|---|
| | calculation not possible; nm = not measured;units = μmol N $m^{-2}$ $h^{-1}$; negative value = flux to sediment) | |
| Table 6.2 | Values of the first order rate constant for nitrate reduction used in the model output with (M+Fit$P_D$) and without (M-Fit$P_D$) equations 6.6 and 6.7 (units ; $y^{-1}$; NB $k_{o2}$ = 8.7 $y^{-1}$ ; $k_{so4}$ = 10 $y^{-1}$ ; the latter two parameters are the mean values for the four sites in the Gt. Ouse, Table 3.5) | 196 |
| Table 6.3 | Comparison of the mean percentage contribution of DNRA to total ammonium production (%DNRA⇒$NH_4^+$) with both $k_{no3}$ values and the mean nitrate concentration in the water column at 6 sites in the lower Gt. Ouse. | 212 |
| Table B2.1a | Parameter sensitivity analysis at site 1 (each parameter decreased by 50%;values represent rate/flux (unit mol $m^{-2}$ $y^{-1}$) associated with each variable; swi = SWI flux; o2r = oxygen respiration; nit = nitrification; s-ox = sulphide oxidation; nr = nitrate reduction; bflx = bottom boundary flux; oxamm = oxic ammonification; subamm = suboxic ammonification; anamm = anoxic ammonification; totamm = total ammonification; sr = sulphate reduction; ox, sub, an = oxic, suboxic, anoxic mineralization; parameters defined in Table 3.2) | 226 |
| Table B2.1b | Parameter sensitivity analysis at site 1 (each parameter increased by 50%;values represent rate/flux (unit mol $m^{-2}$ $y^{-1}$) associated with each variable; swi = SWI flux; o2r = oxygen respiration; nit = nitrification; s-ox = sulphide oxidation; nr = nitrate reduction; bflx = bottom boundary flux; oxamm = oxic ammonification; subamm = suboxic ammonification; anamm = anoxic ammonification; totamm = total ammonification; sr = sulphate reduction; ox, sub, an = oxic, suboxic, anoxic mineralization; parameters defined in Table 3.2) | 227 |
| Table B2.2a | Parameter sensitivity analysis at site 2 (each parameter decreased by 50%;values represent rate/flux (unit mol $m^{-2}$ $y^{-1}$) associated with each variable; swi = SWI flux; o2r = oxygen respiration; nit = nitrification; s-ox = sulphide oxidation; nr = nitrate reduction; bflx = bottom boundary flux; oxamm = oxic ammonification; subamm = suboxic ammonification; anamm = anoxic ammonification; totamm = total ammonification; sr = sulphate reduction; ox, sub, an = oxic, suboxic, anoxic mineralization; parameters defined in Table 3.2) | 228 |
| Table B2.2b | Parameter sensitivity analysis at site 2 (each parameter increased by 50%;values represent rate/flux (unit mol $m^{-2}$ $y^{-1}$) associated with each variable; swi = SWI flux; o2r = oxygen respiration; nit = nitrification; s-ox = sulphide oxidation; nr = nitrate reduction; bflx = bottom boundary flux; oxamm = oxic ammonification; subamm = suboxic ammonification; anamm = anoxic ammonification; totamm = total ammonification; sr = sulphate reduction; ox, sub, an = oxic, suboxic, anoxic mineralization; parameters defined in Table 3.2) | 229 |
| Table B2.3a | Parameter sensitivity analysis at site 3 (each parameter decreased by 50%;values represent rate/flux (unit mol $m^{-2}$ $y^{-1}$) associated with each variable; swi = SWI flux; o2r = oxygen | 230 |

respiration; nit = nitrification; s-ox = sulphide oxidation; nr = nitrate reduction; bflx = bottom boundary flux; oxamm = oxic ammonification; subamm = suboxic ammonification; anamm = anoxic ammonification; totamm = total ammonification; sr = sulphate reduction; ox, sub, an = oxic, suboxic, anoxic mineralization; parameters defined in Table 3.2)

Table B2.3b Parameter sensitivity analysis at site 3 (each parameter increased by 50%;values represent rate/flux (unit mol $m^{-2}$ $y^{-1}$) associated with each variable; swi = SWI flux; o2r = oxygen respiration; nit = nitrification; s-ox = sulphide oxidation; nr = nitrate reduction; bflx = bottom boundary flux; oxamm = oxic ammonification; subamm = suboxic ammonification; anamm = anoxic ammonification; totamm = total ammonification; sr = sulphate reduction; ox, sub, an = oxic, suboxic, anoxic mineralization; parameters defined in Table 3.2) 231

Table B2.4a Parameter sensitivity analysis at site 4 (each parameter decreased by 50%;values represent rate/flux (unit mol $m^{-2}$ $y^{-1}$) associated with each variable; swi = SWI flux; o2r = oxygen respiration; nit = nitrification; s-ox = sulphide oxidation; nr = nitrate reduction; bflx = bottom boundary flux; oxamm = oxic ammonification; subamm = suboxic ammonification; anamm = anoxic ammonification; totamm = total ammonification; sr = sulphate reduction; ox, sub, an = oxic, suboxic, anoxic mineralization; parameters defined in Table 3.2) 232

Table B2.4b Parameter sensitivity analysis at site 4 (each parameter increased by 50%;values represent rate/flux (unit mol $m^{-2}$ $y^{-1}$) associated with each variable; swi = SWI flux; o2r = oxygen respiration; nit = nitrification; s-ox = sulphide oxidation; nr = nitrate reduction; bflx = bottom boundary flux; oxamm = oxic ammonification; subamm = suboxic ammonification; anamm = anoxic ammonification; totamm = total ammonification; sr = sulphate reduction; ox, sub, an = oxic, suboxic, anoxic mineralization; parameters defined in Table 3.2) 233

## Preface

Sediments play an important role in regulating biogeochemical processes. One such process is denitrification. Denitrification has been the focus of much research particularly because of concern over increased nitrogen loads to coastal environments. Diagenetic modelling helps us to understand the biogeochemical controls of the processes involved. The model of early diagenesis presented here was developed to investigate estuarine sedimentary biogeochemical dynamics in a temperate, high nutrient, UK North Sea estuary.

This thesis is divided into seven chapters. Chapter 1 is an introduction to the sedimentary nitrogen cycle and an historical background to the theory and modelling of early diagenesis. The aims and structure of this thesis are also presented in Chapter 1. Chapter 2 describes the observed data relied upon by the model. Chapter 3 deals with the development and calibration of the diagenetic model with emphasis on formulas for the first order rate constant for organic decay. Chapter 3 also examines the sensitivity of the model to changes in its parameters. In Chapter 4 attention focuses on how changes in the thickness of the diffusive boundary layer (DBL) immediately above the sediment water interface affect nutrient/oxygen exchange and mineralization pathways in the sediment. In Chapter 5, the model is modified to investigate seasonal patterns in oxygen and nutrient fluxes across the sediment water interface as well as the monthly changes in porewater profiles. The next chapter (Chapter 6) focuses on how temperature can be used to determine the proportion of nitrate reduction that follows both denitrification and dissimilarity nitrate reduction to ammonium (DNRA). The final chapter (Chapter 7) presents a summary and overall conclusions of this work.

**Acknowledgments**

The story of this Ph.D. is a long and tortuous one. The love and support of the following people ensured that this work was completed.

Firstly, without the incomparable and unquantifiable love and friendship of my most precious wife, Tamaris, there would be no life, let alone a Ph.D. Thank you for always helping me to see better. Because of you, I knew I would finish.

Thank you, David, for your super vision (yes, the gap is intentional) and for your visits to my office to ensure things were going to plan. I especially enjoyed our occasional discussions on films and theatre. To Tom and David, I appreciate the amount of time you gave me to write up this work. Also thank you both for your concern over my RSI. I am also indebted to Rachel and Duncan for their useful comments and guidance along the way. A great deal of gratitude goes to Dave Nedwell and Mark Trimmer for use of their data and for very beneficial discussions. Special mention goes to my voice recognition software (Voicepower Pro), for without it, this work would never have been written and a last minute 'big thanks' to Janes Altunbas for formatting my tables and contents list.

For the ceaseless and immeasurable love and support of my wonderful parents throughout my life and for the genes you have sentenced me with, I am eternally thankful. To my amazing little girl, Rozanna, thank you for the joy you give me. And to my latest precious little girl, Natalia, thank you for being so restless in mummy's tummy... this really speeded up the writing process!

To my dearest aunt, thank you for always showing an interest in my work. This helped a great deal. (Za moju najdrazu tetku, hvala ti puno sto si uvek pokazala interesovanje za moj doktorat. To mi je mnogo pomoglo.).Thank you to Rosemarie and Derrick for willing me on all the way from downunder and for bringing Tamaris into this world.

I would also like to thank all the friends who kept wondering how my Ph.D. was progressing: Aunty Marion, Graham, Suzie, Toby, Helen, Flash, Andrew, Katya, Kris, Lucas, Nico, Lu and many others - you ensured that I was always one step ahead of embarrassment!

Finally, this work, instigated by the MAFF/DOE-funded Joint Nutrient Study (JONUS), was inspired by the brilliance of Robert Berner and Bernie Boudreau, by the exceptionally gifted group at NIOO-CEMO and by the transcendence of Jan Vermeer and Cole Porter.

# 1. Introduction

## 1.1 Global perspective

Estuaries are the main transition zones between freshwater and marine environments. They serve a variety of important functions ranging from transport, industry and tourism to drainage of waste from domestic, industrial and agricultural practices. In the past few decades, there has been increasing concern over the polluted status of estuaries (and associated water ways) caused by the discharge of nitrogen and phosphorus based chemicals from land. It is estimated that 70% of the nitrogen entering the world's oceans from rivers and estuaries can be attributed to anthropogenic activities (Wollast, 1983; Galloway *et al.,* 1995). Although both nitrogen (N) and phosphorus (P) loads have increased (Howarth *et al.,* 1996), N is of particular concern as it is generally thought to be the limiting nutrient in estuaries (Boynton *et al.,* 1982). Such nutrient enrichment has the potential to stimulate primary production which may lead to a number of harmful environmental effects (e.g. water column anoxia, fish kills, noxious algal blooms) as observed in many coastal areas around the world (Baltic, Rosenberg *et al.,* 1990; Graneli *et al.,* 1990; German Bight, Radach *et al.,* 1990; Chesapeake Bay, Harding *et al.,* 1994; Cooper, 1995; southern North Sea, Cadee, 1986; Cadee and Hegeman, 1991). However, actual inputs of nutrients to coastal seas are difficult to establish (Balls, 1994; Nixon *et al*, 1995) because attenuation of the nutrient flux through estuaries is known to occur (Nedwell, 1975; Billen *et al.,* 1985; Law *et al.,* 1991; Trimmer *et al.,* 1998). Estuaries can reduce the transfer of riverine organic material to the coastal zone in two major ways : by

burial or by gaseous emission (Middelburg *et al.,* 1995). Sediment burial is an important removal pathway for suspended material, particulate organic matter (POM) and dissolved components following fixation, sorption or precipitation (Berner and Berner, 1987). Gaseous removal of dissolved nutrients and particulate organic matter is achieved following biogeochemical transformations such as POM remineralisation to carbon dioxide and denitrification of nitrate to dinitrogen or nitrous oxide (Seitzinger, 1988; Billen 1990; Middelburg *et al.,* 1995). A relationship between nutrient attenuation processes such as denitrification and water residence time have been demonstrated (Nixon *et al.,* 1996). However, because most estuarine processes are highly non-linear (Heip *et al.,* 1995) there continue to be difficulties in estimating the true net output of material (nutrients) from estuaries to coastal seas. These difficulties can be resolved by improving understanding of the biogeochemical processes controlling nutrient fluxes to sea. This work focuses on such an understanding.

## 1.2 Sediments as biogeochemical reactors

Sediments are a major reservoir of carbon, nitrogen, phosphorus and sulphur (Van Cappellen *et al.,* 1993). On geological time scales, oceanic sedimentary burial is a critical global sink mechanism controlling the distribution and cycling of these elements (Berner and Berner, 1987). Most estimates of the burial rate of organic carbon in marine sediments range between 40 and 180 Tg $y^{-1}$ (Van der Weijden, 1992, p17). Emerson and Hedges (1988) estimate that 10-20% of global oceanic primary production escapes the euphotic zone, 4% of which is permanently buried. More than 80% of this burial takes place on the continental shelves (Tyson, 1995).

On shorter time scales, a range of competing processes actively regulate the cycling of carbon, nitrogen, phosphorus and sulphur in all marine and freshwater environments including lakes, estuaries, coastal bays and shelf and deep seas (e.g. Wollast, 1982; Seitzinger and Nixon, 1985; Trimmer *et al.,* 1998). For instance, ammonium remineralised from organic matter (OM) can be assimilated by growing algae, can be adsorbed onto sediment particles or converted to other forms of nitrogen by microbial processes (Rosenfeld, 1981; Blackburn and Henriksen, 1983).

With few exceptions, biogeochemical processes in sediments are coupled to the microbially-mediated degradation of OM deposited from the overlying water. In contrast to the deeper (≥1m to 10m), long-term sedimentary reservoir, the surface sediment, which receives the sedimenting OM, is an active biogeochemical reactor in which a large number of microbial reactions, redox processes, precipitation-dissolution reactions and adsorption-desorption processes occur simultaneously, creating steep vertical gradients in chemical properties (Van Cappellen *et al.,* 1993). To understand and quantify these processes, an interdisciplinary approach is needed which takes into account the physics, biology and chemistry of the system. This approach is known as the study of early diagenesis.

## 1.3 Early diagenesis

Berner (1980, p.3) defines diagenesis as the "sum total of processes that bring about changes in a sediment or sedimentary rock subsequent to deposition in water" and confines his definition of early diagenesis to "changes occurring during burial to a few hundred meters where elevated temperatures are not encountered and where uplift above sea-level (or lake level) does not occur, so that the pore spaces are continually filled with

water". Early diagenesis encompasses all the chemical, physical, and biological changes undergone by a sediment after its initial deposition which occur in the zone where the sediment is still unconsolidated (Bates and Jackson, 1987). Down to a sediment depth of a few hundred metres, temperature tends to remain below 25°C, which means that bacterial processes can proceed and standard thermodynamic considerations can be applied to calculate chemical equilibria (Berner, 1980).

Examples of early diagenetic processes include the formation of concretions, the compactive dewatering of clay muds, the bacterial decomposition of sedimentary organic matter (OM) including remineralisation of sedimentary nutrients. Diagenetic processing such as cementation, reworking, authigenesis, replacement, crystallization, leaching and hydration, which continues under conditions of higher pressures (up to 1 kb) and temperatures (up to ~300 °C), is said to be complete when the sediment has been converted to a compact sedimentary rock (Bates and Jackson, 1987).

In this work, the study of early diagenesis is confined to the degradation of organic matter in estuarine sediments and to its effect on pore water chemistry. Particular emphasis is on the modelling of porewater concentration profiles and the calculation of solute fluxes across the sediment water interface (SWI). The focus of this work is on the cycling of nitrogen.

## 1.4 The early diagenesis of organic matter

The key cause of change in porewater composition is the degradation of OM during early diagenesis (Van der Weijden, 1992). Microbial degradation tends to be an oxidative process requiring electron acceptors. The energy source for metabolic processes is derived from the

redox reaction between reductants (electron donors, e.g. organic carbon) and external oxidants (electron acceptors, e.g. oxygen). Examples of oxidation include oxygen and sulphate reduction and nitrate respiration (i.e. denitrification). The alternative metabolic process employed by certain bacteria is fermentation. Fermentation is an anaerobic, non-oxidative, energy-yielding process in which substrates are gradually transformed by a series of balanced redox reactions in such a way that part of the substrate is oxidised at the expense of another part being reduced (Fenchel and Finlay, 1995, p. 38). Here, electron transport phosphorylation is absent and no membrane-bound enzymes are involved (e.g. cytochrome oxidases). There are no external electron acceptors and ATP is formed by substrate level phosphorylation (SLP).

The organic matter that arrives at the SWI is a complex mixture of compounds with different decomposition reactivities. The initial extracellular hydrolysis of large biopolymers, carried out by fermentative and hydrolytic bacteria (Tyson, 1995, p. 50), tends to be fast (Nedwell, 1987). The reduced products (i.e. soluble molecules such as amino acids) of this first step contain most of the chemical energy present in the original substrates. Consequently, other bacteria further down the metabolic chain can make use of this chemical energy (Fenchel and Jørgensen, 1977) depending on the availability of oxidants. Stumm and Morgan (1970) and Froelich *et al.* (1979) showed that the order in which available oxidants are utilised is determined by the relative amounts of free energy produced during their consumption. Table 1.1 shows this series of idealised diagenetic reactions in order of their energy yields per mole of carbon. This thermodynamic order of utilization (which is relative to the *in situ* pH) results in an ecological succession of bacterial floras and a depth stratified series of biogeochemical zones some of which may

Table 1.1. Sequence of diagenetic redox reactions for the major pathways of organic matter degradation (OM = $(CH_2O)_x(NH_3)_y$ ; x=106 and y=16 for all reactions; # in $kJmol^{-1}$ of $CH_2O$; adapted from Tromp *et al.,* 1995)

| Process | Reaction | #ΔG° |
|---|---|---|
| Aerobic respiration | $OM + (x+2y)O_2 \Rightarrow xCO_2+yHNO_3+(x+y)H_2O$ | -475 |
| Nitrate reduction | $5OM + 4xNO_3^- \Rightarrow 5xCO_2 + 2xN_2 + 5yNH_3 + 3xH_2O + 4xHCO_3^-$ | -448 |
| Manganese reduction | $OM + 2xMnO_2 + 3xCO_2 + xH_2O \Rightarrow 2xMn^{++} + 4xHCO_3^- + yNH_3$ | -349 |
| Iron reduction | $OM + 4xFe(OH)_3 + 3xCO_2 + xH_2O \Rightarrow 4xFe^{++} + 8xHCO_3^- + 3xH_2O + yNH_3$ | -114 |
| Sulphate reduction | $2OM + xSO_4^{=} \Rightarrow xH_2S + 2xHCO_3^- + 2yNH_3$ | -77 |
| Methane production | $OM \Rightarrow xCH_4 + xCO_2 + 2yNH_3$ | -58 |

overlap due to similarity in Gibbs free energy yields (e.g. denitrification and manganese reduction, Table 1.1). This biogeochemical zonation scheme relies on the idea that specific groups of bacteria use only a single electron acceptor in a particular zone. However, many bacteria are capable of using different electron acceptors ( e.g. sulphate reducers that can reduce nitrate, Mitchell *et al.,* 1986; reducers of ferric iron, nitrate and sulphate, Sorensen, 1982, 1987). This switching ability by bacteria together with a number of recent studies (e.g. Canfield *et al.,* 1993; Postma and Jackobsen, 1996) have indicated that the idea of sequential biogeochemical zonation is an oversimplification. New advances in sampling porewater geochemistry have revealed new biogeochemical interactions such as the coupling between the cycles of manganese and nitrogen (Luther *et al.,* 1997) and the cycles of iron and sulphur (Mortimer *et al.,* 2002). It seems that the classic diagenetic zonation

defined by Froelich *et al.* (1979) needs to be re-evaluated in light of the newly observed complex recycling reactions in sediments.

Oxygen is the most powerful oxidant (Van Cappellen *et al*, 1993) and therefore the preferred electron acceptor. Hence, for sediments accumulating under oxygenated bottom waters, aerobic respiration dominates the surface layer. When oxygen is fully respired, anaerobic respiration takes over using oxidants in more or less the following order : $NO_3^-$, $MnO_2$, $FeO_2$/FeOOH, $SO_4^=$ (Van der Weijden, 1992). With the exhaustion of the external electron acceptors, the removal of the remaining organic detritus proceeds via fermentation processes. Methane is the common end-product of the latter.

The resulting zonation of the sediment in relation to available oxidants and decomposition pathways yields zones of varying thicknesses. Zones of respiratory pathways are between millimetres to a few centimetres thick, whereas zones of methanogenesis may be several hundered metres deep (Cragg *et al.,* 1990). The upper oxygenated region of the sediment is referred to as the oxic layer. Sediment horizons in which respiratory processes with some degree of oxygen tolerance occur ( e.g. denitrification), are referred to as the suboxic layer. At depths in the sediment where oxygen is fully exhausted, the layer is referred to as anoxic. In this layer, processes such as sulphate reduction and methanogenesis can occur.

In global oceanic terms, aerobic respiration and sulphate reduction are responsible for most of the degradation of organic matter in sediments (Jørgensen, 1982; Canfield, 1989, 1992). In freshwater sediments, anaerobic decomposition is usually dominated by methanogenesis (Gaillard *et al.,* 1987; Kuivila *et al.,* 1988). Which decomposition pathway dominates (i.e. aerobic vs. anaerobic) is dependent on the sediment accumulation rate. An

increase in the latter means that a greater amount of metabolisable carbon survives oxic degradation. Consequently, more of the metabolisable carbon reaching the sediment surface can be degraded by suboxic (via $NO_3^-$, $MnO_2$, $FeO_2$/FeOOH) mineralisation, sulphate reduction or methanogenesis (Toth and Lerman, 1977; Billen, 1982; Jørgensen, 1982). Sulphate reduction can account for more than half of the total mineralisation in shelf (Jørgensen, 1982; Canfield, 1992) and estuarine (Nedwell and Trimmer, 1996) sediments.

With increasing water depth, the flux of metabolisable carbon to the sediment and the sediment accumulation rate decrease. This results in a greater fraction of the metabolisable carbon being removed by oxic mineralisation, leaving behind a more resistant fraction which the fermenters and sulphate reducers can only metabolise slowly, if at all (Berner, 1978; Tyson, 1995). Under these (deep sea) conditions, oxic mineralisation can be responsible for up to 99% of the total mineralisation (Martin and Sayles, 1994). Hence, sulphate reduction is almost fully absent resulting in an incomplete utilisation of pore water sulphate (Jørgensen, 1982; Canfield, 1992). Accumulation rates greater than 100 cm $ka^{-1}$ generally means that oxygen and sulphate are responsible for an equal share of the respiration of organic matter (Bralower and Thierstein, 1987; Canfield, 1989). Below accumulation rates of 1-2 cm $ka^{-1}$ oxygen becomes 100-1000 times more important than sulphate (Tyson, 1995) as the preferred electron acceptor. This yields a sediment column that often remains oxic throughout (Muller and Mangini, 1980; Canfield, 1989; Cranston and Buckley, 1990).

As depth in sediment is a measure of time since deposition,the overall rate of decay in sediments decreases exponentially with the age. Evidence indicates that this decrease is not due to differences in the efficiency of aerobic and anaerobic bacterial

degradation of metabolisable OM (Stumm and Morgan, 1970; Henrichs and Reeburgh, 1987; Emerson and Hedges, 1988; Canfield, 1989; Lee, 1992). Instead it is more likely to be due to the changing lability of OM with depth because the labile components are removed first (Godschalk and Wetzel, 1978; Van Cappellen *et al.,* 1993) yielding particulate organic matter (POM) that becomes progressively refractory with depth. Exceptionally, Sun *et al.* (1993) report a case of higher degradability of OM in anoxic sediments compared to the overlying oxic layers. Here, the quantity of particular structures (in this case chlorophyll a) meant that it was easier for the anaerobic bacteria to breakdown than for the aerobic bacteria. Normally the decrease in lability or bioavailability is paralleled by a decline in bacterial biomass which itself is part of the pool of sedimentary POM. Thus it was previously concluded that after a few hundred meters into the sediment all that remains are recalcitrant phases from the organic detritus deposited from the water column and the *in situ* synthesised material (Metcalf and Eddy, 1979). However, Parkes *et al.* (1994) found viable sediment bacterial populations at depths greater than 500 m where organic matter is considered to be refractory. More recently Zengler *et al.,*(1999) have found evidence of sedimentary bacteria capable of degrading particular hydrocarbons previously thought of as decay resistant. This extends the depths to which early diagenetic processes takes place and therefore the overall thickness of the biosphere.

## 1.5 Flux of solutes across the sediment-water interface

Early diagenesis is an important control of the chemical composition of natural waters (Berner, 1980, p.53). Diagenetic reactions occuring at or close to the sediment-

water interface (SWI), generate sharp solute concentration gradients between the sediment and the water column. This results in a diffusive flux of dissolved species across the SWI which can be enhanced by biological irrigation and/or wave and current stirring,. In the cases of some major ions in seawater (e.g. $Mg^{++}$, $K^{+}$) the sedimentary flux is larger than the riverine input to the oceans (Sayles, 1979; Martin and Sayles, 1994). In the case of nutrients, up to 80% of the nitrogen and phosphorus required by phytoplankton in estuaries may be derived from sedimentary nutrient regeneration (Fisher *et al.,* 1982). In shallow coastal environments, the effect of turbulent diffusive processes caused by the actions of waves and currents acting on the sediments, can increase the flux of dissolved species by more than a 100-fold (Vanderborght *et al.,* 1975; Lohse *et al.,* 1996). The importance of early diagenetic fluxes across coastal and estuarine sediments has been highlighted by many authors with respect to nutrient inputs (Blackburn and Henriksen, 1983; Christensen *et al.,* 1987; Seitzinger *et al.,* 1984, Seitzinger and Nixon, 1985; Seitzinger, 1987, 1988; Kemp *et al.,* 1990). Seitzinger (1988) has shown that in coastal marine sediments, loss of nitrogen as an $N_2$ flux caused by denitrification can exceed the input of nitrogen via $N_2$ fixation. The same author has calculated that in estuaries, sediment denitrification can remove between 20% and 50% of the external nitrogen input. This removal is estimated at 16% for UK estuaries flowing into the North Sea (Trimmer *et al.,* 2000).

### 1.6 Nitrogen and its cycling in estuarine sediments

Nitrogen is an element essential to all life. By volume it makes up almost four fifths of the total composition of the atmosphere, mostly as dinitrogen gas ($N_2$). In many marine and

estuarine habitats, the availability of nitrogen is thought to limit ecosystem productivity (e.g. Stewart, 1975; Billen, 1990). Consequently, there is a need to establish the forms in which nitrogen is present in the environment, the routes by which they are transformed, the microorganisms involved and the rates at which these processes occur.

In sediments, as in most other environments, nitrogen exists in both inorganic and organic forms. Generally, inorganic nitrogen exists either as gases in the atmosphere and dissolved in water or as compounds in aqueous solution. Organic nitrogen can exist in both aqueous and solid states. The geomicrobially important inorganic forms include ammonium, ammonium ion, nitrite, nitrate and gaseous oxides of nitrogen. The geomicrobially important organic nitrogen compounds include humic and fulvic acids, proteins, peptides, amino acids, purines, pyrimidines, pyridines, other amines and amides.

Chemically, nitrogen occurs in the following oxidation states: -3 ($NH_3$), -2 (e.g. $N_2H_4$), -1 (e.g. $NH_2OH$), 0 ($N_2$), +1 ($N_2O$), +2 (e.g. NO), +3 (e.g. $HNO_2$), +4 (e.g. $N_2O_4$), +5 (e.g. $HNO_3$). Oxidation states -3, -1, 0, +1, +2, +3 and +5 are the biologically reactive forms as they can be enzymatically altered (Ehrlich, 1996). The main forms of nitrogen found in estuarine environments are nitrate, nitrite, ammonium, dinitrogen and organic nitrogen (Herbert, 1982). Sources of nitrogen to estuaries include agricultural and urban run-off, sewage discharges, sludge dumping, precipitation and biological nitrogen fixation. During their route from land to sea, these various nitrogenous compounds undergo transformations and interactions to form the biogeochemical nitrogen cycle (see Figure 1.1).When oxygen is limiting or absent, nitrate is initially reduced to nitrite. At this point, two pathways are possible. One leads to the production of gaseous end-products in a

Figure 1.1 The sedimentary nitrogen cycle (DNRA = dissimilatory nitrate reduction to ammonium)

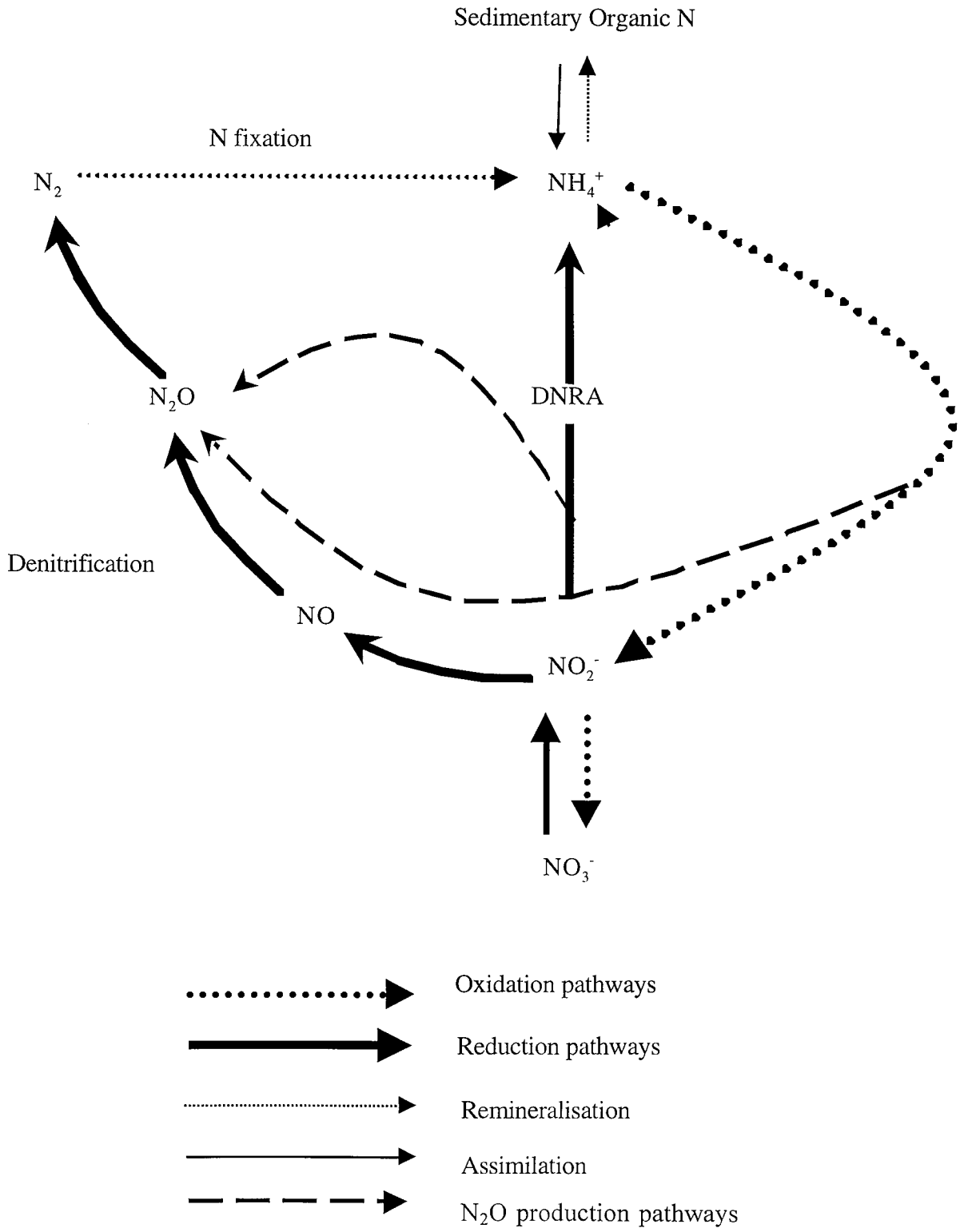

process known as denitrification. The other reduces nitrite, rapidly and directly, to ammonium and is called dissimilatory nitrate reduction to ammonium (DNRA).The latter should not be confused with assimilatory nitrate reduction to ammonium that heterotrophic bacteria carry out for nutritional requirements rather than for energetic gain (e.g. ATP production), as in DNRA. Both denitrification and DNRA have important ecological significance in that the former leads to loss of nitrogen from an ecosystem while the latter retains nitrogen in a biologically reactive form. Denitrification has been shown to counteract nitrogen inputs to estuaries (Seitzinger and Nixon, 1985; Trimmer *et al.,* 1998) while DNRA can contribute significantly to the regulation of some ecosystems (Cole, 1990).

The rate limiting step of the nitrogen cycle is nitrogen fixation whereby molecular nitrogen is reduced to ammonium by a specialised group of prokaryotic microorganisms (Cole and Brown,1980). The ammonium can then be assimilated into cell material or be oxidised in the nitrification process.

The following sections deal in more detail with some of the above components of the nitrogen cycle.

## 1.7 Organic nitrogen mineralisation (ammonification)

The release of ammonium from organic matter (principally from proteins and polynucleotides) is a multi-step process which starts with extracellular enzymatic hydrolysis and can take place under both oxic and anoxic conditions. Extracellular enzymes are those which act outside the bacterial cell and may be free or cell bound (Marxsen and Witzel, 1991). This initial step is thought to be the rate limiting stage in

organic matter degradation in sediments (Billen, 1982). As previously mentioned (section 1.4) the reduced products of hydrolysis (i.e. soluble molecules such as amino acids) contain most of the chemical energy present in the original substrates. Use of these products results in the production of ammonium. An example of such a process is the deamination of amino acids:

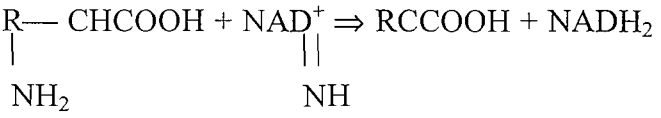

$$\begin{array}{l} R\text{---}\,CHCOOH + NAD^{+} \Rightarrow RCCOOH + NADH_2 \\ \quad\;| \qquad\qquad\qquad\quad\;\; || \\ \quad NH_2 \qquad\qquad\qquad\;\; NH \end{array}$$

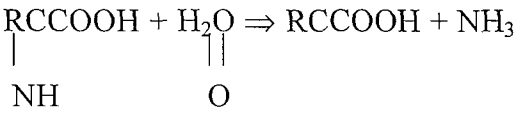

$$\begin{array}{l} RCCOOH + H_2O \Rightarrow RCCOOH + NH_3 \\ \quad\;| \qquad\quad\;\; || \\ \quad NH \qquad\quad\;\; O \end{array}$$

The $NH_3$ reacts with water to form ammonium hydroxide, which dissociates to form ammonium ion:

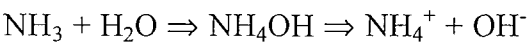

$$NH_3 + H_2O \Rightarrow NH_4OH \Rightarrow NH_4^{+} + OH^{-}$$

Organic matter mineralisation in coastal environments has been estimated to supply up to 80% of the nutrient requirement by phytoplankton (Fisher *et al.*, 1982). There are many methods for measuring the rate of the process (see Blackburn, 1988). It is usually the net rate (total minus N-assimilation) that is measured. The net rate is important because it determines the rate of recycling of nitrogen to the water column (Blackburn, 1988). However, it should be noted that most of these methods exclude the role of benthic macrofauna which will significantly underestimate the true *in situ* rate of mineralisation (Eriksen, 1988) and escape of ammonium to the water column.

## 1.8 Nitrification

Nitrification, or ammonium oxidation, involves two main steps (Kaplan, 1983):

step 1 $NH_4^+ + 1.5O_2 \Rightarrow NO_2^- + H_2O + 2H^+$ $\Delta G = -65kcal$

step 2 $NO_2^- + 0.5O_2 \Rightarrow NO_3^-$ $\Delta G = -18kcal$

Intermediate compounds such as hydroxylamine and by-products such as nitrous oxide are produced (Kaplan, 1983). Both steps are carried out by the chemoautotrophic bacteria, *Nitrosomonas* and *Nitrocystis* spp. (step 1) and by *Nitrobacter* and *Nitrococcus* spp. (step 2). With the exception of a few facultative bacteria such as *Nitrobacter winogradskyi*, most nitrifiers are obligate aerobes (Ehrlich, 1996). These autotrophs are highly inefficient, relative to heterotrophs, at converting energy from the oxidations to cell material. For instance, *Nitrosomonas* generates approximately 1 to 4% and *Nitrobacter* 3 to 10% of the cell material that would be expected from a heterotroph with the same amount of available energy (Fenchel and Blackburn, 1979). As these authors suggest, the reason for this is probably because ATP and reducing power have to be used by autotrophs in the reduction of carbon dioxide. Heterotrophic nitrification (i.e. ammonium oxidation in the presence of an organic substrate) has been observed (Verstraete, 1975; Killham, 1986), although rates are significantly slower than by autotrophic means. Examples of such nitrifying bacteria include *Arthrobacter* spp. (Ehrlich, 1996) and *Thiosphaera pantotropha* (Robertsen and Kuenen, 1990). Some (Killham, 1986; Ehrlich, 1996) have argued that heterotrophic nitrification is of little ecological importance because little nitrite or nitrate accumulates. Others (Robertsen and Kuenen, 1990) maintain that because *Tsa. pantotropha* simultaneously denitrifies the nitrite it produces, heterotrophic nitrification can be seriously underestimated unless complete nitrogen budgets are made.

Strong evidence exists (Van de Graaf, 1995; Jetten *et al.,* 1999; Strous *et al.,* 2002) that ammonium can be anaerobically oxidised by nitrate to dinitrogen in a process named Anammox and has been used to explain observations in estuarine and freshwater sediments (Ogilvie *et al.,* 1997a; Van Luijn *et al.,* 1998). Recently, the bacterium, *Candidatus brocadia anammoxidans* has been identified as carrying out this process (Strous *et al.,* 2002).

The importance of nitrification is that it produces an oxidised form of nitrogen which may participate in denitrification reactions resulting in a loss of N from the sediment (Fenchel and Blackburn, 1979). Other important consequences include the production of an anionic nitrogen species which, unlike ammonium ions, do not readily adsorb to clays rendering them a useful alternative nutrient source to plants. The contribution of sedimentary nitrification to the nitrous oxide budget, although observed (e.g. Jørgensen *et al.,* 1984) has not been quantified. It is noteworthy that Dore *et al.* (1998) have shown its significance in the water column of the subtropical North Pacific Ocean. Seitzinger and Kroeze (1998) in developing a model of the global $N_2O$ budget highlight the need for much field work before reliable estimates of the $N_2O$ source from nitrification can be made. Overall, it is the tight coupling of nitrification to denitrification that has been the main focus of previous studies (e.g. Kim *et al.,* 1997; Kemp *et al.,* 1990).

### 1.8.1 Factors regulating nitrification

The rate of nitrification is regulated by chemical, physical and biological factors. These include temperature, concentrations of oxygen, ammonium, carbon dioxide, sulphide and dissolved organic matter, pH, salinity, reactive surface area and macrofaunal and

macrophyte presence. These have been reviewed in detail by Henriksen and Kemp (1988) and so only a summary of the major factors will be given.

As with many biological processes, temperature effects on nitrification have been successfully described using the Arrhenius equation. $Q_{10}$ values commonly range between 2 and 3 (Carlucci and Strickland, 1968; Hansen, 1980; Helder and De Vries, 1983) over a wide range of temperatures (2-38°C) from different habitats. However, values as high as 17.6 (Berounsky and Nixon, 1990) have been found in coastal waters (Narrangansett Bay). The optimum temperature range for nitrification is 25°C-35°C (Henriksen and Kemp, 1988) although significant rates have been measured at -2°C (Horrigan ,1981 quoted in Henriksen and Kemp, 1988).

Oxygen is required for both steps (1 and 2) in nitrification. Ultimately, therefore, the rate of nitrification is limited by the rate of oxygen diffusion into the sediment. The range in oxygen concentrations at which nitrification is limited is 1.1 to 6.2 μM $O_2$ (see references in Henriksen and Blackburn, 1988). However, high oxygen levels (2-5 times air saturation) have been shown to be both toxic and inhibitory to nitrification (Henriksen and Kemp, 1988). The affinity for oxygen, usually expressed via the half-saturation constant, $K_m$, is highly variable for both steps. $K_m$ values for ammonium and nitrite oxidation show high variability ranging from as low as 0.1 μM $NH_4^+$ for oceanic waters (Olson, 1981; Hashimoto *et al.,* 1983) to between 70-700 μM $NH_4^+$ for ammonium oxidation and 350-600 μM $NO_2^-$ for nitrite oxidation (Painter, 1970; Focht and Verstraete, 1977). The value of $K_m$ is negatively correlated with temperature (Fenchel and Blackburn, 1979) suggesting a possible reason for the large (seasonal) variability in the affinity of nitrifiers for substrates, especially in shallower waters.

Changes in the sedimentary distribution and concentration of oxygen caused by the activities of macrobenthos (Henriksen, 1990) and microphytobenthos (Risgaard-Petersen *et al.,* 1994) have been shown to impact on rates of nitrification. For instance, 24 hour variations in the photosynthetic activity of benthic microphytes create diurnal variations in rates of nitrification (Risgaard-Petersen *et al.,* 1994). The linings of sediment burrows are environments of high potential nitrification rates (Henriksen *et al.,* 1983) because of the high concentrations of ammonium (via excretion) and the increased flux of oxygen into the sediments caused by bio-irrigation (Kristensen, 1988).

Although the regulating role of oxygen in nitrification is well known, recent work (Aller, 1994; Luther *et al.,* 1997) has implicated other oxidants (e.g. $MnO_2$) in sedimentary ammonium oxidation. Known as either suboxic or anoxic nitrification, it has been observed both in laboratory experiments (Hulth *et al.,* 1999) and in marine sediments (Mortimer *et al.,* 2002) but its significance in the sedimentary nitrogen budget is as yet unknown.

The effect of pH on nitrification has not been studied in natural aquatic sediments (Strauss *et al.,* 2002). However, a number of studies elsewhere (e.g. soils, pure cultures) have found that a narrow range in pH (7-8.5) defines the optimal activity of nitrifying bacteria (Henriksen and Kemp, 1988). However, nitrifying bacteria can withstand a broader pH spectrum between 4 and 9 (Engel and Alexander, 1958; Antoniou *et al.,* 1990; Paavolainen and Smolander, 1998), with the upper limit determined by the levels of free ammonium (Prakasam and Loehr, 1972) which is toxic to nitrifiers. The relationship between increasing pH (to optimum values) and higher nitrification rates relates to the increased availability of unprotonated ammonia ($NH_3$). The latter is thought to be the true substrate for nitrification (Suzuki *et al.,* 1974). There is evidence that low pH has a

negative effect on enzyme activity which may also explain the lower rates of nitrification at sub-optimum pH levels (Prosser, 1989). The energy required to maintain the internal cell pH below the environmental pH once the pH rises above the optimum value for nitrification, may counterbalance the advantage of the increased availability of $NH_3$. (Wood, 1988). This may explain the reduction in nitrification rates for pH values greater than ~8. In a survey of nitrification rates from 36 streams in the northern USA, Strauss *et al.* (2002) derived a multiple regression model which showed that nitrification was regulated by several variables with ammonium availability and pH being the most important. However, no single variable could explain more than 20% of the variability in nitrification rates, highlighting differences in the significance of various regulating factors among the streams. Contrastingly, in a single area, year long study of estuarine nitrification rates, Bianchi *et al.* (1999) found that ammonium availability accounted for 74% of the variability in nitrification rates.

The role of organic carbon has also been implicated as an important regulator of nitrification rates in aquatic sediments (Strauss and Lamberti, 2000). These authors found that higher C:N ratios lowered rates of nitrification and that higher quality organic carbon (glucose) had a stronger inhibitory effect on nitrification than lower quality organic carbon (sugar maple leaf extract). Strauss and Lamberti (2000) hypothesised that this was caused by the greater competitiveness of heterotrophic bacteria over nitrifying bacteria for available ammonium.

## 1.9 Nitrate reduction - denitrification and DNRA

Many bacteria use nitrate instead of oxygen as a terminal electron acceptor. Consequently, nitrate is 'respired' or 'reduced' and the process generally occurs only under anaerobic conditions. The first step of nitrate reduction involves the conversion of nitrate to nitrite. The half reaction is:

$$NO_3^- + 2H^+ + 2e \Rightarrow NO_2^- + H_2O$$

Subsequent steps follow either denitrification (production of gaseous nitrogen oxides) or dissimilatory reduction of nitrate to ammonia (DNRA). Denitrification is a multi-step process in which a series of nitrogen oxides are produced ending with the formation of dinitrogen gas:

$$NO_2^- + 2H^+ + e \Rightarrow NO + H_2O$$

$$2NO + 2H^+ + 2e \Rightarrow N_2O + H_2O$$

$$N_2O + 2H^+ + 2e \Rightarrow N_2 + H_2O$$

The reduction of nitrite to ammonium can be summarised as:

$$NO_2^- + 7H^+ + 6e \Rightarrow NH_3 + 2H_2O$$

The standard free energy changes of the overall reactions,

$2NO_3^- + 2H^+ + 5H_2 \Rightarrow N_2 + 6H_2O$ -1120.5 kJ (denitrification)

$NO_3^- + 2H^+ + 4H_2 \Rightarrow NH_4^+ + 3H_2O$ -599.6 kJ (DNRA)

suggest that the energy gain from denitrification and DNRA is similar. The ecological significance of these two nitrate competing processes is that denitrification leads to a loss of nitrogen from the ecosystem while DNRA retains nitrogen in the highly reactive biologically preferred form. The fact that DNRA competes for nitrate with denitrification in sediments (Sorensen, 1978; Enoksson and Samuelsson, 1987) may suggest that DNRA is a significant consumer of nitrate. A literature review (Table 1.2) shows that DNRA (measured using $^{15}N$ assay techniques and/or estimated from measurements of both denitrification using the acetylene blockage technique and nitrate exchange at the sediment water interface) can account for a high proportion of the total nitrate reduction that takes place in sediments. Sorensen (1978) has shown that in organic rich sediments, DNRA may account for up to one third of the carbon oxidation.

Denitrification is carried out, predominantly, by heterotrophic, facultative anaerobic respiratory bacteria (Seitzinger, 1988). Some organisms can reduce nitrite but not nitrate to nitrogen gas (Pichinoty *et al.,* 1976a in Delwiche, 1981) while others lack nitrous oxide reductase activity and therefore produce only nitrous oxide (Greenberg and Becker, 1977). Examples of denitrifying bacteria include the genera *Alcaligenes, Pseudomonoas, Paracoccus* and *Thiobacillus*.

Denitrification is fuelled by nitrate derived from two sources: 1) from the overlying water by diffusion (molecular and/or turbulent) and 2) from nitrification. Denitrification

fuelled from overlying nitrate is termed $D_w$ and 'coupled nitrification-denitrification' is referred to as $D_n$. It is generally acknowledged (see Middelburg *et al.,* 1996a) that as water column nitrate levels decrease (i.e. as water moves along the land-sea axis), the ratio of $D_n$:$D_w$ increases. For instance, in the offshore areas of the southern North Sea, where nitrate concentrations are <~32μM (Hydes and Edmonds, 1992), nitrification fuels denitrification (Lohse *et al.,* 1993). Contrastingly, in UK estuaries where nitrate exceeds 1000μM, $D_w$ dominates (Nedwell and Trimmer, 1996).

Table 1.2 Percentage contribution of dissimilatory nitrate reduction to ammonium (DNRA) in sedimentary nitrate reduction at different locations around the world (ABT = Acetylene Blockage Technique; est.nit= estimate of nitrification).

| % | Location | Method | Reference |
|---|---|---|---|
| 7 - 53 | Coastal/Estuarine (Tokyo Bay), Japan | $^{15}N$ assay + ABT | Koike and Hattori, 1978 |
| 56 | Coastal/Marine (Limfjorden), Denmark | $^{15}N$ assay + ABT | Sørensen, 1978 |
| 5 - 30 | Coastal/Intertidal sediments, New Zealand | $^{15}N$ assay + ABT | Kaspar, 1983 |
| 40 -70 | Coastal/Estuarine, Japan | $^{15}N$ assay + ABT | Nishio *et al.,* 1983 |
| 0 - 18 | Coastal, New Zealand (South Island) | $^{15}N$ assay + ABT | Kaspar *et al.,* 1985 |
| 65-90 | Estuarine (Norsminde Fjord), Denmark | ABT | Jørgensen and Sørensen, 1985 |
| 32 | Coastal/Marine, The Netherlands | $^{15}N$ assay + ABT | Goeyens *et al.,* 1987 |
| 70 | Estuarine (Norsminde Fjord), Denmark | ABT | Jørgensen and Sørensen, 1988 |
| 4-21 | Estuarine (Norsminde Fjord), Denmark | $^{15}N$ assay + ABT | Jørgensen, 1989 |
| 97 | Coastal (Hiroshima Bay), Japan | ABT + est.nit | Kim *et al.,* 1997 |
| 54 | Estuarine (Lower Gt. Ouse), U.K. | ABT | Trimmer *et al.,* 1998 |
| 18-100 | Coastal (Carteau Cove), France | $^{15}N$ assay + ABT | Bonin *et al.,* 1998 |
| 15-75 | Estuarine (Baffin Bay), Texas, USA | $^{15}N$ enrichment | An and Gardner, 2002 |
| 98 | Coastal Lagoon, France | $^{15}N$ assay + ABT | Gilbert *et al.,* 1998 |

While denitrification has received much attention (e.g. Seitzinger and Nixon, 1985; Seitzinger,1987; Hydes *et al.,* 1999), less research (e.g. Cole and Brown, 1980; Sorensen, 1987; Cole, 1990) has concentrated on DNRA. DNRA was originally observed in

fermenting bacteria (Woods, 1938) while Sorensen (1978) and Koike and Hattori (1978) provided early evidence for this process in coastal sediments. Since then others have observed the process in sediments (Enoksson and Samuelsson, 1987; Jørgensen and Sorensen, 1988; Gilbert *et al.,* 1998) while some have tried to explain the mechanism and function of DNRA (Sorensen, 1987; Stouthamer, 1988; Tiedje, 1988; Cole, 1990). It is presently believed that the function of DNRA is to use nitrite or nitrate as 'electron sinks' to reoxidise NADH, but this is not directly coupled to ATP production (Cole and Brown, 1980; Sorensen, 1987). Furthermore, the accommodation of eight electrons per nitrogen in the nitrate to ammonium step in often electron acceptor limited anaerobic environments makes DNRA a favourable process (Tiedje, 1988). A range of bacteria are now known to be able to dissimilate nitrate to ammonium and include the genera *Desulfovibrio, Klebsiella, Clostridium, Achromobacter* and *Escherichia.* (Cole, 1990). A growing number of non-fermenting bacteria are also known to be capable of DNRA including respiratory bacteria such as denitrifiers (MacFarlane and Herbert, 1982; Mancinelli, 1986) and sulphate reducers (Mitchell *et al.,* 1986; Seitz and Cypionka, 1986). It is interesting to note that nitrate reduction can also be an abiotic process, especially where significant amounts of $Fe^{2+}$ or $H_2S$ accumulate in the redoxcline (Sorensen, 1987). However, although this is a recognised process, its contribution to total nitrate reduction in sediments is unknown. In this thesis, DNRA refers only to the bacterially mediated process.

Microbes capable of nitrate reduction are widely distributed in nature (Cole and Brown, 1980; Tiedje, 1988). Hence, any restriction to nitrate reduction will probably be related to environmental conditions that regulate the process rather than to a lack of microorganisms.

### 1.9.1 Factors regulating nitrate reduction

Factors that control denitrification rates include temperature, concentrations of oxygen and nitrate and organic matter supply (Seitzinger, 1988). The effect of temperature on nitrification and oxygen dynamics makes it difficult to assess the direct effect of temperature on denitrification. Nowicki (1994) under controlled laboratory conditions demonstrated a $Q_{10}$ response which increased from 1.8 to 4.5 with increasing nutrient enrichment. Using sediment 'warming' techniques, some (Hill, 1983) have demonstrated four fold increases in rates of denitrification with increasing temperatures (0°C-20°C) while others (Andersen, 1977), over a similar temperature range (5°C-20°C), have found no effect. Seasonal rates of denitrification over a year have shown minima in late winter when temperatures were 17°C and maxima in late spring at 21°C, even though highest temperatures (25°C) occurred in summer (Seitzinger, 1987). In intertidal sediments, Kieskamp *et al.* (1991) found highest denitrification rates in winter and lowest in summer. These were correlated to nitrate concentrations in the overlying water rather than to temperature. Similarly, for a tidal mudflat, Koch *et al.* (1992) measured lowest rates in summer and highest in winter thereby excluding temperature as a controlling factor. At a coastal site, Jensen *et al.* (1988), found that seasonality in denitrification could not be explained by temperature changes and was, instead, determined by the supply of organic matter (the dynamics of primary production /sedimentation). Temperature has also been found to select for different types of nitrate reducers. Kaplan *et al.* (1977) showed in a temperate salt marsh, that two distinct denitrifying bacterial populations with different temperature optima were selected for throughout the year. Chemostat experiments on salt marsh (King and Nedwell, 1984) and estuarine sediments (Ogilvie *et al.*, 1997b) have

shown that colder temperatures (≤10°C) select for denitrifying bacteria while at higher temperatures, nitrate ammonifying bacteria dominate the nitrate reducing community. This suggests that denitrifiers are psychrophilic.

The relationship of nitrate concentrations to denitrification rates has been well studied (see review by Seitzinger, 1988) . The response can be described using Michaelis-Menten type kinetics with half-saturation constants varying between 27 μM $NO_3^-$ and 344 μM $NO_3^-$ (Seitzinger, 1988). Note that these values come from sediment slurry experiments which may not represent *in situ* activity. For instance, microenvironmental sedimentary gradients of nitrate can be important (Duff *et al.,* 1984; Jenkins and Kemp, 1984). Nevertheless, Trimmer *et al.* (1998) showed that denitrification rates ($D_w$) in estuarine sediments approach an asymptotic rate (~<200 μmol N $m^{-2} h^{-1}$) for overlying nitrate concentrations greater than 400 μM. As mentioned earlier, seasonal changes in nitrate concentrations in the overlying water have been used to explain seasonality in denitrification rates (Koch *et al.,* 1992; Kieskamp *et al.,* 1991). King and Nedwell (1987) showed in anoxic estuarine sediment slurries kept at constant temperature (5°C) that increasing nitrate concentrations (100 μM-900 μM) increased denitrification as a percentage of total nitrate reduction from between 30-50% to >70%. A similar finding by Nedwell (1982) suggests that high nitrate concentrations favour the activity of denitrifiers over ammonifiers.

Availability of organic matter affects denitrification in a number of ways. The conversion of nitrate to nitrogen gas ($N_2O$, $N_2$) is coupled to the mineralisation of organic carbon. Hence, the lower the supply of organic matter the lower the rate of denitrification. A less direct control of mineralisation on denitrification is in the production of ammonium

which fuels nitrifiction. Hence in low nitrate waters, where $D_n$ is dominant, denitrification will be limited by mineralisation rates. Furthermore, sediments with high organic carbon content (reduced environments) where the ratio of electron donor (carbon) to electron acceptor (nitrate) is high, DNRA is stimulated (Cole, 1990) which may compete with denitrification for nitrate (Tiedje *et al.,* 1982). In addition, consumption of oxygen during organic mineralisation controls oxygen distributions in the sediment which may affect denitrification. The seasonal cycle of sedimentary rates of denitrification has been correlated to phytoplankton dynamics (Jensen *et al.,* 1988).

In sediments, denitrification (and DNRA) takes place close to the oxic-anoxic interface (Christensen and Sorensen, 1986) and so the presence or absence of oxygen is an important regulating factor. Most studies (see Seitzinger, 1988) show that oxygen concentrations below ~6.25 μM $O_2$ are needed for denitrification to occur. However, denitrification at air saturation by*Thiosphaera pantotropha* has been documented (Robertsen and Kuenen, 1984) but the significance of aerobic denitrification is unknown. Oxygen concentrations can influence the proportioning of $N_2O$ to $N_2$ in denitrification (Jørgensen *et al.,* 1984). These authors showed that decreasing $O_2$ concentrations in the range 0.1-10 kPa $O_2$ increased the proportion of $N_2$ to $N_2O$ from ~50% to >90%. The effect of oxygen on nitrification (section 1.8.1) can also influence denitrification rates.

The inhibitory effect of oxygen on denitrifiers is well described (Payne, 1973) but less is known about the activity in the redoxcline which separates oxidised sediment from deeper reduced layers. In this transition zone, nitrate reduction is known to interact with other forms of anaerobic metabolism such as sulphate reduction (Sorensen, 1986). For instance, Sorensen *et al.* (1980) showed that nitrous oxide accumulated near to strongly

reduced layers because of specific inhibition of $N_2O$ reductase by $H_2S$. More recently, (Luther *et al.,* 1997) have demonstrated the role of $MnO_2$ as an oxidant for nitrification in $D_n$ which has now been observed in marine sediments (Mortimer *et al.,* 2002)

It is likely that the direct controls on DNRA are similar to those on denitrification: oxygen, nitrate, organic matter, temperature. However, only a small amount of work has been done on this subject. Herbert (1982) took sediment samples from a range of British estuaries and coastal sites and amended them with two concentrations of nitrate, 2 mM $KNO_3^-$ and 10 mM $KNO_3^-$. The addition of lower nitrate meant that the major end-product of nitrate dissimilation was ammonium. In contrast, the higher nitrate

Table 1.3. Factors controlling the pathway of nitrate reduction (DEN=denitrification, DNRA=dissimilatory nitrate reduction to ammonium)

| Factor | Effect | Reference |
|---|---|---|
| *in situ* $NO_3^-$ concentration | High favours DEN<br>Low favours DNRA | King & Nedwell, 1987 |
| Carbon : $NO_3^-$ ratio | High favours DNRA<br>Low favours DEN | Rehr & Klemme, 1989 |
| Temperature | Selective pressure on bacteria (colder favours DEN, warmer favours DNRA) | Ogilvie *et al.,* 1997b |
| Sulphide concentration | Inhibits coupled denitrification<br>Acts as electron donor for DNRA | An and Gardner, 2002 |
| Carbon source | e.g. Glycerol favoured by ammonifiers<br>Acetate favoured by denitrifiers | Herbert, 1982 |

supplements meant that nitrate dissimilation proceeded only as far as nitrite. As mentioned above in this section, temperature and nitrate concentrations influence the

proportioning of denitrification to DNRA in nitrate reduction. Other influences have been found (Table 1.3). These include the ratio of carbon to nitrate (i.e. the electron donor to electron acceptor ratio) (Rehr and Klemme, 1989) and the carbon source (e.g. glycerol is used by ammonifying bacteria while acetate is favoured by denitrifiers) (Herbert, 1990).

## 1.10 Diagenetic modelling philosophy

Boudreau (1997, p.1) states: "The study of sedimentary chemistry and its associated processes is becoming far more mathematical. This new emphasis is being driven by pressures originating from both basic research and field applications. In particular, pressing environmental problems, such as predicting the fate and transfer rates of contaminants in aquatic sediments, now demand numerical answers. Furthermore, there is a growing desire to gain a quantitative understanding of the reasons for the natural chemical changes observed in sediments as they are buried."

With this increase in demand for models from both the scientific and environmental management communities, it is important to understand what can be achieved with such a tool. The primary question before developing a model of early diagenesis or of any process, must be "why develop a model in the first place?". A number of reasons can be put forward:

- Measurements seldom indicate how varied processes may be; only the net results are yielded.
- The timescale of many diagenetic processes are longer than the lifetime of any investigator.

- Adequately set up models can easily be used to study future possible effects. This is a hard task for experimentalists
- Models can be used to test hypotheses proposed to explain field observations and hence help to verify understanding.
- Models permit a systematic and comparative treatment of data covering a wide range of sedimentary environments
- Models may reveal processes not suspected during the qualitative interpretation of data and can thereby suggest areas of further research and fieldwork.

While acknowledging these advantages, models are useless without adequate data sets both in terms of quality and temperal-spatial resolution. Thus, a modeller must either be part of a data collecting field programme or have access to literature derived data. Furthermore, if the above six points are accepted as satisfactory reasons for developing a model , it is important to note that modelling is more than just the manipulation of equations. For a sound modelling strategy, a number of important steps are needed. These are listed in a recent text by Boudreau (1997) and for the purposes of aiding the reader these are repeated below:

- Identification of the problem to be addressed; what is the precise question that needs answering?
- Formulation of the appropriate model; i.e. what are the correct equations for the problem?
- Solution of the model; i.e. by what means can an accurate answer be obtained
- Interpretation of the results in the context of early diagenesis; i.e. does the model describe the processes under consideration?

It is within the context of these four steps that the modelling strategy of this thesis is based. Before describing this strategy it is important to place it within the context of historical developments.

## 1.11 The history and development of models of early diagenesis

Berner (1964) was the first to apply a model to sedimentary biogeochemical processes. He recognised that vertical gradients in porewater composition are in general much greater than lateral gradients and thus treated early diagenesis in terms of one dimensional depth models (Berner 1964, 1974, 1980). There have been attempts to model the sediment in terms of 2D and 3D coordinates but lack of detailed multidimensional data has confined these models to numerical experimentation (Boudreau and Taylor, 1989) or to calculations of pore water distributions around irrigation burrows (Aller, 1980, 1983, 1984). The pioneering work of Berner (1964, 1974) culminated in the publication of his classic text in 1980 entitled 'Early diagenesis : a theoretical approach'. In this book, the 1D general diagenetic equation was proposed for a dissolved species that undergoes sediment advection, molecular diffusion and kinetic reaction:

$$\underbrace{\frac{\partial(\phi C)}{\partial t}}_{\text{Rate of change}} = \underbrace{-\frac{\partial}{\partial z}\left[-D_C\phi\frac{\partial C}{\partial z}+\omega\phi C\right]}_{\text{Advection–Diffusion}} + \underbrace{\phi\sum R}_{\text{Reaction}} \qquad 1.1$$

where

$C$ = solute concentration (units of mass per unit volume of pore water)

$D_C$ = molecular diffusion coefficient for solute C (units of surface area of sediment per unit time)

$\omega$ = sediment advection rate (units of length per unit time)

R = reaction rate (units of mass per unit volume of pore water per unit time)

$\phi$ = porosity (ratio of the volume of water to total sediment volume)

z = depth in sediment

t = time

The transport components of equation 1.1 are made up of diffusion and advection. Diffusive fluxes are formulated using Fickian laws of diffusion. Advection considers the bulk flow of a solute (or particles if POC is modelled) and can be due to burial, compaction and/or externally impressed flow (Boudreau, 1997). Both diffusive and advective fluxes are described in equation 1.1 as *local* transport processes. That is, at a given depth, the transport fluxes rely on the concentration (advection) and the concentration gradient (diffusion) at that location. However, *nonlocal* transport can also occur, whereby material is transported between points that are not adjacent to each other. This may be caused by both physical (wave and current action) and bio-physical (deposit feeding benthos) action. In such cases, equation 1.1 must be modified to account for nonlocal transport. Nonlocal transport phenomena are not considered in this study on account of a lack of bioturbating fauna at the sampling sites (section 2.1.2). Nevertheless, in bioturbated sediments, bioturbation (usually confined to the top 10 cm, Boudreau, 1998) is often assumed to be diffusive on the grounds that mixing is rapid, small-scale and random (Boudreau, 1986). This mixing can act in two different ways with respect to solids (e.g. organic matter) and dissolved substances (e.g. oxygen) with direct consequences for equation 1.1. Bioturbation can either i) mix or ii) not mix solids and fluids together. In the first case, called interphase mixing, porosity gradients are removed and bioturbation must be included in equation 1.1 (Boudreau, 1997). In the second case, called intraphase mixing,

porosity gradients are not affected and equation 1.1 does not require a bioturbation term (Boudreau, 1986). Most often, intraphase mixing is assumed (e.g. Soetaert *et al.,* 1996), due to the presence of porosity gradients in most marine sediments. This assumption also has the advantage of simplifying the diagenetic equation for dissolved substances. However, when modelling solids (e.g. organic carbon) in bioturbated sediments, the bioturbation process must be included. Meysman (2001) presents the latest modelling theory for including bioturbation into diagenetic models as well as providing an extensive review of how bioturbation has been previously dealt with.

The final component on the right hand side of equation 1.1 parameterises the biological and chemical reactions of diagenesis. A description of this term in the equation will now be considered in the context of the historical development of diagenetic models.

### 1.11.1 The reaction terms of diagenesis

Following on from Berner (1964, 1974), Vanderborght *et al.* (1977) applied simplified versions of equation 1.1 to North Sea sediments to investigate nutrient diagenesis. These models relied on zero- and first- order kinetics (equations 1.2 and 1.3) to describe steady state porewater distributions and the equations were solved by analytical means.

$$\frac{dC}{dt} = -k_c \qquad \text{(zero order)} \qquad 1.2$$

$$\frac{dC}{dt} = -k\,C \qquad \text{(first order)} \qquad 1.3$$

where $k_c$ is a zero order rate constant, $k$ is a first order rate constant.

In these models oxidant behaviour is not explicitly coupled to the oxidation of organic matter. Other models followed (Berner, 1980; Billen, 1982; Goloway and Bender,

1982; Jahnke *et al.,* 1982; Grundmanis and Murray, 1982) which remedied this problem by modelling the particulate organic carbon (POC) with what Berner (1980) referred to as one-G[1] models, i.e.

$$\frac{\mathrm{dPOC}}{\mathrm{dt}} = -k\,\mathrm{POC} \qquad 1.4$$

where the loss of a particular oxidant (e.g. oxygen) is modelled using stoichiometric relationships (Table 1.1). For example, a model of nitrate reduction would yield

$$\frac{dNO_3^-}{dt} = -\mathrm{k}\ \gamma_{NO3}^{POC}\ \phi POC \qquad 1.5$$

where $\gamma_{NO3}^{POC}$ is the ratio of mole of nitrate used per mole of POC oxidised (i.e. 0.8, see Table 1.1). In such models, the rate constant $k$ is assumed to be constant and "can be regarded as a measure of the weighted average of the reactivity of the organic matter and, to a lesser degree, the kinetic efficiency of the decomposition pathway(s), in the depth range of the sediment under study." (Van Cappellen *et al.,* 1993). Furthermore, in one-G models (e.g. Goloway and Bender, 1982; Grundmanis and Murray, 1982; Emerson *et al.,* 1985), all of the organic carbon is available for microbial breakdown. This has the advantage of allowing the depth distribution of metabolisable organic carbon to be obtained independently of any other species in the system (Van Cappellen *et al.,* 1993). However, these early one-G models were limited by the fact that there was no explicit account of the flux of organic carbon to the sediment surface and as a result, there was no way of linking the magnitude of the POC rain rate to the fraction that was buried or mineralised. Attempts to model such a link were first tried by Jahnke *et al.* (1982), Bender and Heggie

[1] "I used G for organic matter because throughout my diagenetic modeling (eg see my book [Berner, 1980]) I use C for the conentration of dissolved substances in interstitial waters and I didn't want any confusion when I mixed organic matter decomposition with other processes for which the symbol C was used. Also capital G resembles C except for the additional crossbar. It is as simple as that." (pers. comm. R.A. Berner)

(1984) and Emerson *et al.* (1985) but they suffered from a problem that previous models also shared. In the case where more than one oxidant (electron acceptor) was considered (e.g. Goloway and Bender, 1982; Jahnke *et al.,* 1982) a layered model was setup to describe the succession of electron acceptors used by bacteria. The thickness of each layer had to be imposed from measured porewater profiles while at the boundary of adjacent layers, boundary conditions had to be implemented to satisfy mass balance criteria. In particular, zero level (concentration) conditions for electron acceptors had to be introduced to avoid modelling negative concentrations (e.g. Jahnke *et al.,* 1982; also see Rabouille and Gaillard, 1991a). That is, since the rate of change is limited only by the availability of the organic matter (and not the oxidant concentration), it is inevitable that oxidant concentrations become negative unless a zero level condition is set within the model domain.

Boudreau and Westrich (1984) first pointed out that biogeochemical couplings of greater complexity than just described were not generally taken into account because it leads to numerical problems. This resulted in the next generation of models (Rabouille and Gaillard, 1991a,b; Tromp *et al.,* 1995; Van Cappellen and Wang, 1995; Boudreau, 1996; Dhakar and Burdige, 1996; Furrer and Wehrli, 1996; Soetaert *et al.,* 1996; Wang and Van Cappellen, 1996) which made use of the Monod (1949) rate law in the kinetic description of organic matter degradation. This law allows the latter to be correctly coupled to the reduction of an electron acceptor (Rabouille and Gaillard, 1991a; Soetaert *et al.,* 1996). That is,

$$\frac{\mathrm{dPOC}}{\mathrm{dt}} = -k\ \mathrm{POC}\ \frac{\mathrm{Ox}}{\mathrm{Ox} + \mathrm{k_m}} \qquad 1.6$$

and

$$\frac{dOx}{dt} = -k\ \gamma_{Ox}^{POC}\ \phi POC\ \frac{Ox}{Ox + k_m} \qquad 1.7$$

This coupling of the two processes means that the rates of change are limited by the concentrations of both the organic carbon (POC) and the oxidant (Ox) simultaneously. Thus, from equations 1.6 and 1.7 it can be seen that as the concentration of the oxidant approaches zero, so does the rate of change. This is in contrast to the formulations used in earlier diagenetic models (equations 1.4 and 1.5).

Another important development in the description of organic decay in diagenetic models concerns the decreasing lability of POC with depth or time after deposition (see section 1.4). This has led to two major approaches in kinetic formulation: 1) the continuum approach which accounts for variability of the rate constant $k$ with depth/time after deposition (Middelburg, 1989; Boudreau and Ruddick, 1991) and 2) the multi-G approach in which a finite number of metabolisable fractions of organic carbon with fixed mineralisation rates is considered (Westrich and Berner, 1984; Soetaert *et al.*, 1996). Soetaert *et al.* (1996) argued that although the continuum approach was conceptually superior, that multi-G formulations were less problematic, in terms of numerical solution, and more easily incorporated into models. The multi-G model is characterised by

$$\frac{dG_i}{dt} = -\sum k_i\ G_i \qquad 1.8$$

where $G_i$ = metabolisable organic carbon concentration of the $i^{th}$ fraction

$k_i$ = rate constant of the $i^{th}$ fraction

The total decomposable organic carbon concentration is then given by $G=\sum G_i$. This yields a system in which the variability of the overall rate constant ($k$) in equations 1.4 to 1.7 is

interpreted in terms of the changes in the relative distribution of the different fractions of POC. An added advantage of this approach is that different stoichiometry (i.e. separate but fixed C:N ratios) can be imposed on each fraction of organic carbon ($G_i$) to simulate observed changes in C:N with depth (Soetaert *et al.,* 1996).

## 1.12 Modelling strategy

### 1.12.1 Overall aim and objectives

The overall aim of this work is to develop a model of early diagenesis for a temperate estuary exposed to globally high nitrate concentrations such as those found in UK estuaries (Nedwell and Trimmer, 1996; Ogilvie *et al.,* 1997a; Trimmer *et al.,* 1998). Emphasis is placed on the nitrogen cycle, particularly nitrate reduction and its role in attenuating the flux of nitrogen from land to sea. Models prior to the present work have either been developed for the deep sea (Rabouille and Gaillard, 1991b; Dhakar and Burdige, 1996), for global application including shelf sediments (Boudreau, 1996; Soetaert *et al.,* 1996) or for shallow sediments with low overlying nitrate concentrations (Blackburn *et al.*, 1994).

The individual objectives are to:

- find the most appropriate representation of the first order rate constant for organic decay
- carry out a parameter sensitivity analysis to gain a better understanding of the coupling between the different model processes

- quantify the possible errors in measuring solute fluxes across the SWI when the likely presence of a diffusive boundary layer is neglected
- examine the causes in the intra-annual changes in measured solute fluxes across the SWI and thereby test the model assumptions
- implement DNRA as an alternative pathway to denitrification in nitrate reduction

Each of the above objectives sets the structure of the thesis

### 1.12.2 Structure of the thesis and justification of the objectives

In Chapter 2, a description of the data relied upon in this thesis is given. The data come from a temperate, high nutrient estuary on the North Sea coast of England (the Gt. Ouse). Most of the data have been published (Nedwell and Trimmer, 1996; Trimmer *et al.*, 1998).

In the first science Chapter (Chapter 3), the development and calibration of the diagenetic model is described. This is achieved by calibration against annually integrated data (mineralization rates and fluxes across the SWI) derived from pooled seasonal data (Nedwell and Trimmer, 1996). The model is then fitted to this data enabling first order rate constants for each of the three main organic carbon oxidation pathways (oxygen, nitrate and sulphate reduction) to be derived. The intention is to examine a number of different ways to parameterise organic decay with respect to a best-fit to the observed data (Nedwell and Trimmer, 1996). A comparison is made between the stoichiometric models drawn up by Nedwell and Trimmer (1996) to quantify mineralisation pathways in the Gt. Ouse sediments and the results from this model which uses kinetic equations. In the same Chapter, an extensive parameter sensitivity analysis is also carried out as part of the model development.

In Chapter 4, the calibrated model is used to assess the importance of changes in the thickness of the diffusive boundary layer (DBL) on early diagenetic processes. The DBL is the stagnant microlayer directly above the SWI through which molecular diffusion is the assumed dominant mode of transport for dissolved substances. Various authors (Morse, 1974; Boudreau and Guinnasso, 1982; Santschi *et al.,* 1991; Martin and Sayles, 1994) have suggested that neglect of the DBL can lead to erroneous flux estimates and consequently to errors in estimates of both benthic community respiration and sedimentary nutrient budgets. The presence of the DBL is inhibited in high current regions such as shallow water environments and recent modelling investigations (Jørgensen and Boudreau, 2001) suggest that in shallow sediments, changes in the thickness of the DBL have a negligible effect on oxygen consumption rates and organic carbon preservation. This might indicate that investigations into the effect of the DBL are unwarranted for a diagenetic model of estuarine sediments. However, two important points need to be made. Firstly, near-bed current measurements in macrotidal estuaries suggest that the DBL can exist for significant periods of time (section 4.2). Secondly, Jørgensen and Boudreau (2001) assumed that organic carbon mineralization is mediated only by sulphate reduction in shallow sediments. As will be seen, the contribution of the different pathways of sedimentary organic carbon mineralization (oxygen respiration, denitrification and sulphate reduction) is highly variable in the Gt. Ouse sediments. The model investigates how these sediments respond to changes in the thickness of the DBL focusing not only on oxygen consumption as in Jørgensen and Boudreau (2001), but also on nitrate-, ammonium- and sulphate-based processes.

Controls on seasonality in early diagenetic processes and fluxes in the Gt. Ouse is addressed in Chapter 5. The model developed in Chapter 3, is adapted to allow simulations of seasonality to be made. This is facilitated by incorporating changes in observed sediment temperatures and solute concentrations in the overlying water into the model. The overall aim is to test whether the model can reproduce and explain the observed seasonality in the Gt. Ouse sediments which also tests the robustness of the first order rate constants derived in Chapter 3.

In the final science Chapter (Chapter 6), the model in Chapter 5 is adapted to investigate the role of temperature in proportioning nitrate reduction into denitrification and DNRA. Less than half (46 %) of the nitrate flux into the sediments of the lower Gt. Ouse was denitrified, the rest ending up as ammonium (Trimmer *et al.,* 1998). This result was added to a literature review showing that DNRA can account for a high proportion of the total nitrate reduction that takes place in sediments (Table 1.2). DNRA may also account for up to one third of the sedimentary carbon oxidation in coastal environments (Sorensen, 1978). Previous diagenetic models (Blackburn, 1990; Middelburg *et al.,* 1996a) treat nitrate reduction as denitrification, in which standard stoichiometry (Table 1.1), converts all of the nitrate into $N_2$ gas. Note that the model used by Middelburg *et al.* (1996a) is based on the model of Soetaert *et al.* (1996) in which nitrate reduction is coupled to the anaerobic oxidation of ammonium (the Anammox process-see section 1.8). A number of factors have been shown to influence the proportioning of nitrate reduction into denitrification and DNRA (section 1.9.1). In this Chapter, the role of temperature is investigated.

The final Chapter (Chapter 7) presents a summary and the overall conclusions of this work.

## 2. Description of the data: the Gt. Ouse estuary

The data used to develop, calibrate and validate the model comes from the Joint Nutrient Study (JONUS - Anon, 2001). The JONUS programme investigated the fate and behaviour of nutrients as they are carried through rivers and estuaries into coastal seas. The period of the programme was between April 1991 and April 1995.

The data from the Gt. Ouse estuary were used. This estuary system is on the east coast of England and discharges into the North Sea (Figure 2.1). Most of the data have been published (Nedwell and Trimmer, 1996; Trimmer *et al.,* 1998). Consequently, only relevant information is summarised in this section.

The Gt. Ouse data was collected in two regions: the upper section (sites 1 to 4, Nedwell and Trimmer, 1996) which is narrow (<70m), shallow (1 to 7m at low tide) and predominantly canalized and the lower section (sites 4 to 9, Trimmer *et al.,* 1998) which broadens to a wide expanse (~ 15km at site 9) that covers an extensive area of intertidal sediments at the edge of The Wash embayment (Figure 2.1). The Gt. Ouse is characterised by globally high concentrations of nitrate ( upper section: annual mean of 700μM, range 265μM - 1240μM; lower section: 21μM - 830μM) compared with other rivers draining into the North Atlantic (Howarth *et al.,* 1996) and has an annual load of 0.6 to 1 Gmole $NO_3^-$ (Nedwell and Trimmer, 1996). Nedwell and Trimmer (1996) calculated that in the fast flowing narrow stretch of the Gt. Ouse, ~1% of the nitrogen load was lost by denitrification. This potentially increases to more than 50% as the sediment surface area to water column ratio increases over the more extensive mudflats of the lower estuary (Trimmer *et al.,* 1998). The freshwater flow averaged 32 $m^3s^{-1}$ and 50 $m^3s^{-1}$ in 1992 and 1993, respectively (Nedwell and Trimmer, 1996) and the Gt. Ouse contributed 10%

Figure 2.1. Map showing study area and site locations in the Great Ouse estuary

Upper estuary (sites 1-4)

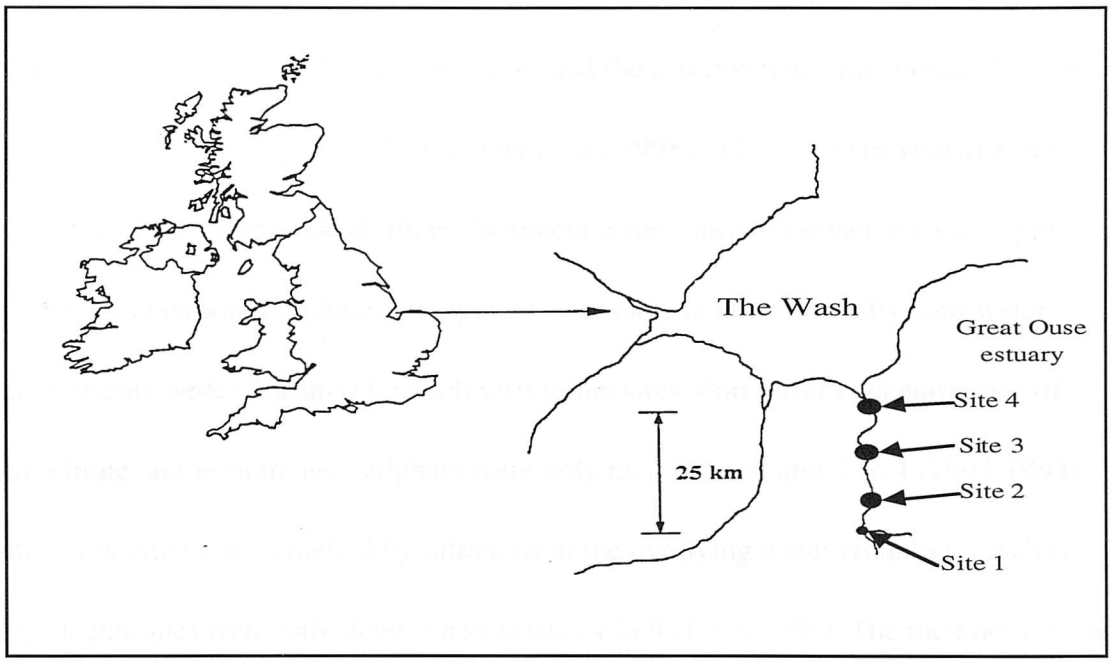


Lower estuary (sites 4-9)

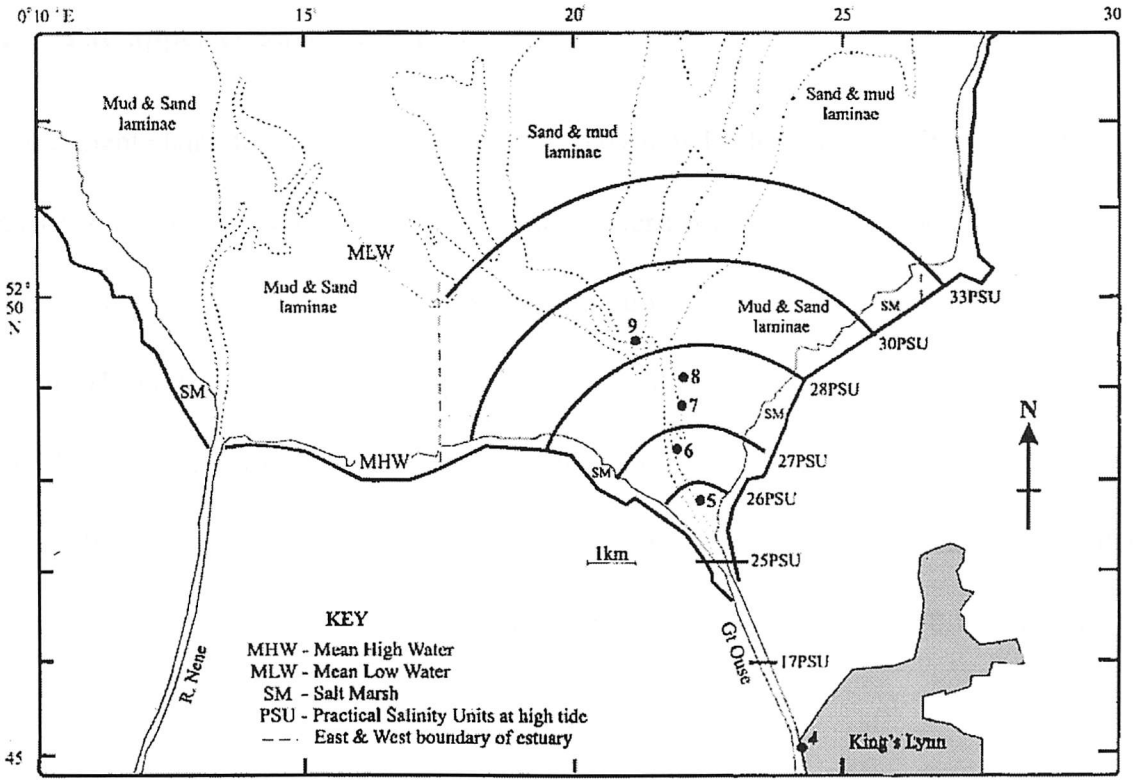

(1992) and 16% (1993) of the total UK riverine load of total oxidized nitrogen to the North Sea (Nedwell and Trimmer, 1996).

The upper estuary was sampled on 7 occasions between December 1992 and November 1993 (Nedwell and Trimmer, 1996) and the lower estuary was visited 11 times between April 1994 and April 1995 (Trimmer *et al.*, 1998). All sites were visited at low tide and remained submerged at all times. Sediment water nutrient exchange and oxygen uptake (core incubations), sediment temperature, organic content, porosity, and water column nutrients were measured for each visit to the sites. Porewater concentrations of oxygen, nitrate, ammonium and sulphate were only measured at sites 1 to 4 (1992-1993) and rates of denitrification fuelled by nitrate from the overlying water column (acetylene blockage technique) were only determined at sites 4 to 9 (1994-1995). The methodology is described in Nedwell and Trimmer (1996) and in Trimmer *et al.* (1998).

## 2.1. The upper estuary (sites 1-4)

The sediment characteristics of sites 1 to 4 are shown in Table 2.1a. The sites cover a distance of 25km between landward site 1 and seaward site 4 (Figure 2.1) and are predominantly very fine sandy sediments (63-125 μm diameter) with a mean porosity of 0.505 ml $H_2O$ $ml^{-1}$ sediment (Table 2.1a). The molar C:N ratios (range over four sites : 26.4-52.1) and the mean organic carbon content (range 262.87 - 181.27 molC $m^{-2}$ in top 0-15cm) differ between sites. Sites 1 and 2 are essentially freshwater sites (annual high water salinity range of site 1 = 0.25-0.62) and sites 3 and 4 are brackish (range = 0.51-18.86 for site 4).

Benthic oxygen demand and nutrient exchange were measured using core incubations lasting up to 24 hours. Sulphate reduction rates were collected from replicate vertical sediment cores (20cm long x 2.4cm inner diameter) and analysed at 1cm intervals over incubation periods lasting 16 to 24 hours. Oxygen porewater concentrations were measured with a Clarke-type microelectrode in a hyperdermic needle at 0.5mm intervals in the sediment. The remaining porewater variables (nitrate, ammonium and sulphate) were measured by slicing the sediment cores used in the oxygen and nutrient flux measurements at 1cm intervals for the 0 to 5cm horizon and at 9cm, 10cm, 14cm and 15cm depths. TOC and TON contents were determined with a CHN analyser at similar depth intervals. Temperature was measured with a mercury thermometer inserted in the sediment and porosity determined from wet and dry weights of known volumes of sediment.

Benthic oxygen demand was higher at sites 1 and 2 (7 visit mean of 27±25 (SD) and 30±26 mol $O_2$ $m^{-2}$ $y^{-1}$, respectively) than at sites 3 and 4 (7 visit mean of 14± 9 and 11±6 mol $O_2$ $m^{-2}$ $y^{-1}$, respectively). Oxygen fluxes correlated well with temperature at sites 1 ($p<0.05$, $r=0.78$) and 2 ($p<0.05$,0.88), but not at sites 3 and 4. However, pooling all of the oxygen flux data yields a significant ($p<0.05$) positive correlation with temperature suggesting a coupling to organic degradation rates. Sites 1, 3 and 4 were consistent sinks for nitrate (7 visit mean of 3.94 mol $NO_3^-$ $m^{-2}$ $y^{-1}$) and sources of ammonium (7 visit mean of 0.37 mol $NH_4^+$ $m^{-2}$ $y^{-1}$). No statistically significant nitrate fluxes were measured at site 2 even though porewater profiles of nitrate suggested that it should be a sink for nitrate. Annual mean ammonium effluxes of 18 μmol $m^{-2}$ $h^{-1}$ were measured at site 2. Pooling all ammonium fluxes together yields a significant ($p<0.05$) positive correlation with temperature again suggesting a link to organic degradation.

Table 2.1a. Sediment characteristics for the 4 sites in the upper Gt. Ouse investigated between December 1992 and November 1993. (Adapted from Nedwell and Trimmer, 1996).

| Site | % of top 5cm of sediment | | | Mean porosity[d] | Mean organic carbon (% dry wt)[e] | Mean C:N ratio (molar) |
|---|---|---|---|---|---|---|
| | FS[a] | VFS[b] | S[c] | | | |
| 1 | 7 | 76 | 17 | 0.55±0.02 | 1.81±0.12 | 26.82±1.1 |
| 2 | 47 | 48 | 5 | 0.46±0.01 | 2.12±0.17 | 55.50±3.6 |
| 3 | 26 | 71 | 3 | 0.50±0.02 | 1.21±0.12 | 36.41±2.1 |
| 4 | 32 | 58 | 10 | 0.51±0.01 | 1.12±0.12 | 30.56±1.1 |

[a]FS:Fine sand 250-125μm. [b]VFS: very fine sand 125-63μm. [c]S:silt/clay <63μm.
[d]Porosity: ml $H_2O$ $ml^{-1}$ sediment, ± SE, n=21. [e]Mean of 4 replicates at 7 depths 1-15cm, ±SE, n=21

Table 2.1b. Sediment characteristics of the 6 sites in the lower Gt. Ouse investigated between April 1991 and April 1995 (taken from Trimmer *et al.*, 1998).

| Site | Particle size[a] (>50% w/w) | Porosity (ml $H_2O$ $ml^{-1}$ sed.) | Organic carbon (%dry wt) | C:N ratio (mol:mol) |
|---|---|---|---|---|
| 4 | VFS | 0.38±0.01 | 0.10±0.01 | 5 |
| 5 | S/C | 0.57±0.03 | 0.78±0.23 | 13 |
| 6 | VFS | 0.38±0.01 | 0.21±0.03 | 17 |
| 7 | S/C | 0.61±0.02 | 2.23±0.35 | 19 |
| 8 | S/C | 0.45±0.03 | 0.44±0.17 | 18 |
| 9 | FS | 0.56±0.02 | 0.36±0.08 | 8 |

No seasonal trend was found for nitrate fluxes. Overall, nitrate fluxes were an order of magnitude greater than ammonium fluxes suggesting that the Gt. Ouse sediments are a sink of dissolved inorganic nitrogen (DIN). Note that nitrite and urea fluxes were shown to be insignificant components of the total flux of DIN (Nedwell and Trimmer, 1996).

Annual rates of sulphate reduction varied between 0.16 mol $SO^{=}_4$ $m^{-2}$ $y^{-1}$ at site 2 and 5.31 mol $SO^{=}_4$ $m^{-2}$ $y^{-1}$ at site 1. The rates were significantly correlated ($p<0.05$, $r=0.57$ and $r=0.68$, respectively) to sediment temperature at sites 2 and 4 but not at sites 1 and 3. The annual budget of the sedimentary organic carbon shows that the relative proportions of each mineralization pathway was different among the sites (Table 2.2). Most of the organic carbon was degraded via sulphate at site 1 (67%) whereas the majority of the degradation occurred via oxygen at the remaining sites (≥50%).

The intra-annual variability of selected determinands in the water column and sediment at the 4 sites are shown in Figure 2.2. These determinands are used as forcing functions in the model (Chapter 5). Sediment temperature varied between 2°C and 18°C (Figure 2.2a). Oxygen concentrations ranged between 390 μM and 280 μM in the sampling period (Figure 2.2b). Nitrate concentrations in the water column varied between 1240 μM in winter (January 1992) and 265 μM in summer (August 1993) across the four sites (Figure 2.2c). Water column

Table 2.2. Annual budget of sedimentary organic carbon in the upper Gt. Ouse (adapted from Nedwell and Trimmer, 1996)

| Site | Annual electron acceptor reduction rates (mol $m^{-2}$ $y^{-1}$) | | | Stoichiometric carbon mineralization via each electron acceptor (mol $m^{-2}$ $y^{-1}$) | | | % of organic carbon degradation via each electron acceptor (mol $m^{-2}$ $y^{-1}$) | | |
|---|---|---|---|---|---|---|---|---|---|
| | $O_2$ | $NO_3^-$ | $SO_4^{=}$ | $O_2$ | $NO_3^-$ | $SO_4^{=}$ | $O_2$ | $NO_3^-$ | $SO_4^{=}$ |
| 1 | 12.84 | 2.54 | 5.31 | 2.16 | 3.09 | 10.62 | 14 | 19 | 67 |
| 2 | 15.69 | 0.00 | 0.16 | 15.28 | 0.00 | 0.32 | 98 | 0 | 2 |
| 3 | 28.01 | 1.98 | 6.05 | 15.57 | 2.42 | 12.10 | 52 | 8 | 40 |
| 4 | 23.43 | 6.83 | 3.69 | 15.96 | 8.33 | 7.38 | 50 | 26 | 24 |

concentrations of ammonium varied between 21± 8 μM in December 1992 and 2±0.5μM in March 1993 (not shown). In the water column, both nitrate and ammonium concentrations showed changes associated with the freshwater flows (Nedwell and Trimmer, 1996). Concentrations of sulphate, which has a seawater source, showed no clear seasonal pattern and little variation from site 1 to 4 ranging from 1.7 mM to 2.8 mM (annual means), respectively (Figure 2.2d). Seasonal porewater concentrations of ammonium at 15cm depth in the sediment (Figure 2.2e) similarly showed no clear seasonal pattern with highest values at site 4 (4.5 mM) and lowest at site 2 (<0.5 mM).

## 2.2. The lower estuary (sites 4-9)

The lower sites (4-9) cover a distance of ~ 9km with mean salinities range of 17 at site 4 and 29 at site 9. The sediments were mostly very fine sands and sandy clays (<63μm) with porosity in the range 0.38-0.61 ml $H_2O$ $ml^{-1}$ sediment (Table 2.1b). Total organic carbon content (0.1% to 2.23% dry weight) was less than in the sediments of the upper estuary (Table 2.1a) while C:N ratios were lower (5-19) than further upstream. The most organic site was site 7 (2.23% dry weight) which had the highest C:N ratio (19). The lowest organic content and lowest C:N ratio was at site 4 (Table 2.1b). While the C:N ratio encompasses the total measurable organic C and N content (which does not distinguish between refractory and non-refractory material), it does not necessarily follow that lower C:N ratios are indicative of higher reactive organic matter. This is corroborated by the similarity in the annually-integrated rates of oxygen uptake by the sediment at these two sites (4 and 7). Rates of 21 and 28 mol $O_2$ $m^{-2}$ $y^{-1}$ at sites 4 and 7 respectively,

Figure 2.2. Intra-annual changes in determinands at 4 sites in the upper Gt. Ouse

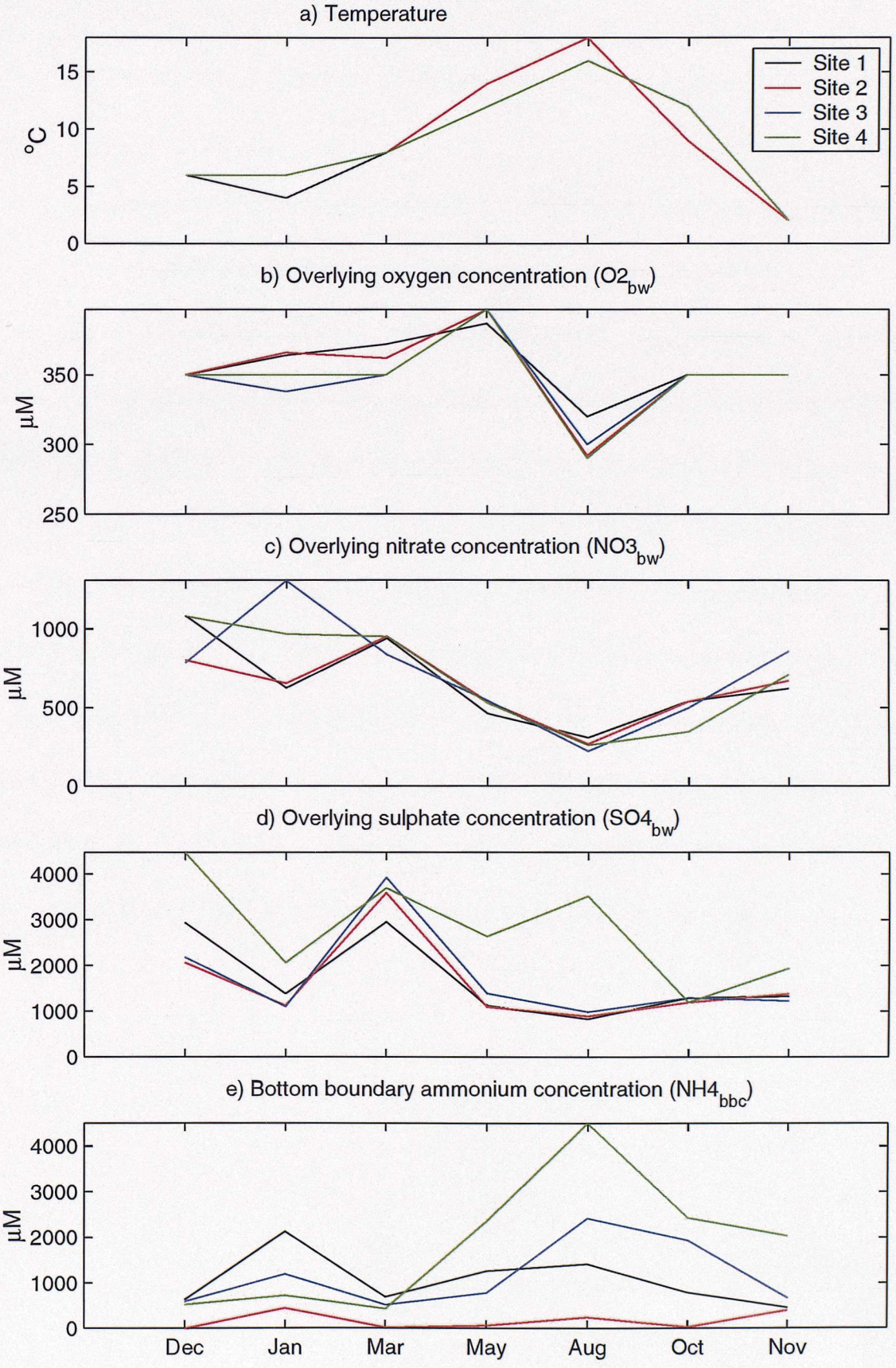

show that while there is a factor of 22 difference in organic content between the sites, rates of organic mineralisation are similar. Benthic oxygen demand was significantly correlated ($p < 0.05$) to temperature at both sites. Oxygen consumption rates were not measured at the other sites.

Sediment temperature ranged from 5°C to 22°C over the year. These sediments were consistent sinks for nitrate (11 visit mean across all sites: 2.72 mol $m^{-2} y^{-1}$) and consistent sources of ammonium (11 visit mean across all sites: 2.37 mol $m^{-2} y^{-1}$). Note that the nitrate flux was lower and the ammonium flux higher than in the sediments of the upper estuary (section 1.13.1). Maximum fluxes of ammonium occurred in November (temperature = 9°C) at each site. Rates of denitrification (that fuelled by nitrate from the overlying water, $D_w$) varied between 4 and 228 μmol N $m^{-2} h^{-1}$ across the sites and accounted for less than half (46%) of the annual flux of nitrate to the sediment. Maximum rates of denitrification occurred in May (14°C) at all sites. Nitrate reduction (DNRA and denitrification) accounted for between 5% and 25% of the total annual organic carbon mineralisation. The remainder of the carbon oxidation was assumed to be mediated by oxygen and sulphate. Note that sulphate reduction rates were not measured.

# 3. Development and calibration of an early diagenesis model for high nitrate, low reactive sediments in a temperate latitude estuary (Great Ouse, UK)

## 3.1. The Model

### 3.1.1. Model description

The model describes the top 15cm of sediment with a series of adjoining vertical boxes each of depth 0.1cm (Figure 3.1). Five variables are modelled : $O_2$, $NO_3^-$, $NH_4^+$, $SO_4^=$ and $S^=$. The biogeochemical cycling of these solutes occurs in three notional zones in the sediment (Figure 3.2) in which bacterial degradation of carbon depends upon different oxidising agents. The mineralisation pathways are oxygen, nitrate and sulphate respiration, all of which produce ammonium. Lack of redox processes involving iron, manganese and fermentation is a model limitation caused by the absence of appropriate data for the Gt. Ouse. This must be considered when assessing the performance of the model.

Sulphide oxidation and nitrification are first order reactions proportional to the sulphide and ammonium concentrations respectively and both processes are limited by the availability of oxygen. Denitrification is limited by nitrate and inhibited by oxygen. This formulation is such that both nitrification and denitrification can occur in the same gridbox. Sulphate reduction is inhibited by both oxygen and nitrate and limited by sulphate availability. The absence of iron and manganese data precludes the modelling of sulphide precipitation/burial processes in these sediments. Any sulphide formed is assumed to be fully available for oxidation. This is reasonable as measurements of total sulphide concentrations over the year at the four sites suggests that sulphide produced from sulphate reduction did not accumulate (Nedwell and Trimmer, 1996). Finally, since

Figure 3.1. 1-dimensional numerical grid scheme of the model

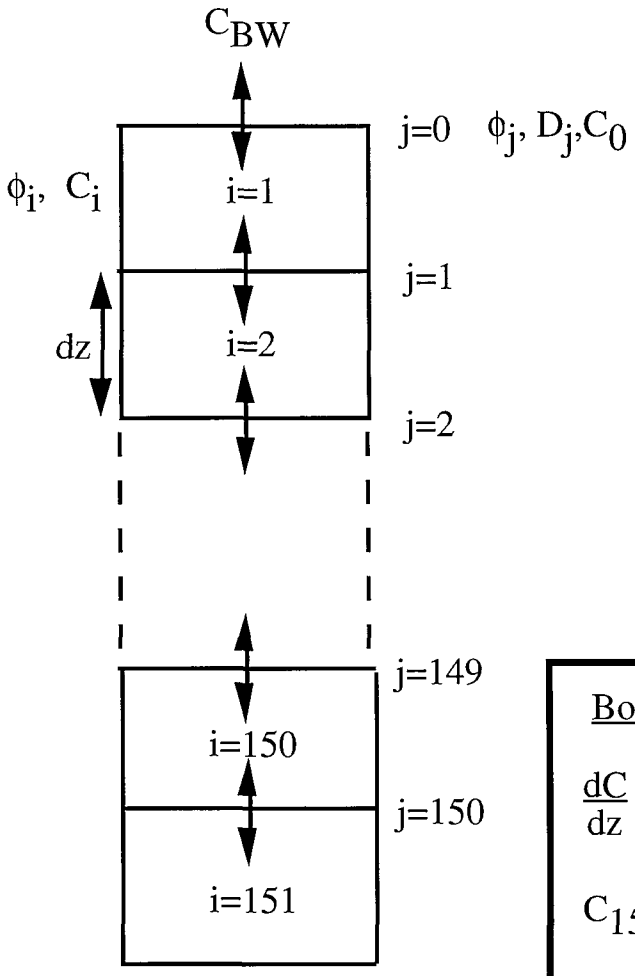


Boundary Conditions

$\frac{dC}{dz} = 0$ for $O_2$, $NO_3^-$, $S^=$, and $SO_4^=$

$C_{151} = C_{obs}$ for $NH_4^+$

$C_{BW}$ = top boundary solute value
$C_{obs}$ = bottom boundary solute value
dz = grid box length (0.1cm)

the model is concerned with a steady state description of diagenesis using annually integrated data for calibration, a temperature function is not included in the kinetics of organic decay.

Figure 3.2. Biogeochemical reactions of the diagenetic model(TOC = total organic carbon)

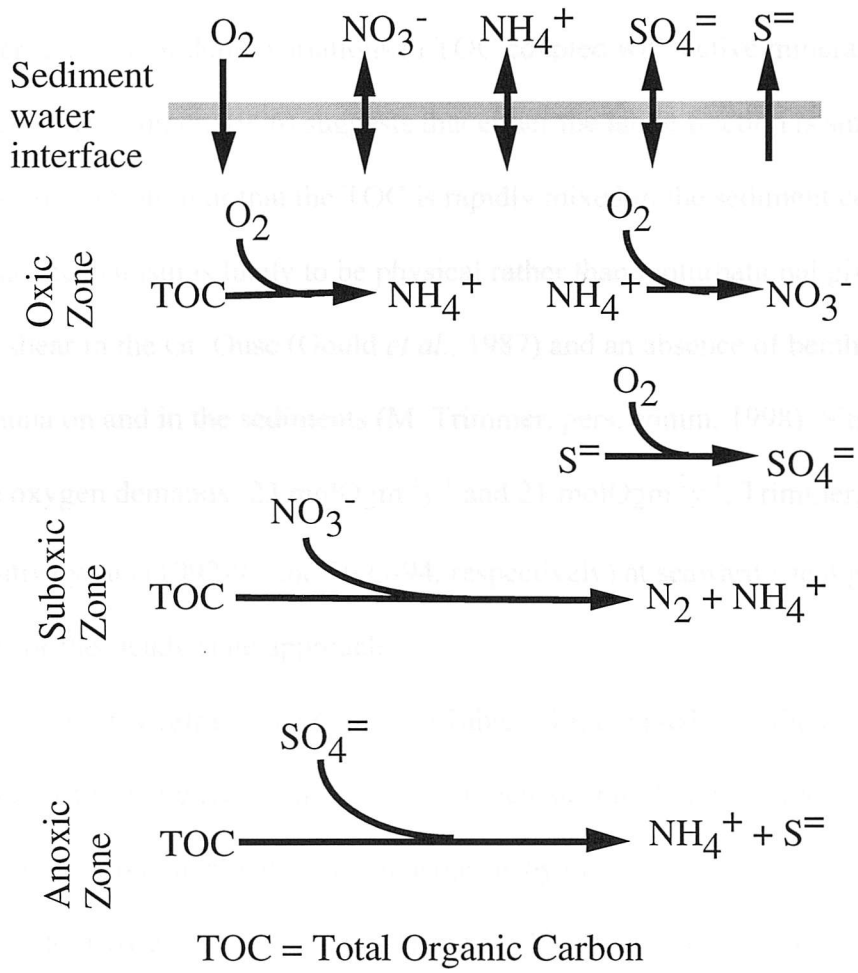


### 3.1.2. Model assumptions

Nedwell and Trimmer (1996) found no change with time or depth in total organic carbon (TOC) profiles in any of the sediments studied. Consequently, this model, calculates porewater profiles and concomitant fluxes across the sediment-water interface (SWI) from data-imposed TOC concentrations (Table 2.1a) which are assumed to be at steady state. The model is calibrated using the annually integrated data reported in Nedwell and

Trimmer (1996). This removes the observed temporal variability of the solute concentrations which will be examined elsewhere (see Chapter 5). By not modelling TOC, there is no need to account for hydrodynamic or bioturbational solid-phase mixing. However, the lack of depth variations in TOC coupled with active mineralisation (Nedwell and Trimmer, 1996) suggests that either the labile fraction is small compared to the bulk concentration or that the TOC is rapidly mixed in the sediment column. If the latter, the mechanism is likely to be physical rather than bioturbational given the high current shear in the Gt. Ouse (Gould *et al.,* 1987) and an absence of benthic macro- and meio-fauna on and in the sediments (M. Trimmer, pers. comm, 1998). Similar annual benthic oxygen demands (23 $molO_2m^{-2}y^{-1}$ and 21 $molO_2m^{-2}y^{-1}$, Trimmer, 1997) for two consecutive years (1992-93 and 1993-94, respectively) at seaward site 4 give additional support for the steady state approach.

The highly refractory sediments (Table 2.1a) coupled with the fact that the Gt. Ouse is a fast flowing river implies that sediment accumulation (advection) rates are low. Therefore, it is assumed that solute transport is by molecular diffusion and that advection is negligible. However, Nedwell and Trimmer (1996) reported physically-induced subsurface irrigation at one of the sites (2) in the Gt. Ouse which may impact on the interpretation of the model results.

Microphytobenthos is not included as core incubations were kept in the dark (Nedwell and Trimmer, 1996), thereby minimising potential benthic algal activity. Additionally, light-dark incubations of intertidal sediments seawards of site 4 have revealed no significant differences in nutrient fluxes across the SWI (D. Thornton, pers. comm., 1998).

Porosity showed little temporal or spatial variation (Table 2.1a). Consequently, a uniform porosity profile is used in the model with the assumption that the porosity at the SWI is close to 1 (0.99).

As the fraction of TOC that is labile is unknown, and since both the molar C:N ratio and the TOC concentrations are constant with depth at each site (Table 2.1a), the one-G model approach has been adopted (Berner, 1980; Tromp *et al.,* 1995; Wang and Van Cappellen, 1996). This assumes a simple first order dependence of organic degradation on the concentration of TOC and has been shown to represent observations well in deep sea sediments (Rabouille and Gaillard, 1991a).

Finally, the core incubation experiments used for the Gt. Ouse sediments (Nedwell and Trimmer, 1996), only account for solute and gas exchange during immersion and ignore deposition-resuspension effects. The model, which is calibrated and validated against this data, is therefore, only valid for periods of sediment submergence and ignores processes such as tidal pumping.

### 3.1.3. Model formulation

The basic model equation for porewater solutes is derived from the general diagenetic reaction-diffusion equation (Berner, 1980).

$$\text{Rate of change of C} = -\frac{1}{\phi}\frac{\partial}{\partial z}\left[D_C \phi \frac{\partial C}{\partial z}\right] + \frac{1}{\phi}\Sigma R \qquad 3.1$$

where C is the solute concentration (nmol $cm^{-3}$ of bulk sediment), $\phi$ is the porosity (dimensionless), $D_C$ is the sediment diffusion coefficient for C ($cm^2\ y^{-1}$) adjusted for

tortuosity and temperature, z is the depth (cm) and R is the set of reaction terms that includes organic decay (see below and Table 3.1). There is no time dependency (i.e. steady state is assumed) and so the left hand side of 3.1 is set to zero.

The kinetics of organic matter degradation are based on a modification of the Monod Law in which the rate is first order with respect to the organic carbon content (G) and limited by the concentration of the electron acceptor ($Ox_1$). Except in oxygen respiration, inhibition of organic decay by other oxidants, $Ox_2$ (e.g. $O_2$ in denitrification), is included i.e.

$$\text{Rate of organic decay} = -k \times G \times \text{LimOx}_1 \times \text{InhibOx}_2$$
$$\text{where } \text{LimOx}_1 = \frac{Ox_1}{Ox_1 + k_s} \text{ and } \text{InhibOx}_2 = 1 - \frac{Ox_2}{Ox_2 + k_{inh}} \qquad 3.2$$

$k$ is the first order rate constant for organic decay, $k_S$ is the Monod constant, $\text{LimOx}_1$ is the limitation function due to oxidant concentration $Ox_1$, $\text{InhibOx}_2$ is the inhibition function due to oxidant concentration $Ox_2$ and $k_{inh}$ is the inhibition constant. The use of $\text{InhibOx}_2$ and $\text{LimOx}_1$ allows a single equation for each variable to be applied continuously over the entire model depth range and provides direct coupling between the various constituents (Rabouille and Gaillard, 1991a; Soetaert *et al.*, 1996). Both inhibition and limitation functions are used to model the sequence of organic matter degradation correctly (Soetaert *et al.*, 1996).

The sediment diffusion coefficient ($D_C$) in equation 3.1 is calculated from porosity, sediment resistivity (F) and temperature following Ullman and Aller (1982) and Soetaert *et al.* (1996). Thus,

$D_C = \frac{\phi}{F}(D_C^0 + D_C^{const}.T)$ where $F = \frac{1}{\phi^m}$

$D_c^0$ is the 0°C free solution diffusion coefficient, $D_c^{const}$ is an ion specific constant (Li and Gregory, 1974), T is the mean temperature and m is an exponent. Here, m=1.3, the lower range value reported for sandy sediments (Iverson and Jørgensen, 1993) which yields

$$D_C = \phi^{0.3}(D_C^0 + D_C^{const}.T) \quad 3.3$$

The loss of oxidants through organic matter degradation is modelled using stoichiometric ratios determined from equations 3.4, 3.5 and 3.6.

$$(CH_2O)_{106}(NH_3)_{16} + 106O_2 = 106CO_2 + 16NH_3 + 106H_2O \quad 3.4$$

$$(CH_2O)_{106}(NH_3)_{16} + 82.8HNO_3 = 106CO_2 + 16NH_3 + 42.4N_2 + 148.4H_2O \quad 3.5$$

$$(CH_2O)_{106}(NH_3)_{16} + 53SO_4^{=} = 106CO_2 + 53S^{=} + 16NH_3 + 106H_2O \quad 3.6$$

The full set of model equations is shown in Table 3.1 and associated parameters are defined in Table 3.2. Note that the effects of adsorption and ion exchange are not included in the ammonium equation (3.11, Table 3.1) on account of the fact that under steady state, the reaction-diffusion equation for diagenesis cancels this term out (see Berner, 1976, p338).

Table 3.1. Model equations for each variable (D is the diffusion term in equation 3.1. The remaining terms represent the sum of R reactions in equation 3.1; TOC= total organic carbon; $k$= first order rate constant for organic decay; $\phi$ = porosity. All other parameters are defined in Table 3.2).

| Variable | Equation | No. |
|---|---|---|
| $O_2$ | $D-\gamma_{O2}^{TOC}\text{OxicMin}-\gamma_{O2}^{NH4}K_{nit}\cdot\frac{O_2}{O_2+k_{sLimO2}}NH_4-\gamma_{O2}^{S}K_{sox}\frac{O_2}{O_2+k_{sSox}}S^{=}$ where $\text{OxicMin}=k\left(\frac{1-\phi}{\phi}\right)\text{TOC}\frac{O_2}{O_2+k_{sO2}}$ | 3.7 |
| $NO_3$ | $D-\gamma_{NO3}^{TOC}\text{SuboxMin}+K_{nit}\cdot\frac{O_2}{O_2+k_{sLimO2}}NH_4$ where $\text{SuboxMin}=k\left(\frac{1-\phi}{\phi}\right)\text{TOC}\frac{NO_3}{NO_3+k_{sNO3}}\left[1-\frac{O_2}{O_2+k_{sInhO2}}\right]$ | 3.8 |
| $SO_4^{=}$ | $D-\gamma_{SO4}^{TOC}\text{AnoxMin}+K_{sox}\frac{O_2}{O_2+k_{sSox}}S^{=}$ where $\text{AnoxMin}=k\left(\frac{1-\phi}{\phi}\right)\text{TOC}\frac{SO_4}{SO_4+k_{sSO4}}\left[1-\frac{O_2}{O_2+k_{sAnoxInhO2}}\right]\left[1-\frac{NO_3}{NO_3+k_{sAnoxInhNO3}}\right]$ | 3.9 |
| $S^{=}$ | $D+\gamma_{SO4}^{TOC}\text{AnoxMin}-K_{sox}\frac{O_2}{O_2+k_{sSox}}S^{=}$ | 3.10 |
| $NH_4^{+}$ | $D+\gamma_{NH4}^{O2}\text{OxicMin}+\gamma_{NH4}^{NO3}\text{SuboxMin}+\gamma_{NH4}^{SO4}\text{AnoxMin}-K_{nit}\frac{O_2}{O_2+k_{sLimO2}}NH4$ | 3.11 |

### 3.1.4. Initialisation and boundary conditions

The observed invariant distribution of organic carbon (Table 2.1a) is imposed at all sites in the model. Initial conditions at each site are derived from the seven month mean of measurements of porewater profiles for oxygen, nitrate, ammonium and sulphate. The free porewater sulphide is arbitrarily set to 10μM in each model box. Boundary conditions are

Table 3.2 : Parameter values and their sources

| Parameter | Source | Description | Value |
|---|---|---|---|
| $D_{O2}^{0}$ | 1 | $O_2$ molecular diffusion coefficient at 0°C | 182.59 $cm^2 y^{-1}$ |
| $D_{NO3}^{0}$ | 1 | $NO_3^-$ molecular diffusion coefficient at 0°C | 308.42 $cm^2 y^{-1}$ |
| $D_{NH4}^{0}$ | 1 | $NH_4^+$ molecular diffusion coefficient at 0°C | 309.05 $cm^2 y^{-1}$ |
| $D_{SO4}^{0}$ | 2 | $SO_4^=$ molecular diffusion coefficient at 0°C | 157.68 $cm^2 y^{-1}$ |
| $D_S^{0}$ | 1 | $S^=$ molecular diffusion coefficient at 0°C | 307.32 $cm^2 y^{-1}$ |
| $D_{O2}^{const}$ | 1 | Temperature coeff. for $O_2$ diffusion | 14.09 $cm^2 y^{-1} (°C)^{-1}$ |
| $D_{NO3}^{const}$ | 1 | Temperature coeff. for $NO_3^-$ diffusion | 12.26 $cm^2 y^{-1} (°C)^{-1}$ |
| $D_{NH4}^{const}$ | 1 | Temperature coeff. for $NH_4^+$ diffusion | 12.16 $cm^2 y^{-1} (°C)^{-1}$ |
| $D_{SO4}^{const}$ | Calc | Temperature coeff. for $SO_4^=$ diffusion | 6.83 $cm^2 y^{-1} (°C)^{-1}$ |
| $D_S^{const}$ | 1 | Temperature coeff. for $S^=$ diffusion | 8.83 $cm^2 y^{-1} (°C)^{-1}$ |
| $K_{nit}$ | 1 | Rate constant for nitrification | 12520 $y^{-1}$ |
| $K_{sox}$ | # | Rate constant for sulphide oxidation | 3.15 x $10^6$ $y^{-1}$ |
| $k_{sLimO2}$ | 1 | Half saturation constant for $O_2$ limitation in nitrification | 1 µM |
| $k_{sInhO2}$ | 1 | Half saturation constant for $O_2$ inhibition in denitrification | 6.25µM |
| $k_{sAnoxInhO2}$ | 1 | Half saturation constant for $O_2$ inhibition in anoxic mineralisation | 8µM |
| $k_{sAnoxInhNO3}$ | 3 | Half saturation constant for $NO_3^-$ inhibition in anoxic mineralisation | 30µM |
| $k_{sO2}$ | 1 | Half saturation constant for $O_2$ limitation in oxic mineralisation | 3µM |
| $k_{sNO3}$ | 1 | Half saturation constant for $NO_3^-$ limitation in denitrification | 30µM |
| $k_{sSO4}$ | 4 | Half saturation constant for $SO_4^=$ limitation in sulphate reduction | 1600µM |
| $k_{sSox}$ | 1 | Half saturation constant for $O_2$ limitation in sulphide oxidation | 1µM |
| $\gamma_{O_2}^{TOC}$ | 5 | Mol $O_2$ used per mol C used in oxic mineralisation | 1 |
| $\gamma_{NO_3}^{TOC}$ | 5 | Mol $NO_3^-$ used per mol C used in suboxic mineralisation | 4/5 |
| $\gamma_{SO_4}^{TOC}$ | 5 | Mol $SO_4^=$ used per mol C used in anoxic mineralisation | 1/2 |
| $\gamma_{NH_4}^{X}$ | 5 | Mol $NH_4^+$ produced per mol C used in mineralisation via X; X = $O_2$, $NO_3^-$, $SO_4^=$ | 1/(C:N)[τ] |
| $\gamma_{O_2}^{X}$ | 1 | Mol $O_2$ used per mol X used in reoxidation; X = $NH_4^+$, $S^=$ | 2 |

[1] Soetaert *et al.* (1996); [2]Li and Gregory (1974); [3]Boudreau (1996); [4]Van Cappellen *et al.* (1993); [5]Nedwell and Trimmer (1996); Calc= method in Soetaert *et al.* (1996); [*]method in Soetaert *et al.* (1996); [#]higher values meant that the model did not conserve mass. [τ]C:N for each site is inTable 2.1a

shown in Table 3.3. Note that the ammonium concentration is fixed at the bottom boundary to provide a continuous flux across this boundary. This is because porewater profiles for ammonium were linear with depth, indicating continued ammonification beyond 15cm into the sediment.

### 3.1.5. The numerical scheme and its solution

The numerical scheme is similar to that of Soetaert *et al.* (1996). All grid cells, each of equal length dz (Soetaert *et al.*, 1996, use unequal length grid boxes), are indexed by a

Table 3.3. Boundary conditions and values (7 visit mean; units: μM) at the 4 sites

| | Top boundary | | | | | Bottom boundary (at 15cm) | | | | |
|---|---|---|---|---|---|---|---|---|---|---|
| Site | $O_2$ | $NO_3^-$ | $NH_4^+$ | $SO_4^=$ | $S^=$ | $O_2$ | $NO_3^-$ | $NH_4^+$ | $SO_4^=$ | $S^=$ |
| 1 | 350 | 654 | 8.2 | 1692 | 0 | $Z_f$ | $Z_f$ | 1052 | $Z_f$ | $Z_f$ |
| 2 | 350 | 635 | 6.4 | 1630 | 0 | $Z_f$ | $Z_f$ | 176 | $Z_f$ | $Z_f$ |
| 3 | 350 | 724 | 3.8 | 1739 | 0 | $Z_f$ | $Z_f$ | 1164 | $Z_f$ | $Z_f$ |
| 4 | 350 | 694 | 17.3 | 2794 | 0 | $Z_f$ | $Z_f$ | 1858 | $Z_f$ | $Z_f$ |

$Z_f$ = Zero flux condition

number i which is defined in the middle of a box (Figure 3.1). Thus, solute concentrations are modelled at the centre of each gridcell. The i indices run from 1 at the top of the sediment to 150 at the bottom. The interfaces between boxes, including the SWI, are defined by a j-index which runs from 0 (the SWI) to 150 (the lower boundary of box i=150). Porosities are defined both at j and i indices while sediment diffusion coefficients are defined only at j positions. The porosity at i=1 is derived by linearly interpolating the values of $\phi$ between the SWI (j=0) and j=1 at each site. For $j \geq 1$ and $i>1$, the porosity-depth gradient is zero and the porosity values are set to those shown in Table 2.1a. This yields a sharp porosity gradient which is confined to the first model layer. It has been shown that porosity gradients have a strong influence on diagenetic processes (Rabouille and Gaillard, 1991a; Soetaert *et al.,* 1996). However, given the resolution of the sampling method (1 centimetre slices of sediment), the sharp porosity gradient must be implemented. That is, the porosity measured represents the average porosity for the sediment depth interval (1cm). Thus, the model porosity profile, when integrated over a 1cm sediment slice, must yield the observed porosity in that slice. As the porosity at the SWI must be close to one, the model porosity profile must decline sharply to represent the observed porosity.

The diffusion term in equation 3.1 is approximated by direct differencing (see Appendix A). This ensures mass conservation, even in the presence of sharp porosity gradients (Van Cappellen *et al.,* 1993). The equations (3.7-3.11, Table 3.1) are solved with an iterative Newton-Raphson type procedure obtained from the LINPACK FORTRAN library at the ftp site netlib.att.com.

### 3.1.6. Parameterisation

#### 3.1.6.1. The first order rate constant for organic decay, *k*

The parameter $k$ (see equation 3.2 and Table 3.1) represents the reactivity of organic material and to a lesser extent, the efficiency of bacterial degradation (Van Cappellen *et al.,* 1993). Four methods could be used to derive $k$: 1) by direct calculation from data yielding $k_{calc}$; 2) by defining $k$ at any depth, z, with an exponential function of the form

$$k_z = k_0 e^{-\alpha z} \qquad 3.12$$

in which the parameters $k_0$ ($k$ in box i=1, Figure 3.1) and $\alpha$ (the coefficient of decrease) are fitted to measured solute fluxes across the SWI; 3) by fitting a separate $k$ to a combination of stoichiometrically determined mineralisation rates and observed solute fluxes across the SWI (thereby deriving $k_{o2}$, $k_{no3}$ and $k_{so4}$ for oxic, suboxic and anoxic mineralisation, respectively) and 4) by fitting equations similar to 3.2 (without $LimOx_1$ and $InhibOx_2$) to organic carbon profiles. Only methods 1, 2 and 3 are investigated since method 4 requires a non-zero depth gradient for TOC. All methods are subjected to inhibition and limitation functions (see equation 3.2). In method 1, $k$ was calculated from

the annually integrated data of Nedwell and Trimmer (1996). As an example, division of the total mineralisation rate derived stoichiometrically at site 4 (31.67 mol $Cm^{-2}y^{-1}$, Table 3.4) by the depth integrated TOC concentration in the top 15cm of sediment (181.27 mol $Cm^{-2}$, Table 3.4) yields a $k_{calc}$ for total mineralisation of 0.175 $y^{-1}$. Similar calculations give $k$ at each site (Table 3.4).

Table 3.4. Calculation of $k_{calc}$ for each site in the upper Great Ouse estuary (see text for further details)

| Site | TOC[1] mol $m^{-2}$ | $C_{Ox\text{-}rate}$[1*] mol $m^{-2}y^{-1}$ | $k_{calc}$ $y^{-1}$ |
|---|---|---|---|
| 1 | 265.87 | 15.87 | 0.0597 |
| 2 | 243.63 | 15.60 | 0.0640 |
| 3 | 199.13 | 30.09 | 0.1510 |
| 4 | 181.27 | 31.67 | 0.1750 |

[1] Data from Nedwell and Trimmer (1996) integrated over 0-15cm
[*] Total mineralisation rate

The derivation of $k$ in this way takes no account of the actual depth over which mineralisation was taking place. A constant $k$ throughout the sediment column (method 1) assumes equal maximum degradation rates for the different mineralisation pathways and is the approach adopted by most diagenetic models (e.g. Soetaert *et al.*, 1996).

From hereon, model runs are termed according to the kinetic method used. Thus, $M_{calc}$ is the run using method 1, $M_{exp}$ uses method 2 and model run $M_{fit}$ uses method 3. It is important to note that $M_{calc}$ does not involve a fitting process. In contrast, both $M_{fit}$ and $M_{exp}$ results are derived by a calibration and fitting process. The output from the application of methods 2 and 3 is that achieved with best fit parameter values.

## 3.2. Results

### 3.2.1. Values of *k*

The calculated $k_{calc}$ values for the $M_{calc}$ runs at the four sites in the Gt. Ouse are shown in Table 3.4. The values increase by a factor of ~3x between sites 1 (0.0597 $y^{-1}$) and 4 (0.175 $y^{-1}$). The values of *k* for model runs $M_{exp}$ and $M_{fit}$ are shown for all sites in Table 3.5.

Table 3.5. Values of *k* for model runs $M_{fit}$ and $M_{exp}$ derived by fitting the model to stoichiometrically determined mineralisation rates (Nedwell and Trimmer, 1996). Units: $y^{-1}$ ($k_{o2}=k$ for oxic mineralisation; $k_{no3}=k$ for suboxic mineralisation; $k_{so4}=k$ for anoxic mineralisation; $k_0=k$ in top sediment model box (box i=1, Figure 3.1); $\alpha$=coefficient of decrease; z=depth. See text for further details)

| | Fitted ($M_{fit}$) | | | Exponential ($M_{exp}$) : $k_z=k_0e^{-\alpha z}$ | |
|---|---|---|---|---|---|
| Site | $k_{o2}$ | $k_{no3}$ | $k_{so4}$ | $k_0$ | $\alpha$ ($cm^{-1}$) |
| 1 | 1.23 | 0.24 | 34.7 | 5.68 | 0.0 |
| 2 | 7.85 | 0.0004 | 0.06 | 17.34 | 9.0 |
| 3 | 12.39 | 0.19 | 5.23 | 19.55 | 1.5 |
| 4 | 13.40 | 3.63 | 1.73 | 22.08 | 5.2 |

The fitted values of $k_0$ (Table 3.5) for the $M_{exp}$ runs increase by a factor of 3.8 between sites 1 and 4. The coefficient of decrease, $\alpha$, is least (0 $cm^{-1}$) at site 1 and greatest (9 $cm^{-1}$) at site 2. $M_{fit}$ values at sites 2 and 3 yield similar patterns i.e. $k_{o2}>k_{so4}>k_{no3}$. In contrast, at site 4 $k_{o2}>k_{no3}>k_{so4}$. At site 1, $k_{so4}$ is approximately one and two orders of magnitude greater than $k_{o2}$ and $k_{no3}$ respectively. Intersite differences show that $k_{o2}$ increases by a factor of ~11 between sites 1 and 4 while no such pattern is seen for $k_{no3}$ and $k_{so4}$.

### 3.2.2. SWI Fluxes

The site by site comparison of modelled ($M_{calc}$, $M_{exp}$, $M_{fit}$) and observed SWI fluxes for oxygen, nitrate and ammonium is shown in Figures 3.3a-c. $M_{calc}$ underestimates all measured fluxes by an average of 66% (Figure 3.3a-c). The only exceptions are for nitrate (Figure 3.3b) and ammonium (Figure 3.3c) at site 3 where model fluxes are similar to measurements.

$M_{exp}$ fluxes of oxygen (Figure 3.3a) are well correlated (r=0.96, n=4, p=0.02) to the data. In contrast, $M_{exp}$ nitrate fluxes (Figure 3.3b) across all sites do not correlate well (r=0.06, p=0.75) with the measurements. Only at site 4 does the modelled nitrate flux of 8.49 mol $NO_3^- m^{-2} y^{-1}$ compare favourably with the observed flux of 6.83 mol $NO_3^- m^{-2} y^{-1}$. At site 3, the model overestimates the nitrate flux by a factor of 7 and produces a flux of 3.80 mol $NO_3^- m^{-2} y^{-1}$ at site 2 where no significant fluxes were observed (Nedwell and Trimmer, 1996). Similarly, compared to measurements, ammonium fluxes in $M_{exp}$ (Figure 3.3c) are poorly modelled (r=0.04, p=0.81). Removal of site 3 results from the regression analysis, where the model overestimates the measurement by a factor of 7.5, improves the fit (r=0.77, p=0.3). At site 1, the model flux (0.44 mol $NH_4^+ m^{-2} y^{-1}$) is higher than the observed flux (0.36 mol $NH_4^+ m^{-2} y^{-1}$), and at sites 2 and 4 the model underestimates the observations.

$M_{fit}$ fluxes of oxygen and nitrate (Figure 3.3a and 3.3b, respectively) compare well (r=0.99, p<0.001) with observations at all sites. Note that nitrate release is modelled (0.02 mol $NO_3^- m^{-2} y^{-1}$) at site 2 (Figure 3.3b) where no significant nitrate fluxes were measured. Ammonium fluxes (Figure 3.3c) in $M_{fit}$ are less well correlated (r=0.67, p<0.33) to the data. $M_{fit}$ fluxes are underestimated by approximately 40% (intersite mean) for sites 1, 2

Figure 3.3a-c. Modeled and measured (Nedwell and Trimmer, 1996) solute exchange across the sediment water interface at 4 sites in the upper Gt. Ouse ($M_{fit}$= separate $k$ fitted to each mineralization pathway; $M_{exp}=k$ defined by $k_z=k_0e^{-\alpha z}$; $M_{calc}=k$ calculated from data, see Table 3.5. Note that observed data are annual integrals from 7 monthly measurements)

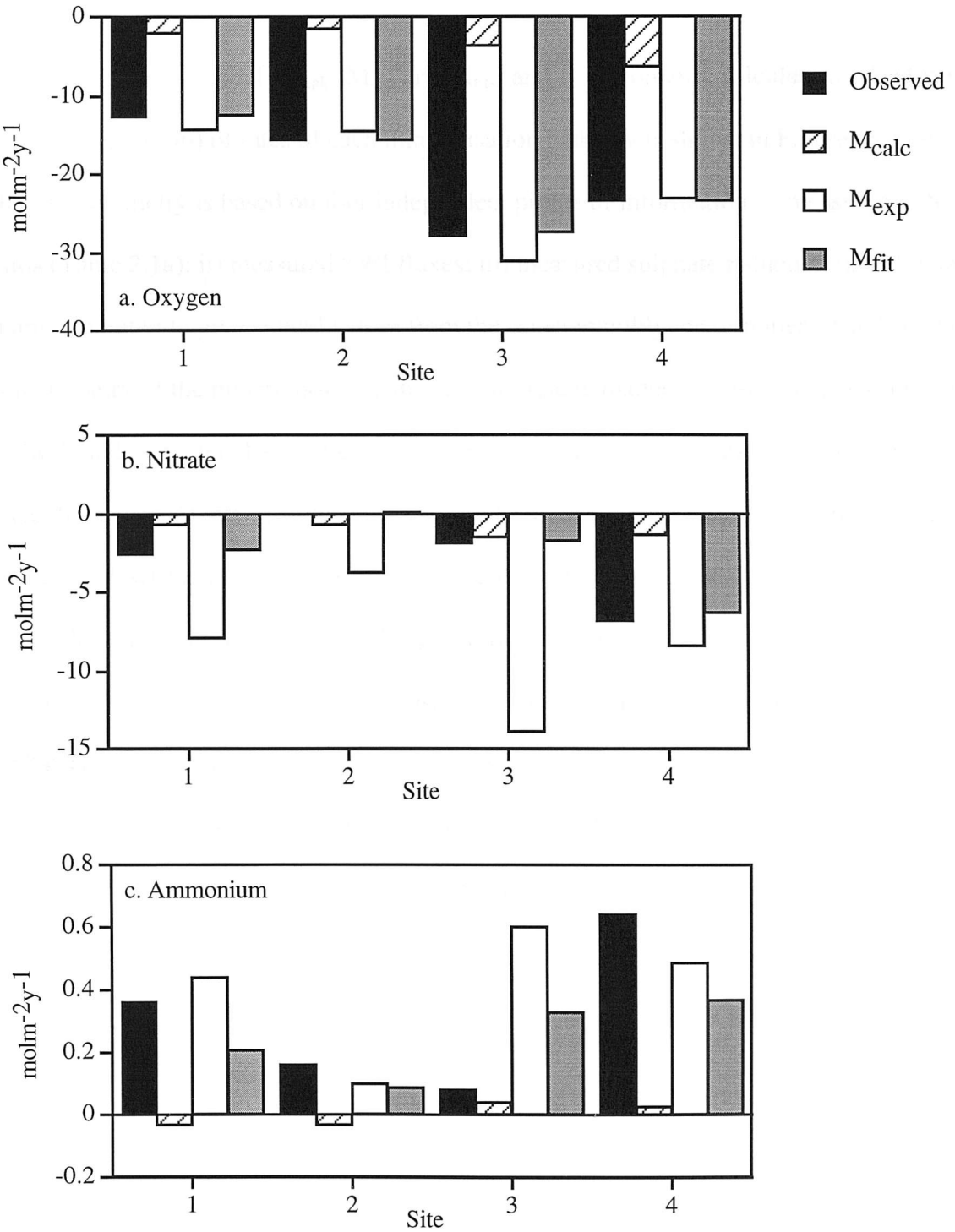

and 4 and at site 3, the model ammonium flux (0.29 mol $NH_4^+ m^{-2} y^{-1}$) is 3.7 times greater than the observed flux (0.08 mol $NH_4^+ m^{-2} y^{-1}$).

### 3.2.3. Mineralisation Rates

The comparison of model ($M_{calc}$, $M_{exp}$ and $M_{fit}$,) and stoichiometric calculations (Nedwell and Trimmer, 1996) of rates of each mineralisation pathway is shown in Figures 3.4a-c. This stoichiometry is based on four independent pieces of information: i) measured C:N ratios (Table 2.1a); ii) measured SWI fluxes; iii) measured sulphate reduction rates ( ii and iii are integrated to give annual values from the seven monthly measurements) and iv) the stoichiometry of the mineralisation pathways of organic matter (see equations 3.4-3.6 and Nedwell and Trimmer, 1996). Note that anoxic mineralisation (equation 3.6) is simply twice the measured rate of sulphate reduction. From hereon, the term stoichiometry will be used to describe the mineralisation rates derived by Nedwell and Trimmer (1996).

$M_{calc}$ rates of mineralisation by all pathways (Figure 3.4a-c) do not correspond well to the stoichiometric calculations. Rates of oxic mineralisation in $M_{calc}$ (Figure 3.4a) are 24% of the stoichiometrically determined rates for site 1, and less than 3% at the remaining sites. Nitrate based mineralisation (Figure 3.4b) in $M_{calc}$ yields carbon oxidation rates which are 44%, 83% and 26% of the stoichiometry at sites 1, 3 and 4 respectively. Anoxic mineralisation rates in $M_{calc}$ are less than the stoichiometric rates at sites 1, 3 and 4 (1.06, 3.03 and 2.57 mol $Cm^{-2}y^{-1}$ cf. 10.6, 12.1 and 7.38 mol $Cm^{-2}y^{-1}$, respectively) but greater at site 2 by a factor of 2.9.

$M_{exp}$ rates of oxic mineralisation give a fit to the stoichiometry with a correlation of r=0.33 (p=0.43). Model rates of oxic mineralisation (Figure 3.4a) are 6.3 and 1.2 times greater than that derived stoichiometrically at sites 1 and 3, respectively. In contrast, the

Figure 3.4a-c. Modeled and stoichiometric (Nedwell and Trimmer (1996) calculations of oxic, suboxic and anoxic mineralization rates at each site in the upper Gt. Ouse ($M_{fit}$= separate *k* fitted to each mineralization pathway; $M_{exp}$=*k* defined by $k_z=k_0e^{-\alpha z}$; $M_{calc}$=*k* calculated from data, see Table 3.5. Note that observed data are annual integrals from 7 monthly measurements)

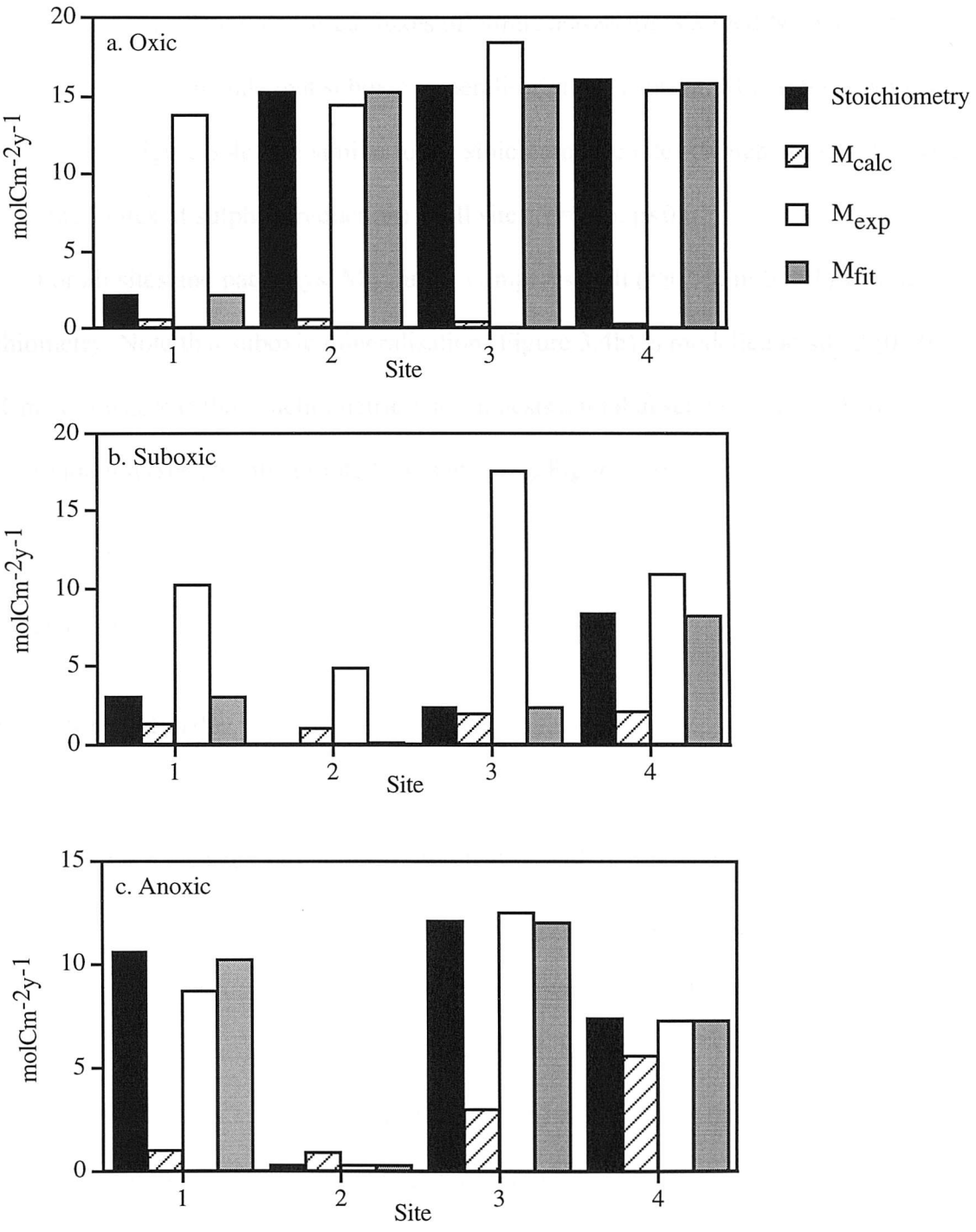

model closely resembles stoichiometric oxic mineralisation rates at sites 2 and 4. Suboxic mineralisation in $M_{exp}$ (Figure 3.4b) is higher than stoichiometric determinations at all sites. At sites 1, 3 and 4, $M_{exp}$ overestimates stoichiometric calculations by factors of 3.3, 7.3 and 1.3 respectively. At site 2, suboxic mineralisation is modelled at 2.94 mol $Cm^{-2}y^{-1}$ where a lack of significant measured fluxes of nitrate across the SWI led Nedwell and Trimmer (1996) to conclude that suboxic mineralisation was absent. $M_{exp}$ rates of anoxic mineralisation (Figure 3.4c) are similar to the stoichiometric rates (which are simply twice the measured rates of sulphate reduction) at all sites ($r=0.96$, $p<0.02$).

For all sites and pathways, $M_{fit}$ output compares well ($r\geq0.99$, $p\leq0.001$) with the stoichiometry. Note that suboxic mineralisation (Figure 3.4b) is modelled at site 2 (0.09 mol $Cm^{-2}y^{-1}$) whereas the stoichiometric rate suggests a total absence of nitrate based carbon oxidation (see also the nitrate fluxes at site 2, Figure 3.3b).

## 3.3.Discussion

### 3.3.1. *k*, the first order rate constant

The value of *k* is a measure of the reactivity of TOC with depth (and time) and to a lesser extent the kinetic efficiency of the mineralisation pathways (Van Cappellen *et al.,* 1993). The calculated *k* values ($k_{calc}$, Table 3.4) are at the lower limit of the range reported for a wide variety of coastal sediments (e.g. 0.1-2.8 $y^{-1}$; McNichol *et al.,* 1988; 0.005-53 $y^{-1}$, Andersen, 1996; 0.2-7 $y^{-1}$ ; Middelburg *et al.,* 1996b) and suggests that the bulk of the organic matter at the Gt. Ouse sites is highly refractory with reactivity decreasing landward from site 4 to 1. Similarly, $k_0$, obtained with equation 12 (see Table 3.5), suggests that TOC reactivity decreases from site 4 to site 1. This trend is reflected in the

increase of the C:N ratio towards the freshwater sites (Table 2.1a). In comparison to $k_{calc}$, $k_0$ is greater than two orders of magnitude higher at all sites. However, $k_{calc}$ and $k_0$ are not directly comparable. The latter reflects only the TOC reactivity at the SWI whereas $k_{calc}$, as previously mentioned, is the depth-integrated TOC reactivity of the sampled sediment column (15cm). Thus $k_{calc}$ is uniform with depth while $k_0$ decreases exponentially away from the SWI. The degree to which $k_0$ decreases is determined by $\alpha$ (equation 3.12). At sites 2, 3 and 4 $\alpha$ values (Table 3.5) are higher than those derived for other coastal areas (e.g. $\alpha<1$, Mackin and Swider, 1989) which suggests that the distribution of reactive organic matter is highly restricted to the upper sediment. Such distributions are typical of those observed in deep sea sediments (Emerson *et al.*, 1985) where the amount of organic material reaching the sea floor is small enough to allow oxic mineralisation to dominate the consumption of reactive carbon (Bender and Heggie, 1984). In contrast, shallow areas usually experience high deposition of organic matter and a smaller proportion is degraded oxically within the usually very shallow surface oxic layer. Reactive carbon is buried below the oxic layer so pathways of anoxic degradation are more important in the sum of total benthic mineralisation (Jørgensen, 1982). This case is suggested at site 1 where $k_z$ does not vary with depth ($\alpha = 0$, Table 3.5). In addition, Mackin and Swider (1989) showed that in fine-grained coastal sediments with lower overlying nitrate concentrations than that found in the Gt. Ouse, the lower the depth attenuation of reactive carbon (i.e. $\alpha$), the less oxygen contributes to total mineralisation. This may explain why at site 1 Nedwell and Trimmer (1996) calculated that oxygen contributed least (14%) to total benthic mineralisation. This compares to between 50% and 98% at the other sites.

Values of $k$ derived for $M_{fit}$ (Table 3.5) reveal a similar trend between sites. $k_{o2}$ decreases from site 4 to site 1 by more than an order of magnitude. This consistent pattern probably reflects the landward increase in the C:N ratio (Table 2.1a) which itself indicates

an increase in both age and refractory nature of the bulk TOC. However, values of $k_{so4}$ and $k_{no3}$ do not show such a pattern. $k_{no3}$ is least (4 x $10^{-4}$ $y^{-1}$) at site 2 and highest (3.63 $y^{-1}$) at site 4 while $k_{so4}$ is maximum (34.7 $y^{-1}$) at site 1 and lowest (1.73 $y^{-1}$) at site 2. In sediments where reactive organic carbon decreases with depth, it is expected that $k_{o2}>k_{no3}>k_{so4}$. This pattern is only shown at site 4 (Table 3.5). At site 1 $k_{so4}$ is ~28 times greater than $k_{o2}$ and at sites 2 and 3 $k_{so4}>k_{no3}$. This can be indicative of at least three things: 1) that inputs of labile organic matter are high enough to allow most of the degradation to be anoxic; 2) that the sulphate reducing bacteria are more effective degraders than both aerobic and nitrate reducing bacteria for similar labile organic matter or 3) that the type of material available for degradation is decomposed faster (and more easily) under anoxic conditions. 1) is usually explained by high accumulation rates of labile organic matter in excess of that which can be respired by oxygen (Jørgensen, 1982). Rates of sedimentation >0.1 cm $y^{-1}$ generally mean that sulphate is at least as important as oxygen in oxidising organic matter (Bralower and Thierston, 1987; Canfield, 1989). High sedimentation rates would therefore explain why at site 1 sulphate reduction accounts for nearly 70% of total carbon oxidation (Nedwell and Trimmer, 1996). In contrast, it has been argued that in this narrow, fast flowing, canalised river, sedimentation is likely to be low and so a further explanation is required. The evidence concerning explanation 2) is conflicting. In some cases (e.g. Sun *et al.,* 1993), anaerobic degradation rates have been shown to be faster than aerobic rates of decomposition, while in others (e.g. Benner *et al.,* 1984) the opposite has been demonstrated. However, most of the evidence (e.g. Lee, 1992; Harvey *et al.,* 1995) suggests that there are no differences between aerobic and anaerobic decomposition rates. In support of the third explanation, Sun *et al.* (1993) have shown that degradation rate constants for diatom-derived chlorophyll-a in intertidal sediments are up to 7 times greater under anoxic compared to oxic conditions. These authors point out that the

differences in the rate constants are associated with the presence and quantity of particular types of structural associations of the degradable organic material (chlorophyll a). This means that organic material not easily degraded by aerobic bacteria can be more readily decomposed by anoxic microorganisms. It is therefore proposed that in these physically well mixed sediments, the differences between $k_{o2}$, $k_{no3}$ and $k_{so4}$ at sites 1, 2 and 3 reflect a higher lability of the organic carbon in the anoxic zone relative to the oxic layer. The nature of the organic material means that it is more reactive under anoxic conditions.

### 3.3.2. Model Runs

$M_{calc}$ runs yield poor comparisons with the data (Figure 3.3a-c, Figure 3.4a-c) because of the nature of the calculation of $k_{calc}$. $k_{calc}$ represents a net value for carbon reactivity which accounts for all inhibiting and limiting factors that affect mineralisation rates. When $k_{calc}$ is implemented in the model its value is reduced by the actions of $LimOx_1$ and $InhibOx_2$ (equation 3.2). The final value of $k_{calc}$, therefore, is the result of factors which are repeatedly accounted for, firstly (and implicitly) in the calculation and then in the model. This yields the low rate constants and thus the low model process rates.

The absolute magnitude of $k_{calc}$ depends strongly on the sediment depth considered which itself is dependent on the depth over which mineralisation is assumed to be active. The smaller the depth considered, the higher the $k_{calc}$ value. For example, integration over the top 5cm (instead of 15cm) of sediment would increase $k_{calc}$ by a factor of 3. For the Gt. Ouse sites, this can only be considered at site 1 where estimates of the depth of sulphate reduction are shown to be in the 0-5cm depth range (Trimmer *et al.*, 1997). At the only other site (site 4) where similar estimates were made, active mineralisation occurred over the entire 15cm sediment core (Trimmer *et al.*, 1997). Recalculating $k_{calc}$ at site 1 so that

only the top 5cm of sediment is integrated over, $k_{calc}$ is increased to ~$0.18y^{-1}$. This is still much lower that the $k$ values derived for site 1 in $M_{fit}$ and $M_{exp}$ (Table 3.5). Similar calculations for the other sites yield the same conclusions. Consequently, rate constants calculated via method 1 and similar approaches (e.g. McNichol *et al.,* 1988; Middelburg *et al.,* 1996b) while providing important information on the turnover times of bulk sedimentary organic carbon, should not be used in diagenetic models which include inhibition and limitation functions. Doing so will significantly reduce the value of the calculated rate constant.

The results of runs in $M_{exp}$ (Figure 3.3a-c, Figure 3.4a-c) show that the use of $k_z$ in the Gt. Ouse sediment sites does not reproduce the data consistently among the sites. Oxic mineralisation rates, total benthic oxygen demand and sulphate reduction rates are modelled satisfactorily. This suggests that $\alpha$ (in equation 3.12) yields a reasonable depth profile of reactive organic carbon (i.e. decreasing $k_z$ with depth). By implication, a factor other than $\alpha$ must be responsible for the high model nitrate fluxes (Figure 3.3b) and denitrification rates (Figure 3.4b) at all sites. $k_z$ type formulations have been widely used (e.g. Mackin and Swider, 1989) and are comparable to diagenetic models which explicitly model organic carbon concentrations (e.g. Soetaert *et al.,* 1996). However, these models have not been applied to regions where nitrate concentrations are as high as those in the Gt. Ouse (annual average ~700μM). At such high concentrations, nitrate no longer limits the rate of denitrification (Nedwell, 1975; Nedwell and Trimmer, 1996; Trimmer *et al.,* 1998). This has important consequences for the model. To illustrate this point, Figure 3.5 compares the model profiles in the top 1cm of sediment of $k_{no3}$ (from $M_{fit}$) and $k_z$ (from $M_{exp}$) as applied in equation 3.8 (Table 3.1), for site 3. The maximum possible values of these rate constants (Max $k_{no3}$ and Max $k_z$) are plotted alongside the actual model values.

Figure 3.5. Comparison of profiles of first order rate constants for denitrification, $k_z$ and $k_{no3}$, at site 3. (Both constants are modified by oxygen inhibition and nitrate limitation, see equation 3 .8 in Table 3.1. For comparison, the maximum value of both rate constants is also profiled)

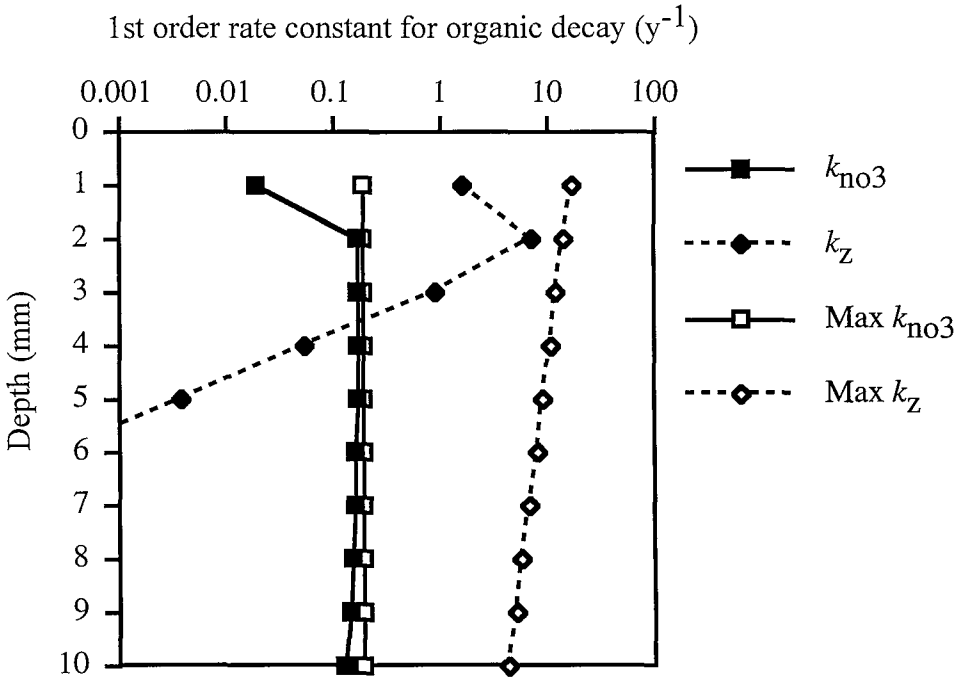


$k_z$ is a function of α, the *in situ* nitrate concentration and oxygen inhibition. $k_{no3}$ is only modified by nitrate and oxygen levels. Both rate constants increase in the first 1mm as oxygen inhibition decreases (Figure 3.5). At 2mm depth, $k_z$ reaches a maximum of $7.4y^{-1}$ compared to a maximum of $0.18y^{-1}$ for $k_{no3}$. The lower $k_{no3}$ does not deplete the nitrate pool as fast as $k_z$. Consequently, nitrate remains less limiting (i.e. $NO_3^- \sim Ks_{no3}$, equation 3.8 and Table 3.1) and $k_{no3}$ is close to its maximum value (Max $k_{no3}$ Figure 3.5; $0.19y^{-1}$ Table 3.5). In contrast, $k_z$, between 1 and 3mm depths, causes greater denitrification. At depths >3mm, $k_z$ denitrification depletes nitrate to limiting concentrations and $k_z$ decreases faster with depth compared to $k_{no3}$.

The higher $k_z$ near the SWI (depth<4mm) is caused by two factors: 1) $k_0$ (Table 3.5), which is fitted to correspond well to measured oxygen fluxes (Figure 3.3a) and 2) the

nitrate removing capacity of denitrification. As oxygen concentrations become less inhibitory, the initial rate of denitrification increases. Opposing this increase is the corresponding decrease in nitrate concentrations. However, in this high nitrate environment, denitrification during this initial phase cannot remove enough nitrate for the nitrate to be sufficiently limiting (i.e. nitrate is not sufficiently less than $Ks_{no3}$, equation 3.8). Consequently, $k_z$ cannot be reduced to a value (i.e. $k_{no3}$) which gives the correct nitrate flux (see Figure 3.3b, $M_{fit}$ vs. measured value). Instead $k_z$ at 2mm is ~41 times greater than $k_{no3}$ which therefore yields a high nitrate flux to the sediment.

It might be argued that the use of a 2-G model (Berner, 1980) may overcome these problems. The more labile fraction of TOC would be mostly mineralised by oxygen and the more refractory portion would be mostly mineralised by sulphate. The oxidation of sulphide (and ammonium) could account for the remainder of the observed oxygen demand. Thus, denitrification would be the sum of the nitrate based carbon oxidation of part of the remainder of both fractions of TOC. Consequently, the measured TOC was split into two fractions: a labile part (= 0.6% of the measured TOC (Nedwell, 1987)) with an assumed Redfield C:N ratio of 6.6, and a refractory part (the remainder) with the measured C:N ratio (Table 2.1a). Each fraction was modelled with its own $k_0$ and $\alpha$. This 2-G model could reproduce all observations but with an unrealistic $k_0$ for the labile fraction of $>3x10^5$ $y^{-1}$ and a nitrification rate constant $>10^6$ $y^{-1}$. The inverse linear dependency of the rate constant, $k_0$, to the TOC concentration means that an increase in the assumed percentage of the labile fraction of the TOC (i.e. 0.6%) would decrease $k_0$. As this labile fraction is unknown and no alternative to the Nedwell (1987) quantification exists, tuning the fraction of TOC that is labile to the data would introduce greater uncertainty in the model.

It is concluded that the use of exponential functions for describing organic mineralisation rates is not appropriate for sediments where overlying nitrate concentrations are high.

Some of the discrepancy between the $M_{exp}$ model and the measured nitrate fluxes at site 2 (Figure 3.3b) may be due to the absence of advection in the model. Nedwell and Trimmer (1996) note the occurrence of subsurface irrigation at this site which will influence porewater profiles. However, as the discrepancy between $M_{exp}$ and observed nitrate fluxes occurs at all remaining sites, where it is reasonable to assume that diffusion is the dominant mode of solute transport (see assumptions), the conclusion remains.

Of the three model parameterisations tested, $M_{fit}$ is the closest fit ($r>0.99$, $p<0.001$) to both the observed solute fluxes across the SWI (Figure 3.3a-c) and the stoichiometrically determined rates of mineralisation (Figure 3.4a-c). The discrepancy between model results and those of Nedwell and Trimmer (1996) for suboxic mineralisation and nitrate fluxes at site 2 results from a modification in the way in which $k_{no3}$ was derived. Setting $k_{no3}$ =0 to reproduce the observed zero flux of nitrate (Figure 3.3b) would mean that denitrification was absent at this site. Although Nedwell and Trimmer (1996) concluded that nitrate based carbon oxidation did not occur at site 2, stoichiometric analysis showed that only 59% of the mineralised organic nitrogen left the sediment as ammonium. This indicates that coupled nitrification-denitrification occurred at this site (Nedwell and Trimmer, 1996) and thus carbon was oxidized by nitrate. Consequently, $k_{no3}$ was derived by ensuring that 41% of the mineralised nitrogen was denitrified.

The goodness of fit of $M_{fit}$ to the data is not surprising and only serves to validate the suitability of Berner's (1980) general diagenetic equation for modelling sedimentary biogeochemical processes. Model fitting exercises are useful in extracting parameter

values, but the $M_{fit}$ approach with its use of separate rate constants for each mineralisation pathway increases the degrees of freedom in the model and thus reduces conceptual simplicity. Given this, $M_{fit}$ ammonium effluxes compare less well to the data at all sites (Figure 3.4c). At site 3, the observed ammonium flux of 0.08 mol $NH_4^+$ $m^{-2}$ $y^{-1}$ could be reproduced with a 10-fold increase in the nitrification rate constant ($K_{nit}$) to 127720 $y^{-1}$ (350 $d^{-1}$, cf. Table 3.2). In contrast, at the remaining sites where model ammonium fluxes underestimate the observations, lower values for $K_{nit}$ could not replicate the data. A zero nitrification rate could only increase the ammonium efflux to 0.51 mol $NH_4^+$ $m^{-2}$ $y^{-1}$ (site 4), to 0.14 mol $NH_4^+$ $m^{-2}$ $y^{-1}$ (site 2) and to 0.26 mol $NH_4^+$ $m^{-2}$ $y^{-1}$ (site 1) compared with observed fluxes of 0.64 mol $NH_4^+$ $m^{-2}$ $y^{-1}$, 0.16 mol $NH_4^+$ $m^{-2}$ $y^{-1}$ and 0.36 mol $NH_4^+$ $m^{-2}$ $y^{-1}$, respectively. These differences may not be significant given the uncertainties associated with the calculation of the annually integrated SWI nutrient fluxes (i.e. the calculation is based on 7 monthly measurements). However, the deep oxygen penetration at site 2 (Nedwell and Trimmer, 1996) suggests that a zero rate of nitrification is unlikely at this site. Alternatively, the deficit in the modelled ammonium flux at sites 1, 2 and 4 may be due to either a lack of other mineralisation pathways in the model (e.g. iron and manganese reduction) or to a lack of model nitrate ammonification. Addition of alternative mineralisation pathways would contrast with the stoichiometric models of Nedwell and Trimmer (1996) which showed that all of the measured ammonium fluxes could be accounted for by oxygen, nitrate and sulphate based carbon oxidation. In Nedwell and Trimmer (1996), the measured benthic oxygen demand was accounted for by sulphide oxidation and two types of stoichiometry for oxic mineralisation : 1) where the nitrogen end product is ammonium (equation 3.4) and 2) where oxygen respiration is coupled to the production of $N_2$ via nitrification-denitrification, i.e.

$$(CH_2O)_{106}(NH_3)_{16}+118O_2=106CO_2+8N_2+130H_20 \quad 3.13$$

Equation 3.13 was used in cases where all of the measured ammonium flux could be accounted for by oxic mineralisation (equation 3.4) and sulphate reduction (equation 3.6) alone. To account for the remaining oxygen demand, oxygen respiration was coupled to nitrification-denitrification (equation 3.13). The absence of direct measurements of denitrification fuelled by nitrification (i.e. $D_n$) means that this cannot be verified. It is therefore possible that the oxygen could be used to reoxidise other reduced compounds such as iron ($Fe^{2+}$) or manganese ($Mn^{2+}$). In their oxidised form, iron and manganese could then be used to respire the same fraction of the organic carbon that would result via equation 3.13. This would not upset the mass balance for carbon in Nedwell and Trimmer (1996). However, with this model the number of mineralisation pathways needed to satisfy the nitrogen budget would be increased. While it would be possible to incorporate additional pathways of organic decay and to calibrate the parameters (e.g. $k_{Fe}$ for iron reduction) against the measured ammonium fluxes (and thereby improve the model fit), this would further increase the number of model parameters and thus the degrees of freedom. Additionally, the lack of data for iron and manganese in the Gt. Ouse sediments means that inclusion of processes related to these elements would amount to guesswork.

The alternative reason for the low model ammonium fluxes is a lack of nitrate ammonification. It has been suggested (Nedwell, 1982; King and Nedwell, 1987; Trimmer *et al.,* 1998) that in high nitrate environments like the Gt. Ouse, nitrate reduction will favour the denitrification pathway instead of nitrate ammonification. However, this does not rule out the presence of nitrate ammonification which can account for ≤10% of the total nitrate reduction at nitrate concentrations in excess of 500μM (see Table 1 in Nedwell , 1982). Similar percentages (4% at site 1 and 6% at site 4) of the measured

nitrate fluxes to the sediment (equivalent to total nitrate reduction) are required to account for the model deficit in ammonium fluxes (this calculation cannot be done at site 2 due the zero nitrate flux measurement). It is thus concluded that a lack of nitrate ammonification in the model is a likely cause for the underestimates in model ammonium fluxes (the introduction of DNRA into the model is the subject of Chapter 6).

### 3.3.3. Parameter sensitivity analysis (PSA)

The ability of a model to predict rates and fluxes at regional and global scales is dependent on the parameter set and the appropriateness of the formulations of the processes under consideration. If a universal set of parameters and equations has been derived, then differences in space (and time) can be related to differences in forcing (e.g. variations in the flux of organic carbon to the sediment, temperature variations etc.). Hence, for a model to be universally robust it is desirable for the model to be insensitive to as many parameters as possible and that important parameters (those that the model is most dependent on) can be easily determined.

Parameter sensitivity analysis (PSA) is an important tool that can help towards achieving this goal of universal robustness in a model. PSA improves understanding by quantifying the dependence of the model on its parameters. Consequently, parameters may be grouped according to how sensitive the model is to changes in those parameters. Parameter sensitivity analyses have been carried out on other diagenetic models. For instance, Soetaert *et al.* (1996) and Middelburg *et al.* (1996a) focused on the effect of parameter changes on pathways of organic carbon mineralization. From this, Middelburg *et al.* (1996a) derived a reduced version of their model which predicted rates of denitrification from a subset of the original parameter set. However, it is unclear whether

these authors included all parameters in their PSA. Here, the aim is to determine and quantify the model's dependence on all of its parameters and to pinpoint parameters that significantly alter all aspects of the model.

To quantify the sensitivity of the model to its parameters, the simple approach of Fasham *et al.* (1990) was used. The method involved changing the value of one parameter at a time, running the model and calculating the percentage change in the model results compared to the reference run. The latter was the $M_{fit}$ output (Figures 3.4 and 3.5). There were 21 parameters that were varied in the model: the first 20 in Table 3.2 and the porosity. The first order rate constants for organic decay ($k_{o2}$, $k_{no3}$, $k_{so4}$) were not included in this exercise as they have essentially already been tested in previous sections in this Chapter. The effect of changes in the thickness of the diffusive boundary layer[1] on model behaviour is dealt with separately in the next Chapter (Chapter 4). Each parameter was modified by ±50%. The one exception was the first order rate constant for sulphide oxidation, $K_{sox}$, which was set as high as possible to account for the fact that sulphide did not accumulate in these sediments (section 3.1.1). Values higher than that used in the standard run ($3.15 \times 10^6$ $y^{-1}$, Table 3.2) meant that the model did not conserve mass. Hence, only a reduction in value was considered. This yielded 41 runs, one for each parameter change. The greater the percentage change in a model statistic (e.g. oxygen flux across the SWI) due a parameter change, the greater the sensitivity of the model to that parameter. The sensitivity was calculated for SWI fluxes and diagenetic rates and the analysis was applied to all sites.

The model parameters can be grouped into those that affect transport and those that affect reactions in the sediment. The first 10 parameters in Table 3.2 are used to calculate effective diffusion coefficients for the model solutes (equation 3.3) and the other

[1] The diffusive boundary layer is the microlayer (~1mm thick) directly above the sediment water interface through which diffusion is the dominant transport process for solutes.

10 parameters are found in the reaction terms of the diagenetic equations (equations 3.7-3.11, Table 3.1). Porosity is included in both diffusion (equation 3.3) and reaction terms (equations 3.7-3.11). Changes in parameters which increase the rate of diffusion of solutes (e.g. diffusion coefficients, porosity) decrease the time available for those solutes to react but can also increase the supply of the solute ( e.g. oxygen) to the sediment. Conversely, in a particular horizon, reduced diffusion rates increase the reaction times for solutes but can lower their supply from the overlying water. The degree to which this balance between diffusion and reaction occurred was assessed by the PSA.

The sensitivity of the model to each parameter was judged according to the following 4 groupings: low sensitivity ( <10%), moderate sensitivity ( 10%-25%), high sensitivity (26 %-50%) and extreme sensitivity (>50%). Each variable and its associated processes are dealt with in turn. The effects of porosity are dealt with separately on account of its extreme sensitivity on model processes. The results of the PSA are shown in Tables 3.6 to 3.9. Actual model rates and fluxes (ie magnitudes) and their response to parameter changes are shown in Tables B2.1-B2.4 in Appendix B.

### 3.3.3.1. Oxygen processes

The change in rates in the oxygen based reactions was less than 10% for most parameter changes at all sites (Tables 3.6-3.9). Parameters that changed oxygen consumption rates by between 10% and 25% ( ie moderate model sensitivity) were the 0°C free solution diffusion coefficient for oxygen ($D_{o2}^0$, Table 3.7a,b, 3.8a, 3.9a {sites 2-4}) ammonium ($D_{nh4}^0$, Table 3.6a, 3.8a,b, 3.9a {sites 1, 3 and 4}) and sulphate ($D_{so4}^0$, Table 3.6-3.9 {sites 1-4}), the half saturation constant for nitrate inhibition in anoxic

Table 3.6a. Parameter sensitivity analysis at site 1 (each parameter decreased by 50%; values represent percentage change in rate/flux associated with each variable; swi=SWI flux; o2r= oxygen respiration; nit= nitrification; s-ox= sulphide oxidation; nr= nitrate reduction; bf lx= bottom boundary flux; oxamm= oxic ammonification; subamm= suboxic ammonification; anamm= anoxic ammonification; totamm= total ammonification; sr= sulphate reduction; ox, sub,an= oxic, suboxic, anoxic mineralization; parameters defined in Table 3.2)

| Parameter | Oxygen | | | | Nitrate | | | Ammonium | | | | | | | Sulphate | | | Sulphide | | | Carbon | | | |
|---|---|---|---|---|---|---|---|---|---|---|---|---|---|---|---|---|---|---|---|---|---|---|---|---|
| | swi | o2r | nit | s-ox | swi | nit | nr | swi | bflx | $ox_{amm}$ | $sub_{amr}$ | $an_{amm}$ | $tot_{amr}$ | nit | swi | sr | s-ox | swi | sr | s-ox | ox | sub | an | total |
| $D_{O2}^{0}$ | -5 | -1 | -3 | -6 | | -3 | | -3 | 1 | -1 | | | -6 | -4 | -3 | 37 | -6 | -6 | 37 | -6 | -6 | -1 | | -6 | -4 |
| $D_{NO3}^{0}$ | 5 | | | 6 | -23 | | -22 | | 1 | | -22 | | 6 | -1 | | 13 | 6 | 6 | 13 | 6 | 6 | | -22 | 6 | -1 |
| $D_{NH4}^{0}$ | | | 12 | | -1 | 12 | | -1 | -41 | | | | | | 12 | | | | | | | | | |
| $D_{SO4}^{0}$ | -15 | | -1 | -19 | | -1 | | -12 | 2 | | | | -19 | -13 | -1 | -44 | -19 | -19 | -44 | -19 | -19 | | | -19 | -13 |
| $D_{S}^{0}$ | 1 | | -1 | 1 | | -1 | | | | | | | | | -1 | -39 | | 1 | -39 | | 1 | | | | |
| $D_{O2}^{const}$ | -2 | | -1 | -2 | | -1 | | -1 | | | | | -2 | -1 | -1 | 14 | -2 | -2 | 14 | -2 | -2 | | | -2 | -1 |
| $D_{NO3}^{const}$ | 1 | | | 2 | -8 | | -8 | | | | -8 | | 2 | | | 4 | 2 | 2 | 4 | 2 | 2 | | -8 | 2 | |
| $D_{NH4}^{const}$ | | | 3 | | | 3 | | -4 | -15 | | | | | | 3 | | | | | | | | | |
| $D_{SO4}^{const}$ | -6 | | -1 | -7 | | -1 | | -4 | 1 | | | | -7 | -5 | -1 | -17 | -7 | -7 | -17 | -7 | -7 | | | -7 | -5 |
| $D_{S}^{const}$ | | | | | | | | | | | | | | | | -1 | | | -1 | | | | | | |
| $K_{nit}$ | -1 | | -49 | | 2 | -49 | | 8 | | | | | | | -49 | | | | | | | | | |
| $K_{sox}$ | -1 | | 2 | -2 | | 2 | | | | | | | | | 2 | 93 | | -2 | 93 | | -2 | | | | |
| $k_{sLimO2}$ | | | 2 | | | 2 | | | | | | | | | 2 | | | | | | | | | |
| $k_{sInhNO3}$ | | | | | | | | | | | | | | | | | | | | | | | | |
| $k_{sAnoxInhO2}$ | | | | | | | | | | | | | | | | -1 | | | -1 | | | | | |
| $k_{sAnoxInhNO3}$ | -15 | | -2 | -19 | | -2 | | -12 | | | | | -19 | -13 | -2 | -43 | -19 | -19 | -43 | -19 | -19 | | | -19 | -13 |
| $k_{sO2}$ | | 1 | | | | | | | | 1 | | | | | | | | | | | | 1 | | | |
| $k_{sNO3}$ | 1 | | | 1 | 3 | | 3 | 1 | | | 3 | 1 | 1 | | | 2 | 1 | 1 | 2 | 1 | 1 | | 3 | 1 | 1 |
| $k_{sSO4}$ | 11 | | 2 | 14 | | 2 | | 9 | | | | | 14 | 9 | 2 | 33 | 14 | 14 | 33 | 14 | 14 | | | 14 | 9 |
| $k_{sSox}$ | | | -1 | | | -1 | | | | | | | | | -1 | | | | | | | | | | |
| $\phi$ | -11 | 60 | -24 | -25 | -23 | -24 | -23 | -2 | -59 | 60 | -23 | -25 | -13 | -24 | | 25 | -25 | -25 | 25 | -25 | -25 | 60 | -23 | -25 | -13 |

Table 3.6b. Parameter sensitivity analysis at site 1 (each parameter increased by 50%; values represent percentage change in rate/flux associated with each variable; swi=SWI flux; o2r= oxygen respiration; nit= nitrification; s-ox= sulphide oxidation; nr= nitrate reduction; bf lx= bottom boundary flux; oxamm= oxic ammonification; subamm= suboxic ammonification; anamm= anoxic ammonification; totamm= total ammonification; sr= sulphate reduction; ox, sub,an= oxic, suboxic, anoxic mineralization; parameters defined in Table 3.2)

| Parameter | Oxygen | | | | Nitrate | | | Ammonium | | | | | | | Sulphate | | | Sulphide | | | Carbon | | | |
|---|---|---|---|---|---|---|---|---|---|---|---|---|---|---|---|---|---|---|---|---|---|---|---|---|
| | swi | o2r | nit | s-ox | swi | nit | nr | swi | bflx | $ox_{amm}$ | $sub_{amm}$ | $an_{amm}$ | $tot_{amm}$ | nit | swi | sr | s-ox | swi | sr | s-ox | ox | sub | an | total |
| $D_{O2}^{0}$ | 5 | 1 | 4 | 6 | | 4 | | 3 | -1 | 1 | | | 6 | 4 | 4 | -37 | 6 | 6 | -37 | 6 | 6 | 1 | | 6 | 4 |
| $D_{NO3}^{0}$ | -3 | | | 1 | -3 | 19 | 1 | 18 | 1 | -1 | | 18 | -3 | 1 | 1 | -8 | -3 | -3 | -8 | -3 | -3 | | 18 | -3 | 1 |
| $D_{NH4}^{0}$ | | | | -6 | | | -6 | | 9 | 41 | | | | | -6 | | | | | | | | | |
| $D_{SO4}^{0}$ | 14 | | | 2 | 17 | | 2 | | 1 | -2 | | | 18 | 12 | 2 | 41 | 18 | 17 | 41 | 18 | 17 | | | 18 | 12 |
| $D_{S}^{0}$ | | | | 1 | -1 | | 1 | | | | | | | | 1 | 38 | | -1 | 38 | | -1 | | | | |
| $D_{O2}^{const}$ | 2 | | | 1 | 2 | | 1 | | 1 | | | | 2 | 1 | 1 | -14 | 2 | 2 | -14 | 2 | 2 | | | 2 | 1 |
| $D_{NO3}^{const}$ | -1 | | | | -1 | 7 | | 7 | | | | 7 | -1 | | | -3 | -1 | -1 | -3 | -1 | -1 | | 7 | -1 | |
| $D_{NH4}^{const}$ | | | | -3 | | | -3 | | 3 | 15 | | | | | -3 | | | | | | | | | |
| $D_{SO4}^{const}$ | 6 | | | 1 | 7 | | 1 | | 4 | -1 | | | 7 | 5 | 1 | 17 | 7 | 7 | 17 | 7 | 7 | | | 7 | 5 |
| $D_{S}^{const}$ | | | | | | | | | | | | | | | | 1 | | | 1 | | | | | | |
| $K_{nit}$ | 1 | | | 47 | | -2 | 47 | | -8 | | | | | | 47 | | | | | | | | | | |
| $K_{sox}$ | | | | -1 | 1 | | -1 | | | | | | | | -1 | -33 | | 1 | -33 | | 1 | | | | |
| $k_{sLimO2}$ | | | | -1 | | | -1 | | | | | | | | -1 | | | | | | | | | | |
| $k_{sInhNO3}$ | | | | | | | | | | | | | | | | | | | | | | | | | |
| $k_{sAnoxInhO2}$ | | | | | | | | | | | | | | | | 1 | | | 1 | | | | | | |
| $k_{sAnoxInhNO3}$ | 1 | | | 2 | 13 | | 2 | | 8 | | | | 13 | 9 | 2 | 3 | 13 | 13 | 3 | 13 | 13 | | | 13 | 9 |
| $k_{sO2}$ | | -1 | | | | | | | | | -1 | | | | | | | | | | | -1 | | | |
| $k_{sNO3}$ | -1 | | | | -1 | -3 | | -3 | -1 | | | -3 | -1 | -1 | | -2 | -1 | -1 | -2 | -1 | -1 | | -3 | -1 | -1 |
| $k_{sSO4}$ | -7 | | | -1 | -9 | | -1 | | -5 | | | | -9 | -6 | -1 | -2 | -9 | -9 | -2 | -9 | -9 | | | -9 | -6 |
| $k_{sSox}$ | | | | 1 | | | 1 | | | | | | | | 1 | | | | | | | | | | |
| $\phi$ | -18 | -46 | 149 | -16 | -23 | 149 | -16 | -31 | 70 | -46 | -16 | -17 | -21 | 149 | | -97 | -17 | -16 | -97 | -17 | -16 | -46 | -16 | -17 | -21 |

Table 3.7a. Parameter sensitivity analysis at site 2 (each parameter decreased by 50%; values represent percentage change in rate/flux associated with each variable; swi=SWI flux; o2r= oxygen respiration; nit= nitrification; s-ox= sulphide oxidation; nr= nitrate reduction; bf lx= bottom boundary flux; oxamm= oxic ammonification; subamm= suboxic ammonification; anamm= anoxic ammonification; totamm= total ammonification; sr= sulphate reduction; ox, sub,an= oxic, suboxic, anoxic mineralization; Δ= change in direction)

| Parameter | Oxygen | | | | Nitrate | | | Ammonium | | | | | | | Sulphate | | | Sulphide | | | Carbon | | | |
|---|---|---|---|---|---|---|---|---|---|---|---|---|---|---|---|---|---|---|---|---|---|---|---|---|
| | swi | o2r | nit | s-ox | swi | nit | nr | swi | bflx | $ox_{amm}$ | $sub_{am}$ | $an_{amm}$ | $tot_{amn}$ | nit | swi | sr | s-ox | swi | sr | s-ox | ox | sub | an | total |
| $D_{O2}^{0}$ | -12 | -13 | -19 | | Δ | -19 | | -9 | 1 | -13 | | | -12 | -19 | 12 | | | 12 | | | -13 | | | -12 |
| $D_{NO3}^{0}$ | | | | 13 | 31 | | -5 | | -2 | | -5 | 14 | | | 1 | 13 | 13 | 1 | 13 | 13 | | -5 | 13 | |
| $D_{NH4}^{0}$ | | | 9 | | 69 | 9 | | -7 | -46 | | | | | 9 | | | | | | | | | | |
| $D_{SO4}^{0}$ | | | | -19 | 4 | | | | 5 | | | -19 | | | -2 | -19 | -19 | -2 | -19 | -19 | | | -19 | |
| $D_{S}^{0}$ | | | | | | | | | | | | | | | -6 | | | -6 | | | | | | |
| $D_{O2}^{const}$ | -4 | -4 | -7 | | -52 | -7 | | -3 | | -4 | | | -4 | -7 | 2 | | | 2 | | | -4 | | | -4 |
| $D_{NO3}^{const}$ | | | | 4 | 6 | | -1 | | -1 | | -1 | 4 | | | | 4 | 4 | | 4 | 4 | | -1 | 4 | |
| $D_{NH4}^{const}$ | | | 2 | | 19 | 2 | | -2 | -17 | | | | | 2 | | | | | | | | | | |
| $D_{SO4}^{const}$ | | | | -7 | 1 | | | | 2 | | | -7 | | | -1 | -7 | -7 | -1 | -7 | -7 | | | -7 | |
| $D_{S}^{const}$ | | | | | | | | | | | | | | | -2 | | | -2 | | | | | | |
| $K_{nit}$ | | | -48 | | Δ | -48 | | 19 | -1 | | | | | -48 | | | | | | | | | | |
| $K_{sox}$ | | | | | | | | | | | | | | | 26 | | | 26 | | | | | | |
| $k_{sLimO2}$ | | | 9 | | 66 | 9 | | -3 | | | | | | 9 | | | | | | | | | | |
| $k_{sInhNO3}$ | | | | | | | | | | | | | | | | | | | | | | | | |
| $k_{sAnoxInhO2}$ | | | | | | | | | | | | | | | | | | | | | | | | |
| $k_{sAnoxInhNO3}$ | | 1 | 1 | -33 | 5 | 1 | | | 5 | 1 | | -33 | | 1 | -4 | -33 | -33 | -4 | -33 | -33 | 1 | | -33 | |
| $k_{sO2}$ | 1 | 1 | -9 | | -68 | -9 | | 4 | | 1 | | | 1 | -9 | 5 | | | 5 | | | 1 | | | 1 |
| $k_{sNO3}$ | | | | 1 | -25 | | 4 | | | | 4 | 1 | | | | 1 | 1 | | 1 | 1 | | 4 | 1 | |
| $k_{sSO4}$ | | | | 23 | -4 | | | | -3 | | | 23 | | | 2 | 23 | 23 | 2 | 23 | 23 | | | 23 | |
| $k_{sSox}$ | | | | | | | | | | | | | | | -3 | | | -3 | | | | | | |
| ϕ | 20 | 21 | -33 | -14 | Δ | -33 | -3 | 36 | -64 | 21 | -4 | -14 | 2 | -33 | 200 | -14 | -14 | 200 | -14 | -14 | 21 | -4 | -14 | 2 |

Table 3.7b. Parameter sensitivity analysis at site 2 (each parameter increased by 50%; values represent percentage change in rate/flux associated with each variable; swi=SWI flux; o2r= oxygen respiration; nit= nitrification; s-ox= sulphide oxidation; nr= nitrate reduction; bf lx= bottom boundary flux; oxamm= oxic ammonification; subamm= suboxic ammonification; anamm= anoxic ammonification; totamm= total ammonification; sr= sulphate reduction; ox, sub,an= oxic, suboxic, anoxic mineralization; parameters defined in Table 3.2)

| Parameter | Oxygen | | | | Nitrate | | | Ammonium | | | | | | Sulphate | | | Sulphide | | | Carbon | | | |
|---|---|---|---|---|---|---|---|---|---|---|---|---|---|---|---|---|---|---|---|---|---|---|---|
| | swi | o2r | nit | s-ox | swi | nit | nr | swi | bflx | $ox_{amm}$ | $sub_{am}$ | $an_{amm}$ | $tot_{amn}$ | nit | swi | sr | s-ox | swi | sr | s-ox | ox | sub | an | total |
| $D_{O2}^0$ | 12 | 12 | 17 | | 133 | 17 | | 9 | -1 | 12 | | | 12 | 17 | -3 | | | -3 | | | 12 | | | 12 |
| $D_{NO3}^0$ | | | | -6 | -7 | | 1 | | 1 | | | 1 | -6 | | -1 | -6 | -6 | -1 | -6 | -6 | | 1 | -6 | |
| $D_{NH4}^0$ | | | -4 | | -35 | -4 | | 5 | 46 | | | | | -4 | | | | | | | | | |
| $D_{SO4}^0$ | | | | 14 | -3 | | | | -4 | | | | 14 | | 1 | 14 | 14 | 1 | 14 | 14 | | | 14 | |
| $D_S^0$ | | | | | | | | | | | | | | | 8 | | | 8 | | | | | | |
| $D_{O2}^{const}$ | 4 | 4 | 6 | | 5 | 6 | | 3 | | 4 | | | 4 | 6 | -2 | | | -2 | | | 4 | | | 4 |
| $D_{NO3}^{const}$ | | | | -3 | -3 | | 1 | | | | | | -3 | | -1 | -3 | -3 | -1 | -3 | -3 | | 1 | -3 | |
| $D_{NH4}^{const}$ | | | -2 | | -15 | -2 | | 2 | 17 | | | | | -2 | | | | | | | | | |
| $D_{SO4}^{const}$ | | | | 6 | -1 | | | | -2 | | | | 6 | | | 6 | 6 | | 6 | 6 | | | 6 | |
| $D_S^{const}$ | | | | | | | | | | | | | | | 2 | | | 2 | | | | | | |
| $K_{nit}$ | | | 43 | | 337 | 43 | | -17 | 1 | | | | | 43 | | | | | | | | | | |
| $K_{sox}$ | | | | | | | | | | | | | | | -6 | | | -6 | | | | | | |
| $k_{sLimO2}$ | | | -5 | | -42 | -5 | | 2 | | | | | | -5 | | | | | | | | | | |
| $k_{sInhNO3}$ | | | | | | | | | | | | | | | | | | | | | | | | |
| $k_{sAnoxInhO2}$ | | | | | | | | | | | | | | | | | | | | | | | | |
| $k_{sAnoxInhNO3}$ | | | | 21 | -3 | | | | -2 | | | | 21 | | 2 | 21 | 21 | 2 | 21 | 21 | | | 21 | |
| $k_{sO2}$ | -1 | -1 | 5 | | 39 | 5 | | -3 | | -1 | | | -1 | 5 | -2 | | | -2 | | | -1 | | | -1 |
| $k_{sNO3}$ | | | | -1 | 22 | | -3 | | | | -4 | -1 | | | | -1 | -1 | | -1 | -1 | | -3 | -1 | |
| $k_{sSO4}$ | | | | -15 | 2 | | | | 2 | | | | -14 | | -2 | -14 | -15 | -2 | -14 | -15 | | | -15 | |
| $k_{sSox}$ | | | | | | | | | | | | | | | 2 | | | 2 | | | | | | |
| $\phi$ | -16 | -16 | 58 | -38 | 728 | 58 | -41 | -39 | 96 | -16 | -42 | -37 | -17 | 58 | -9 | -38 | -38 | -9 | -38 | -38 | -16 | -41 | -38 | -17 |

Table 3.8a. Parameter sensitivity analysis at site 3 (each parameter decreased by 50%; values represent percentage change in rate/flux associated with each variable; swi=SWI flux; o2r= oxygen respiration; nit= nitrification; s-ox= sulphide oxidation; nr= nitrate reduction; bf lx= bottom boundary flux; oxamm= oxic ammonification; subamm= suboxic ammonification; anamm= anoxic ammonification; totamm= total ammonification; sr= sulphate reduction; ox, sub,an= oxic, suboxic, anoxic mineralization; parameters defined in Table 3.2)

| Parameter | Oxygen | | | | Nitrate | | | Ammonium | | | | | | | Sulphate | | | Sulphide | | | Carbon | | | |
|---|---|---|---|---|---|---|---|---|---|---|---|---|---|---|---|---|---|---|---|---|---|---|---|---|
| | swi | o2r | nit | s-ox | swi | nit | nr | swi | bflx | $ox_{amm}$ | $sub_{am}$ | $an_{amm}$ | $tot_{amm}$ | nit | swi | sr | s-ox | swi | sr | s-ox | ox | sub | an | total |
| $D_{O2}^{0}$ | -26 | -56 | -38 | 15 | 8 | -38 | 6 | -18 | | -56 | 6 | 17 | -22 | -38 | 81 | 17 | 15 | 81 | 17 | 15 | -56 | 6 | 17 | -22 |
| $D_{NO3}^{0}$ | 1 | | | 3 | -23 | | -22 | | 1 | | -22 | 3 | -1 | | 4 | 3 | 3 | 4 | 3 | 3 | | -22 | 3 | -1 |
| $D_{NH4}^{0}$ | | | 26 | | -1 | 26 | | -8 | -4 | | | | | 26 | | | | | | | | | | |
| $D_{SO4}^{0}$ | -8 | 2 | -3 | -22 | | -3 | | -7 | 2 | 2 | | -22 | -8 | -3 | -29 | -22 | -22 | -29 | -22 | -22 | 2 | | -22 | -8 |
| $D_{S}^{0}$ | | | | 1 | | | | | | | | | | | -39 | | 1 | -39 | | 1 | | | | |
| $D_{O2}^{const}$ | -4 | -8 | -4 | 2 | 1 | -4 | 1 | -2 | | -8 | 1 | 3 | -3 | -4 | 12 | 3 | 2 | 12 | 3 | 2 | -8 | 1 | 3 | -3 |
| $D_{NO3}^{const}$ | | | | 1 | -7 | | -7 | | | | -7 | 1 | | | 1 | 1 | 1 | 1 | 1 | 1 | | -7 | 1 | |
| $D_{NH4}^{const}$ | | | 7 | | | 7 | | -2 | -14 | | | | | 7 | | | | | | | | | | |
| $D_{SO4}^{const}$ | -3 | 1 | -1 | -8 | | -1 | | -3 | 1 | 1 | | -8 | -3 | -1 | -11 | -8 | -8 | -11 | -8 | -8 | 1 | | -8 | -3 |
| $D_{S}^{const}$ | | | | | | | | | | | | | | | -1 | | | -1 | | | | | | |
| $K_{nit}$ | | | -49 | | 2 | -49 | | 4 | | | | | | -49 | | | | | | | | | | |
| $K_{sox}$ | -1 | | | -3 | | | | | | | | | | | 92 | | -3 | 92 | | -3 | | | | |
| $k_{sLimO2}$ | | | 1 | | | 1 | | | | | | | | 1 | | | | | | | | | | |
| $k_{sInhNO3}$ | | | | | | | | | | | | | | | | | | | | | | | | |
| $k_{sAnoxInhO2}$ | -1 | | | -2 | | | | -1 | | | | -2 | -1 | | -2 | -2 | -2 | -2 | -2 | -2 | | | -2 | -1 |
| $k_{sAnoxInhNO3}$ | -8 | 2 | -3 | -22 | | -3 | | -7 | | 2 | | -22 | -8 | -3 | -29 | -22 | -22 | -29 | -22 | -22 | 2 | | -22 | -8 |
| $k_{sO2}$ | 1 | 3 | 1 | | | 1 | | 1 | | 3 | | | 1 | | 1 | | | 1 | | | 3 | | | 1 |
| $k_{sNO3}$ | | | | | 3 | | 3 | | | | 3 | | | | 1 | | | 1 | | | | 3 | | |
| $k_{sSO4}$ | 6 | -3 | 2 | 18 | | 2 | | 5 | | -3 | | 18 | 6 | 2 | 24 | 18 | 18 | 24 | 18 | 18 | -3 | | 18 | 6 |
| $k_{sSox}$ | | | | | | | | | | | | | | | -1 | | | -1 | | | | | | |
| $\phi$ | 11 | 38 | -19 | -25 | –23 | -19 | -23 | 1 | -59 | 38 | -23 | -24 | 8 | -19 | | -24 | -25 | | -24 | -25 | 38 | -23 | -24 | 8 |

Table 3.8b. Parameter sensitivity analysis at site 3 (each parameter increased by 50%; values represent percentage change in rate/flux associated with each variable; swi=SWI flux; o2r= oxygen respiration; nit= nitrification; s-ox= sulphide oxidation; nr= nitrate reduction; bf lx= bottom boundary flux; oxamm= oxic ammonification; subamm= suboxic ammonification; anamm= anoxic ammonification; totamm= total ammonification; sr= sulphate reduction; ox, sub,an= oxic, suboxic, anoxic mineralization; parameters defined in Table 3.2)

| Parameter | Oxygen | | | | Nitrate | | | Ammonium | | | | | | | Sulphate | | | Sulphide | | | Carbon | | | |
|---|---|---|---|---|---|---|---|---|---|---|---|---|---|---|---|---|---|---|---|---|---|---|---|---|
| | swi | o2r | nit | s-ox | swi | nit | nr | swi | bflx | $ox_{amm}$ | $sub_{am}$ | $an_{amm}$ | $tot_{amn}$ | nit | swi | sr | s-ox | swi | sr | s-ox | ox | sub | an | total |
| $D_{O2}^{0}$ | 4 | 3 | 3 | 4 | −1 | 3 | -1 | 3 | | 3 | -1 | 4 | 3 | 3 | -17 | 4 | 4 | -17 | 4 | 4 | 3 | -1 | 4 | 3 |
| $D_{NO3}^{0}$ | -1 | | | -2 | 19 | | 18 | 1 | -1 | | 18 | -2 | 1 | | -2 | -2 | -2 | -2 | -2 | -2 | | 18 | -2 | 1 |
| $D_{NH4}^{0}$ | | | -13 | | | -13 | | 7 | 40 | | | | | -13 | | | | | | | | | | |
| $D_{SO4}^{0}$ | 7 | -3 | 2 | 21 | | 2 | 1 | 6 | -2 | -3 | 1 | 21 | 7 | 2 | 28 | 21 | 21 | 28 | 21 | 21 | -3 | 1 | 21 | 7 |
| $D_{S}^{0}$ | | | | -1 | | | | | | | | | | | 38 | | -1 | 38 | | -1 | | | | |
| $D_{O2}^{const}$ | 2 | 2 | 2 | 1 | | 2 | | 1 | | 2 | | 1 | 1 | 2 | -7 | 1 | 1 | -7 | 1 | 1 | 2 | | 1 | 1 |
| $D_{NO3}^{const}$ | | | | -1 | 7 | | 7 | | | | 7 | -1 | | | -1 | -1 | -1 | -1 | -1 | -1 | | 7 | -1 | |
| $D_{NH4}^{const}$ | | | -5 | | | -5 | | 2 | 14 | | | | | -5 | | | | | | | | | | |
| $D_{SO4}^{const}$ | 3 | -1 | 1 | 8 | | 1 | | 2 | -1 | -1 | | 8 | 3 | 1 | 11 | 8 | 8 | 11 | 8 | 8 | -1 | | 8 | 3 |
| $D_{S}^{const}$ | | | | | | | | | | | | | | | 1 | | | 1 | | | | | | |
| $K_{nit}$ | | | 47 | | −2 | 47 | | -4 | | | | | | 47 | | | | | | | | | | |
| $K_{sox}$ | | | | 1 | | | | | | | | | | | -32 | | 1 | -32 | | 1 | | | | |
| $k_{sLimO2}$ | | | -1 | | | -1 | | | | | | | | -1 | | | | | | | | | | |
| $k_{sInhNO3}$ | | | | | | | | | | | | | | | | | | | | | | | | |
| $k_{sAnoxInhO2}$ | 1 | | | 2 | | | | 1 | | | | 2 | 1 | | 2 | 2 | 2 | 2 | 2 | 2 | | | 2 | 1 |
| $k_{sAnoxInhNO3}$ | 6 | -2 | 2 | 17 | | 2 | | 5 | | -2 | | 17 | 6 | 2 | 23 | 17 | 17 | 23 | 17 | 17 | -2 | | 17 | 6 |
| $k_{sO2}$ | -1 | -2 | | | | | | -1 | | -2 | | | -1 | | -1 | | | -1 | | | -2 | | | -1 |
| $k_{sNO3}$ | | | | | -3 | | -3 | | | | -3 | | | | -1 | | | -1 | | | | -3 | | |
| $k_{sSO4}$ | -4 | 1 | -1 | -1 | | -1 | | -3 | | 1 | | -1 | -4 | -1 | -13 | -1 | -1 | -13 | -1 | -1 | 1 | | -1 | -4 |
| $k_{sSox}$ | | | | | | | | | | | | | | | 1 | | | 1 | | | | | | |
| $\phi$ | -27 | -47 | 1 | | −7 | 1 | -7 | -15 | 69 | -47 | -7 | -1 | -25 | 1 | -41 | -1 | | -41 | -1 | | -47 | -7 | -1 | -25 |

Table 3.9a. Parameter sensitivity analysis at site 4 (each parameter decreased by 50%; values represent percentage change in rate/flux associated with each variable; swi=SWI flux; o2r= oxygen respiration; nit= nitrification; s-ox= sulphide oxidation; nr= nitrate reduction; bf lx= bottom boundary flux; oxamm= oxic ammonification; subamm= suboxic ammonification; anamm= anoxic ammonification; totamm= total ammonification; sr= sulphate reduction; ox, sub,an= oxic, suboxic, anoxic mineralization; parameters defined in Table 3.2)

| Parameter | Oxygen | | | | Nitrate | | | Ammonium | | | | | | | Sulphate | | | Sulphide | | | Carbon | | | |
|---|---|---|---|---|---|---|---|---|---|---|---|---|---|---|---|---|---|---|---|---|---|---|---|---|
| | swi | o2r | nit | s-ox | swi | nit | nr | swi | bflx | $ox_{amm}$ | $sub_{amm}$ | $an_{amm}$ | $tot_{amn}$ | nit | swi | sr | s-ox | swi | sr | s-ox | ox | sub | an | total |
| $D_{O2}^{0}$ | -15 | -2 | -9 | -3 | 15 | -9 | 15 | -5 | | -2 | 15 | -2 | -7 | -9 | 41 | -2 | -3 | 41 | -2 | -3 | -2 | 15 | -2 | -7 |
| $D_{NO3}^{0}$ | 2 | | -1 | 5 | -27 | -1 | -26 | -5 | 1 | | -26 | 5 | -6 | -1 | 9 | 5 | 5 | 9 | 5 | 5 | | -26 | 5 | -6 |
| $D_{NH4}^{0}$ | | | 11 | | | 11 | | -1 | -40 | | | | | 11 | | | | | | | | | | |
| $D_{SO4}^{0}$ | -7 | 1 | -1 | -23 | | -1 | | -5 | 2 | 1 | | -23 | -5 | -1 | -37 | -23 | -23 | -37 | -23 | -23 | 1 | | -23 | -5 |
| $D_{S}^{0}$ | | | | 1 | | | | | | | | | | | -39 | | 1 | -39 | | 1 | | | | |
| $D_{O2}^{const}$ | -2 | -2 | -1 | -2 | 1 | -1 | 1 | -1 | | -2 | 1 | -1 | -1 | -1 | 14 | -1 | -2 | 14 | -1 | -2 | -2 | 1 | -1 | -1 |
| $D_{NO3}^{const}$ | | | | 2 | -9 | | -8 | -2 | | | -8 | 2 | -2 | | 3 | 2 | 2 | 3 | 2 | 2 | | -8 | 2 | -2 |
| $D_{NH4}^{const}$ | | | 3 | | | 3 | | -3 | -14 | | | | | 3 | | | | | | | | | | |
| $D_{SO4}^{const}$ | -2 | | | -8 | | | | -2 | 1 | | | -8 | -2 | | -13 | -8 | -8 | -13 | -8 | -8 | | | -8 | -2 |
| $D_{S}^{const}$ | | | | | | | | | | | | | | | -1 | | | -1 | | | | | | |
| $K_{nit}$ | -1 | | -49 | | 1 | -49 | | 9 | | | | | | -49 | -1 | | | -1 | | | | | | |
| $K_{sox}$ | -1 | | 1 | -2 | | 1 | | | | | | | | 1 | 94 | | -2 | 94 | | -2 | | | | |
| $k_{sLimO2}$ | | | 1 | | | 1 | | | | | | | | 1 | | | | | | | | | | |
| $k_{sInhNO3}$ | | | | | -1 | | -1 | | | | -1 | | | | | | | | | | | -1 | | |
| $k_{sAnoxInhO2}$ | | | | | | | | | | | | | | | | | | | | | | | | |
| $k_{sAnoxInhNO3}$ | -1 | | | -4 | | | | -1 | | | | -4 | -1 | | -7 | -4 | -4 | -7 | -4 | -4 | | | -4 | -1 |
| $k_{sO2}$ | 1 | 2 | | | | | | 1 | | 2 | | | 1 | | 1 | | | 1 | | | 2 | | | 1 |
| $k_{sNO3}$ | 1 | | | 2 | 3 | | 3 | 1 | | | 3 | 2 | 1 | | 4 | 2 | 2 | 4 | 2 | 2 | | 3 | 2 | 1 |
| $k_{sSO4}$ | 4 | | | 13 | | | | 3 | | | | 14 | 3 | | 22 | 14 | 13 | 22 | 14 | 13 | | | 14 | 3 |
| $k_{sSox}$ | | | | | | | | | | | | | | | -1 | | | -1 | | | | | | |
| $\phi$ | 23 | 45 | -18 | -25 | -29 | -18 | -29 | 2 | -59 | 45 | -29 | -24 | 1 | -18 | 18 | -24 | -25 | 18 | -24 | -25 | 45 | -29 | -24 | 1 |

Table 3.9b. Parameter sensitivity analysis at site 4 (each parameter increased by 50%; values represent percentage change in rate/flux associated with each variable; swi=SWI flux; o2r= oxygen respiration; nit= nitrification; s-ox= sulphide oxidation; nr= nitrate reduction; bf lx= bottom boundary flux; oxamm= oxic ammonification; subamm= suboxic ammonification; anamm= anoxic ammonification; totamm= total ammonification; sr= sulphate reduction; ox, sub,an= oxic, suboxic, anoxic mineralization; parameters defined in Table 3.2)

| Parameter | Oxygen | | | | Nitrate | | | Ammonium | | | | | | | Sulphate | | | Sulphide | | | Carbon | | | |
|---|---|---|---|---|---|---|---|---|---|---|---|---|---|---|---|---|---|---|---|---|---|---|---|---|
| | swi | o2r | nit | s-ox | swi | nit | nr | swi | bflx | $ox_{amm}$ | $sub_{amm}$ | $an_{amm}$ | $tot_{amn}$ | nit | swi | sr | s-ox | swi | sr | s-ox | ox | sub | an | total |
| $D_{O2}^{0}$ | 2 | 1 | 2 | 5 | -1 | 2 | -1 | 1 | | 1 | -1 | 4 | 1 | 2 | -39 | 4 | 5 | -39 | 4 | 5 | 1 | -1 | 4 | 1 |
| $D_{NO3}^{0}$ | -1 | | 1 | -4 | 22 | 1 | 22 | 4 | -1 | | 22 | -4 | 5 | 1 | -7 | -4 | -4 | -7 | -4 | -4 | | 22 | -4 | 5 |
| $D_{NH4}^{0}$ | | | -5 | | | -5 | | 9 | 4 | | | | | -5 | | | | | | | | | | |
| $D_{SO4}^{0}$ | 6 | -1 | 1 | 19 | | 1 | | 4 | -2 | -1 | | 2 | 4 | 1 | 32 | 2 | 19 | 32 | 2 | 19 | -1 | | 2 | 4 |
| $D_{S}^{0}$ | | | | -1 | | | | | | | | | | | 38 | | -1 | 38 | | -1 | | | | |
| $D_{O2}^{const}$ | 1 | 1 | 1 | 2 | -1 | 1 | -1 | | | 1 | -1 | 1 | 1 | 1 | -14 | 1 | 2 | -14 | 1 | 2 | 1 | -1 | 1 | 1 |
| $D_{NO3}^{const}$ | | | | -2 | 8 | | 8 | 2 | | | 8 | -2 | 2 | | -2 | -2 | -2 | -2 | -2 | -2 | | 8 | -2 | 2 |
| $D_{NH4}^{const}$ | | | -2 | | | -2 | | 3 | 14 | | | | | -2 | | | | | | | | | | |
| $D_{SO4}^{const}$ | 2 | | | 8 | | | | 2 | -1 | | | 8 | 2 | | 13 | 8 | 8 | 13 | 8 | 8 | | | 8 | 2 |
| $D_{S}^{const}$ | | | | | | | | | | | | | | | 1 | | | 1 | | | | | | |
| $K_{nit}$ | 1 | | 47 | | -1 | 47 | | -9 | | | | | | 47 | 1 | | | 1 | | | | | | |
| $K_{sox}$ | | | | 1 | | | | | | | | | | | -33 | | 1 | -33 | | 1 | | | | |
| $k_{sLimO2}$ | | | -1 | | | -1 | | | | | | | | -1 | | | | | | | | | | |
| $k_{sInhNO3}$ | | | | | 1 | | 1 | | | | 1 | | | | | | | | | | | 1 | | |
| $k_{sAnoxInhO2}$ | | | | | | | | | | | | | | | | | | | | | | | | |
| $k_{sAnoxInhNO3}$ | 1 | | | 3 | | | | 1 | | | | 3 | 1 | | 4 | 3 | 3 | 4 | 3 | 3 | | | 3 | 1 |
| $k_{sO2}$ | -1 | -1 | | | | | | -1 | | -1 | | | -1 | | -1 | | | -1 | | | -1 | | | -1 |
| $k_{sNO3}$ | -1 | | | -2 | -3 | | -3 | -1 | | | -3 | -2 | -1 | | -3 | -2 | -2 | -3 | -2 | -2 | | -3 | -2 | -1 |
| $k_{sSO4}$ | -3 | | | -9 | | | | -2 | | | | -9 | -2 | | -14 | -9 | -9 | -14 | -9 | -9 | | | -9 | -2 |
| $k_{sSox}$ | | | | | | | | | | | | | | | 1 | | | 1 | | | | | | |
| $\phi$ | -34 | -49 | 28 | -6 | -3 | 28 | -2 | -18 | 69 | -49 | -2 | -7 | -27 | 28 | -86 | -7 | -6 | -86 | -7 | -6 | -49 | -2 | -7 | -27 |

mineralization ($k_{sAnoxInhNO3}$,Table 3.6a,b {site 1}, 3.8a,b {site 3}) and the half saturation constant for sulphate limitation in anoxic mineralization ($k_{sSO4}$, Table 3.6a {site 1}, 3.7a {site 2}). Parameters that caused high model sensitivity (26%-50% changes in model output) were the first order rate constant for nitrification ($K_{nit}$, Table 3.6-3.9 {sites 1-4}), $k_{sAnoxInhNO3}$ (Table 3.7a,b {site 2}), $D_{o2}^0$ and $D_{nh4}^0$ (Table 3.8a {site 3}) and porosity, $\phi$ (Table 3.6-3.9 {sites 1-4}). Extreme model sensitivity (>50% changes in model output) was caused by porosity (Table 3.6a,b { site 1}, 3.8a { site 3}) and $D_{o2}^0$ (Table 3.8a {site 3}). It is clear that some parameters caused different levels of sensitivity at different sites. For instance, a reduction in $D_{o2}^0$ caused a reduction in the oxygen flux to the sediment of 26% at site 3 (Table 3.8a) which compares to a reduction of 5% at site 1 (Table 3.6a). As would be expected, some parameters induced different levels of sensitivity for reductions in value compared to increases in value e.g. a 50% increase in porosity increased oxygen consumption via nitrification by 58% whereas a 50% reduction in porosity decreased the rate of the same process by 33% at site 2 (Table 3.7a,b). Similarly, a reduction in the value of $k_{sAnoxInhNO3}$ at site 1 decreased the oxygen flux to the sediment by 15% (Table 3.6a) whereas an increase in $k_{sAnoxInhNO3}$ increased the oxygen flux by 1% (Table 3.6b). This non-linearity in model response is a consequence of the non-linear nature of the model formulations.

The effect of $D_{o2}^0$ on oxygen processes was not straightforward. In particular, oxygen processes were highly sensitive to changes in $D_{o2}^0$ at site 3 (Table 3.8a) but were only of low sensitivity at the other sites (Table 3.6a, 3.7a, 3.9a). Furthermore, oxygen consumption via sulphide oxidation increased at site 3 and decreased at the other sites in response to lowered $D_{o2}^0$. These differences may be understood by following the sequence of model responses firstly, at sites 1, 2 and 4 together and secondly, at site 3. Reducing $D_{o2}^0$ decreased the supply of oxygen to the sediment (5%-26%) which reduced rates of

oxygen respiration (1%-13%) relative to the standard run ( $M_{fit}$) (Table 3.6a, 3.7a, 3.9a). The reduction in diffusion within the sediment meant that, relative to the standard run, reaction times were higher than diffusion times. Hence, oxygen penetration (and concentration) was decreased (not shown) even though oxygen consumption had been reduced. This limited and caused a reduction in rates of sulphide oxidation. Consequently, sulphate supply from sulphide oxidation was reduced which in turn lowered rates of sulphate reduction relative to $M_{fit}$. This series of causal relationships explain the model sensitivities to $D_{o2}^0$ at sites 1, 2 and 4 (Table 3.6, 3.7, 3.9). In contrast there was a different sequence of events caused by a reduction in $D_{o2}^0$ at site 3. The modelled oxygen processes were highly sensitive to a 50% reduction in $D_{o2}^0$ (Table 3.8a). This was because the oxygen flux to the sediment was highest at site 3 (Figure 3.3a, Table 2.2) implying that oxygen penetration depths were lowest at this site (ie the oxic zone was thinnest at site 3). Consequently, limitation by oxygen on oxygen respiration was greatest at site 3, yielding an increased sensitivity of oxygen respiration (56% reduction, Table 3.8a) to a reduction in $D_{o2}^0$ relative to other sites (1-13%, Table 3.6a, 3.7a, 3.9a). This large decrease in the rate of oxic mineralization at site 3 and the lowering of porewater oxygen concentrations relative to the standard run enabled sulphate reduction to occur closer to the SWI which enhanced the rate of sulphate reduction (17%, Table 3.8a). The increase in sulphate reduction was high enough to fuel an increase in the rate of sulphide oxidation in the presence of the limiting effects of the lowered oxygen concentrations. In conclusion, sulphate reduction and sulphide oxidation decreased in response to a reduction in $D_{o2}^0$ at sites 1, 2 and 4 but increased at site 3. Hence, the lower the oxygen penetration depth ( ie the higher the oxygen consumption rates), the greater the sensitivity of oxygen based rates to reduced oxygen supply to the sediment. An increase in $D_{o2}^0$ only affected oxygen processes at site 2 where increased oxygen supply (12%) fuelled a similar increase (12%)

in oxic mineralization (note that organic carbon mineralization was dominated by the oxic mineralization pathway at this site, Table 2.2 and Figure 3.4a-c).

The effect of $D_{nh4}^0$ on oxygen was mediated through the response of nitrification and the sensitivity was greatest at site 3 (Table 3.8a,b). A reduction in $D_{nh4}^0$ meant that ammonium reaction times (ie nitrification rates) increased relative to diffusion times. Conversely, an increase in $D_{nh4}^0$ lowered the time available for ammonium oxidation and consequently decreased nitrification rates. The sensitivity of nitrification was greatest at site 3 because oxygen concentrations were most limiting at this site (as discussed in the previous paragraphs).

The effect of changes in $D_{so4}^0$ on oxygen processes can be illustrated by considering the response of the model to a 50% reduction in value. Lowering the value of $D_{so4}^0$ reduced the supply of sulphate to the anoxic zone (2%-44%) and hence lowered the rate of both sulphate reduction (19%-23%) and sulphide oxidation (19%-23%) at all sites (Table 3.6a-3.9a). This decreased the rate of oxygen consumption via sulphide oxidation (by 19%-23%) which increased the depth of oxygen penetration and in turn lowered further the rate of sulphate reduction. This coupled feedback mechanism acting on sulphate reduction explains why the magnitude of the decrease in the sulphate flux did not match the magnitude of the decrease in rates of sulphate reduction. For example, the sulphate flux reduced from 0.0847 mol $m^{-2}$ $y^{-1}$ to 0.0535 mol $m^{-2}$ $y^{-1}$ while rates of sulphate reduction fell from 3.6612 mol $m^{-2}$ $y^{-1}$ to 2.8225 mol $m^{-2}$ $y^{-1}$ for a 50% reduction in $D_{so4}^0$ at site 4, (Table B2.4). Note also that the largest decrease in the oxygen flux (15%) caused by a reduction in $D_{so4}^0$ occurred at site 1 (Table 3.6a) where oxygen consumption was dominated by sulphide oxidation (ie where sulphate reduction dominated the degradation of organic matter, Figure 3.4a-c and Table B2.2).

The parameter $k_{sAnoxInhNO3}$, is the concentration of nitrate which determines the level of inhibition on sulphate reduction (equation 3.9) and therefore the degree of overlap between the suboxic and anoxic zone. Smaller values deepen the anoxic zone while larger values move the anoxic zone closer to the SWI. This counter-intuitive response to $k_{sAnoxInhNO3}$ results from the formulation of inhibition functions in the diagenetic equations (equations 3.2 and 3.9). Reductions in $k_{sAnoxInhNO3}$ lowered rates of both sulphate reduction and sulphide oxidation (4%-33%) and hence total oxygen consumption was reduced at all sites (Table 3.6a-3.9a). Conversely, increases in $k_{sAnoxInhNO3}$ increased oxygen consumption via sulphide oxidation (Tables 3.6b-3.9b).

The parameter $k_{sSO4}$ is the half saturation constant for anoxic mineralization which is the sulphate concentration at which sulphate reduction proceeds at half the maximum rate. As a result, a reduction in $k_{sSO4}$ increased rates of sulphate reduction and enhanced oxygen consumption by sulphide oxidation by between 13% and 23% at all sites (Table 3.6a-3.9a). An increase in $k_{sSO4}$ had the opposite effect (1%-15% reduction in oxygen consumption by sulphide oxidation at all sites, Table 3.6b-3.9b). The impact on the flux of oxygen to the sediment was small (0%-7%) at all sites except site 1 where a reduction in $k_{sSO4}$ yielded an increase of 11%. The latter was fuelled by the dominance of sulphide oxidation in the oxygen budget (Table B2.1).

The high model sensitivity of nitrification to $K_{nit}$ at all sites (43%-49%, Table 3.6-3.9) had a low impact on total oxygen consumption rates as nitrification rates accounted for less than 1% of the oxygen budget (Table B2.1-B2.4).

### 3.3.3.2. Nitrate processes

As with the oxygen processes, the effect of parameter changes on nitrate based reactions was not uniform among the sites and the response of the model to reductions compared to increases in parameter values was non-linear. This meant that changes in parameters induced different levels of sensitivity at different sites. Nitrate based processes were insensitive (induced changes <8%) to most parameter changes (Table 3.6-3.9). The largest percentage changes occurred as a result of changes in the 0°C free solution diffusion coefficients for nitrate ($D_{NO3}^0$), ammonium and oxygen, the first order rate constant for nitrification, $K_{nit}$ , the half saturation constants for oxygen in both oxic mineralization ($k_{sO2}$) and nitrification ($k_{sLimO2}$), the half saturation constant for nitrate limitation in denitrification ($k_{sNO3}$) and porosity.

A decrease in $D_{NO3}^0$ reduced the flux of nitrate into the sediment by 23% at sites 1 and 3 and by 27% at site 4 causing a similar decrease in denitrification (Table 3.6a, 3.8a, 3.9a). In contrast, the flux of nitrate from the sediment was increased by 31% at site 2 (Table 3.7a). A 50% increase in $D_{NO3}^0$ increased the flux of nitrate and consequently the rate of denitrification by up to 22% at sites 1, 3 and 4 (Table 3.6b, 3.8b, 3.9b) but decreased the efflux of nitrate by 7% at site 2 (Table 3.7b).

Reductions in $D_{NH4}^0$ increased nitrification rates at all sites (9%-26%, Table 3.6b-3.9b). This was caused by reduced diffusion rates of ammonium which increased the time available for nitrification. The largest increase occurred at site 3 where oxygen penetration was least (section 3.3.3.1). Limitation by oxygen on nitrification was, therefore, greatest at site 3, yielding the increased sensitivity of ammonium oxidation to a reduction in $D_{NH4}^0$. The nitrate efflux was highly (26%-50% range in change, Table 3.7b) and extremely (>50% change, Table 3.7a) sensitive to changes in $D_{NH4}^0$ at site 2. This was because the

low rates of denitrification were unchanged compared to the standard run (note that $k_{no3}$=0.0004 $y^{-1}$, Table 3.5) while the magnitude of the changes in the nitrification rate was high relative to the magnitude of the efflux of nitrate (Table B2.2).

The response of modeled nitrate processes to changes in $D_{O2}^0$ was variable and of low to extreme sensitivity. A reduction in $D_{O2}^0$ decreased rates of nitrification by 3% to 38% as a result of the reduced flux of oxygen into the sediment. The highest decrease occurred at site 3 (Table 3.8a) where highest rates of oxygen consumption meant that oxygen concentrations were most limiting compared to the other sites (section 3.3.3.1). Lowered $D_{O2}^0$ increased the rate of denitrification and consequently the nitrate flux by 15% at site 4 where $k_{no3}$ was highest among the sites (Table 3.5), but had little effect elsewhere on denitrification. The flux of nitrate was reversed at site 2 as reduced nitrification rates became lower than rates of denitrification (Table 3.7a). An increase in $D_{O2}^0$ yielded a moderate to extreme increase in rates of nitrification (17%) and the nitrate efflux (133%) by increasing the supply of oxygen to the sediment at site 2 (Table 3.7b). At this site, rates of nitrification were greater than rates of denitrification (Table B2.2). Elsewhere, the sensitivity was low to an increase in $D_{O2}^0$. The nitrate efflux at site 2 was also extremely sensitive (-52%, Table 3.7a) to a 50% reduction in the temperature coefficient for the oxygen diffusion coefficient ($D_{O2}^{const}$).

Nitrification rates were highly sensitive (47%-49%) to changes in $K_{nit}$ at all sites (Table 3.6-3.9). Increased values of $K_{nit}$ enhanced rates of nitrification while lowered values decreased rates of nitrification. The effect on fluxes of nitrate was negligible at all sites except site 2 where rates of nitrification exceeded rates of denitrification in the standard run (Table B2.2). The reduction in nitrification caused by lower $K_{nit}$, reversed the flux from 0.0109 mol $NO_3^-$ $m^{-2}$ $y^{-1}$ to -0.0292 mol $NO_3^-$ $m^{-2}$ $y^{-1}$ (Table B2.2a) while increased rates of nitrification enhanced the nitrate efflux by 337% at site 2 (Table 3.7b).

The modelled nitrate efflux was highly to extremely sensitive to changes in the half saturation constants for oxygen limitation on nitrification ($k_{sLimO2}$) and oxic mineralization ( $k_{sO2}$) at site 2 (Table 3.7a,b). Both of these parameters are the concentration of oxygen at which nitrification and oxic mineralization proceed at half the maximum rate (and the rates becomes increasingly limited by oxygen). Hence lower values of $k_{sLimO2}$ increased rates of nitrification ( e.g. 66%, Table 3.7a) and higher values of $k_{sLimO2}$ decreased rates of nitrification ( e.g. 42%, Table 3.7b). Similarly, reduced values of $k_{sO2}$ reduced oxic mineralization rates although only negligibly (≤1% at all sites). The effect of this small change at site 2, where oxic mineralization dominated total organic carbon oxidation rates and hence rates of ammonification, was to reduce the amount of ammonium available for nitrification and to consequently reduce the nitrate efflux (68%, Table 3.7a). An increase in $k_{sO2}$ had the opposite effect and increased the efflux of nitrate by 39% at site 2 (Table 3.7b).

Changes in the half saturation constant for nitrate limitation in denitrification, $k_{sNO3}$, induced small changes in rates of denitrification ( ≤4% at all sites). These changes had more of an impact at site 2 where the change in magnitude of rates of denitrification (e.g. 50% reduction in $k_{sNO3}$ increased rates of denitrification by 0.0032 mol N $m^{-2}$ $y^{-1}$) were large in comparison to the magnitude of the efflux of nitrate (0.0109 mol $NO_3^-$ $m^{-2}y^{-1}$, Table B2.2a). Consequently, the nitrate efflux was reduced by 25% (Table 3.7a) and increased by 22% (Table 3.7b) for a decrease and increase in $k_{sNO3}$, respectively, at site 2. Note that the nitrification rate was unchanged by $k_{sNO3}$.

Changes in nitrate processes brought about by changes in porosity are dealt with separately (section 3.3.3.6).

### 3.3.3.3. Ammonium processes

Ammonium processes were moderately sensitive to the 0°C free solution diffusion coefficients for oxygen, , nitrate, ammonium and sulphate, the temperature coefficient for ammonium diffusion ($D_{NH4}^{const}$), the half saturation constant for nitrate inhibition in anoxic mineralization ($k_{sAnoxInhNO3}$) and the half saturation constant for sulphate limitation in sulphate reduction ($k_{sSO4}$) at most sites. At other sites, the model was highly sensitive to the 0°C free solution diffusion coefficient for ammonium and oxygen and the first order rate constant for nitrification. Extreme sensitivity was caused by the 0°C free solution diffusion coefficient for oxygen (site 3) and porosity (all sites). As noted earlier (section 3.3.3.1) and evident in the list above, changes in the same parameters caused different levels of sensitivity at different sites.

Reductions in $D_{O2}^{0}$ caused the highest percentage changes in ammonium processes to occur at site 3 (Table 3.8a). Changes in the rates of the pathways of organic carbon mineralization caused by changes in $D_{O2}^{0}$ have been described in section 3.3.3.1. These changes were directly related to the changes in rates of ammonification at the sites. Overall, total ammonification rates were decreased by 22% at site 3 (Table 3.8a), by 12% at site 2 (Table 3.7a) and by negligible amounts elsewhere. This lowered the ammonium efflux by 18% at site 3 even though rates of nitrification were reduced by 38% (note that rates of nitrification were an order of magnitude lower than rates of ammonification, Table B2.3a).

Changes in ammonium production from suboxic mineralization induced by changes in $D_{NO3}^{0}$ were caused by changes in the flux of nitrate to the sediment. Hence, a reduction in $D_{NO3}^{0}$ decreased the flux of nitrate, the rate of denitrification and the rates of suboxic ammonification at sites 1, 3 and 4 (22%-26%, Table 3.6a, 3.8a, 3.9a). Conversely,

a 50% increase in $D_{NO3}^0$ increased rates of suboxic ammonification at these sites (18%-22%, Table 3.6b, 3.8b, 3.9b). However, these changes had little effect on ammonium effluxes and total ammonification rates.

Changes in $D_{NH4}^0$ affected only the bottom flux of ammonium at all sites. As the depth of the bottom boundary of the model (15cm) is far from the reaction zones of the model (top 1-5cm), there was little difference between the concentration gradient of ammonium across the bottom boundary between sensitivity runs (note that the fixed bottom boundary condition for ammonium, Table 3.3, was unchanged in the sensitivity runs). Hence a change in $D_{NH4}^0$ of ±50% produced a similar percentage change (±40-46%) in the bottom boundary flux (Table 3.6-3.9). Changes in $D_{NH4}^{const}$ had a similar effect although the percentage changes on the bottom flux were lower (14%-17%, Table 3.6-3.9).

A reduction in $D_{SO4}^0$ lowered rates of anoxic ammonification (19%-23%, Table 3.6a-3.9a) because the sulphate flux to the sediment was decreased at all sites (see section 3.3.3.1). Conversely, a higher value of $D_{SO4}^0$ increased rates of anoxic ammonification (14%-20%, Table 3.6b-3.9b). The effects on ammonium effluxes and total rates of ammonification were >10% at site 1 only where sulphate reduction was the dominant pathway in organic carbon oxidation.

The effects of $k_{sAnoxInhNO3}$ and $k_{sSO4}$ on sulphate reduction have been discussed (section 3.3.3.1). Lower values of $k_{sAnoxInhNO3}$ decreased rates of anoxic ammonification (4%-33%, Table 3.6a-3.9a) while lower values of $k_{sSO4}$ increased rates of anoxic ammonification (3%-23%, Table 3.6a-3.9a). Higher values of both parameters caused similar but opposite percentage changes (Table 3.6b-3.9b). The greatest impact on ammonium effluxes and total rates of ammonification occurred at site 1 (>10%) where sulphate reduction was the dominant pathway in organic carbon oxidation.

Changes in $K_{nit}$ have been discussed previously (sections 3.3.3.1 and 3.3.3.2). Thus, only at site 2 where rates of nitrification were higher than rates of denitrification did the large percentage changes in nitrification have a moderate impact on ammonium effluxes (17%-19%, Table 3.7a,b). Changes in ammonium processes caused by changes in porosity are discussed below ( section 3.3.3.6).

### 3.3.3.4. Sulphate and sulphide processes

Sulphur processes were moderately sensitive (and in some cases, highly sensitive) to $D_{O2}^{0}$, $D_{NO3}^{0}$, $D_{SO4}^{0}$, $D_{S}^{0}$, $D_{O2}^{const}$, $D_{SO4}^{const}$, $k_{sSO4}$ and $k_{sAnoxInhNO3}$. The impact of changes in these parameters on sulphur processes has been discussed in the context of other processes in the previous sections (3.3.3.1-3.3.3.3). Highest sensitivity was due to the first order rate constant for sulphide oxidation, $K_{sox}$, and to porosity. Changes in $K_{sox}$ produced large changes in SWI fluxes: a 50% decrease in this parameter enhanced the fluxes by over 90% (Table 3.6a, 3.8a, 3.9a). SWI fluxes were less sensitive to changes in $K_{sox}$ at site 2 (-6%, 26%, Table 3.7a,b). These large percentage changes at the sites arose from small percentage changes (<3%) in rates of sulphide oxidation where the latter were between factors of 30 and 65 times that of the SWI fluxes at sites 1, 3 and 4 (Table B2.1, B2.3 and B2.4) and were over 3 orders of magnitude greater than the SWI flux at site 2 (Table B2.2). The effects of porosity are dealt with later (section 3.3.3.6).

### 3.3.3.5. Carbon mineralisation

Rates of total organic carbon mineralization were unaffected (<10% changes) by changes in most parameters (Table 3.6-3.9). Only changes in $D_{O2}^0$, $D_{SO4}^0$ and porosity caused relatively high percentage changes in total organic carbon oxidation rates. A reduction in $D_{O2}^0$ lowered the rate at sites 2 (12%, Table 3.7a) and 3 (22%, Table 3.8a) and an increase in $D_{O2}^0$ enhanced the rate at site 2 (12%, Table 3.7b). The sensitivity at site 2 was due to the fact that oxic mineralization dominated (98%) both the breakdown of organic carbon (Table 2.2) and the oxygen budget (Table B2.2) and so changes in the supply of oxygen to the sediment by changing $D_{O2}^0$ directly affected rates of total organic carbon mineralization. The response to a reduction in $D_{O2}^0$ at site 3 occurred because of the 56% reduction in oxic mineralization induced by increased oxygen limitation at this already oxygen limited site (section 3.3.3.1). Changes in $D_{SO4}^0$ produced a moderate response in carbon mineralization rates at site 1 because sulphate reduction was the dominant organic carbon oxidation pathway: increased $D_{SO4}^0$ enhanced the supply of sulphate (41%) for anoxic mineralization (which increased by 18%) and consequently increased rates of total carbon oxidation (12%, Table 3.6b) while a decrease in $D_{SO4}^0$ had the opposite effect (Table 3.6a). The implications of changes in organic carbon mineralization rates for organic matter preservation is dealt with in the following section on porosity effects (3.3.3.6).

### 3.3.3.6. Porosity

The extreme sensitivity of model processes caused by the changes in porosity arose from the dependency of both diffusion (equation 3.3) and reaction (equations 3.7-3.11, Table

3.1) on porosity. A decrease in porosity decreases the effective diffusion coefficient (equation 3.3) but also increases rates of organic carbon mineralization through the multiplying effects of the porosity term $(1-\phi)/\phi$ in equations 3.7-3.11 (Table 3.1). The converse occurs for an increase in porosity. Consequently, the effect of changes in porosity on model processes depends on the balance between changes in diffusion and changes in reaction. The result of this sensitivity analysis shows that the model response to changes in porosity depended on the budget of both oxygen and organic mineralization via each electron acceptor. For example, a reduction in porosity increased the flux of oxygen to the sediment at sites 2 to 4 (20%-23%), where oxic mineralization dominated both organic degradation (Table 2.2) and the oxygen budget (Table B2.2-B2.4) but decreased the flux at site 1 (11%), where anoxic mineralization dominated total organic degradation (Table 2.2) and where sulphide oxidation dominated total oxygen consumption (Table B2.1). These differences in sensitivity among the sites can be explained in the following way. Rates of oxic mineralization were increased by lower porosity (45%-60%) which reduced both rates of nitrate reduction (3%-29%) and sulphate reduction (14%-25%) at all sites (Table 3.6a-3.9a). Changes in oxic mineralization rates were more important than changes in the porosity term $(1-\phi)/\phi$ in determining rates of both nitrate and sulphate reduction. The increase in oxic mineralization at sites 2 to 4 meant that total oxygen consumption was dominated by oxic mineralization rather than by sulphide oxidation. Hence, the oxygen flux increased at these sites. In contrast, sulphide oxidation dominated total oxygen consumption at site 1. Consequently, the 25% decrease in both sulphate reduction and sulphide oxidation brought about by the 60% increase in oxic mineralization, caused the reduction in the oxygen flux at site 1 (Table 3.6a).

Interestingly, and counter-intuitively, the reduced rates of sulphate reduction increased the flux of sulphate to the sediment (2%-200%) at all sites (Table 3.6a-3.9a).

This resulted from the fact that the absolute decrease in sulphate reduction was different from that of sulphide oxidation. This increased the magnitude of the difference between sulphate reduction and sulphide oxidation which caused the enhanced sulphate fluxes. The large percentage change in sulphate flux at site 2 resulted from a small absolute increase from 0.0001 mol $SO_4^{=}$ $m^{-2}$ $y^{-1}$ ($M_{fit}$) to 0.0003 mol $SO_4^{=}$ $m^{-2}$ $y^{-1}$ in response to changes in sulphate reduction and sulphide oxidation of a similar magnitude (Table B2.2a).

Changes in porosity had a high impact on nitrate processes. Nitrate fluxes decreased by between 23% and 29%, rates of suboxic mineralization (denitrification) decreased by between 3% and 29% and nitrification rates decreased in the range 18%-33% as a result of lower porosity. These changes were driven by the increase in oxic mineralization which reduced denitrification rates and consequently the nitrate flux. Changes in nitrification were caused by the reduction (59%-60%) in the diffusive supply of ammonium through the base of the model sediment column at all sites. This resulted from the reduction in the diffusion coefficient for ammonium caused by the lowered porosity values (equation 3.3). The response of nitrification had little effect on the nitrate flux as the latter were fuelled by rates of denitrification at sites 1, 3 and 4. The exception was at site 2 where a reduction in porosity changed the direction of the nitrate flux from an efflux to an influx as rates of nitrification became lower than rates of denitrification, in contrast to the standard run (Table B2.2a).

Reduced porosity had a negligible effect on ammonium effluxes at all sites except site 2 where an increase of 36% was modeled (Table 3.7a). The lowest modelled flux of ammonium occurred at this site (0.097 mol $m^{-2}$ $y^{-1}$, Figure 3.3c) where oxic mineralization (15.32 mol C $m^{-2}$ $y^{-1}$) fully dominated rates of organic decay (15.71 mol C $m^{-2}$ $y^{-1}$, Table 2.2). This meant that a 21% increase in oxic mineralization caused an increase of 20% in rates of ammonification (Table 3.7a) yielding the increased ammonium efflux.

Changes in porosity had a variable effect on rates of total organic matter mineralization. Lower porosity increased rates by less than 10% at sites 3 and 4. A higher increase of 20% occurred at site 2 which was fuelled by the increase in oxic mineralization (organic carbon oxidation was dominated by oxygen respiration at this site, (Table 2.2). In contrast to the effects of lowered porosity at sites 2, 3 and 4, reduced porosity decreased organic carbon mineralization rates at site 1 (13%). This was caused by the decrease in sulphate reduction (25%, Table 3.6a) which accounted for the majority (67%) of the carbon mineralization budget (Table 2.2)

Changes in organic oxidation rates caused by changes in porosity (and other parameters e.g. $D_{so4}^{0}$, Table 3.6a) imply changes in organic carbon preservation. For example, reduced porosity increased total organic carbon mineralization rates by 20% at site 2 (Table 3.7a) which meant that less organic carbon was preserved compared to the standard run. Rabouille and Gaillard (1991a) found similar results with a model of deep sea organic carbon mineralization coupled to oxygen consumption (note that when these authors included compaction ie a decrease in porosity with depth, this representated an increase in porosity relative to their standard run with no compaction). However, reduced porosity decreased total organic carbon mineralization rates and consequently increased carbon preservation at site 1 where sulphate reduction dominated the carbon mineralization budget (Table 2.2). The model of Rabouille and Gaillard (1991a) could not have predicted this result at site 1 because organic carbon mineralization was only coupled to oxygen consumption (a reasonable description for deep sea sediments). However these same authors published a more complex model (Rabouille and Gaillard, 1991b) which included the cycling of other electron acceptors but did not carry out a similar sensitivity analysis on this model. In any case, their model would need to be applied to sediments in which sulphate reduction was an important pathway of organic

carbon mineralization. Soetaert *et al.* (1996) developed a diagenetic model that included similar processes to those in the model presented here, but was applied to deeper (shelf to abyssal) sediments. They found that a decrease in porosity reduced the rate of oxic mineralization because the lower diffusion coefficient reduced the flux of oxygen into the sediment. This response conflicts with that of the model presented here: a decrease in porosity increased oxic mineralization rates (Table 3.6a-3.9a). This meant that in the model presented here, the enhanced biological demand for oxygen (via $(1-\phi)/\phi$) counteracted the effects of the reduced diffusion coefficient for oxygen on the oxygen flux (via equation 3.3) resulting in an increased flux of oxygen to the sediment. The exception was at site 1 where sulphate reduction dominated the organic mineralization rates (Table 2.2). Soetaert *et al.* (1996) also showed that lower porosity decreased the percentage contribution of oxic mineralization to total organic carbon mineralization. In contrast, lower porosity increased the percentage contribution of oxic mineralization at the expense of the other mineralization pathways (Table 3.10).

Table 3.10. The effect of ±50% changes in porosity on the percentage contribution of oxic, suboxic and anoxic mineralization to total organic carbon mineralization

| Site | 1 | | | 2 | | | 3 | | | 4 | | |
|---|---|---|---|---|---|---|---|---|---|---|---|---|
| | oxic | suboxic | anoxic | oxic | suboxic | anoxic | oxic | suboxic | anoxic | oxic | suboxic | anoxic |
| Mfit | 14 | 20 | 66 | 98 | 0 | 2 | 52 | 8 | 40 | 50 | 26 | 24 |
| +50% | 10 | 21 | 69 | 98 | 0 | 2 | 37 | 10 | 53 | 35 | 35 | 30 |
| - 50% | 25 | 18 | 57 | 98 | 0 | 2 | 66 | 6 | 28 | 67 | 17 | 16 |

One possible reason for the difference in model responses to changes in porosity between this model and that of Soetaert *et al.* (1996) may be due to the use of different values of the exponent m, in equation 3.3. Here, m=1.3 (sandy sediments) whereas in Soetaert *et al.* (1996), m=3 (muddy sediments). These differences yield an equation for

the diffusion coefficient which includes porosity raised to the power of 0.3 (equation 3.3) rather than 2 (Soetaert *et al.,* 1996, p1025) which means that in the latter case, changes in porosity will produce a greater change in diffusion compared to the value used in this model. However, running the model with m=3 in equation 3.3 did not change this model's response to porosity. Consequently, an explanation for the differences in responses to changes in porosity between the models remains unknown.

An increase in porosity reduced the rates of all pathways of organic mineralization (1%-49 %, Table 3.6b-3.9b) through the multiplying effects of the term ( 1-$\phi$)/$\phi$ in equations 3.7-3.11 (Table 3.1). This contrasts with the effects of decreased porosity, where increased rates of oxic mineralization caused the reductions in denitrification and sulphate reduction (Table 3.6a-3.9a). It is concluded that within the range of the porosity values used in this sensitivity analysis, the effects on reaction terms (rates of organic carbon mineralization) outweigh the effects on the diffusion terms ( diffusion coefficients) in determining the behaviour of diagenetic processes and solute fluxes across the SWI.

Denitrification contributed equally with oxygen respiration towards the organic mineralization budget at site 4 when porosity was increased, accounting for more of the budget than sulphate reduction. This was because the first order rate constant for denitrification ($k_{no3}$=3.63 $y^{-1}$) was higher than the first order rate constant for sulphate reduction ($k_{so4}$=1.73 $y^{-1}$) at this site (Table 3.5). Elsewhere, the contribution of denitrification to total organic carbon oxidation was negligibly affected.

### 3.3.3.7. PSA and model robustness

To evaluate the model robustness it is necessary to focus on the parameters to which the model was most sensitive. All model processes (e.g. organic carbon mineralization rates)

and fluxes (e.g. the oxygen flux across the SWI) were moderately to extremely sensitive to porosity and diffusion parameters (Table 3.6-3.9). Parameters associated with the reaction terms of the diagenetic equations (3.7-3.11, Table 3.1) such as $k_{sAnoxInhNO3}$ and $k_{sSO4}$ also changed fluxes and organic carbon mineralization rates by moderate (10%-25%) to high (26%-50%) amounts in sediments where sulphate reduction was the dominant mineralization pathway (site 1, Table 3.6a). Other parameters had a high impact on one particular aspect of the model without affecting rates of organic carbon oxidation e.g. $K_{nit}$ on rates of nitrification and $K_{sox}$ on fluxes of sulphate and sulphide across the SWI (Table 3.6-3.9). The following addresses each of these parameters in turn.

The influence of the component diffusion coefficients (e.g. $D_{O2}^0$) that make up the bulk diffusion coefficient (equation 3.3) on model processes is unlikely to be of significance in the real world. In reality there is no reason to believe that changes in the diffusion coefficient of one solute are independent of changes in the diffusion coefficient of other solutes. In shallow coastal sediments subjected to active hydrodynamic conditions (unlike deep sea sediments), solute transport across the SWI can be enhanced by processes such as turbulence (Lohse *et al.,* 1996). Under such conditions, changes in transport will affect all solutes. To investigate this, two model runs were made in which the bulk diffusion coefficient for all model variables ($D_C$, equation 3.3) was changed by ±50%. The results are shown in Table 3.11. A reduction in $D_C$ reduced all fluxes and processes at all sites (except nitrification at site 1 and the SWI flux of sulphate and sulphide at site 2). Rates of organic carbon mineralization decreased by between 18% and 40 % across the sites. This reflected the reduction in supply of electron acceptors (oxygen, nitrate and sulphate) from the overlying water. Conversely, an increase in $D_C$ increased the diffusive supply of the electron acceptors which enhanced rates of organic carbon mineralization (14 %-22%). The increase in organic carbon mineralization rates was mostly fuelled by

Table 3.11. Model sensitivity to ±50% changes in the bulk diffusion coefficient ( equation 2.3) for all variables.
( swi=SWI flux; o2r= oxygen respiration; nit= nitrification; s-ox= sulphide oxidation; nr= nitrate reduction; bf lx= bottom boundary flux; $ox_{amm}$= oxic ammonification; $sub_{amm}$= suboxic ammonification; $an_{amm}$= anoxic ammonification; $tot_{amm}$= total ammonification; sr= sulphate reduction; ox, sub,an= oxic, suboxic, anoxic mineralization)

| Site | Oxygen | | | | Nitrate | | | Ammonium | | | | | | | Sulphate | | | Sulphide | | | Carbon | | | |
|---|---|---|---|---|---|---|---|---|---|---|---|---|---|---|---|---|---|---|---|---|---|---|---|---|
| | swi | o2r | nit | s-ox | swi | nit | nr | swi | bflx | $ox_{amm}$ | $sub_{amm}$ | $an_{amm}$ | $tot_{amm}$ | nit | swi | sr | s-ox | swi | sr | s-ox | ox | sub | an | total |
| -50% | | | | | | | | | | | | | | | | | | | | | | | | |
| 1 | -26 | -1 | 5 | -33 | -33 | 5 | -32 | -38 | -50 | -1 | -32 | -33 | -28 | 5 | -52 | -33 | -33 | -52 | -33 | -33 | -1 | -32 | -33 | -28 |
| 2 | -18 | -18 | -18 | -21 | -60 | -18 | -11 | -20 | -54 | -18 | -12 | -21 | -18 | -18 | 10 | -21 | -21 | 10 | -21 | -21 | -18 | -11 | -21 | -18 |
| 3 | -41 | -63 | -31 | -12 | -24 | -31 | -24 | -42 | -50 | -63 | -24 | -13 | -40 | -31 | -24 | -13 | -12 | -24 | -13 | -12 | -63 | -24 | -13 | -40 |
| 4 | -31 | -33 | -8 | -30 | -16 | -8 | -16 | -35 | -50 | -33 | -16 | -30 | -28 | -8 | -45 | -30 | -30 | -45 | -30 | -30 | -33 | -16 | -30 | -28 |
| +50% | | | | | | | | | | | | | | | | | | | | | | | | |
| 1 | 20 | 1 | 0 | 25 | 25 | 0 | 24 | 31 | 50 | 1 | 24 | 25 | 22 | 0 | 30 | 25 | 25 | 30 | 25 | 25 | 1 | 24 | 25 | 22 |
| 2 | 16 | 16 | 14 | 6 | 99 | 14 | 1 | 20 | 59 | 16 | 1 | 6 | 16 | 14 | 40 | 6 | 6 | 40 | 6 | 6 | 16 | 1 | 6 | 16 |
| 3 | 13 | 3 | -9 | 26 | 24 | -9 | 23 | 21 | 50 | 3 | 23 | 27 | 14 | -9 | 55 | 27 | 26 | 55 | 27 | 26 | 3 | 23 | 27 | 14 |
| 4 | 9 | 2 | -2 | 25 | 28 | -2 | 27 | 24 | 50 | 2 | 27 | 25 | 14 | -2 | 17 | 25 | 25 | 17 | 25 | 25 | 2 | 27 | 25 | 14 |

the increase in sulphate reduction at all sites except site 2 where oxic mineralization dominated the organic carbon mineralization budget. This contrasts with the effect of reducing $D_C$ where reductions in total organic carbon oxidation rates were fuelled by changes in different pathways at different sites. For example, at site 1 where sulphate reduction is the dominant pathway in the breakdown of organic carbon, the 33 % decrease in anoxic mineralization caused the 28% reduction in total organic carbon mineralization. In contrast, at site 2 where oxic mineralization dominated, the reduction in the latter was responsible for the reduction in total organic carbon oxidation rates.

These results reflect the even distribution of organic carbon with depth in the sediments of sites 1 to 4 (section 3.1.2). This distribution explains why increases in diffusion coefficients increased rates of organic carbon mineralization. For example, increased diffusion increases the penetration depth of oxygen; the same amount of organic carbon is available at these lower depths as there is closer to the SWI; consequently, depth integrated oxic mineralization rates increase. In sediments where organic carbon concentrations decrease exponentially with depth (the more common situation), an increased diffusive supply of oxygen would also increase depth integrated rates of oxic mineralization but to a lesser degree. Consequently, the percentage changes in the output of this model caused by changes in diffusion parameters apply only to sediments in which organic material is well mixed with depth. However, the qualitative effects of changes in the diffusion parameters on model processes may apply to sediments in which organic carbon concentrations decrease with depth.

The effect of porosity on model processes has been shown to be important both in this PSA and in other studies (Rabouille and Gaillard, 1991a; Soetaert *et al.*, 1996). Soetaert *et al.* (1996) did not include porosity in their Monte Carlo type sensitivity analysis but investigated its effect separately. Middelburg *et al.* (1996a) carried out a

similar Monte Carlo analysis on the model developed by Soetaert *et al.* (1996) to determine the sensitivity of predicted rates of denitrification. It is unclear whether porosity was included in their analysis, but it is curious that it does not feature in the metamodel derived by Middelburg *et al.* (1996a) to estimate denitrification rates in marine sediments. The importance of porosity shown here and by others suggest that it is important to have measurements of porosity when modelling diagenesis in particular sediments. Alternatively, a model of porosity, rather than imposed profiles of porosity in diagenetic models, may be the way forward.

A range of values exist in the literature for some of the reaction parameters. The value of the half saturation constant for sulphate limitation in sulphate reduction, $k_{sSO4}$, was set to 1600 μM $SO_4^-$ after Van Cappellen *et al.* (1993). However, values as low as 200 μM $SO_4^-$ have been determined for marine sulphate reducing bacteria (Ingvorsen *et al.*, 1984). The PSA revealed that a 50% reduction in $k_{sSO4}$ to 800 μM $SO_4^-$, enhanced sulphate reduction rates by between 14 % and 23% across the sites with a maximum increase in total organic carbon mineralization rates of 9% at site 1 (Table 3.6a). Using a value of $k_{sSO4}$=200 μM in the model enhanced total organic carbon mineralization rates by 24% at site 1 reflecting the importance of the changes in sulphate reduction (not shown).

Table 3.12. The effect of changes in $k_{sAnoxInhNO3}$ on the percentage contribution of oxic, suboxic and anoxic mineralization to total organic carbon mineralization

| Site | 1 | | | 2 | | | 3 | | | 4 | | |
|---|---|---|---|---|---|---|---|---|---|---|---|---|
| $k_{sAnoxInhNO3}$ ($\mu M\ NO_3^-$) | oxic | suboxic | anoxic | oxic | suboxic | anoxic | oxic | suboxic | anoxic | oxic | suboxic | anoxic |
| 30 ($M_{fit}$) | 14 | 20 | 66 | 98 | 0 | 2 | 52 | 8 | 40 | 50 | 26 | 24 |
| 15 | 16 | 24 | 60 | 98 | 0 | 2 | 46 | 11 | 43 | 44 | 32 | 24 |
| 5 | 20 | 28 | 52 | 98 | 0 | 2 | 61 | 11 | 28 | 46 | 32 | 22 |

For the half saturation constant for nitrate inhibition in anoxic mineralization ($k_{sAnoxInhNO3}$), no values exist from experimental work. This parameter has been allocated values of 5 μM $NO_3^-$ (Soetaert *et al,* 1996), 15 μM $NO_3^-$ (Boudreau *et al.,* 1998) and 30 μM $NO_3^-$ (Boudreau, 1996). This PSA showed that a 50% reduction in $k_{sAnoxInhNO3}$ (ie.from 30 μM $NO_3^-$ to 15 μM $NO_3^-$) lowered the flux of oxygen by 15% and decreased rates of both sulphate reduction and total organic carbon mineralization by 19% and 13%, respectively at site 1 (Table 3.6a). Running the model with $k_{sAnoxInhNO3}$ =5 μM $NO_3^-$ caused further decreases in both oxygen fluxes (12%-36%) and total organic carbon mineralization rates (8%-29%) across the sites, with the largest effect occurring at site 1 where sulphate reduction was the dominant organic carbon mineralization pathway. These different values of $k_{sAnoxInhNO3}$ also changed the percentage contribution of each electron acceptor to total organic carbon mineralization with lower values increasing the relative importance of oxygen respiration at the expense of sulphate reduction (Table 3.12).

These examples of parameter changes suggest that it is unwise to consider parameters as universally constant in space. Consequently, when undertaking PSA as part of diagenetic model development, all parameters should be included in the exercise before model robustness can be assessed

## 3.4. Conclusions

The first order rate constant $k$, represents the reactivity of sedimentary organic carbon and as such must decrease with depth and time. Three ways of implementing $k$ in a diagenetic model for sediments subjected to high overlying nitrate concentrations and have been tested: 1) The commonly used exponential formulation ($k_z = k_0 e^{-\alpha z}$), while modelling oxic and anoxic processes well, overestimates measured nitrate fluxes because nitrate levels at

these high concentrations cannot limit (reduce) the value of $k_z$ in the zone of denitrification. 2) data calculated constants ($k_{calc}$ = depth integrated total mineralisation rate÷depth integrated carbon inventory) underestimate diagenetic rates. Factors in the model (e.g. $LimOx_1$) that decrease the rate constant value with depth have already been accounted for in the calculation of $k_{calc}$. Consequently, the actual rate constant in the model is lowered. It is concluded that $k$ values commonly derived in this way are not suitable in diagenetic models which use limitation/inhibition functions. 3) Fitting first order rate constants to individual pathways of mineralisation is the only way to satisfactorily reproduce the data. This increases the degrees of freedom in the model and thus, casts doubt on the ability of diagenetic models for estuaries with high nitrate loads to be universally applicable.

The model ($M_{fit}$) underestimates the observed ammonium fluxes at 3 sites. It is proposed that this is due to a neglect of other mineralisation pathways (e.g. DNRA) in the model which is likely to be active in the Gt. Ouse sediments.

Different model processes and fluxes are sensitive to varying degrees to changes in a number of parameters. If the results of the PSA are restricted to the effects on organic carbon mineralization rates then only a few parameters are found to be important. These are $D_{O2}^0$, $D_{SO4}^0$, the bulk diffusion coefficient ($D_C$, equation 3.3) and porosity. In addition, using the range of values of $k_{sAnoxInhNO3}$ and $k_{sSO4}$ found in the literature shows that these parameters are also important. These latter two parameters influence the rate of sulphate reduction and so the largest percentage changes occurred at the site where sulphate reduction dominated organic carbon mineralization rates. This highlights the importance of considering a range of sediment environments with different organic carbon mineralization budgets when carrying out parameter sensitivity analysis.

# 4. The diffusive boundary layer and its impact on early diagenetic processes

## 4.1. Introduction

Archer *et al.* (1989) first suggested that the lower the penetration of oxygen into the sediment, the greater the impact of the diffusive boundary layer (DBL - see section 4.2) on oxygen fluxes. This is because a greater proportion of the oxygen concentration gradient is contained within the DBL. In deep sea sediments oxygen penetration is often greater than 2cm, which is deep enough for the DBL to have a negligible effect on oxygen fluxes (Reimers *et al.,* 2001). Narrow oxic layers (<0.5cm) are often observed in shallow sediments where high oxygen consumption rates are fuelled by the greater availability of organic matter compared to the deep sea. The influence of the DBL is therefore expected to be greatest in shallow sediments. However, Jørgensen and Boudreau (2001) in a modelling study, concluded that the DBL had a negligible effect on oxygen consumption rates and organic carbon preservation in shallow sediments. They assumed that oxygen consumption was driven solely by the oxidation of reduced substances (e.g. sulphide). As a result, their conclusions only apply to sediments in which sulphate reduction dominates the breakdown of organic carbon. Only one site (site 1) meets this condition in the shallow sediments of the Gt. Ouse (Table 2.2). Total organic carbon mineralization rates were dominated by oxic mineralization at the remaining sites of the upper estuary (2-4) where mean oxygen penetration depths ranged between 0.3cm and 0.7cm (Nedwell and Trimmer, 1996). In this Chapter, a more complete assessment is made of the effects of different thicknesses of the DBL on early diagenetic processes by examining changes in the porewater profiles of oxygen, nitrate, ammonium and sulphate, the fluxes of these dissolved substances across the SWI and the sedimentary processes.

## 4.2. Structure of the interfacial region

The DBL, also referred to as the diffusive sublayer, is a component of the benthic boundary layer (BBL) which is " that part of the marine environment that is directly influenced by the presence of the interface between the bed and its overlying water." (Dade *et al.,* 2001). The structure of the BBL (Figure 4.1) has been well described (Boudreau and Jørgensen, 2001) and develops under the influence of the mean flow, waves and turbulence (Dade *et al*, 2001). As the sediment surface is approached from above, the vertical motions of turbulence and waves die out. The region below this point is called the viscous sublayer through which the viscous transport of momentum dominates. Closer to the sediment surface (by a factor of ~10, Boudreau, 1997), there is a transition to the upper boundary of the DBL where the eddy diffusion coefficient, K, becomes smaller than the molecular diffusion coefficient, D (Boudreau and Guinasso, 1982). The thickness of the DBL is, therefore, solute dependent as different dissolved substances have different diffusion coefficients (Li and Gregory, 1974) but are independent of K (Glud *et al.,* 1996). K quickly decreases to zero on approaching the sediment surface whereas D remains constant (Jørgensen and Des Marais, 1990). Hence **the DBL is the stagnant microlayer directly above the SWI through which molecular diffusion is the assumed dominant mode of transport for dissolved substances.** Recently, Guss (1998) has demonstrated that in non-bioturbated sediments, dispersive effects (undefined) can cause a more efficient exchange mechanism through the DBL than molecular diffusion alone.

The thickness of the DBL has been measured *in situ* in deep sea sediments and is generally found to be in the range 0.02-0.1 cm (e.g. Santschi *et al.,* 1983, 1991) although values as high as 0.35 cm have been measured (Archer *et al.,* 1989). Archer *et al.* (1989) determined the thickness of the DBL by inserting microelectrode oxygen sensors into the sediment. This method has subsequently been shown to reduce the DBL by up to

Figure 4.1. Schematic diagram of the vertical structure of the benthic boundary layer (BBL). Adapted from Dade *et al.* (2001). z= depth, |u|= flow magnitude.

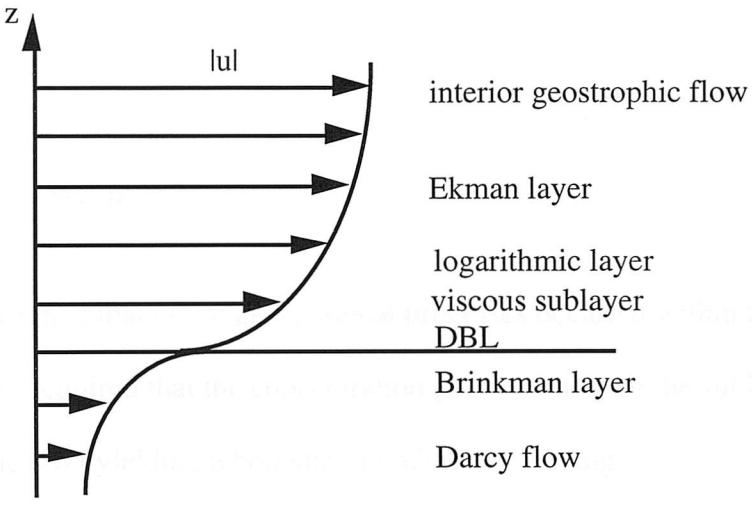


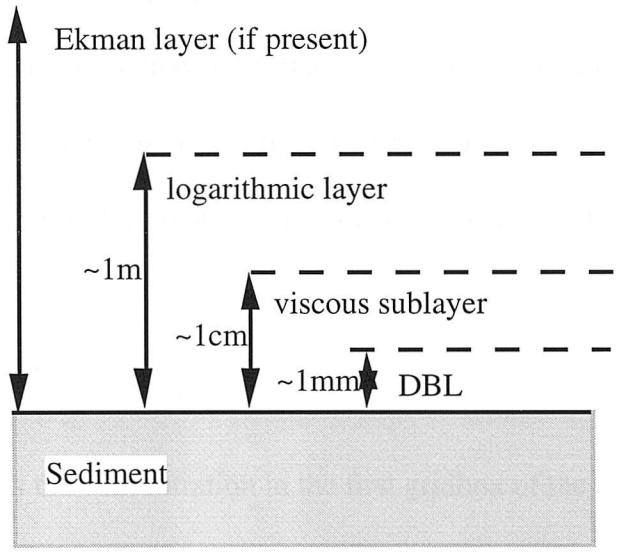


45% (Glud *et al.,* 1994), suggesting that the maximum thickness measured by Archer *et al.* (1989) may be even higher. There are no *in situ* measurements of the DBL in coastal sediments that the author is aware of, although direct measurements from laboratory

incubations of shallow water sediments have revealed DBLs of similar thickness to those in deep sea sediments (Jørgensen and Revsbech, 1985; Sweerts *et al.*, 1989).

In this Chapter, DBL thicknesses in the range 0.01 to 0.1cm were imposed on the model (see below).

### 4.3. Model setup

It was assumed that no biogeochemical processes occurred within the DBL. Hence mass continuity required that the concentration gradient through the sublayer was equal to that across the SWI yielding a boundary condition satisfying:

$$-\left[\phi \frac{\partial C}{\partial z}\right]_{z=0} = \frac{(C_w - C_{swi})}{\delta_D} \text{ (Boudreau, 1997)} \qquad 4.1$$

where $C_w$ is the concentration of the solute in the overlying turbulent flow region at the viscous- diffusive sublayer interface, $C_{swi}$ is the concentration at the SWI, $\phi$ is the porosity, $z$ is depth in the sediment and $\delta_D$ is the diffusive sublayer thickness.
At the SWI (j=0, Figure 4.2), equation 4.1 is discretised according to Boudreau, (1997) to give

$$C_0 = C_1 + \frac{\Delta z}{\delta_D}(C_w - C_{swi}) \qquad 4.2$$

where $C_1$ is the concentration in the first gridbox of the model domain (i=1, Figure 4.2) and $C_0$ is the concentration at an imaginary point at z = -Δz/2 (Δz is the grid spacing=0.1cm, Figure 4.2) and

$$C_{swi} = C_1 + \frac{\frac{\Delta z}{2}}{\left(\delta_D + \frac{\Delta z}{2}\right)}(C_w - C_1) \qquad 4.3$$

It can be seen that as $\delta_D$ approaches 0, $C_{swi}$ approaches $C_w$. Equation 4.2 can thus be substituted into the discretised form of the reaction- diffusion equation used in the model

(equation A2 in Appendix A) to give the rate of change in the top grid box (i=1 and j=0, Figure 4.2) as

$$\text{Rate of change} = -\phi_j D_{C_j} \frac{\left(\frac{\Delta z}{\delta_D}(C_{swi} - C_w)\right)}{\phi_i \Delta z^2} + \phi_{j+1} D_{C_{j+1}} \frac{(C_{i+1} - C_i)}{\phi_i \Delta z^2} + \sum R_i \qquad 4.4$$

Figure 4.2. Numerical grid incorporating the diffusive boundary layer (DBL). See text for details and refer to Figure 3.1

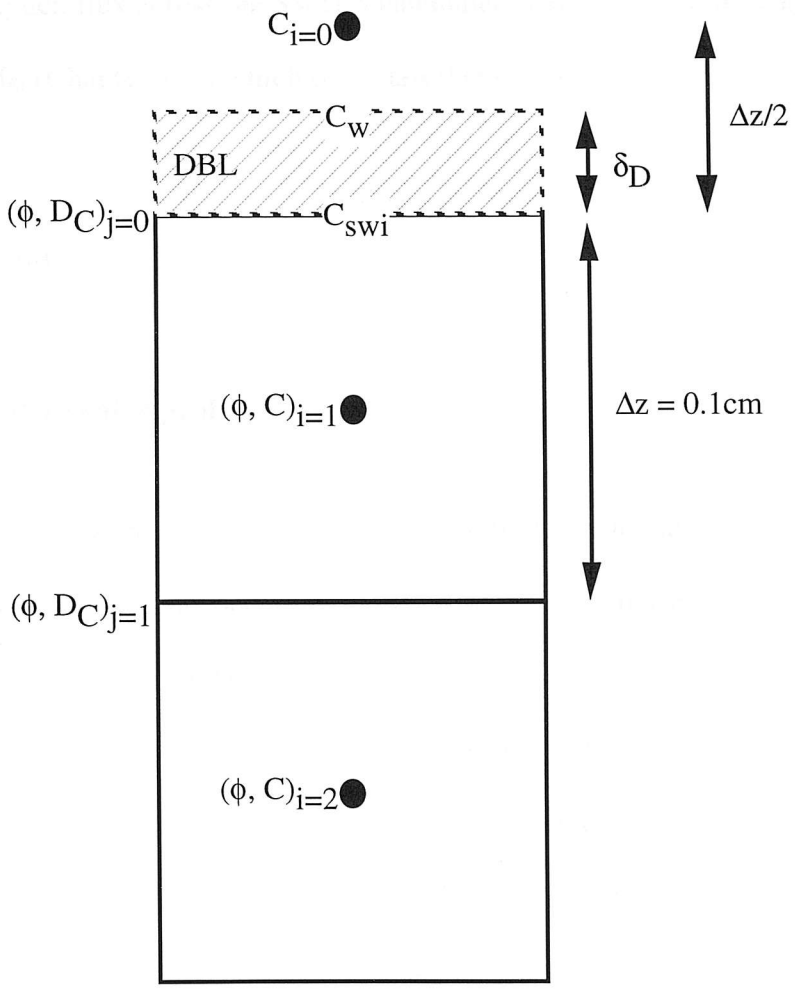


In the core incubations used to measure nutrient and oxygen fluxes in the Gt. Ouse sediments, stirring rates (300 rpm) were high enough to suppress the development of a

DBL (Glud *et al.*, 1996). Thus, a value for $\delta_D$ of 0.0001 cm was used in previous runs of the model (Chapters 3 and 4). Note that equation 4.1 precludes the use of $\delta_D$=0. The dependency of the DBL thickness on the solute (section 4.2) means that sublayer thicknesses vary by less than 10% among all variables (see equation 4.5, section 4.4). These differences had a negligible effect on the results (not shown). For simplicity, it is assumed that the thickness of the DBL is the same for each variable. In this Chapter, DBL thicknesses ($\delta_D$) in the range 0.01 to 0.1cm are imposed on the model. The model is run to a new steady state for each thickness of the DBL. The percentage change in a quantity (e.g. oxygen flux across the SWI) is calculated with respect to its standard value derived from $M_{fit}$ (Chapter 3) in which $\delta_D$ equals 0.0001 cm.

## 4.4. Results

### 4.4.1. Porewater profiles

Changes in the oxygen porewater profiles in response to variations in the thickness of the DBL at each site to are shown in Figure 4.3a-d. An increase in the thickness of the DBL decreases both oxygen penetration and oxygen concentration in the sediment at all sites (Figure 4.3a-d, Table 4.1). Lower oxygen penetration means that a greater proportion of the oxygen concentration gradient is contained in the DBL (Figure 4.3a-d). Note that oxygen concentrations are zero by a depth of 1.5 mm at all sites. This is because the resolution of the model is not high enough to resolve the depth at which oxygen concentrations would otherwise reach zero levels. From the gradients in the profiles over the first 2 millimetres (at sites and DBL thicknesses where the gradient is greater in the 0-0.5mm than in the 0.5-1.5mm depth range) it is possible, by extrapolation to the depth

axis, to approximate the maximum penetration depth of oxygen. Using this method, the penetration depths in order of increasing depth occurred at site 3, 4, 2 and 1. This is supported by the porewater concentrations of oxygen at a depth of 0.05cm which are

Table 4.1 Response of oxygen concentrations (μM) at 0.05 cm in the sediment to changes in the DBL thickness (see also Figure 4.3a)

| DBL thickness (cm) | Site 1 | 2 | 3 | 4 |
|---|---|---|---|---|
| 0.0001($M_{fit}$) | 217.00 | 180.74 | 52.74 | 98.16 |
| 0.01 | 191.45 | 153.64 | 13.28 | 53.86 |
| 0.02 | 165.95 | 128.09 | 3.96 | 21.63 |
| 0.03 | 140.75 | 104.36 | 1.79 | 9.16 |
| 0.04 | 115.83 | 82.51 | 0.89 | 5.08 |
| 0.05 | 91.17 | 62.76 | 0.43 | 3.29 |
| 0.06 | 66.68 | 45.59 | 0.20 | 2.30 |
| 0.07 | 42.20 | 31.71 | 0.10 | 1.68 |
| 0.08 | 17.20 | 21.68 | 0.06 | 1.26 |
| 0.09 | 2.10 | 15.20 | 0.04 | 0.96 |
| 0.10 | 0.40 | 11.23 | 0.03 | 0.73 |

lowest at site 3 and highest at site 1 (Table 4.1). The differences among the sites relates to the differences in rates of oxygen consumption: rates are highest at site 3 and lowest at site 1 (Table 2.2). That is, higher rates of oxygen consumption yield lower oxygen penetration and concentrations in the sediment. This has important consequences for oxygen fluxes across the SWI (section 4.4.2).

Nitrate (Figure 4.4a-d) and sulphate (Figure 4.5a-d) porewater profiles responded to increased sublayer thicknesses in a similar way to oxygen. Thicker DBLs yielded lower nitrate and sulphate concentrations in the sediment. In contrast, an increase in the DBL thickness increased the concentration of ammonium in the sediment (Figure 4.6a-d)

Figure 4.3. The effect of changing DBL thicknesses on oxygen porewater concentrations ( M)

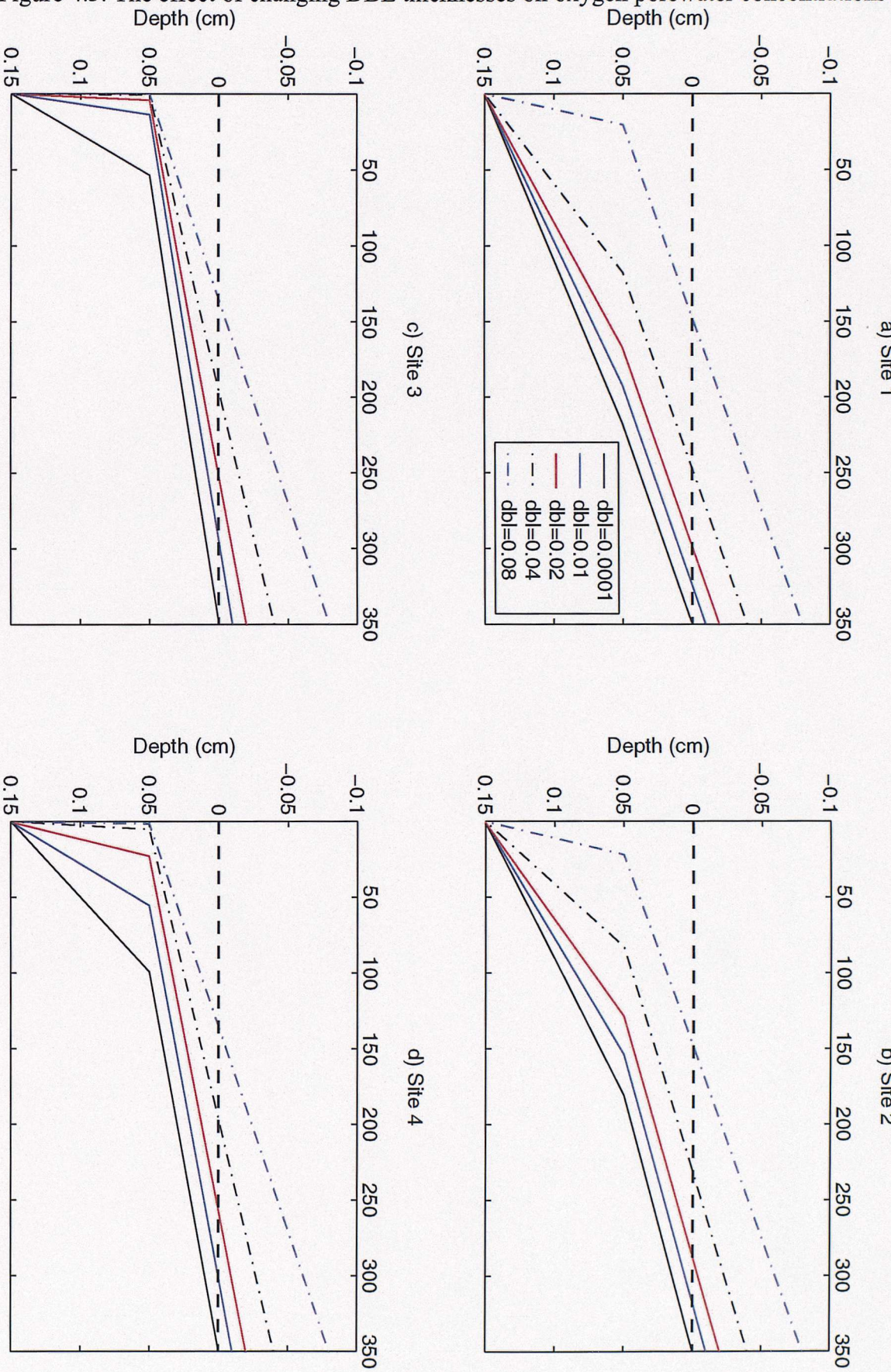

Figure 4.4. The effect of changing DBL thicknesses on nitrate porewater concentrations ( M)

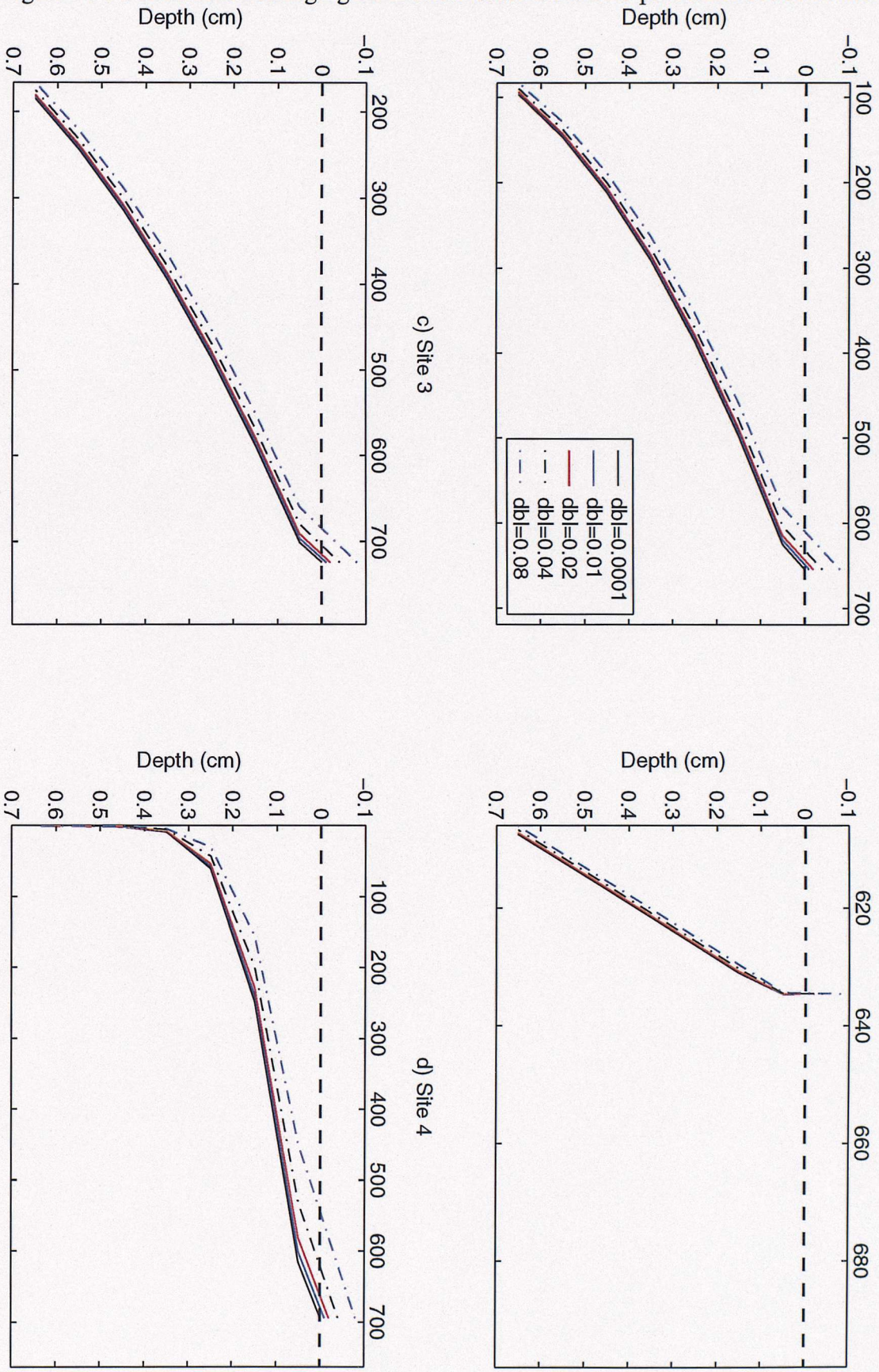

Figure 4.5. The effect of changing DBL thicknesses on sulphate porewater concentrations ( M)

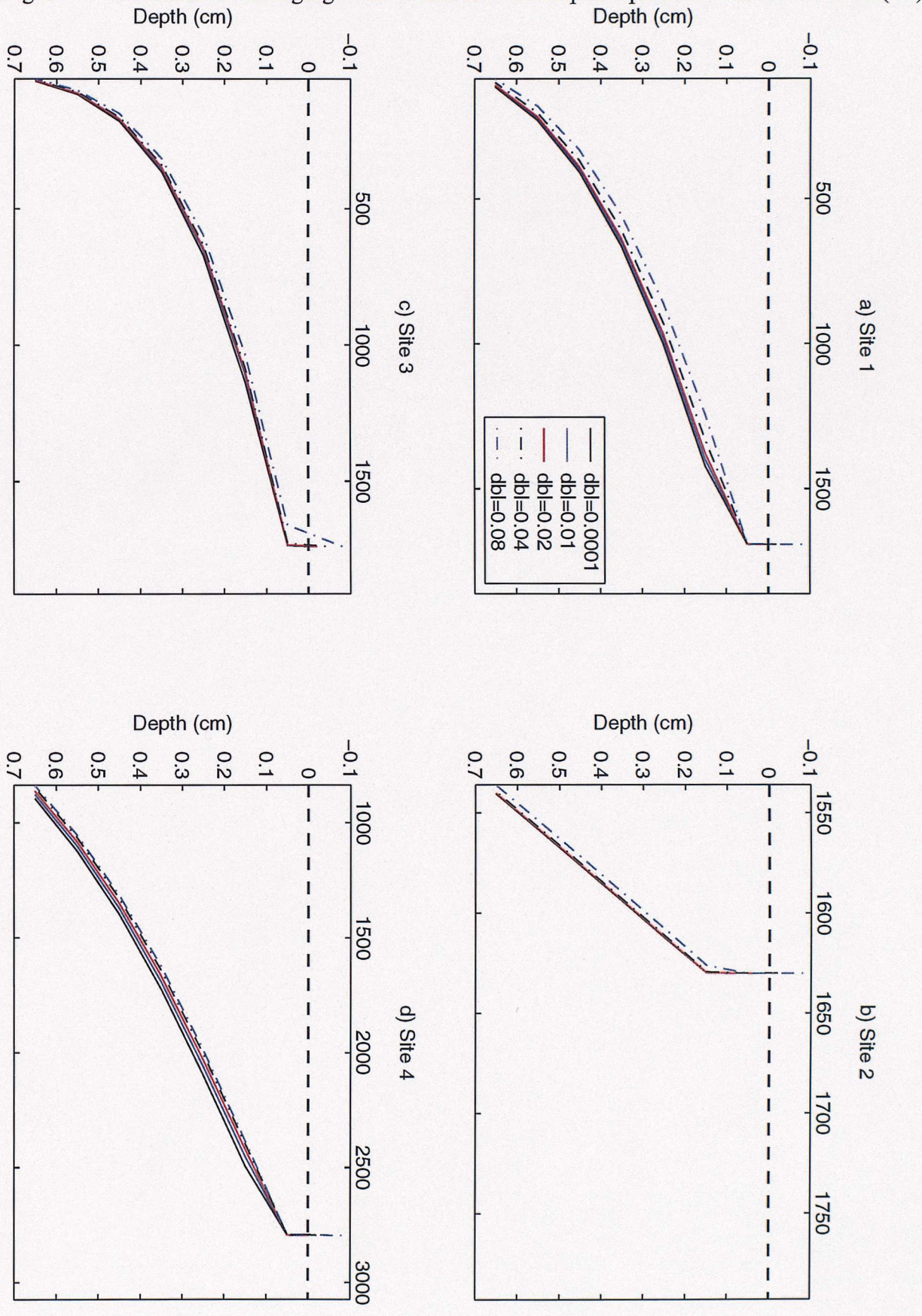

Figure 4.6. The effect of changing DBL thicknesses on ammonium porewater concentrations ( M)

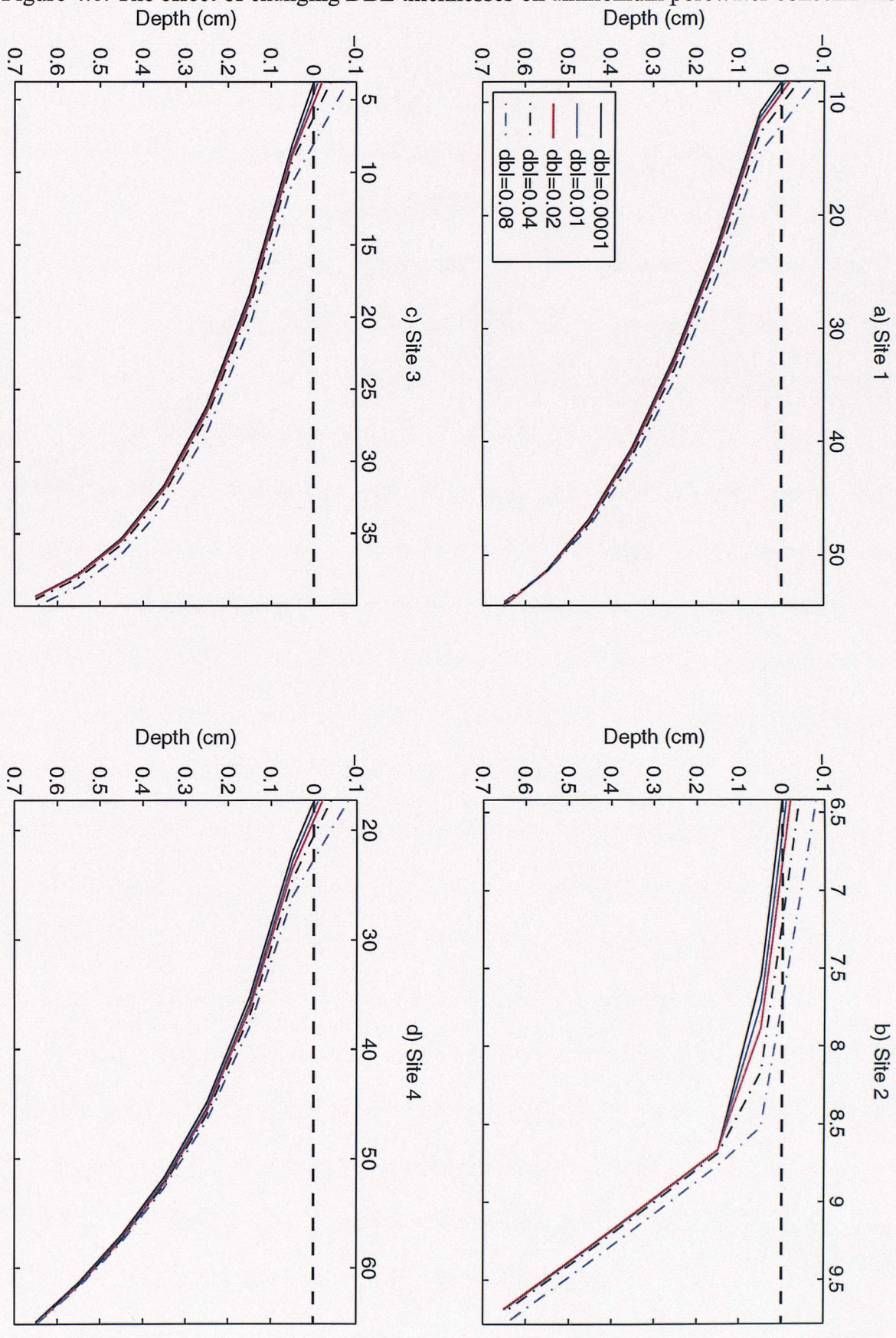

### 4.4.2 SWI fluxes

The changes in fluxes of oxygen, nitrate, sulphate and ammonium across the SWI in response to different thicknesses of the DBL at the 4 sites in the Gt. Ouse are shown in Figure 4.7a-d. Oxygen fluxes decreased with increasing thicknesses in the DBL at all sites although the strength and shape of the response was different at each site (Figure 4.7a). There was least change (<12% reduction) in the flux with increasing DBL thicknesses at site 1. The decrease was quasi- linear at site 2 and reached 33% at the maximum sublayer thickness. The largest reductions in flux were at sites 3 (61%) and 4 (53%). These differences in the response of the oxygen fluxes to changes in the DBL relates to the differences in oxygen penetration among the sites(Figure 4.3a-d). The smallest percentage change in oxygen flux occurred where oxygen penetration was deepest (site 1, Figure 4.3a). Conversely, the oxygen flux was most sensitive to changes in the sublayer thickness where oxygen penetration was least (site 3, Figure 4.3c) and hence where the proportion of the oxygen concentration contained in the DBL was greatest

Nitrate fluxes responded differently among the sites to changes in the thickness of the DBL (Figure 4.7b). The nitrate flux decreased between DBL thicknesses of 0.0001cm and 0.08cm and then increased for thicker DBLs at site 1. These changes were small (±5%). The nitrate flux at site 2 changed direction for DBL thicknesses greater than 0.05cm. This change in direction from an efflux of 0.011 mol $NO_3^-$ $m^{-2}$ $y^{-1}$ in the standard run to an influx of 0.009 mol $NO_3^-$ $m^{-2}$ $y^{-1}$ at the maximum DBL thickness applied means that the flux cannot be plotted on Figure 4.7b. The fluxes of nitrate at sites 3 and 4 responded in a similar way (hyperbolic) to variations in the DBL. Fluxes increased by 11% (site 3) and by 20% (site 4) at a DBL thickness of 0.1cm.

Figure 4.7. The effect of changing DBL thicknesses on solute fluxes across the SWI at 4 sites in the Gt. Ouse.

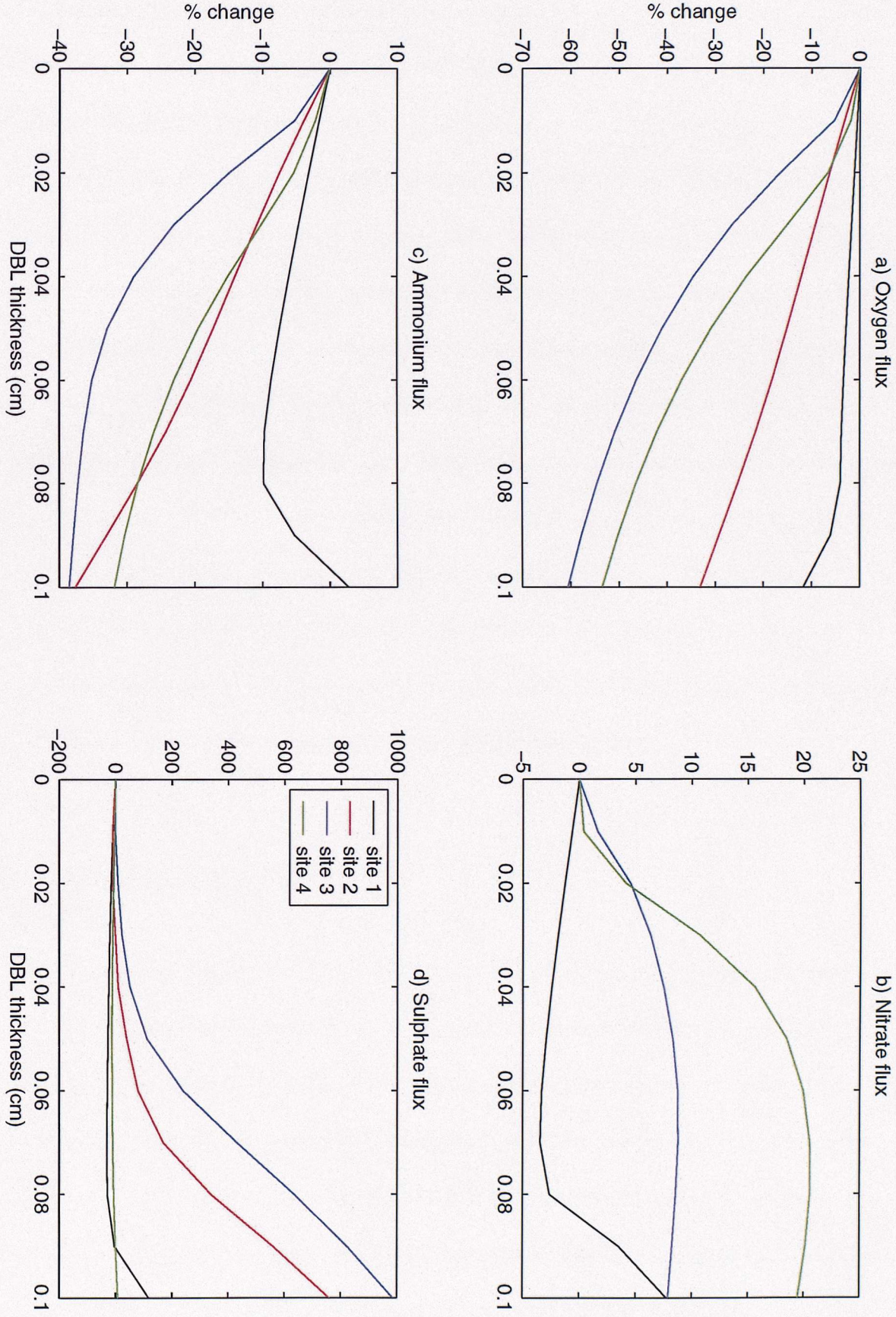

Ammonium effluxes and their response to the DBL are shown in Figure 4.7c. The ammonium efflux decreased (12%) and then increased (3%) as the DBL thickened at site 1. This change in response at site 1 occurred over a change in thickness in the DBL between 0.08cm and 0.09cm. The efflux of ammonium decreased at sites 2, 3 and 4 with increasing sublayer thickness (by 38%, 30% and 27%, respectively, at a DBL thickness of 0.1cm). The decrease in efflux was approximately linear at site 2 and quasi-parabolic at sites 3 and 4. Predicted effluxes were highest at both of these latter sites (Figure 2.4c).

Sulphate fluxes to the sediment increased in response to thicker DBLs at all sites [Figure 4.7d]. The sulphate flux decreased (20%) and then increased (140%) with increasing DBL thickness at site 1. The change from a decrease to an increase occurred for DBL thicknesses between 0.08cm and 0.09cm, similar to the response of the ammonium and nitrate fluxes at this site. The largest increases occured at sites 3 (980%) and 2 (780%). The increase at site 3 represented changes in the flux from 0.18 mol $SO_4^{=}$ $m^{-2}$ $y^{-1}$ to 1.76 mol $SO_4^{=}$ $m^{-2}$ $y^{-1}$ whereas at site 2 the change was in a lower range (<0.0001 mol $SO_4^{=}$ $m^{-2}$ $y^{-1}$). The lowest increase in flux occurred at site 4 (12%).

### 4.4.2. Sedimentary processes

The effects of variations in the thickness of the DBL on sedimentary processes (total carbon oxidation, oxic mineralization, suboxic mineralization (denitrification), anoxic mineralization (sulphate reduction), nitrification and sulphide oxidation) at all sites are shown in Figure 4.8a-g. Rates of total carbon oxidation decreased with increasing DBL thicknesses at all sites (Figure 4.8a). The largest decreases in rates of total carbon mineralization occurred at site 3 (42%) and the smallest change occurred at site 1 (8%). A similar response occurred with the rates of oxic mineralization(Figure 4.8b). The sudden

Figure 4.8. The effect of changing DBL thicknesses on modeled sedimentary processes

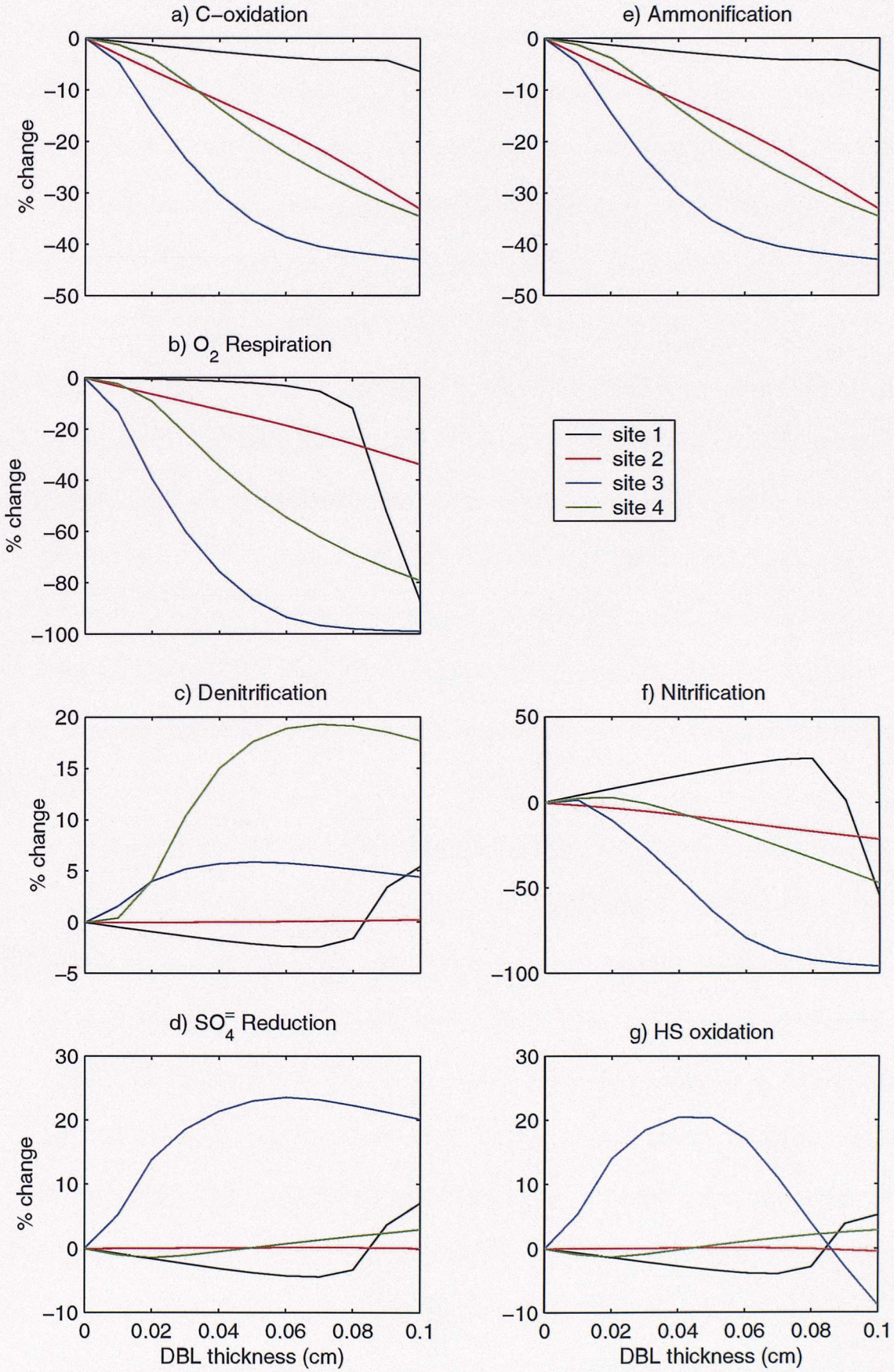

change in the percentage reduction in rates of oxic mineralization beyond a DBL thickness of 0.08cm at site 1 occurred because the oxygen concentration in the porewater became limiting ie the porewater oxygen concentration decreased from 17.2 μM to 2.1 μM at a sediment depth of 0.05cm between DBL thicknesses of 0.08cm and 0.09cm (Table 4.1) which meant that oxygen levels were lower than the half saturation constant for oxygen limitation in oxic mineralization ($k_{sO2}$ = 3 μM, Table 3.2). Rates of oxic mineralization were more than halved once oxygen concentrations became limiting. The responses of both oxic and total carbon mineralization followed the response of the oxygen fluxes to changes in the DBL at each site (Figure 4.3a). This resulted from the fact that a reduction in the flux of oxygen reduced the supply to oxic mineralization. Where oxic mineralization contributed significantly (50-98%, Table 2.2) to the sum of total organic matter degradation (sites 2-4), a decrease in oxic mineralization had the greatest effect on total carbon oxidation (Figure 4.4a). Consequently, the higher the contribution of oxic mineralization to total organic matter oxidation, the greater the sensitivity of the latter to variations in the DBL.

Rates of denitrification did not respond uniformly to increases in the DBL at the sites (Figure 4. 8c). The rate decreased (~3%) and then increased (~6%) with increasing DBL thickness at site 1. This change in response at site 1 occurred between a DBL of 0.08cm and 0.09cm which corresponds to the point at which oxygen concentrations (Table 4.1) became lower than the half saturation constant for oxygen inhibition in denitrification ($k_{sInhO2}$ = 6.25 μM $O_2$, Table 3.2). For oxygen concentrations less than or equal to $k_{sInhO2}$ to, rates of denitrification proceeded at least as fast as half the maximum rate (equation 3.8). Hence the change from a decreased to an increased denitrification rate between a DBL of 0.08cm and 0.09cm at site 1. Rates of denitrification were unaffected by the thickness of the DBL at site 2 where the low rates were fuelled by nitrate derived from

nitrification rather than from the overlying water. An increase in the DBL enhanced rates of denitrification in a similar way (hyperbolic) at sites 3 and 4. The increase was less than 6% at site 3 while rates of denitrification were increased by up to 19% at site 4 where rates of denitrification were higher (Figure 3.4b; note also that $k_{no3} = 3.63\ y^{-1}$ at site 4 while $k_{no3} = 0.19\ y^{-1}$ at site 3, Table 2.5). The increases in denitrification at sites 3 and 4 were facilitated by the lower oxygen concentrations in the sediment and the greater rate of change of oxygen with respect to changes in the DBL thickness compared to site 1 (Table 4.1). The response of denitrification to changes in the DBL explain the response of the nitrate fluxes at sites 1, 3 and 4 (Figure 4.2b). The decrease in oxygen availability with increasing DBL thickness at site 2 (Table 4.1) meant that nitrification rates decreased (see below) and became lower than rates of denitrification. This explains the change in direction of the flux of nitrate at site 2 (section 4.4.2).

Rates of sulphate reduction responded differently to changes in the DBL among the sites (Figure 4.8d). The decrease (~ 3%) and increase (~7%) in rates at site 1 have a similar causation to the response of denitrification rates at this site (Figure 4.8c). This causation is the oxygen concentration in the porewater an its value compared to the half saturation constant for oxygen inhibition in anoxic mineralization, $k_{sAnoxInhO2}$ (=3 μM $O_2$, Table 3.2). The decrease was caused by the high inhibitory concentrations of oxygen (>>$k_{sAnoxInhO2}$) for DBL thicknesses of up to 0.08cm (Table 4.1). For thicker DBLs the oxygen concentration was lower than $k_{sAnoxInhO2}$ e.g. at DBL=0.09cm the oxygen concentration was 2.1 μM at a 0.05cm depth (Table 4.1). This response explains the response of the ammonium efflux to changes in DBL at site 1 (Figure 4.3c). Ammonium production was dominated by sulphate reduction at this site (ie anoxic mineralization was the dominant organic carbon oxidation pathway, Table 2.2) and so changes in sulphate reduction were reflected in changes in the ammonium efflux. Rates of sulphate reduction

were insensitive to changes in the DBL at site 2. Sulphate reduction rates were most sensitive to changes in the DBL at site 3 where rates increased by up to 23% (Figure 4.4d). This increase was facilitated by the low concentrations of oxygen ($<k_{sAnoxInhO2}$) for DBL thicknesses greater than 0.01cm (Table 4.1). Rates of sulphate reduction remained within ± 3% of the standard value for the range of DBL thicknesses used at site 4.

Rates of ammonification are the total production rates of ammonium from organic matter mineralization. Hence, rates of ammonium production decreased with increasing sublayer thicknesses (Figure 4.8e, compare with Figure 4.8a). This decrease in ammonification is paradoxical when set against the increase in concentrations of ammonium in the porewaters at all sites (Figure 4.6a-d). To understand this, it is important to consider that the diffusion path length increases between the bottom boundary of the model at 15cm (Table 2.3) and the top of the DBL. The effect of this is best illustrated by considering the behaviour of a conservative tracer affected only by diffusion between a constant source at depth and a constant sink at the surface (Figure 4.9). An increase in the distance between the positions of two fixed porewater concentrations of a conservative tracer reduces the diffusive flux through the sediment and hence increases the sedimentary concentration. This increase occurred with the ammonium concentrations even though ammonification had been reduced, ie the increase in the diffusion path length with increasing DBL thickness reduced the flux of ammonium through the sediment which counteracted the effects of the reduced ammonium production on ammonium concentrations.

There was a variable response of nitrification to changes in the DBL thickness (Figure 4.8f). Rates of nitrification increased by 45% before decreasing by a similar amount with increasing sublayer thickness at site 1. The initial increase was facilitated by the increased ammonium concentrations in the porewater (Figure 4.6a) and the non-

Figure 4.9. Effect of increasing the diffusion distance between two fixed end point concentrations of an idealized conservative tracer in a model sediment ($C_0$, $C_1$= fixed concentration at the surface and bottom where $C_0 < C_1$; $dz_{1,2}$=diffusion distance between $C_0$ and $C_1$)

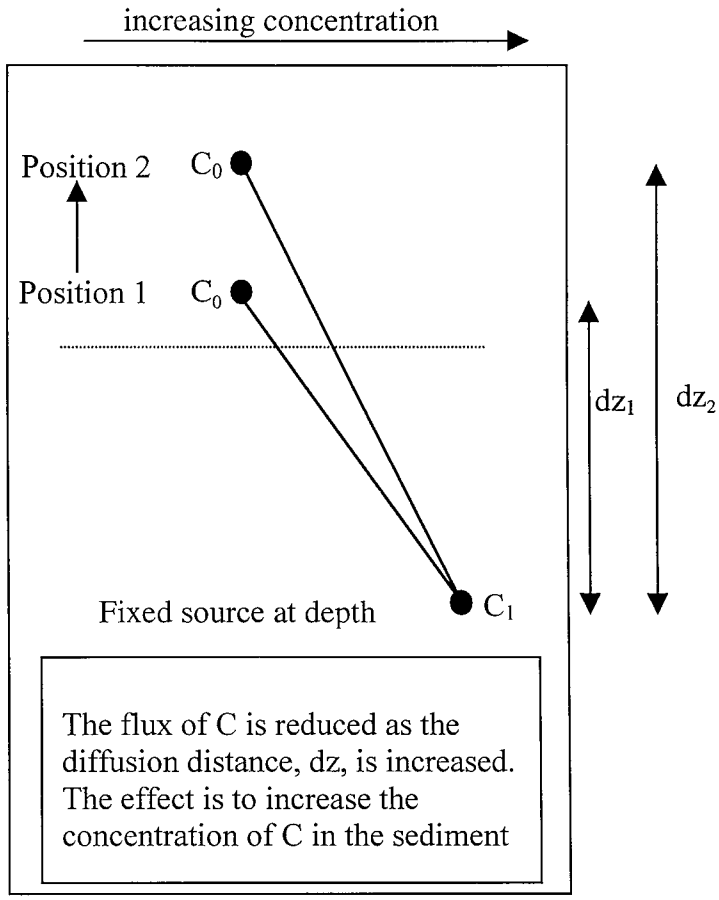


limiting oxygen concentrations (Table 4.1). Rates of nitrification decreased relative to the standard run when oxygen concentrations were lower than the half saturation constant for oxygen limitation in nitrification ($k_{sLimO2}$=1 μM $O_2$, Table 3.2) ie at DBL=0.09cm, the oxygen concentration was 0.4 μM at 0.05cm depth (Table 4.1). Nitrification rates decreased (by a maximum of 20%) with increasing sublayer thickness at site 2. This was because ammonium concentrations were lowest (<10 μM) in the zone of nitrification (upper 2mm) at this site (Figure 4.6b) compared to the other sites (Figure 4.6a, c, d). Hence the effect of the increase in ammonium concentrations with increasing DBL thickness was small (<2 μM) compared to the effect of decreasing oxygen concentrations

at site 2 (Table 4.1). The response of rates of nitrification to changes in the DBL was greatest at sites 3 and 4. The rate of nitrification increased initially with increases in the DBL at both sites and then decreased as soon as oxygen concentrations fell below $k_{sLimO2}$. This change in response from an increase to a decrease occurred for a smaller DBL thickness at site 3 compared to site 4 which resulted from the lower oxygen penetration depth at site 3 compared to site 4 (section 4.3.1.1). The overall reduction was greatest at site 3 where the 90% decrease in nitrification was fuelled by the 95% reduction in ammonium production from oxic mineralization (Figure 4.7b).

Rates of sulphide oxidation (Figure 4.8g) followed a similar pattern to sulphate reduction (Figure 4.8d) in response to variations in the DBL at sites 1 and 4. The response at site 3 where sulphide oxidation rates decreased once the DBL thickness exceeded 0.04cm, was driven by the limiting oxygen concentrations ($\leq$ 0.89 μM, Table 4.1) which were lower than the half saturation constant for oxygen limitation in sulphide oxidation ($k_{sSox}$=1 μM $O_2$, Table 3.2). This reduction in sulphide oxidation meant that in order to sustain the increased rates of sulphate reduction for thicker DBLs at site 3 (Figure 4.7d), the supply of sulphate from the overlying water increased (Figure 4.3d). The large percentage increase in the flux occurred because the changes in the magnitude of both sulphide oxidation and sulphate reduction were large in comparison to the sulphate flux (Table B2.7-B2.10). Similar reasoning explains the response of both sulphide oxidation and sulphate fluxes at site 2 (Figure 4.7d).

## 4.5. Discussion

At steady state the benthic flux is balanced by the integrated reaction rate over the sediment depth. In the model presented here, only the DBL thickness was changed

between runs. The concentration of organic matter in the model sediment and the bottom water boundary conditions were the same at each site between model runs. Hence it is not surprising that changes in the diffusive sublayer thickness (which alters the diffusion time through the DBL) influenced the reaction rates in the sediment. Furthermore, an increase in the diffusive sublayer thickness increased the proportion of the oxygen concentration gradient that is contained within the DBL (Figure 4.5). This explains why increases in DBLs have a greater impact on oxygen fluxes and mineralization rates and supports the earlier predictions of Archer *et al.* (1989) (section 4.1). The narrower the oxic layer relative to the thickness of the DBL, the greater the control of the DBL on solute exchange at the SWI because more of the diffusion time occurs in the DBL compared to the sediment. Also, thinner oxic layers decrease the diffusion path length of nitrate and sulphate between the upper boundary of the DBL and the zones of denitrification and sulphate reduction. However, any effect this might have on nitrate and sulphate fluxes was negligible in the thin oxic layers (<2mm) of the Gt. Ouse sediments. One important implication of a reduction in oxic mineralization is the effect on the ammonium effluxes. These may be reduced by 25-30% (equivalent to 0.13 mol $NH_4^+$ $m^{-2}$ $y^{-1}$) in the presence of a diffusive sublayer of thickness 0.05-0.1cm (site 3, Figure 4.3c). This can limit rates of primary production in areas where 80-94% of the nitrogen required by phytoplankton is regenerated in the sediments (Fisher *et al.,* 1982; Cowan *et al.,* 1996). The large effect of the DBL on nitrification rates (Figure 4.8f) had no effect on rates of denitrification (Figure 4.8c) even at site 2 where $D_n$ accounted for 100% of the total denitrification (Nedwell and Trimmer, 1996). A possible impact of changes in the nitrification rate is the impact on the flux of nitrous oxide from the sediments. Estimates of the global source of nitrous oxide suggest that the oceans account for between 22% and 36% of emmissions (Bouwman *et al.,* 1995). Unfortunately, the relative contribution of sedimentary and water column

processes to the oceanic flux is unknown and controversy exists over whether nitrification or denitrification is more important in the formation of nitrous oxide (see discussion in Suntharalingam and Sarmiento, 2000). Recent work suggests that denitrification is the sedimentary source of nitrous oxide in shallow sediments (GarciaRuiz *et al.,* 1998; Dong *et al.,* 2000) and analysis of porewater profiles indicate that nitrification is the source of nitrous oxide in deeper sediments (Koike and Terauchi, 1996; Usui *et al.,* 1998). In the latter work (Usui *et al.,* 1998) porewater profiles revealed oxygen penetration depths of at least 2cm which is common for deep sea sediments (e.g. Jahnke *et al.,* 1989; Glud *et al.,* 1994). As discussed earlier in this section, such deep oxygen penetration means it is unlikely that changes in the DBL will affect oxygen availability and hence rates of nitrification and emmissions of nitrous oxide.

The predicted effects of the DBL on total organic matter oxidation, rates of denitrification and benthic fluxes can have implications for nutrient and carbon budgets. For instance, changes in rates of organic degradation can influence the preservation of organic matter in sediments although other factors may be more important (Hedges and Kiel, 1995). These authors concluded that 45% of organic matter inputs are preserved on shelf sediments which contrasts with more recent calculations suggesting that shelf seas play only a minor role in the preservation and withdrawal of organic carbon from the global carbon cycle (de Haas *et al.,* 2002). In either case, the presence of a diffusive sublayer may increase the organic carbon preservation capability of shelf sea sediments. For instance, the major region of organic carbon accumulation in the southern North Sea (Figure 2 in de Haas *et al.,* 2002) is the same area where some of the highest organic degradation rates were measured (sites 2 and 3 in Up ton *et al.,* 1993) and is close to where oxygen penetration can be less than 0.1cm ( Lohse *et al.,* 1996) and where weak

tidal currents and infrequent mobilization of the sediment occur (site B in Williams *et al.*, 1998). It is possible to calculate a likely range in DBL thicknesses in this region from:

$$\delta_D = 5Sc^{-1/3}\nu u_* \qquad \text{(Dade } et\ al.,\ 2001) \qquad 4.5$$

where ν is the kinematic viscosity (=0.01 cm $s^{-1}$ , Boudreau, 1997), $u_*$ is the near bed current shear velocity (0.1-0.81 cm $s^{-1}$ measured in September 1989 at site B in Williams *et al.*, 1998) and *Sc* is the Schmidt number (=ν/D, Sideman and Pinczewski 1975 quoted in Boudreau, 1997 where D is the temperature corrected free water diffusion coefficient). Assuming a temperature of ~10°C (September 1989 at site 3 in Figure 4 in Up ton *et al.*, 1993) and using equation 3.3 (with ϕ set to 1) and the relevant parameters in Table 3.2 to calculate the diffusion coefficient for oxygen, yields a DBL thickness of 0.006-0.05 cm. In measuring the benthic oxygen consumption rates in this area, Up ton *et al.* (1993) averaged their measurements over a range of stirring speeds greater than 300rpm. Such speeds are greater than that needed to suppress the DBL (Glud *et al.*, 1996). Results from this modelling study make it possible to speculate that a neglect of the DBL may overestimate total carbon oxidation rates by up to 53% ($\delta_D$ =0.05 at site 3, Figure 4.8a) in these carbon accumulating sediments of the southern North Sea. As the majority of organic degradation was mediated by oxygen (74.7%, Up ton *et al.*, 1993), it is possible that such a reduction in organic matter mineralization may promote carbon preservation. However, such speculation must be treated with caution as the sediments in this region are sandy muds (20-28% mud, Up ton *et al.*, 1993; Lohse *et al.*, 1996; de Haas, 1997; Morris *et al.*, 1998; $D_{50}$=100μm, Williams *et al.*, 1998) in which advective and dispersive porewater fluxes can dominate the transport of solutes in the upper millimetres (Huettel and Gust, 1992; Lohse *et al.*, 1996). This is likely to be the case in the shallow (<7m)

sediments of the Gt. Ouse, where maximum current speeds of 2 m $s^{-1}$ in this fast flowing canalized river system can scour the surface sediments (Gould *et al.,* 1984). Consequently, the potential of the DBL to promote carbon preservation is likely to be greater in fine grained, less permeable sediments with low enough near bed current velocities. An example is Southampton Water (UK) where the sediments are predominantly muddy (Velegrakis, 2000) and near bed current velocities (0.1-7.7 cm $s^{-1}$ for 29% of a 2 month period, J. Waniek, unpublished ADCP mooring data 0.5m above the sediment surface) are close to values for which DBLs in the range 0.016-0.12 cm have been determined in experimental settings (0.3-7.7 cm $s^{-1}$, Jørgensen and Des Marais, 1990; 2.0-8.0 cm $s^{-1}$, Santschi *et al.,* 1991; 2.4-4.6 cm $s^{-1}$, Glud *et al.,* 1995). Consequently, the presence of a DBL should be considered when measuring benthic solute exchange in these environments although sediment permeability and its influence on porewater advection should be taken into account. This acts as a caveat for carbon budget studies which rely on benthic fluxes measured using incubation methods which alter the *in situ* hydrodynamics and change the thickness of the diffusive sublayer.

Jørgensen and Boudreau (2001) modeled the effect of the DBL on oxygen fluxes in coastal and deep sea sediments. It was assumed that oxygen was only consumed by sulphide oxidation in the coastal scenario while benthic oxygen demand was assumed to be driven by oxic mineralization in the deep sea case. A separate model was defined for each example, each one mathematically simple enough to be solved analytically. The diffusive flux across the SWI was then derived to show its relationship to the diffusive sublayer. Jørgensen and Boudreau (2001) found that the diffusive flux at the SWI was independent of the oxygen concentration in the coastal scenario while the deep sea counterpart was dependent on rates of oxygen consumption: the lower the rate, the greater the oxygen penetration and the less influence of the DBL on the oxygen flux.

Consequently, they concluded that the DBL had no impact on oxygen fluxes. These authors then speculated that organic carbon preservation would be unaffected by the DBL in both cases (note that the oxygen flux was related to by-product oxidation rather than to organic degradation in the coastal scenario). To support these model results, Jørgensen and Boudreau (2001) cited the experimental work of Glud *et al.* (1994) which showed that as the DBL decreased from 0.046cm to 0.036cm, the diffusive flux of oxygen was reduced by only 8%. In contrast to the models of Jørgensen and Boudreau (2001), the model presented here simulates oxygen consumption due to both reoxidation processes and organic matter degradation. This model can only be solved numerically at present, ie no analytical solutions exist. For changes in the DBL over the same range as in Glud *et al.* (1994), the change in the oxygen flux was similar ie less than 10% (Figure 4.7a). However, larger changes in the thickness of the diffusive sublayer (0.0001 cm - 0.1 cm) reduced the oxygen flux by between 12% and 60% (Figure 4.7a). The DBL had the least influence on benthic oxygen demand where sulphide oxidation dominated the oxygen budget (site 1, Figure 4.3a) which supports the near shore scenario of Jørgensen and Boudreau (2001) but for different reasons. The model results at site 1 were caused because the oxygen penetration was deepest (Table 4.1) and the oxygen consumption rate was least (Table 2.2) at this site. The effect of the DBL on oxygen fluxes was greatest where oxygen consumption was highest and where oxygen penetration was least (sites 3 and 4). To assume that oxygen consumption is dominated by by-product oxidation in shallow coastal sediments results in the conclusion that the effect of the DBL on benthic fluxes is insignificant. The organic carbon and oxygen budgets of the Gt. Ouse sediments show that near shore sediments are not necessarily respectively dominated by sulphate reduction and sulphide oxidation (Nedwell and Trimmer, 1996). The same is true for coastal sea sediments such as those in the North Sea (e.g. Up ton *et al.*, 1993). This modelling study

suggests that when oxic mineralization is the dominant oxygen consuming process in shallow sediments it is important to account for the effect of the DBL when measuring benthic fluxes.

The application of a 1 dimensional model to investigate changes in the DBL thickness assumes that the sediment surface is flat. In contrast, natural marine sediments are characterized by complex surface topography (e.g. Gunderson and Jørgensen, 1990) and this can affect the structure and flux of solutes across the DBL (Jørgensen and Des Marais,1990). The latter authors calculated that the presence of a microbial mat on the sediment surface increased the diffusive flux by 49% when compared to one dimensional diffusion calculations. Røy *et al.* (2002) encountered errors in these calculations but still found the difference to be approximately 30%. The same authors showed that the difference between 1 dimensional and 3 dimensional diffusive fluxes was less than 10% within the DBL over bioturbated sediments. Røy *et al.* (2002) argued that use of 1D models of the DBL was widely applicable except where extreme horizontal heterogeneity occurred (e.g. bioturbated sediment with active benthic photosynthesis). This supports the 1 dimensional approach used here.

## 4.6. Conclusions

This is the first attempt to look at changes in the DBL on sedimentary processes and on benthic fluxes other than oxygen. The response to changes in the DBL were not uniform among the sites and depended on differences in oxygen penetration depths and first order rate constants for organic mineralization. Generally, fluxes of oxygen and ammonium across the SWI decreased with increasing DBL thickness while fluxes of nitrate and sulphate increased with thicker DBLs. The response of oxygen fluxes to changes in the

DBL in the model support the predictions of Archer *et al.* (1989). That is, the lower the oxygen penetration the greater the sensitivity of oxygen consumption rates to changes in the diffusive sublayer. This is because lower oxygen penetration means that a higher proportion of the oxygen concentration gradient is contained in the DBL.

Rates of denitrification increased by up to 20% at a DBL thickness of 0.1cm. This was fuelled by the lowering of the oxygen penetration depth which in turn fuelled the increase in nitrate fluxes. Similarly, the change in rates of sulphate reduction due to variations in the DBL caused the changes to the sulphate fluxes. Rates of nitrification increased by up to 45% and decreased by up to 90% with increasing DBL thickness. This had little effect on nitrate fluxes except where nitrification rates were greater than rates of denitrification (site 2). In the latter case, the nitrate efflux changed to an influx with increasing sublayer thickness. Consequences for nitrous oxide production from nitrification were argued to be negligible. The largest percentage change due to increasing DBL thicknesses occurred for sulphate fluxes (980%). These were fuelled by the increase in sulphate reduction as the sulphate supply from sulphide oxidation decreased under increased oxygen limitation.

Rates of total organic matter oxidation were lowered (8%-42%) in response to increased thicknesses of the DBL at all sites. The largest percentage change in total organic matter mineralization occurred where oxygen penetration was least and where oxic respiration was the dominant mineralization pathway. This lowering of organic mineralization rates reduced the ammonium effluxes by up to 30%. This could limit rates of primary production in areas where phytoplankton growth is fuelled by nitrogen regenerated in the sediments.

Core incubation derived solute fluxes which use a high stirring rate assume that the DBL is not a controlling factor of early diagenesis. This assumption is appropriate for the

shallow sediments of the Gt. Ouse which experience high current speeds. However in other shallow/coastal sediments, near bed hydrodynamic conditions may favour the development of a DBL. The model results suggest that for the range in measured thicknesses of the DBL, solute fluxes obtained from core incubation experiments may not represent *in situ* fluxes. Coupled with the fact that oxygen consumption can be dominated by oxic mineralization rather than by the oxidation of reduced substances, the DBL can influence organic carbon preservation.

# 5. Modelling observed seasonality in the upper Gt. Ouse sediments

## 5.1. Introduction

Much effort has focussed on trying to understand what factors dominate the regulation of both the sediment water exchanges of nutrients (and oxygen) and the sedimentary processes themselves. Examples of such factors include the supply and quality of organic material (Nixon, 1981; Jensen *et al.,* 1990; Osinga *et al.,* 1996), temperature (Hargrave, 1969; Nedwell and Trimmer, 1996; Trimmer *et al.,* 1998), the redox status of the sediments and the water column (Patrick and Khalid, 1974; Sundby *et al.,* 1992), overlying nutrient concentrations (Kieskamp *et al.,* 1991; Magalhaes *et al.,* 2002) which influence diffusion gradients and thus the direction of the fluxes into or from the sediment, macroinfaunal activity (Aller and Aller, 1998) and the physical stability of the sediment (Vidal, 1994), the last two of which may influence diffusion gradients. The relative importance of these factors varies from one estuary to another. However, some studies have shown that the ultimate control of nutrient fluxes and diagenetic processes is the supply of organic matter to the sediments (Kelly and Nixon, 1984; Jensen *et al.,* 1990; Cowan *et al.,* 1996). All of these factors have seasonal signals which in turn produce the variability observed in diagenetic processes. Understanding this variability is important because nutrients regenerated in the sediments can sustain pelagic primary production (Officer and Ryther, 1980; Jensen *et al.,* 1990; Cowan *et al.,* 1996). Up to 80% of the nitrogen and phosphorus required by phytoplankton in estuaries may be derived from sedimentary nutrient regeneration (Fisher *et al.,* 1982).

The extent to which seasonal changes in observed sediment temperatures and solute concentrations control the observed seasonality in porewater profiles and fluxes across the

SWI of oxygen, nitrate, ammonium and sulphate (not measured) in the upper Gt. Ouse sediments is examined in this Chapter. This will test the assumption of steady state with respect to the organic carbon concentrations as well as the robustness of the calibrated first order rate constants derived by the model in Chapter 3 (Table 3.5).

## 5.2. Changes to the model in Chapter 3 required to account for seasonality

To model all four sites in the upper Gt. Ouse on every occasion measurements were made, the model needs to take account of changes in temperature and changes in the concentration of solutes (nitrate, oxygen, sulphate and ammonium) in the water column. Below is a description of the how these changes have been implemented. Unless stated, all model details (e.g. equations, assumptions) are identical to those in Chapter 3 (section 3.1.2). Note that the thickness of the DBL is 0.0001cm as in $M_{fit}$.

### 5.2.1. Temperature

Model equations have been adapted to account for changes in temperature. This has been done by using an Arrhenius-type temperature function of the form

$$Q10fact = e^{0.07(Temperature-20)} \qquad 5.1$$

This multiplies the reaction terms for rates of nitrification and TOC mineralization via oxygen, nitrate and sulphate in the model equations (Table 3.1). This temperature effect

assumes a $Q_{10}$ of 2 which means that for each 10°C rise in temperature, the rate of a microbiologically mediated process (e.g. oxic mineralisation, denitrification) doubles.

### 5.2.2. Boundary conditions

Top boundary values at the sediment-water interface (SWI) for oxygen, nitrate, ammonium and sulphate are the mean (triplicates) core incubation concentrations in the water column at the end of the incubation period (Figure 2.2). Free sulphide levels are set to zero in the water column for all model runs. A zero flux bottom boundary condition is imposed for oxygen, nitrate, sulphate and free sulphide. For ammonium, the bottom boundary is prescribed with measurements of the porewater concentration at 15cm depth (Figure 2.2).

### 5.2.3. Initial conditions

Measured TOC concentrations (see Table 1.4a) were imposed in each model box and assumed to be evenly distributed with depth. This assumption derives directly from the measurements (Nedwell and Trimmer, 1996). Initial concentrations of oxygen, nitrate, ammonium, sulphate and sulphide were arbitrarily set. Preliminary runs showed that the model outcome was not sensitive to the initial conditions of these variables.

### 5.3. Porewater data and location of the concentration in top 1cm of sediment

To compare observed monthly porewater concentrations with the monthly model output, an approximation of the actual depth of the measured concentrations needs to be calculated. Porewater profiles for nitrate, ammonium and sulphate were taken from core sediment slices (Figure 5.1) at 1cm intervals for the 0 to 5cm horizon, and at 9 to 10 and 14 to 15cm depths (Nedwell and Trimmer, 1996). These coarse resolution porewater measurements represent the mean solute concentration in a particular slice of sediment. No information on the depth location of that mean concentration is provided. This becomes important where sharp gradients exist, such as for nitrate in the upper 1cm of sediment. As this is beyond the resolution of the measurements, for model comparison purposes, the position of the upper 1cm concentration for porewater nitrate is calculated by fitting an exponential function to the data. Any function fitted to the change in concentration of a solute with depth in the sediment must, upon integration over an interval, yield the measured average concentration over that interval (Morse, 1974). Thus

$$\int_{z_0}^{z_1} N_0 e^{-kz} dz = N_{obs} \qquad 5.2$$

where

$N_0$ = measured concentration in overlying water (or at the sediment-water interface)

$N_{obs}$ = average measured concentration for top 1cm slice

$k$ = coefficient of decrease (similar to first order rate constant)

$z$ = depth

$z_0$ = 0cm depth (the sediment-water interface)

$z_1$ = 1cm

Figure 5.1. Converting sediment core measurements into porewater concentration profiles.

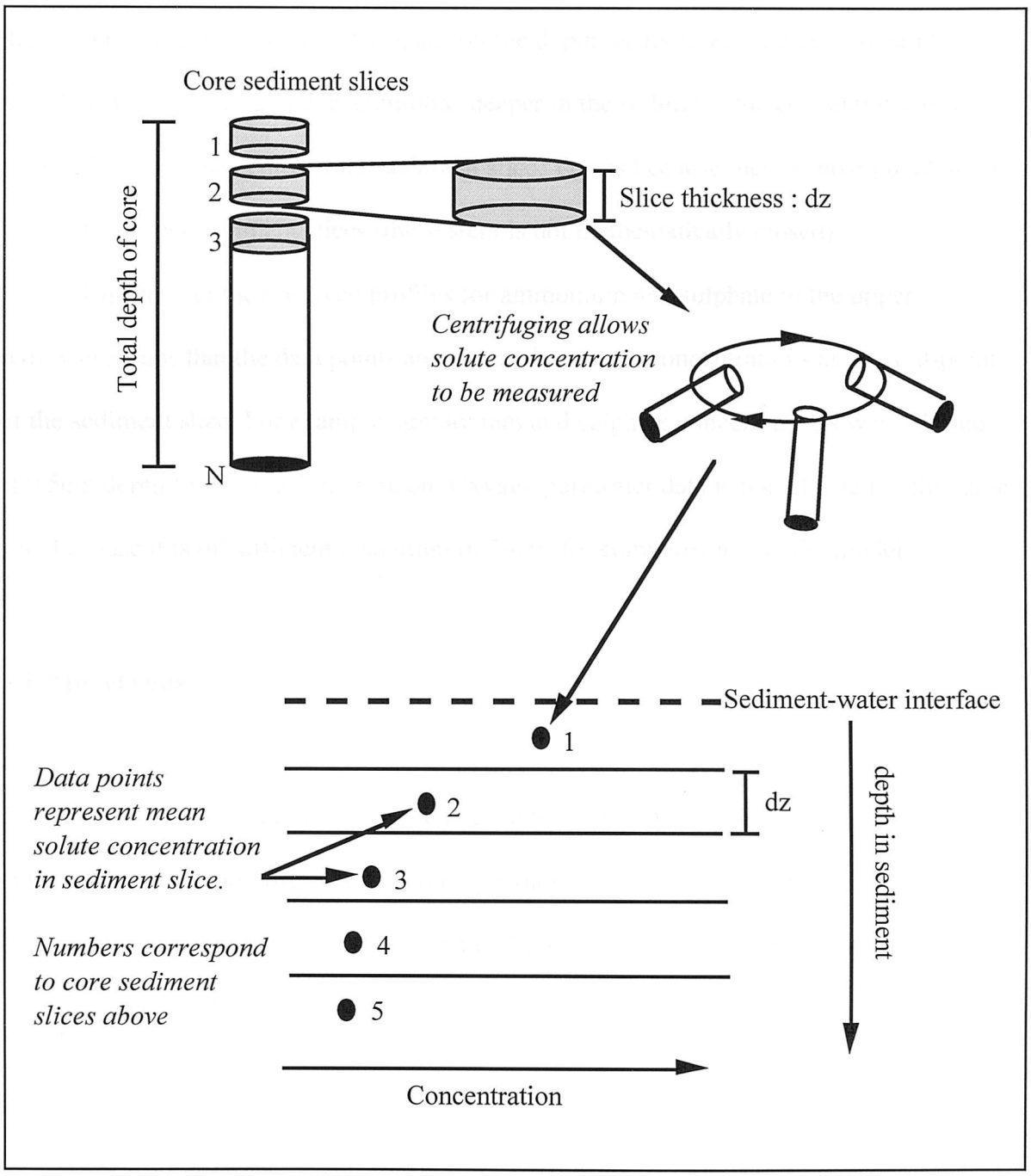

Since $N_0$ , the bottom water concentration, is independent information, the system is mathematically closed and can be solved without the need for other information. Thus, integrating 5.2 with respect to z (depth) and then numerically solving for k (Newton-Raphson method, Press *et al.,* 1990), allows the depth location, z, to be determined for $N_{obs}$. For nitrate porewater concentrations deeper in the sediment, the concentrations are assumed to be in the centre of the sediment slice. This is because there is no equivalent of $N_0$ for the deeper sediment slices (the system is not mathematically closed).

Linearity in the observed profiles for ammonium and sulphate in the upper sediment means that the data points are assumed to be the concentrations at the mid-point of the sediment slice. For example, ammonium and sulphate concentrations were plotted at 0.5cm depth for the top 1cm horizon. Oxygen porewater data is not adjusted in the same way because it is of sufficient resolution (0.5mm) for comparison with the model.

### 5.4. Model runs

The model is run for each month at each of the four sites in the upper Gt. Ouse. Model output is compared to observed porewater profiles of nitrate, ammonium, sulphate and oxygen, to rates of sulphate reduction and to fluxes of oxygen, nitrate and ammonium across the sediment-water interface.

## 5.5. Results

### 5.5.1. Porewater profiles

The monthly modelled and observed porewater concentration profiles of nitrate, ammonium, sulphate and oxygen at the 4 sites in the Gt. Ouse are shown in Figures 5.2, 5.3, 5.4 and 5.5, respectively. Model profiles of nitrate compare well with the observations at sites 1, 3 and 4 (Figure 5.2). Correlation coefficients ($r^2$) are in the ranges 0.78-1.00, 0.69-0.98 and 0.68-1.00, respectively. The model performs poorly against the measurements at site 2 which showed depletion of nitrate in the top 5cm whereas modeled nitrate concentrations showed much smaller decreases over the same sediment depth. Modeled ammonium concentrations in the sediment also compare well to the observed linear increase in concentration with depth at most sites for most months (Figure 5.3). $R^2$ values range between 0.79-0.97 (site 1) , 0.5-0.96 (site 2), 0.74-0.98 (site 3) and 0.81-0.97 (site 4). In contrast, measured sulphate porewater profiles are not represented well by the model (Figure 5.4). The model sulphate concentrations were depleted within the top 4cm at all sites except site 2, where depletion occurred over the top 15cm. The observations, however, rarely showed this pattern of exponential decrease (exceptions include May and August at site 1). With few exceptions, observed sulphate concentrations at 15cm remained greater than 1000 μM. Observed sulphate concentration profiles were highly variable between sites and months. For example, some profiles were nearly vertical ( e.g. October, site 2), some showed a maximum at depth before decreasing ( e.g. March, site 3) and others showed an increase with depth ( e.g. January, site 3).

Modeled porewater profiles of oxygen concentrations showed similar decreases with depth to the measured profiles (Figure 5.5). Values of $r^2$ are between 0.56 and 0.99. across the sites. There were occasions (e.g. March, site 2: $r^2$=0.56) when modeled oxygen

Figure 5.2. Modeled and measured porewater profiles of nitrate at 4 sites in the upper Gt. Ouse

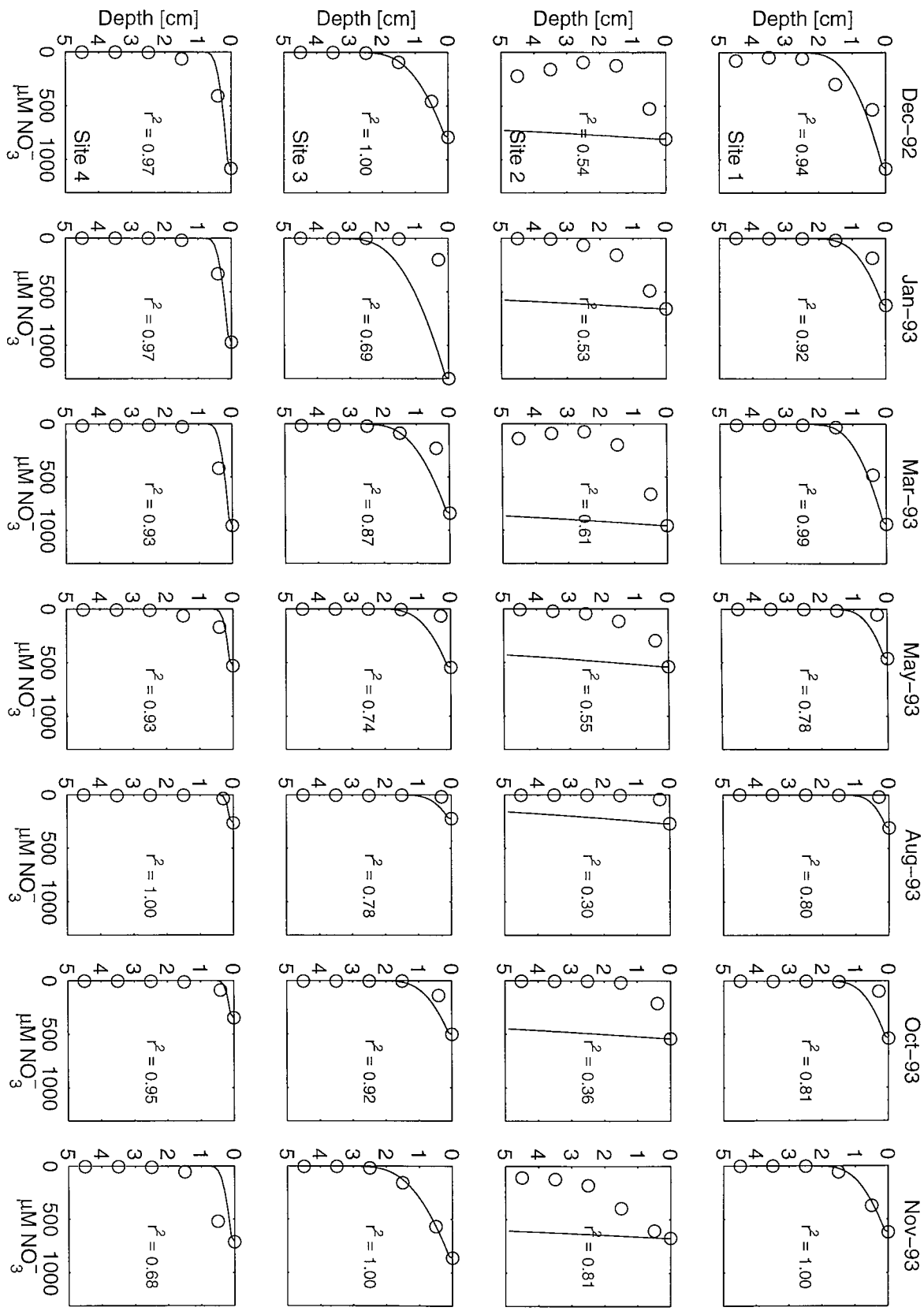

Figure 5.3. Modeled and measured porewater profiles of ammonium at 4 sites in the upper Gt. Ouse

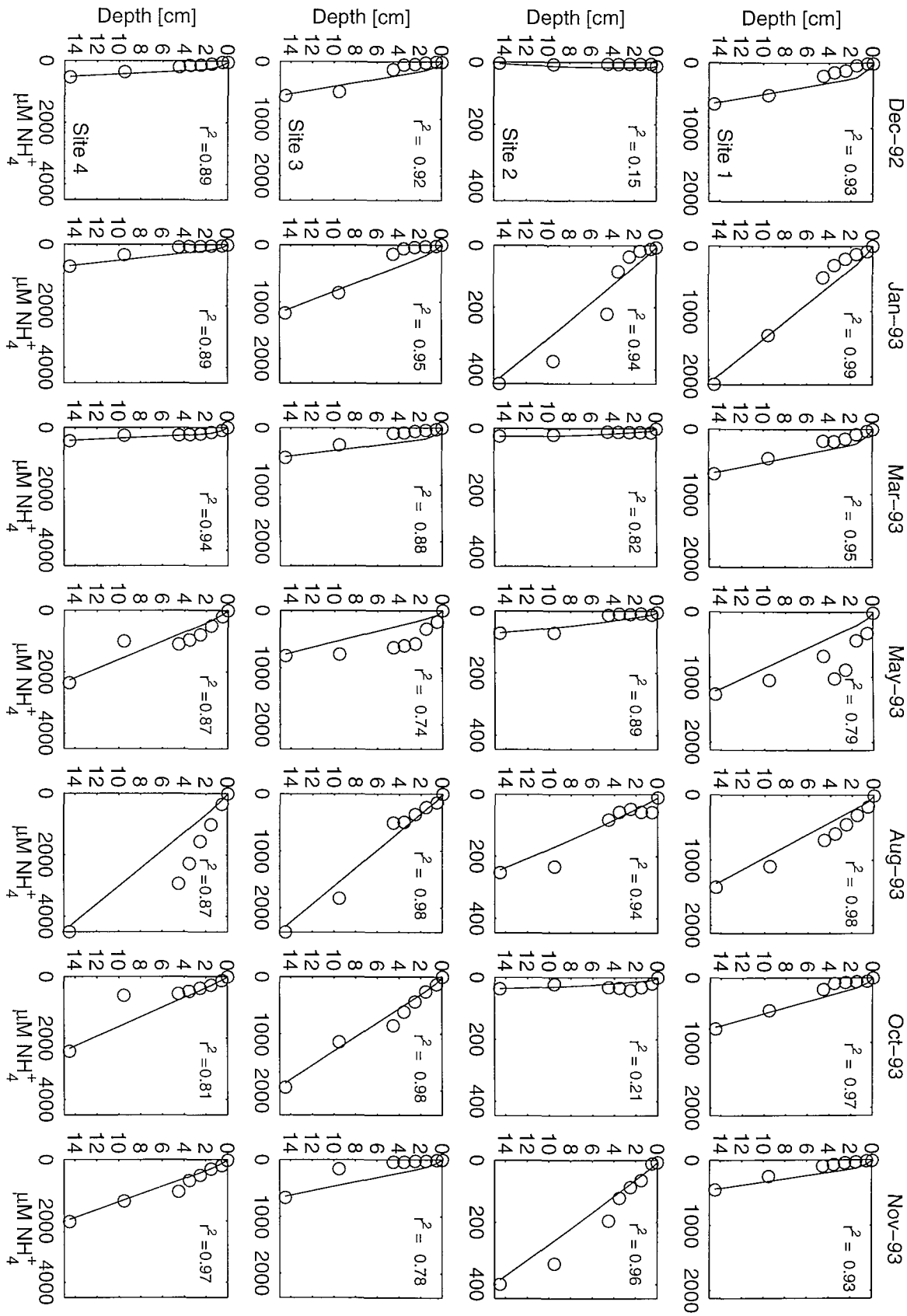

Figure 5.4. Modeled and measured porewater profiles of sulphate at 4 sites in the upper Gt. Ouse

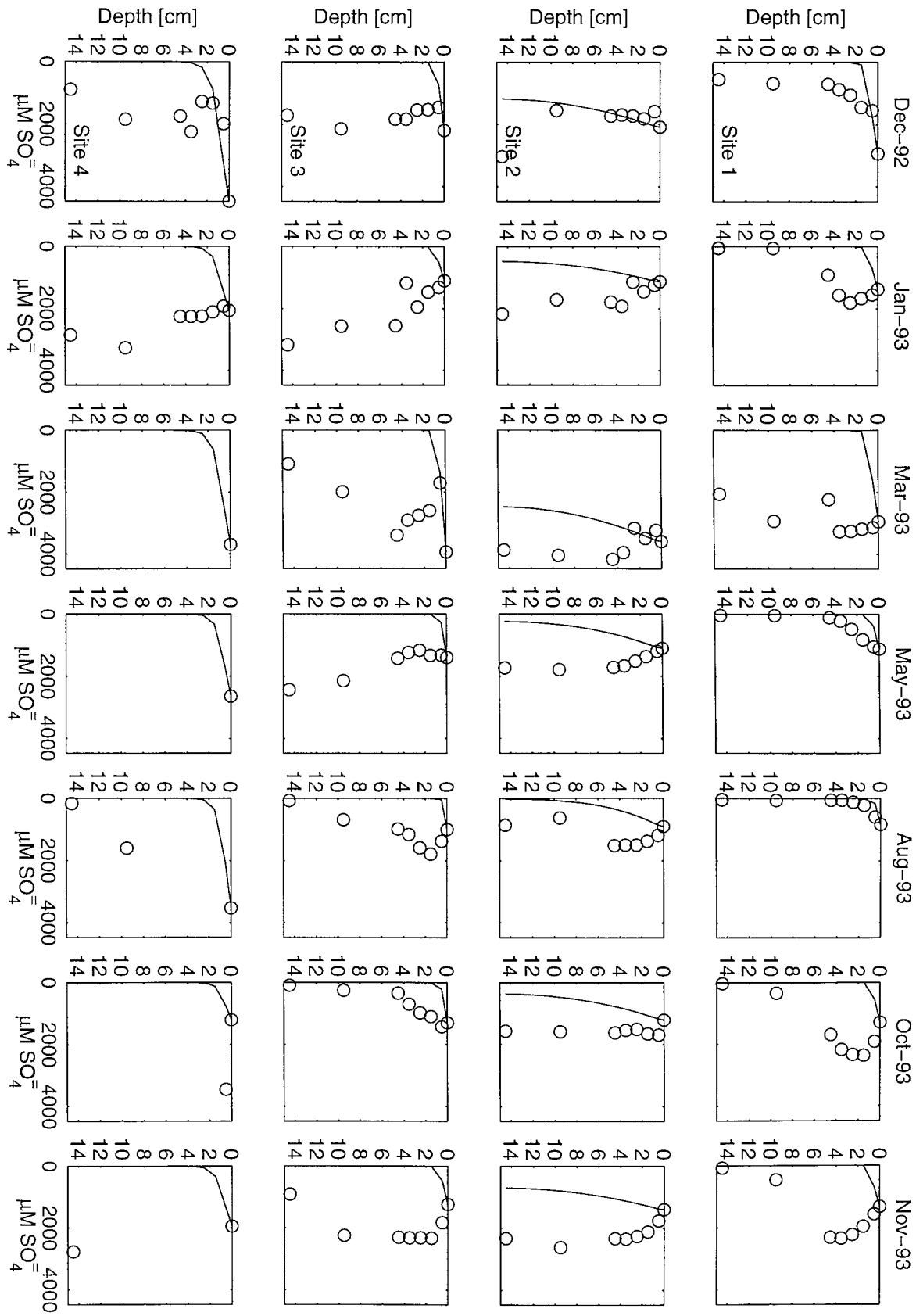

Figure 5.5. Modeled and measured porewater profiles of oxygen at 4 sites in the upper Gt. Ouse

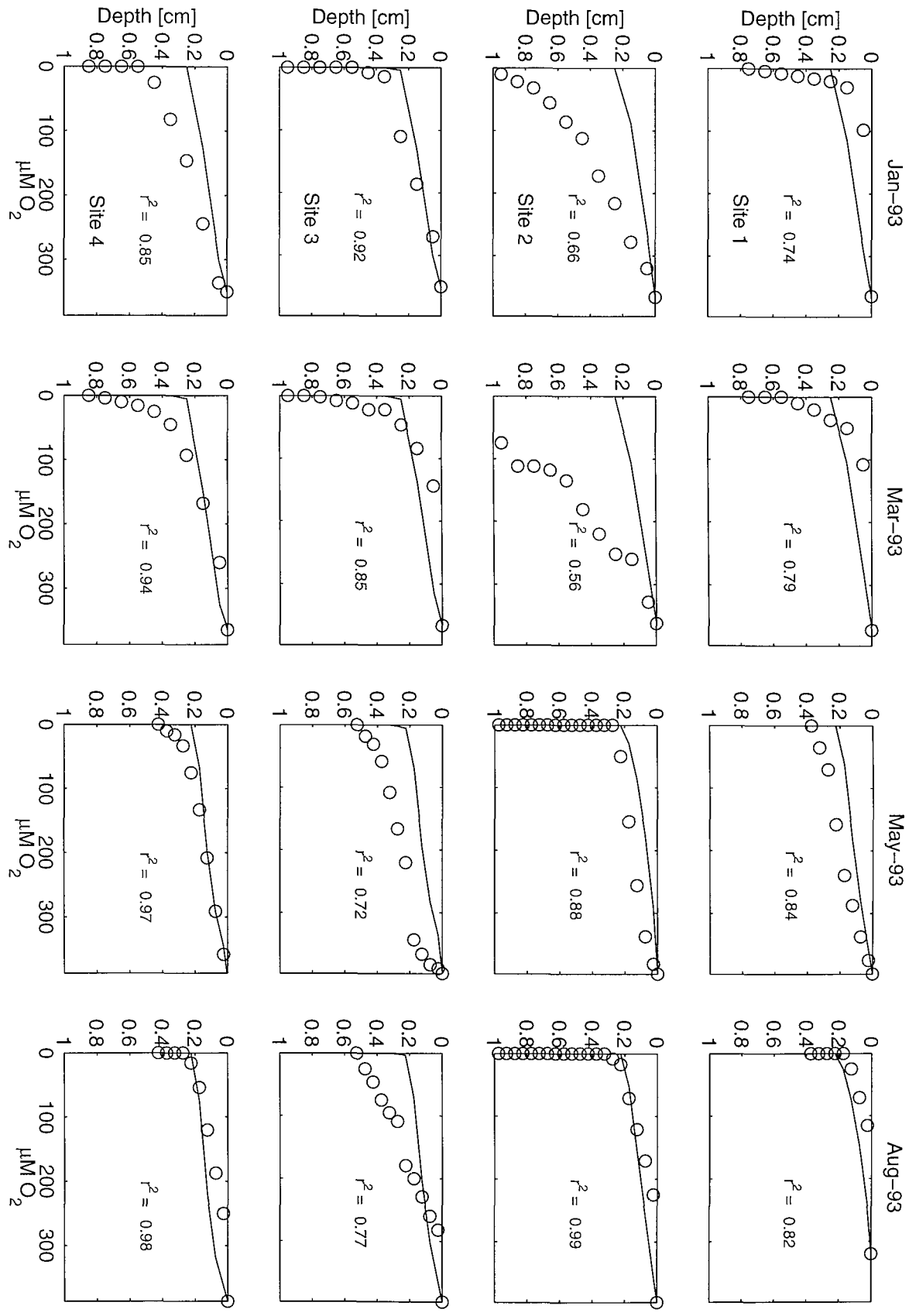

concentrations depleted faster than is suggested by the measured concentrations (ie the modeled oxygen profiles had a steeper gradient compared to the observations).

### 5.5.2. Solute fluxes across the sediment-water interface

Monthly comparisons of modeled and observed fluxes of oxygen, nitrate and ammonium across the SWI are shown for each site in Figures 5.6, 5.7 and 5.8, respectively. Comparisons between modeled and observed oxygen fluxes reveal high variability(Figure 5.6). Overall, model oxygen fluxes were mostly (17 out of the 28 (7 months x 4 sites) samples) lower than observed fluxes by factors of between 0.15 and 0.94. For the remaining comparisons modeled oxygen fluxes were 1.05 to 3.15 times greater than observed fluxes. There were both differences and similarities in the seasonal cycles of the simulated and measured oxygen fluxes at the sites. For example, maximum oxygen fluxes were measured in December at sites 3 and 4 whereas highest oxygen fluxes in the model occurred in August at the same sites. In contrast, the seasonal cycle of observed and modeled oxygen fluxes were similar at sites 1 and 2 with highest fluxes in summer and lowest in winter.

The comparison of modeled and observed fluxes of nitrate also shows high variability (Figure 5.7). There were months when the modelled and measured fluxes were opposite in direction (e.g. December, site 1; May, site 3). At other times, such as in August (sites 3 and 4) and in January (site 1), observed fluxes were 4 to 5 times greater than the modelled simulations. Model nitrate fluxes were between -0.02 and 0.2 mmol $m^{-2}$ $d^{-1}$ at site 2, where no net nitrate fluxes were measured. The model compared more favourably (i.e. to within a factor of ~2) to the observations in March, October and

Figure 5.6. Modeled and measured oxygen fluxes across the SWI at 4 sites in the upper Gt. Ouse

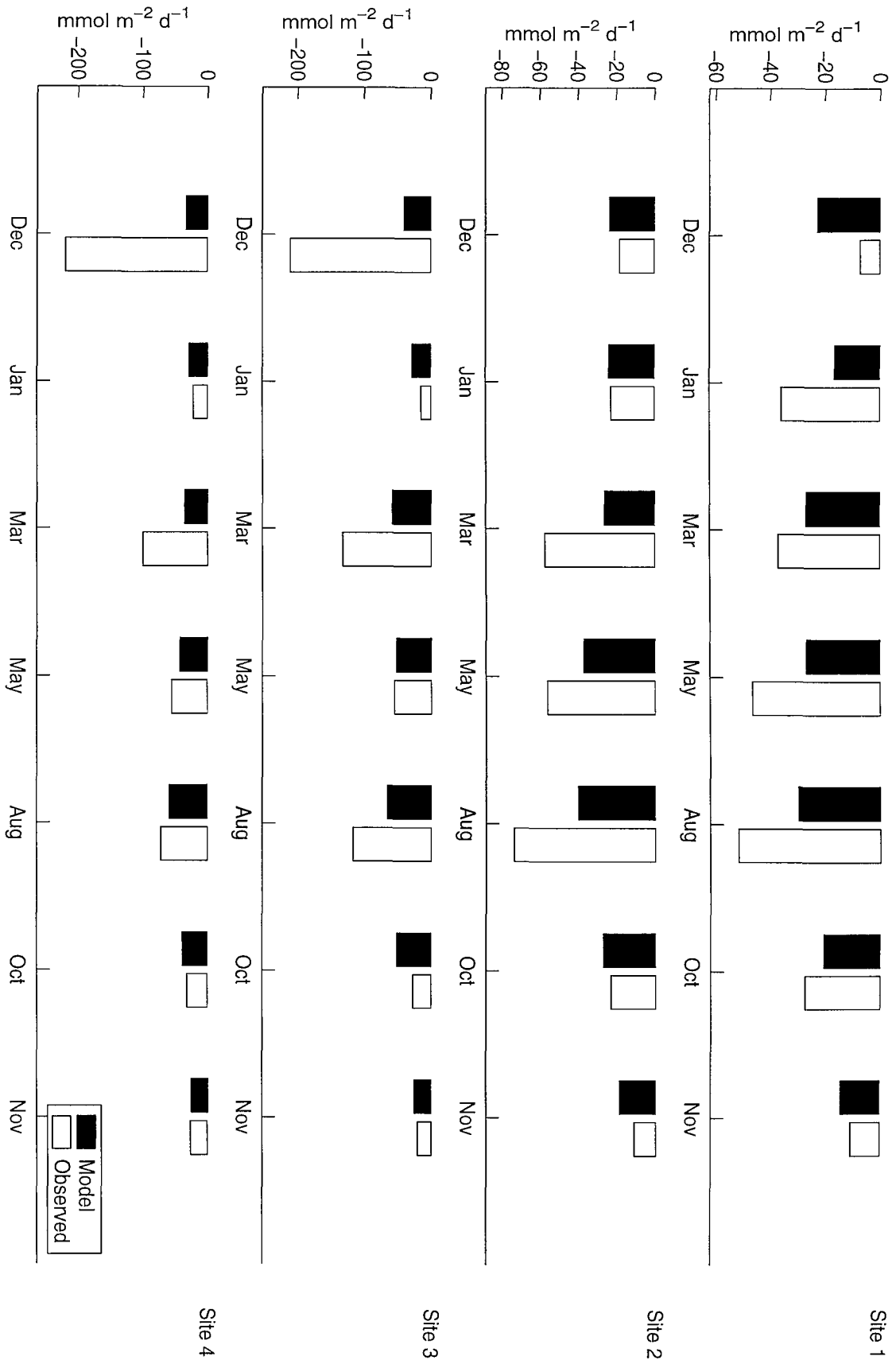

Figure 5.7. Modeled and measured nitrate fluxes across the SWI at 4 sites in the upper Gt. Ouse

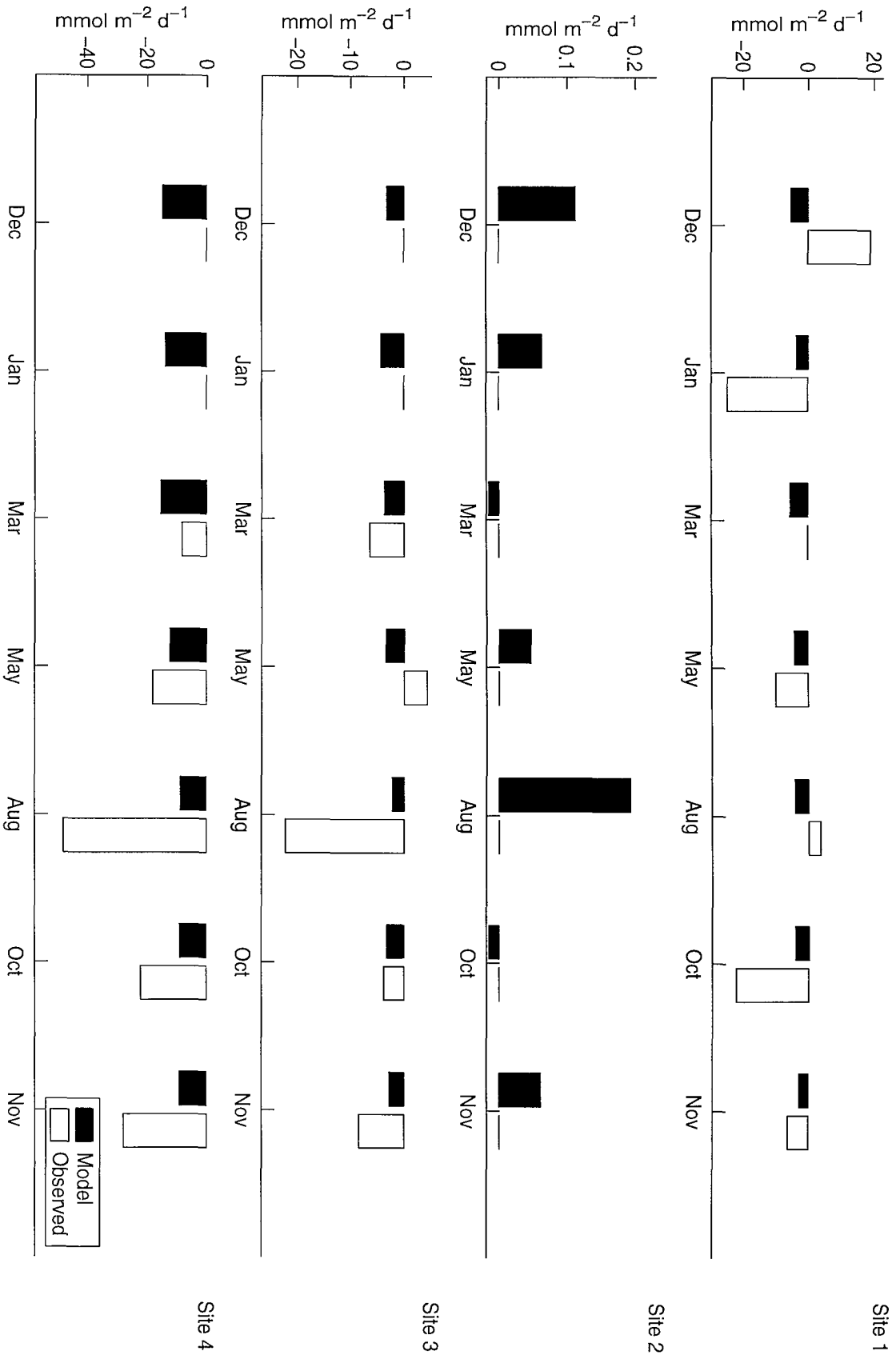

Figure 5.8. Modeled and measured ammonium fluxes across the SWI at 4 sites in the upper Gt. Ouse

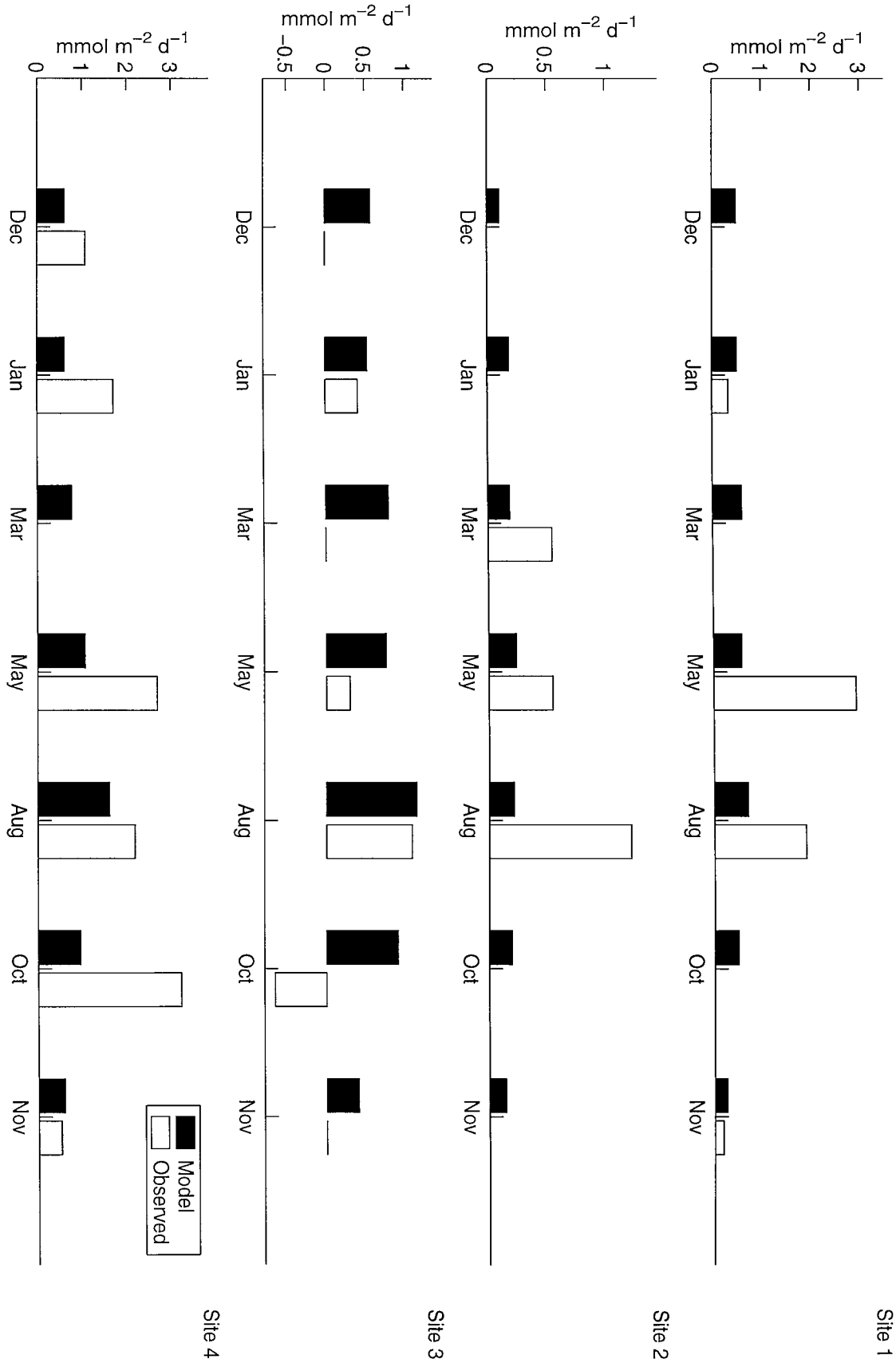

November at site 3, in May, October and November at site 4 and in May and November at site 1. Overall, modeled nitrate fluxes were higher than observed fluxes.

Modelled ammonium fluxes across the SWI compare relatively well (with respect to oxygen and nitrate fluxes) to the observations (Figure 5.8). Modeled fluxes were within ±50% of the observed ammonium fluxes at most times at the four sites. Exceptions were in May and August at site 1, in August at site 2, in May and October at site 3 and in October at site 4.

### 5.5.3. C, N, S and O budgets

The seasonal changes in the percentage contribution of oxic, suboxic and anoxic mineralization to total carbon respiration at the 4 sites is shown in Figure 5.9. Sulphate reduction dominated (>60%) the total respiration at site 1, followed by nitrate reduction (16-23%) and then oxic mineralization which accounted for less than 20%. The dominant pathway of organic decay was via oxygen at site 2 which accounted for more than 95% of the mineralization budget. Most of the mineralization budget at site 3 was taken up by both sulphate reduction (between 33% and 63%) and oxic mineralization (38%-48%) with less than 16% accounted for by nitrate reduction. Oxic mineralization was the dominant pathway at site 4 accounting for 32% to 58% of the carbon budget with sulphate reduction (18-37%) and nitrate reduction (16-39%) taking up similar portions.

The balance of processes (sulphide oxidation, nitrification and oxic mineralization) contributing to total benthic oxygen demand for each site is shown in Figure 5.10. Sulphide oxidation was responsible for most (76-90%) of the oxygen uptake throughout the year at site 1. The oxygen demand was almost entirely (>95% with respect to the other mineralization pathways) attributed to oxic mineralization, the remainder equally

Figure 5.9. Predicted percentage contributions of the different pathways of organic carbon mineralization to total organic carbon mineralization at 4 sites in the upper Gt. Ouse

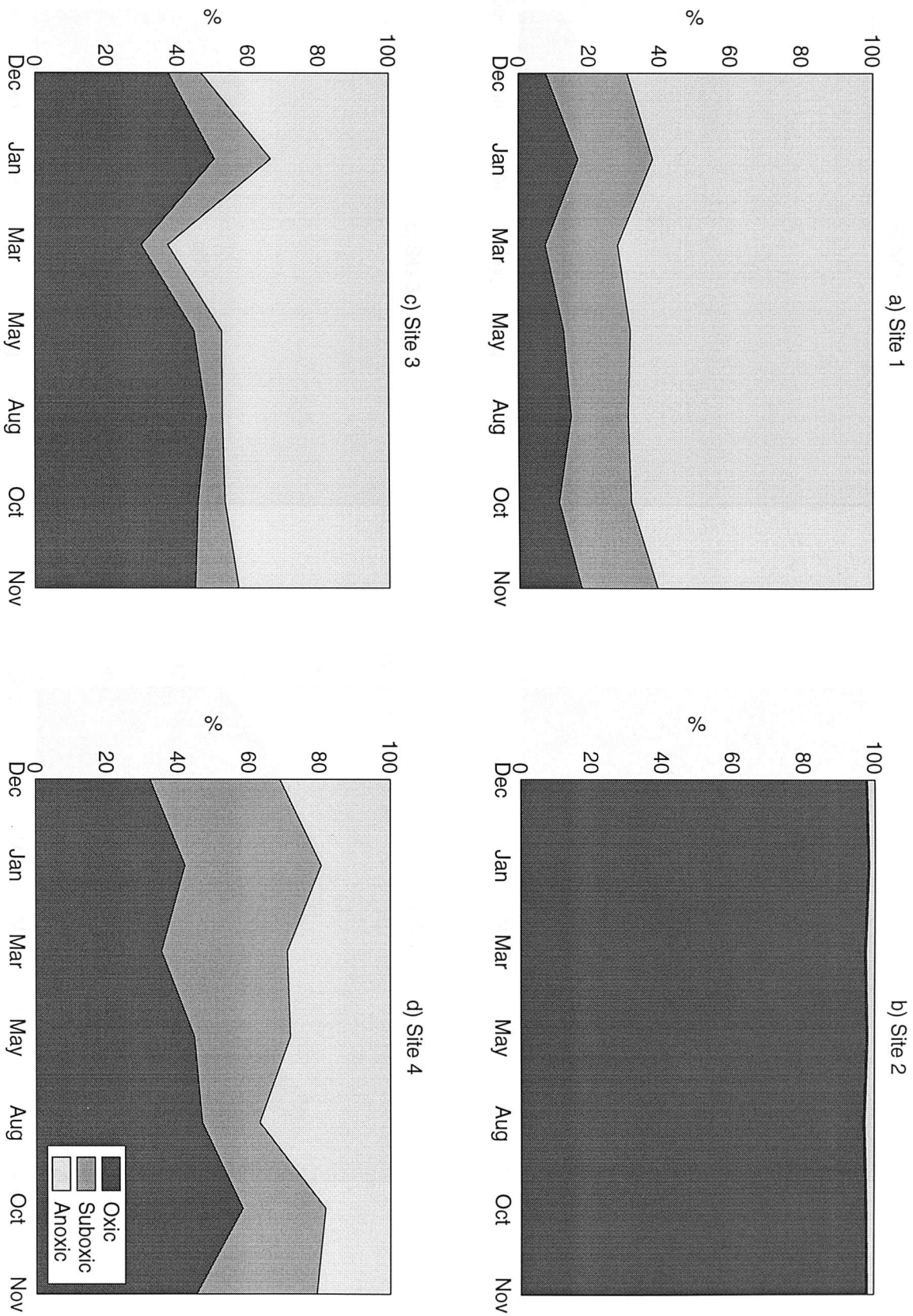

Figure 5.10. Modeled oxygen budget at 4 sites in the upper Gt. Ouse

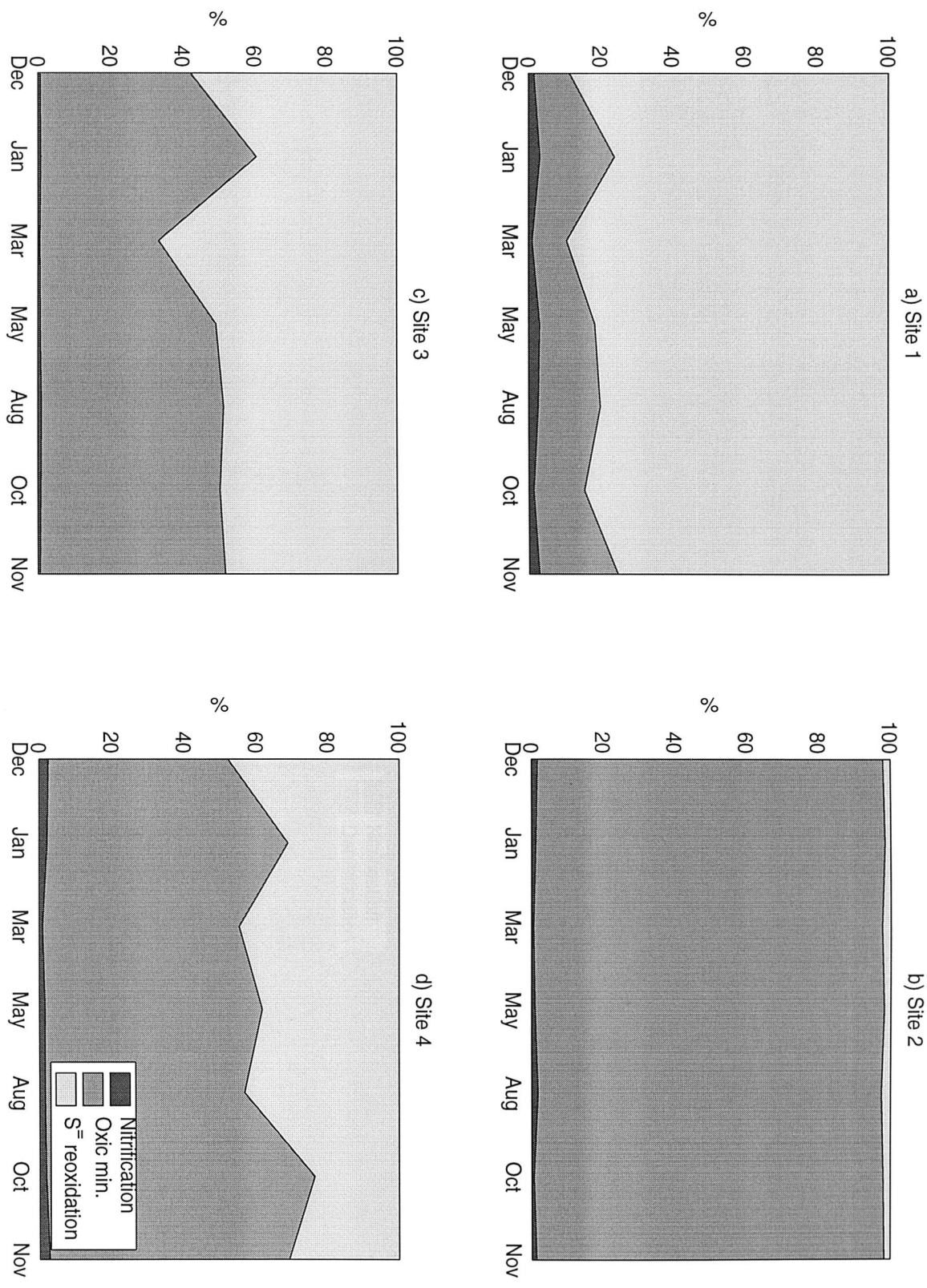

Figure 5.11. Modeled nitrate budget at 4 sites in the upper Gt. Ouse

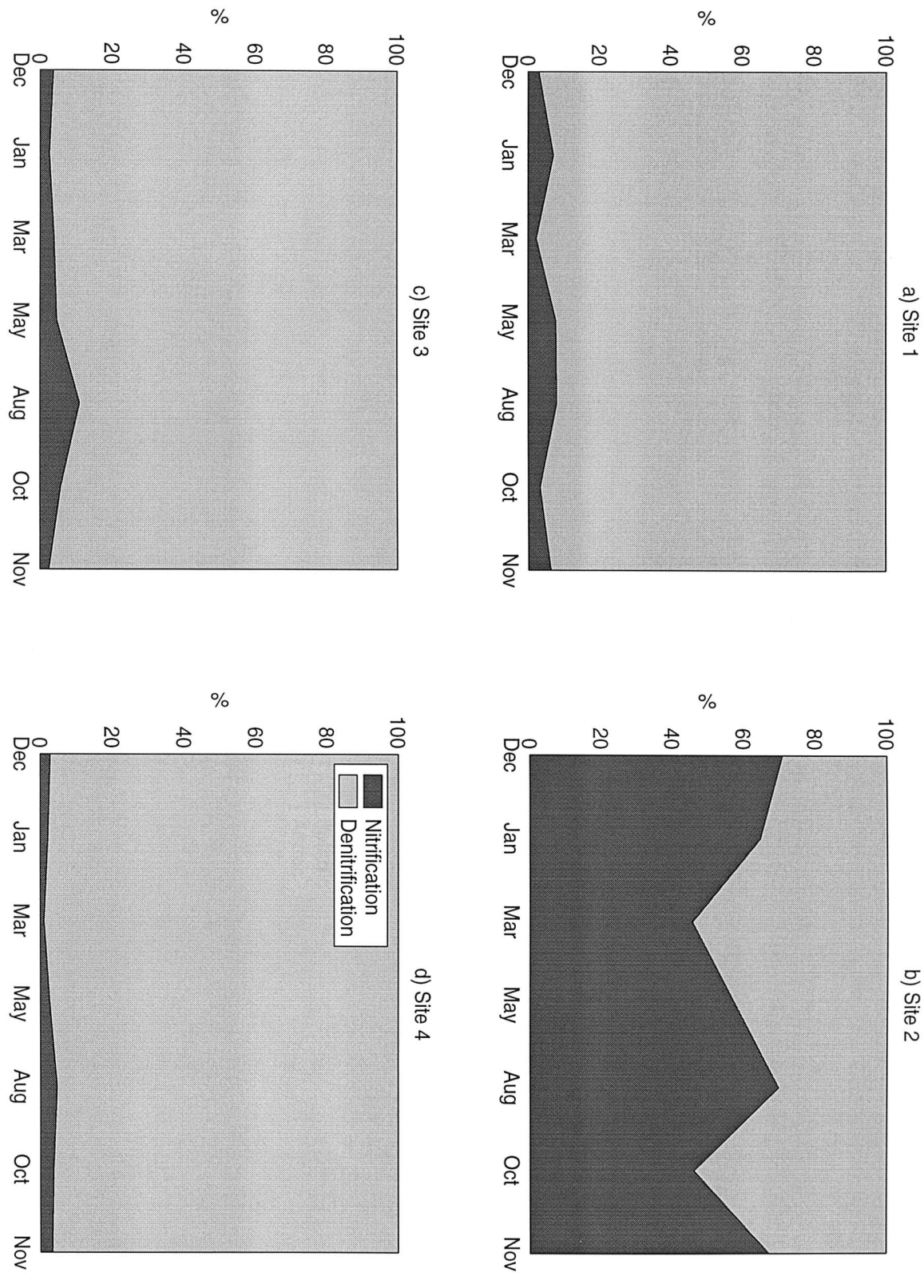

Figure 5.12. Modeled ammonium budget at 4 sites in the upper Gt. Ouse

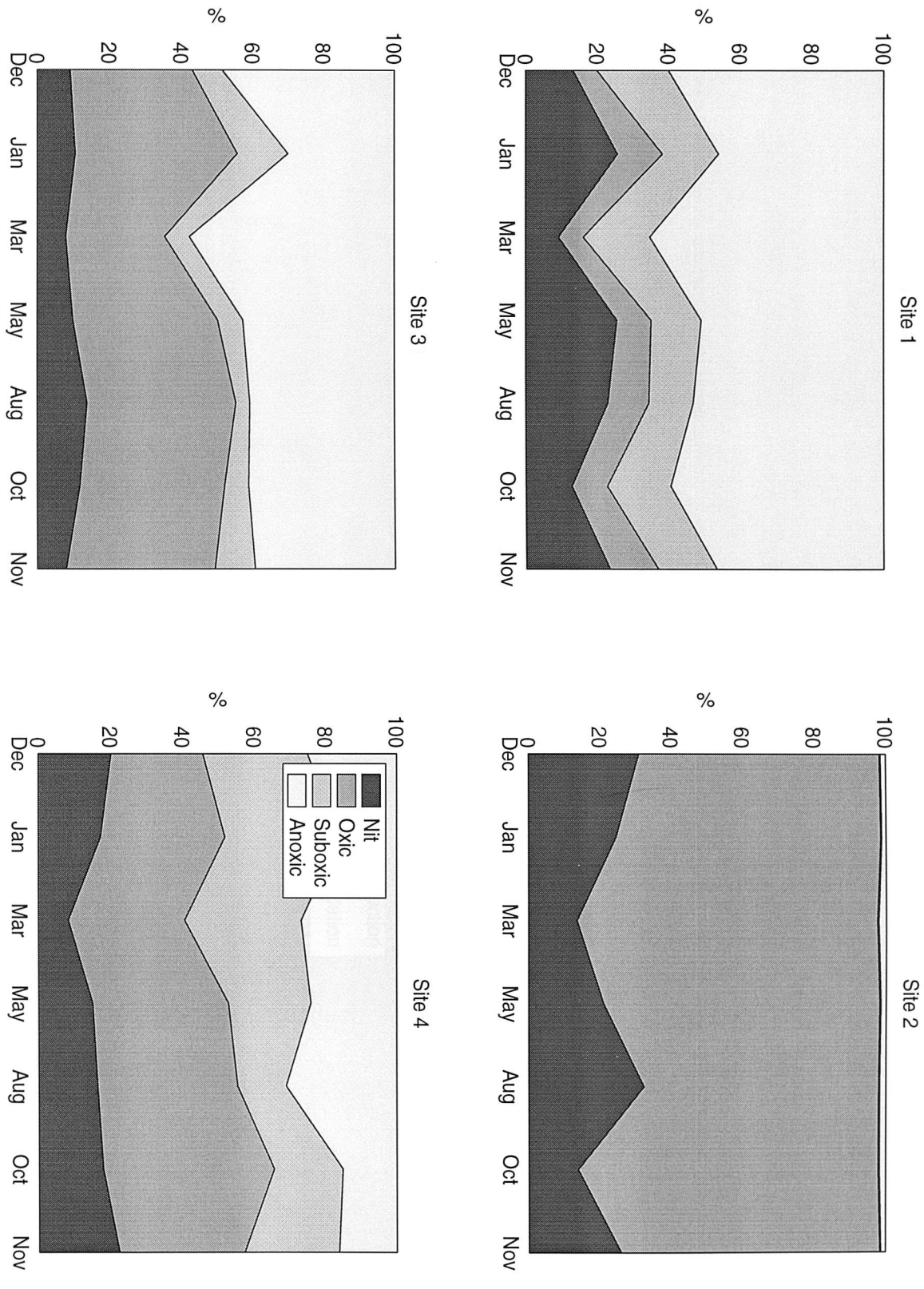

Figure 5.13. Modeled sulphur budget at 4 sites in the upper Gt. Ouse

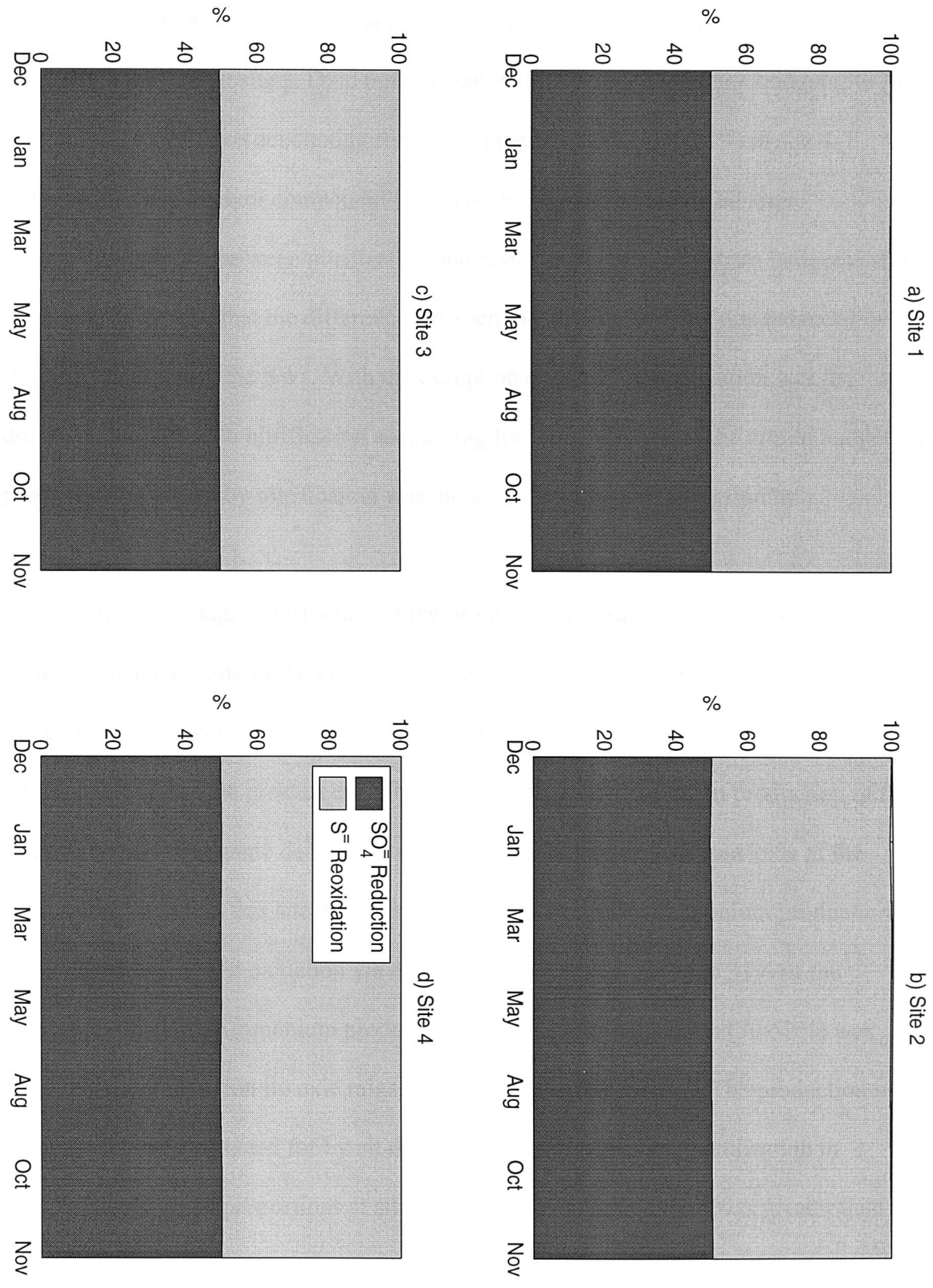

accounted for by the other two oxygen consuming processes at site 2. Oxygen was consumed in equal proportions by sulphide oxidation and oxic mineralization (38-67%) throughout the year at site 3. Oxic mineralization dominated the oxygen budget (50-74%) with sulphide oxidation accounting for most of the remainder (24-47%) at site 4. Nitrification was a minor component (<3%) of the oxygen budget at all sites.

The balance between nitrification and denitrification in the nitrate budget is shown in Figure 5.11. Note that the difference between these two processes was balanced by the flux of nitrate across the SWI. With the exception of site 2, denitrification was the dominant process with nitrification accounting for less than 11% of the nitrate budget. The production of nitrate by nitrification was mostly greater than its reduction by denitrification at site 2.

The percentage contribution of the production-consumption processes of ammonium at each site in the Gt. Ouse is shown in Figure 5.12. Again note that the sum of these processes was balanced by the flux of ammonium across the SWI. Anoxic mineralization was the greatest contributor (62%-72%) to ammonium production of the three pathways of organic decay at site 1 and nitrification was less than 26% of the ammonium budget at this site. Oxic mineralization dominated ammonium production (>95%) at site 2, while oxidation via nitrification accounted for up to 31% of the ammonium budget. Ammonium production by anoxic mineralization (30-57%) was slightly greater than that by oxic mineralization (28-46 %) at site 3. The production of ammonium was accounted for by all three pathways of organic mineralization in approximately equal proportions at site 4. Production of ammonium was greater than its consumption at all sites.

The sulphur budget for all sites is shown in Figure 5.13. The production of sulphate by oxidation of sulphide was balanced by sulphate reduction at all sites.

However, there was a small difference between the two processes which meant that sulphate reduction was greater than its production. This fueled a flux of sulphate from the overlying water into the sediment.

It is clear from these budgets (Figure 5.9-5.13) that the relative contribution of the different pathways for any particular variable (except sulphate) did not remain constant between months at the sites. For example, the order of the rates in the mineralization budget in decreasing magnitude was oxic >suboxic>anoxic in January at site 4 (Figure 5. 9). The order was oxic > anoxic> suboxic in August at the same site. Similarly, anoxic mineralization accounted for ~63% of total organic degradation in March at site 3 (Figure 5.9), even though at other times oxic mineralization was more dominant. The reason for this variability is discussed below.

## 5.6. Discussion

The degree to which the model is successful at reproducing the seasonal cycles of measured quantities ( e.g. porewater profiles, oxygen fluxes across the SWI) depends on the property being considered. A number of discrepancies between modeled and observed data exist which need to be explained. In the following discussion, model output is considered in the same sequence as presented in the results section (5.5). The causes for the seasonality in the predicted solute fluxes are dealt with prior to examining the discrepancy between modeled and observed solute exchange across the SWI.

### 5.6.1. Porewater profiles

The ability of the model to capture the observed seasonality in porewater concentrations depends on which variable is chosen for the comparison. Overall, porewater concentrations of nitrate, ammonium and oxygen were modeled well at most sites both in terms of a qualitative (visual) and a statistical comparison (ie $r^2$). However, some of the oxygen porewater profiles indicated that modeled penetration depths were lower than those observed (e.g. site 1 in May, Figure 5.5). A possible explanation for this lies in the work of Lohse *et al.* (1996) and Glud *et al.* (1996). Lohse *et al.* (1996) had a similar problem with oxygen porewater concentrations in the sandy sediments of the North Sea. To model these profiles successfully, they had to increase the diffusion coefficient by up to 100 times. Lohse *et al.* (1996) concluded that tidal currents induced turbulent diffusion in these sediments. Glud *et al.* (1996) demonstrated that stirring rates and sediment permeability determined the extent of advective porewater transport in benthic flux chambers. Stirring rates of 12 rpm were high enough to change solute transport from diffusive to advective and higher sediment permeabilities meant a greater intensity of advection. The stirring rate was 300 rpm in the core incubations of the sediments from the upper Gt. Ouse but differences in both the experimental setup and sediment characteristics between the study of Glud *et al.* (1996) and of Nedwell and Trimmer (1996) may mean that the effect of the higher stirring rate on oxygen transport in the core incubations may not be as great as it may seem. Firstly, there are differences in the dimensions of the benthic flux chambers (9cm depth x 19cm diameter) and the core incubators (5cm depth by 2.4cm diameter). Secondly, different sized stirrers were used (17cm x 1cm disc in the benthic chamber cf. ~1cm in the core incubator). Thirdly, the sediments used by Glud *et al.* (1996) were coarser (79%-100% of the grain size distribution between 125 μm and 500

μm) than the sediments of the upper Gt. Ouse (53% to 93% ≤ 125 μm) which, in the absence of actual measurements, indicates that the sediments used in this study had lower permeabilities. Consequently, the stirring rate at which advective transport dominated over diffusion may have been higher in the core incubations used by Nedwell and Trimmer (1996) than that suggested by Glud *et al.* (1996). In any case, it is possible that the discrepancy between modeled and observed oxygen porewater profiles was due to the action of transport processes other than diffusion. However, nitrate penetration depths in the model were rarely lower than in the observations. This may be because the sediment depth over with turbulent diffusion dominantes over molecular diffusion is generally less than 0.5cm (Lohse *et al.,* 1996) and would therefore not be observed in the coarse resolution measurements (~1cm) of nitrate porewater profiles (Figure 5.1). Alternatively, if only molecular diffusion dominated the actual oxygen transport then questions arise about the predictions of rates of oxygen consumption. That is, modeled rates of oxygen consumption may have been higher than the actual rates when simulated porewater concentrations of oxygen had a steeper gradient (ie a lower oxygen penetration depth) compared to the observations (e.g. March at site 2). (Note, however, that at other times e.g. August at site 4, modeled profiles matched the observations well ($r^2$=0.99) suggesting that modeled rates of benthic oxygen demand were close to the actual demand).

The lower penetration depths of nitrate in the observations compared to the model at site 2 (Figure 5.2) suggest a greater consumption of nitrate than was modeled. It was possible to simulate the measured porewater profiles of nitrate at site 2 by deriving a value for $k_{no3}$ of 0.09 $y^{-1}$ (Figure 5.14). This compares with the reference run value of $k_{no3}$ = 0.0004 $y^{-1}$ (section 3.6.2). However, the higher parameter value produced much higher rates of denitrification (not shown) than estimated from the stoichiometric calculations of Nedwell and Trimmer (1996). Furthermore, fluxes of nitrate into the sediment were

Figure 5.14. Modeled and measured porewater profiles of nitrate at site 2 in the upper Gt. Ouse with $k_{no3}$=0.09 $y^{-1}$

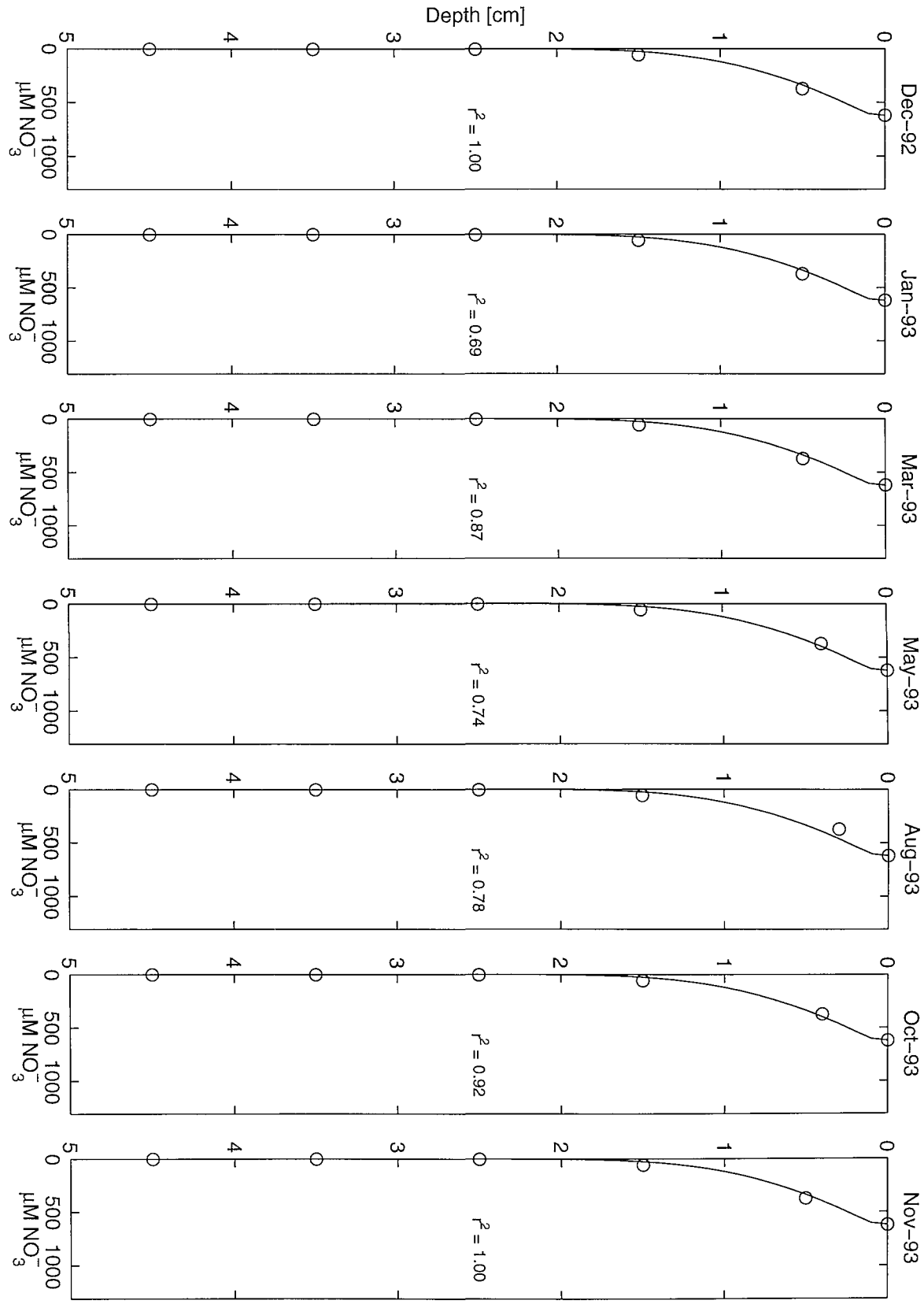

produced which contrasts with the measurements of nitrate exchange at this site where no net flux of nitrate across the SWI was observed (Figure 5.7). The likely solution to the problem of modelling the nitrate porewater profile at site 2 may lie in correctly predicting the balance between nitrate reduction and nitrification.

Measured sulphate concentrations in the porewater were poorly simulated. The reason for this is unclear. The majority of the observed porewater profiles of sulphate suggest a lack of sulphate reduction. However, measurements show that sulphate reduction was active in these sediments (Trimmer *et al.,* 1997). So the question is what caused these unusual porewater profiles? One possibility is to do with tidal pumping in which overlying water is driven into the sediment in response to the ebb and flow of the tide. Under this condition, the supply of sulphate to the sediment would be greater than the bacterial demand. Consequently, porewater concentrations of sulphate would not decrease with depth, a trend seen in the sediments of the upper Gt. Ouse (Figure 5.4). However, a problem arises with this explanation. Why are other variables e.g. nitrate not affected in a similar way? It is unlikely that oxygen and nitrate were consumed faster than the rate of supply from tidal pumping. At the present time an explanation for the sulphate profiles is not forthcoming.

### 5.6.2. Solute fluxes across the SWI: explaining the seasonality in the model

Reasons for the seasonal dynamics of model fluxes (and processes) are easy to predict. For instance, model oxygen fluxes will be controlled by factors affecting seasonality in organic mineralization rates and oxidation processes (e.g. temperature, oxygen, nitrate and sulphate concentrations in the overlying water). However, to what degree each of these factors controls the seasonal dynamics of oxygen fluxes cannot be well predicted and it is

difficult to extract this information from the data alone. To determine this, five model sensitivity runs (Runs 1 to 5, see Table 5.1) were examined. In these runs, different forcing functions (e.g. temperature, boundary concentration values) were kept constant to observe the effect, relative to a reference run, on SWI fluxes in the model. The reference run is the model run presented so far.

Table 5.1 Model sensitivity runs ($O2_{bw}$, $NO3_{bw}$, $SO4_{bw}$ = oxygen, nitrate, sulphate concentration in the overlying water; $NH4_{bbc}$= ammonium concentration in the sediment bottom boundary; values used are the mean across all sites and sample dates)

| Run | Difference from reference run |
|---|---|
| 1 | Constant temperature (10°C) |
| 2 | Constant $O2_{bw}$ (350 μM) |
| 3 | Constant $NO3_{bw}$ (677 μM) |
| 4 | Constant $SO4_{bw}$ (1964 μM) |
| 5 | Constant $NH4_{bbc}$ (1000 μM) |

The results are shown in Figures 5.15-5.18. Each model flux is considered in turn.

### 5.6.2.1. Oxygen fluxes

The effect of the sensitivity runs (Table 5.1), relative to the reference run, on the modeled seasonal oxygen fluxes across the SWI at all 4 sites in the upper Gt. Ouse is shown in Figure 5.15. There seemed to be a clear relationship between oxygen fluxes and temperature at sites 2 (Figure 5.15b) and 4 (Figure 5.15d) where highest fluxes coincided with highest temperatures and vice versa (Figure 2.2a).

Figure 5.15. Effect of Runs 1 to 4 (see Table 5.1) on oxygen fluxes (mmol $m^{-2}$ $d^{-1}$) across the SWI at 4 sites in the upper Gt. Ouse

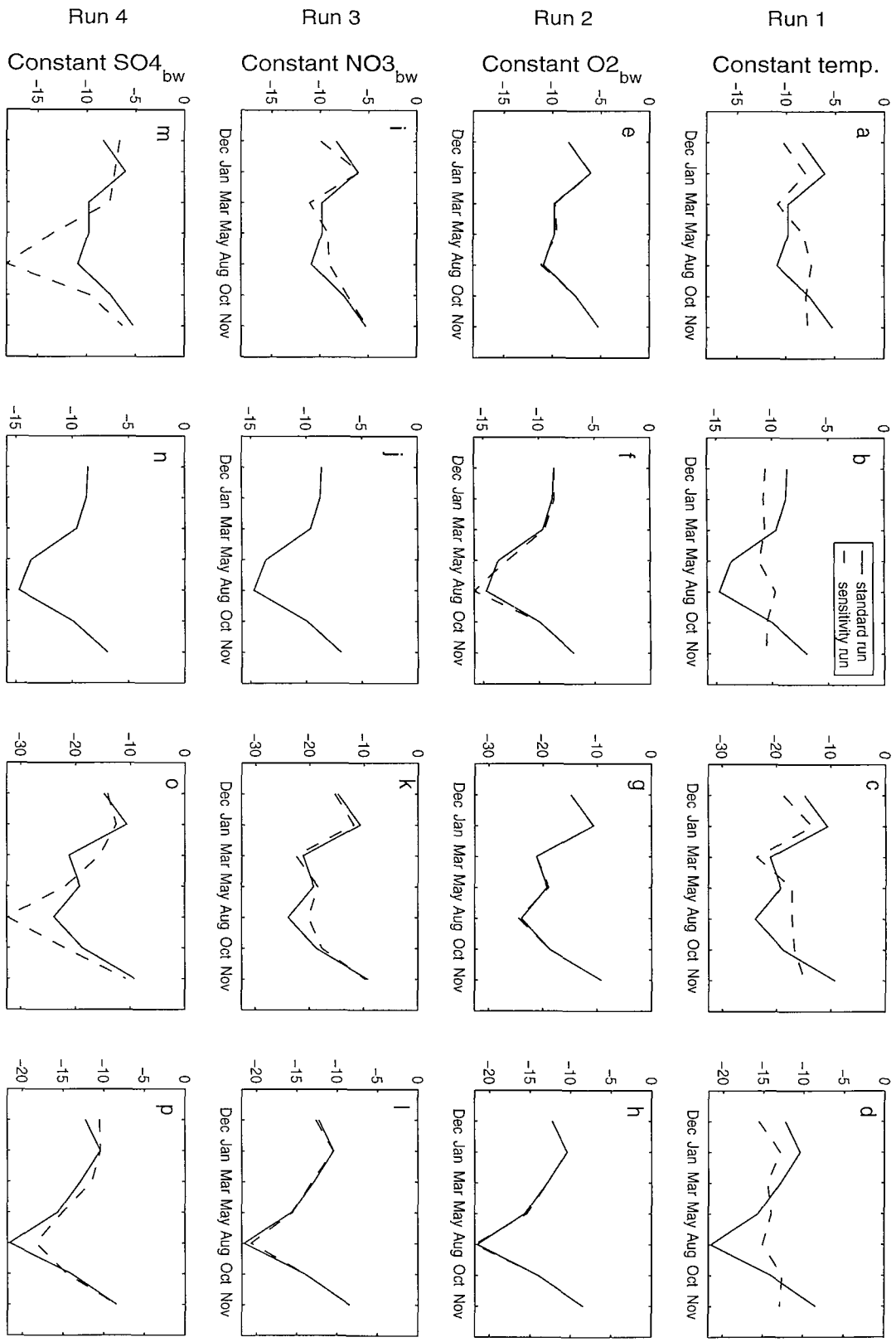

In Run 1, removal of the seasonal temperature signal yielded a completely different seasonality in the oxygen fluxes at sites 2 (Figure 5.15b) and 4 (Figure 5.15d). At sites 1 (Figure 5.15a) and 3 (Figure 5.15c), temperature could not fully explain the seasonal pattern in the oxygen fluxes, especially between December and May. The effect of variations in oxygen concentrations in the overlying water (Run 2) had a negligible effect on oxygen fluxes at all sites (Figure 5.15e-h). Consequently, this run had little effect on other solute fluxes across the SWI and is not shown in subsequent plots.

Constant nitrate concentrations in the overlying water (Run 3) had either no noticeable effect on oxygen fluxes (site 2, Figure 5.15j and site 4, Figure 5.15l) or a dampening effect (August at site 1, Figure 5.15i and 3, Figure 5.15k) when compared to the reference runs. The overlying nitrate concentration through its influence on diffusion of nitrate into the sediment may be expected to have an effect on oxygen fluxes due to its inhibitory effect on sulphate reduction (equation 3.9, Table 3.1). That is, higher overlying nitrate creates a higher nitrate flux which means greater inhibition of sulphate reduction and therefore less sulphide oxidation and therefore lower oxygen demand. Nitrate concentrations in Run 3 were higher than nitrate concentrations in the standard run between March and November (site 1) and between May and October (site 3) (compare Table 5.1 and Figure 2.2c). These higher concentrations of nitrate meant greater inhibition of sulphate reduction, lower rates of sulphide oxidation and consequently lower oxygen demand compared to the standard run (Figure 5.15a,i, Figure 5.15c,k). Nitrate fluxes were directed out of the sediment at site 2 (as rates of nitrification were greater than rates of denitrification, Figure 5.11b) and so overlying nitrate concentrations had no effect here.

Run 4 reveals that sulphate concentrations in the overlying water have a strong control on the variability in oxygen fluxes at sites 1 (Figure 5.15i,m) and 3 (Figure 5.15k,o). The explanation lies in the seasonal dynamics of sulphate cycling. Seasonal

diffusive fluxes of sulphate into the sediment were forced by the changing sulphate concentrations in the overlying water. These boundary concentrations supplied sulphate for anoxic mineralization which in turn produced sulphide. The instantaneous oxidation of sulphide in the model (section 3.1.1) forced the consumption of oxygen in the stoichiometric ratio of 1:2 (Nedwell and Trimmer, 1996). The difference in the influence of sulphate on oxygen fluxes between the sites was related to the differences in magnitude of the first order rate constant for anoxic mineralization, $k_{so4}$. At sites 1 and 3, $k_{so4}$ =34.7 $y^{-1}$ and 5.23 $y^{-1}$, respectively (Table 3.5), which contrasts with the values at sites 2 ($k_{so4}$ = 1.73 $y^{-1}$) and 4 ($k_{so4}$ = 0.06 $y^{-1}$). In other words, sulphate reduction and consequently sulphide oxidation proceeded at higher rates at sites 1 and 3 than at sites 2 and 4. This is reflected in the different proportions of total oxygen consumption accounted for by sulphide oxidation among the sites (76-90% at site 1, 38-67% at site 3, <5% at site 2 and 24-47% at site 4, Figure 5.10a-d).

### 5.6.2.2. Nitrate fluxes

Fluxes of nitrate across the SWI (Figure 5.16a-h) were related to both temperature and to the changing nitrate concentrations in the overlying water. Run with constant temperature (Run 1), the modeled seasonal nitrate fluxes were determined by the seasonal cycle of nitrate concentrations in the top boundary (Figure 5.16a-d). In the absence of changes in nitrate concentrations in the overlying water (Run 3), temperature fully controlled the seasonal cycle of nitrate fluxes to the sediment (Figure 5.16e-h). Overall, temperature controlled the magnitude of the flux while nitrate mostly controlled the seasonality of the flux. At site 2 where nitrate reduction rates were low ($k_{no3}$=0.0004 $y^{-1}$, Table 3.5) nitrate fluxes were directed both out of the sediment (December, January, May, August,

Figure 5.16. Effect of Runs 1 and 3 (see Table 5.1) on nitrate fluxes (mmol $m^{-2}$ $d^{-1}$) across the SWI at 4 sites in the upper Gt. Ouse

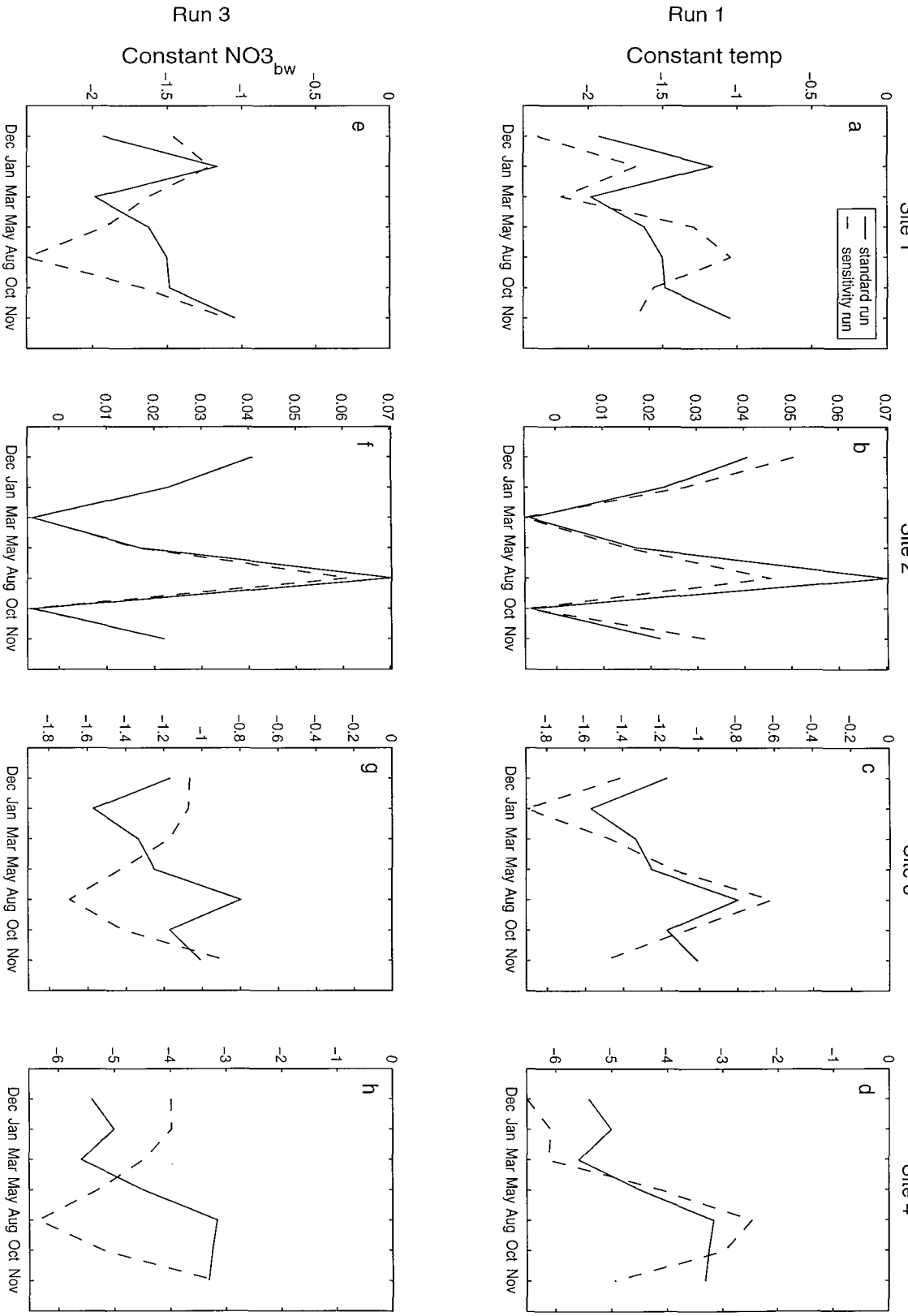

November) and into the sediment (March, October). Consequently, the seasonal cycle of nitrate fluxes at site 2 was controlled by the net balance between nitrification and denitrification where most of the ammonium for nitrification was derived by upward diffusion from the fixed bottom boundary condition.

### 5.6.2.3. Ammonium fluxes

Ammonium was affected by 4 different processes in the model: nitrification and oxic, suboxic and anoxic mineralization. The effect of the forcing data on ammonium fluxes was different among the sites because of the different contributions of these four processes to the ammonium budget (Figure 5.12a-d). Thus, where sulphate reduction contributed 62%-72% to the total production of ammonium throughout the year (site 1, Figure 5.12a), factors controlling anoxic mineralization affected ammonium production and effluxes. In contrast, oxic mineralization (>60%) and nitrification (15-30%) dominated the budget of ammonium at site 2 (Figure 5.12b) and so factors controlling these two processes were important in determining the seasonality in ammonium effluxes. All four processes contributed fairly equally to the ammonium pool at site 4 (Figure 5.12d) and so the dominant factor controlling all these processes affected the seasonal fluxes of ammonium from the sediment.

The seasonal fluxes of ammonium across the SWI in the model and their relationship to forcing data are shown in Figure 5.17a-p. Seasonality in ammonium fluxes were affected by all pathways of organic carbon mineralization, temperature and variations in the ammonium concentration in the fixed bottom boundary. The latter provided an upward diffusive supply of ammonium to the model sediment. The reference run (Figure 5.17a-d) suggests a relationship with temperature in which highest effluxes of

Figure 5.17. Effect of Runs 1, 3, 4 and 5 (see Table 5.1) on ammonium fluxes (mmol $m^{-2}$ $d^{-1}$) across the SWI at 4 sites in the upper Gt. Ouse

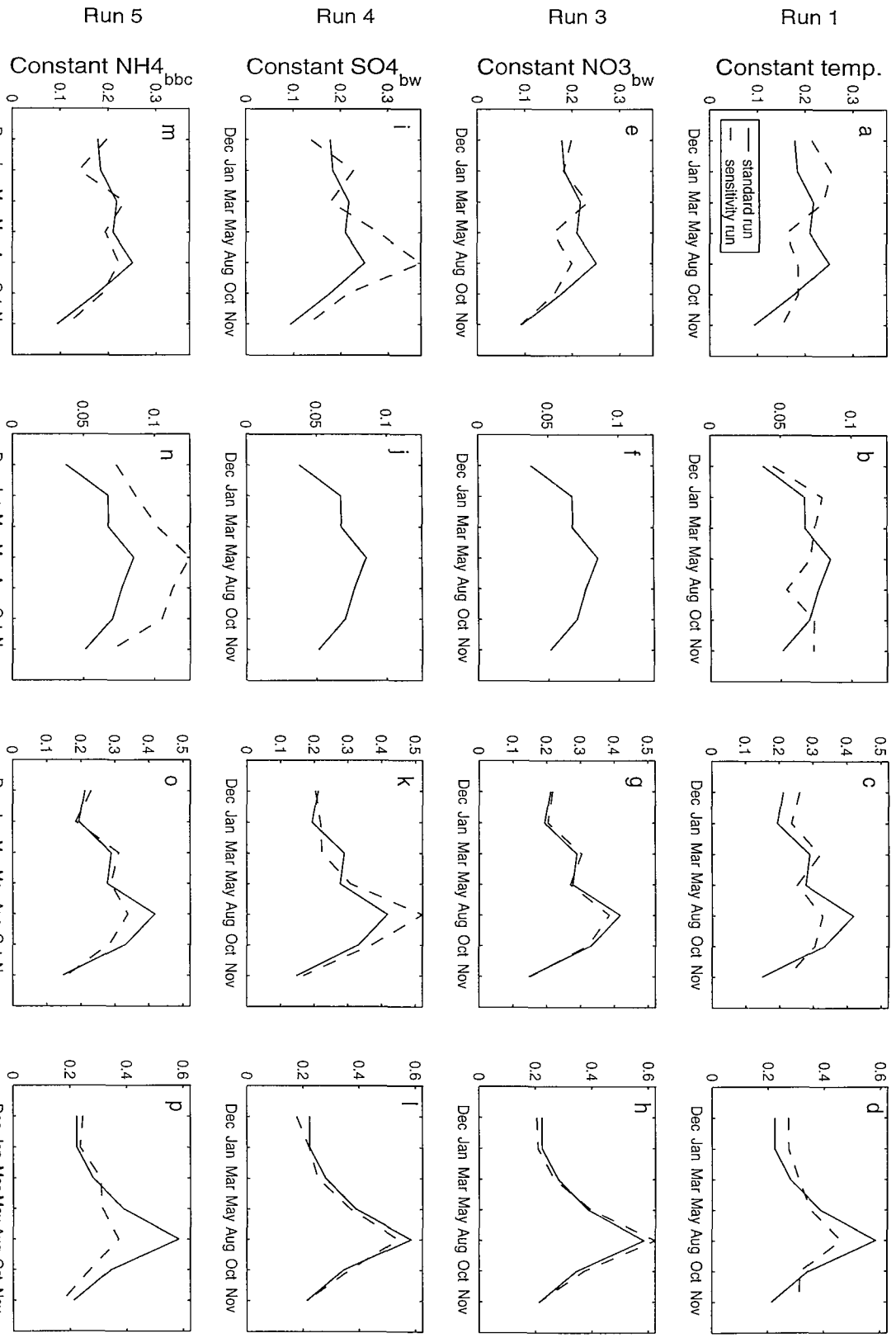

ammonium coincided with highest temperatures and low effluxes occurred at low temperatures (Figure 2.2a). Running the model with constant temperature (Run 1) caused a marked change in the seasonal ammonium fluxes at sites 1 and 2 (Figure 5.17a,b). Ammonium effluxes at sites 3 and 4 were similar to those in the reference run (Figure 5.17c,d), the effect of constant temperature being to dampen the peak in August (Note that temperature is set to 10°C in Run 1 which is less than the 16°C used in the reference run at sites 3 and 4 in August, see Figure 2.2a).

Changes in the overlying nitrate concentration (Run 3) had little effect on the seasonality in ammonium effluxes at sites 2 to 4 (Figure 5.17f-h). Nitrate had a more noticeable effect at site 1 (Figure 5.17c) where sulphate reduction was responsible for most of the ammonium production. Hence the inhibitory effect of nitrate on sulphate reduction (equation 3.9) was greatest at site 1 and this was expressed in the ammonium effluxes.

The effect of overlying sulphate concentrations (Run 4) on the seasonality of the ammonium fluxes was most noticeable at site 1 (Figure 5.17m) where sulphate reduction dominated ammonium production.

Constant bottom boundary concentrations of ammonium (Run 5) meant that there was a constant supply of ammonium to the sediment. Setting the concentration to 1000 $\mu M\ NH_4^+$ in Run 5 meant that, compared to the standard settings (Figure 2.2e), ammonium concentrations and therefore fluxes to the sediment were either reduced or increased at each site depending on the month. The most noticeable effect of Run 5 was at site 2 where ammonium effluxes increased at each month relative to the standard run (Figure 5.17n). This was in response to higher bottom boundary concentrations of ammonium in Run 5 compared to the standard run. The reduction in the ammonium efflux

at site 4 in August (Figure 5.17p) was caused by the lower bottom boundary concentration of ammonium in Run 5 compared to the standard run (4300 μM $NH_4^+$, Figure 2.2e).

The magnitude and seasonality of the ammonium efflux was controlled to varying degrees by temperature, the overlying sulphate concentration and the supply of ammonium from depth at the sites.

### 5.6.2.4. Sulphate fluxes (and sulphate reduction)

Fluxes of sulphate and their relation to forcing data are shown in Figure 5.18a-l. A comparison between the reference run and Run 1 at each site shows that seasonal temperature changes had little effect on seasonal sulphate fluxes (Figure 5.18a-d).

Removal of the seasonal signal in overlying nitrate concentrations (Run 3) had a variable effect among the sites (Figure 5.18e-h). Changes in overlying nitrate concentration changed the nitrate fluxes to the sediment (Figure 5.16a-d) which varied the inhibitory effect of nitrate on sulphate reduction and hence on the sulphate fluxes. Setting $NO3_{bw}$ to 677 μM meant that from December to March nitrate concentrations in the overlying water were lower than in the reference run and higher from May onwards (Figure 2.2c). Consequently nitrate fluxes were lower in December to March and higher thereafter relative to the reference run. This reduced or enhanced rates of sulphate reduction and therefore sulphate fluxes to the sediment (Figure 5.18e-h). Apart from increases or decreases in sulphate fluxes, the seasonal cycle was negligibly affected by changes in overlying nitrate concentrations.

Figure 5.18. Effect of Runs 1, 3 and 4 (see Table 5.1) on sulphate fluxes (mmol $m^{-2}$ $d^{-1}$) across the SWI at 4 sites in the upper Gt. Ouse

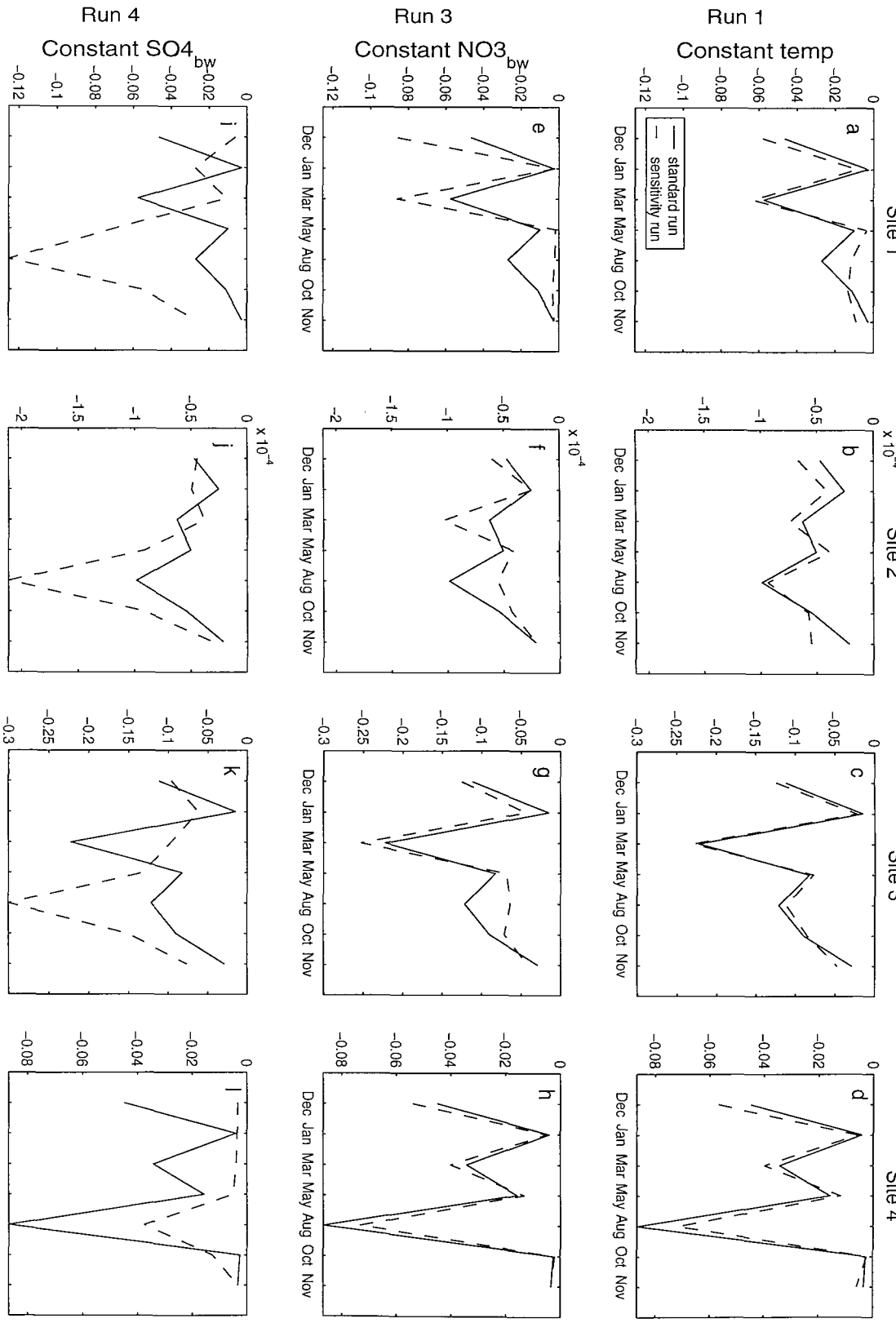

The major control on seasonality was the variability in the sulphate concentrations in the overlying water. This is shown in Run 4 (5.20i-l) where constant sulphate concentrations yielded a significantly different seasonal cycle in sulphate fluxes compared to the reference run. Thus the changing availability of sulphate in the water column ultimately controlled and limited the demand by sulphate reduction in the model.

A summary of all of these results is presented in Table 5.2.

Table 5.2. Summary of controls on seasonality in the model (T= temperature; $SO4_{bw}$, $NO3_{bw}$ = overlying concentrations of sulphate and nitrate, respectively; $NH4_{bbc}$= bottom boundary concentration of ammonium)

| SWI flux | Site 1 | Site 2 | Site 3 | Site 4 |
|---|---|---|---|---|
| Oxygen | T, $SO4_{bw}$, $NO3_{bw}$ | T | T, $SO4_{bw}$, $NO3_{bw}$ | T, $SO4_{bw}$ |
| Nitrate | $NO3_{bw}$ | $NH4_{bbc}$ | $NO3_{bw}$ | $NO3_{bw}$ |
| Ammonium | T, $SO4_{bw}$, $NO3_{bw}$ | T, $NH4_{bbc}$ | T, $SO4_{bw}$ | T, $NH4_{bbc}$ |
| Sulphate | $SO4_{bw}$ | $SO4_{bw}$ | $SO4_{bw}$ | $SO4_{bw}$ |

### 5.6.3. Solute fluxes across the SWI : explaining the seasonality in the observations with reference to the model predictions

Nedwell and Trimmer (1996) showed that oxygen fluxes at sites 1 and 2 were significantly correlated to temperature, in line with studies in other temperate systems (Hopkinson *et al.,* 1999; Cabrita and Brotas, 2000). In contrast, there was no simple explanation for the variation with temperature in oxygen fluxes at sites 3 and 4 suggesting that other environmental factors may be important. Cowan *et al.* (1996) found that oxygen demand in a temperate latitude coastal environment was correlated to both bottom water temperatures and oxygen concentrations in the overlying water. However, these authors concluded that availability of labile organic carbon was ultimately controlling benthic

fluxes. Thamdrup *et al.* (1998) showed that area specific aerobic (oxic) mineralization had a weak temperature dependence in a temperate estuary. This was caused by differences in the seasonal activities of various populations of aerobic bacteria adapted to different ranges in temperature (ie thermophiles and non-thermophiles). Seasonal variations in the flux of labile organic matter and/or the presence of mixed bacterial populations with different temperature optima may explain the observed oxygen fluxes at sites 3 and 4 where oxygen consumption rates were dominated by oxic mineralization (Figure 5.10). The model presented here takes no account of variations in either sedimentary organic carbon concentrations from month to month or different bacterial populations. The measurements of TOC used in this model did not distinguish between labile and refractory fractions and to the author's knowledge there exist no data for fluxes of organic carbon to either the Gt. Ouse or other similar estuarine sediments. Concentrations of chlorophyll, if had been measured, may have been a good indicator of labile organic carbon on account of being strongly correlated to oxygen fluxes (Magalhaes *et al.,* 2002) and nutrient fluxes (Banta *et al.,* 1995; Grenz *et al.,* 2000) in temperate estuarine sediments. This makes it difficult to validate a model which includes the flux and sedimentary incorporation of labile organic carbon. The lack of dynamic simulations of concentrations of organic matter presents a limitation of this model. The possibility of including different bacterial populations with a range of optimal temperatures may be an area of future work.

The analysis of seasonality in the modeled oxygen fluxes (section 5.6.2.1) may partly explain the comparable behaviour of simulated and observed oxygen fluxes between December and March at sites 3 and 4 (Figure 5.6). Fluxes were higher in December and March than in January in both the model and the observations. This pattern was determined by variations in the overlying sulphate concentrations (compare Figure 5.15c,d and Figure 5.15o,p).

The variability in the comparison between modeled and observed nitrate fluxes (Figure 5.7) is probably related to differences in factors controlling both rates of denitrification and the fluxes themselves. Actual rates of nitrate reduction (denitrification) are a function of concentrations of nitrate and oxygen, temperature and organic carbon supply and lability (section 1.9). In the absence of measurements of both denitrification rates and concentrations of labile organic carbon, a link to the observed nitrate fluxes in the sediments of the upper Gt. Ouse cannot be defined. Similar unclear seasonal cycles in nitrate fluxes exist for other temperate sediments (Wadden Sea, Kristensen *et al.,* 1997; San Francisco Bay, Grenz *et al.,* 2000). Some have had to speculate on the role of factors such as sediment mixing and porewater advection in an attempt to understand seasonal nitrate fluxes (Hopkinson *et al.,* 2001). Elsewhere, strong correlations exist between nitrate fluxes and other factors (e.g. overlying nitrate concentrations, Tagas estuary, Magalhaes *et al.,* 2002; temperature, Weser estuary, Sagemann *et al.,* 1996). In the model, seasonal denitrification rates were controlled by nitrate (section 5.6.2.3, Table 5.2). One way to generate some of the high observed fluxes of nitrate (e.g. August at site 4, Figure 5.7) in the model was to increase the organic carbon concentration in the sediment by an order of magnitude (not shown). Such a large increase is unrealistic. Another way to simulate the observed nitrate flux was to increase the diffusion coefficient for nitrate by a factor of 15 (not shown). In doing so, the modeled nitrate fluxes between December and March at site 4 (Figure 5.7) were much greater than the observed fluxes, but at other sites the comparison with the observations improved. It is therefore possible that a combination of transport processes other than diffusion and changes in organic carbon concentrations ( ie the labile fraction) was responsible for the observed fluxes. These factors were neglected in the model and may explain the discrepancies between predicted and measured nitrate (and oxygen) fluxes across the SWI. This speculation casts doubt on the

assumption that organic carbon concentrations remained constant over time in the upper Gt. Ouse sediments.

Ammonium fluxes were significantly correlated ($p<0.05$) to temperature when all the measurements from all the sites were pooled together (Nedwell and Trimmer, 1996). However the seasonal signal in the measured ammonium fluxes at each site (Figure 5.8) was not clear. For instance, the largest measured efflux of ammonium occurred in May at site 1 (Figure 5.8) even though temperature was at a maximum in August (Figure 2.2a). In contrast, the largest ammonium efflux was measured when temperature was highest at site 2 (August). A number of factors have been attributed to controlling the seasonal flux of ammonium in estuarine and coastal sediments. These include temperature and the C:N ratio of the surficial sediments (Forja *et al.,* 1994; Clavero *et al.,* 2000), the activities of sediment biota (Asmus *et al.,* 2000), chlorophyll concentrations (Banta *et al.,* 1995; Vidal *et al.,* 1997), salinity, through adsorption-desorption effects (Hopkinson *et al.,* 1999) and a combination of porosity, overlying ammonium concentrations and chlorophyll pigments (Grenz *et al.,* 2000). Some factors (e.g. chlorophyll), but not others (e.g. sediment biota, C:N ratios - see section 3.1.2), may contribute to the variability in the observed fluxes in the upper Gt. Ouse sediments. A lack of adequate data does not allow for correlations to be derived to understand the seasonal cycle of ammonium effluxes in these sediments.

The magnitude of the ammonium effluxes in the model was mostly within a factor of 2 of the observations. However, modeled and observed seasonality was different. The analysis of model seasonality (section 5.6.2.3) showed that temperature, overlying concentrations of sulphate and nitrate and bottom boundary concentrations of ammonium controlled the seasonal ammonium effluxes to varying degrees at the four sites in the upper Gt. Ouse (Table 5.2). While these factors may not control the seasonality of the observed ammonium effluxes, they may contribute to the magnitude of these fluxes.

### 5.6.4. Differences in model performance: porewater profiles vs. SWI fluxes

The simulations of porewater profiles (Figure 5.2, 5.3, 5.5) suggest that the model mostly reproduces both the seasonality and the individual measurements of the observations. In contrast, the model performs less well when compared to fluxes of nutrients and oxygen across the SWI (Figure 5.6, 5.7, 5.8). This discrepancy in the performance of the model may be related to the experimental determination of the SWI fluxes and porewater concentration profiles. For instance, the large difference between modelled and observed nitrate fluxes in August at sites 3 and 4 (Figure 5.7) is not seen in the comparison of the porewater profiles of nitrate for the same month and site (Figure 5.2). Also, the nitrate flux is directed out of the sediment in May at site 3 (Figure 5.7) even though the porewater profiles suggest an inward flux. In part , this may be due to the inability of the porewater determinations to resolve concentrations at less than 1cm depth intervals. A higher resolution technique for measuring profiles may reveal that in the example of May at site 3 (Figure 5.7), there may be a nitrate maxima within the first 1cm of sediment. More importantly, the measurement of the SWI fluxes is calculated from a change in concentration of nitrate in the water column of a core incubation for a period of up to 24 hours. This is then followed by the determination of the porewater profiles. This sequence does not mean that the latter reflects the value of the flux. At steady state (i.e. when the nitrate flux to the sediment does not change with respect to a constant nitrate concentration or input), the experimental sequence would be valid. That is, the nitrate flux would be the same at any point in time during the incubation. It has been shown (Trimmer, 1997) that above concentrations of 400μM nitrate in the water column, the flux of nitrate becomes asymptotic in the Gt. Ouse sediments. Below this value, the nitrate flux

into the sediment becomes proportional to the nitrate concentration in the overlying water. In August at site 4, the nitrate concentration in the water column at the start of the core incubation was 399μM and diminished to 261μM by the end of the experiment (these values are the mean of triplicates). It follows that the flux of nitrate would not be the same at any point during the incubation. The porewater profile determined after this period would therefore only reflect the flux of nitrate at the end of and not during the experiment. The same is true in August at all other sites where nitrate concentrations in the overlying water are <400 μM (Figure 2.2c). Such considerations need to be taken into account when trying to model both the flux and porewater profiles of particular solutes.

Another reason for the discrepancy between modeled porewater profiles and SWI fluxes may be due to the neglect of advective/turbulent transport processes in the model (section 5.6.1). Similar results in which benthic chamber fluxes were higher than those determined from diffusion models applied to porewater profiles have previously been reported (e.g. Rasmussen and Jørgensen, 1986). This lack of advection highlights a potential limitation in the model.

### 5.6.5. C, N, S and O budgets

The reason for the differences in the budgets of most of the variables between the sites is largely due to the differences in the values of the first order rate constants for organic decay (Table 3.5). The value of $k_{so4}$ is highest (34.7 $y^{-1}$) at site 1, which explains (1) why sulphate reduction dominates the pathways of organic mineralization (Figure 5.9a), (2) why ammonium production is greatest from anoxic mineralization (Figure 5.12a) and (3) why most of the oxygen budget is accounted for by sulphide oxidation (Figure 5.10a). In contrast, at site 2, $k_{so4}$ is lowest (0.06$y^{-1}$) and $k_{o2}$ is much greater than $k_{no3}$ (7.85 $y^{-1}$ cf.

0.0004 $y^{-1}$). This explains the dominance of oxic mineralization in terms of (1) the mineralization budget (Figure 5.9b), (2) the oxygen budget (Figure 5.10b) and (3) the ammonium budget (Figure 5.12b). At site 4, the value of $k_{o2}$ is highest (13.4 $y^{-1}$) which explains why oxic mineralization dominates. Also, the value of $k_{no3}$ is at a maximum (3.63 $y^{-1}$) which explains why nitrate reduction shares a similar proportion of the mineralization budget with sulphate reduction throughout the year (Figure 5.9d). The dominance of denitrification over nitrification in the nitrate budget (Figure 5.11a,c,d) may seem strange given that $k_{no3}$ is much less than the first order rate constant for ammonium oxidation ($K_{nit}$=12520 $y^{-1}$, Table 3.2). This is because the equation for suboxic mineralization (Table 3.1, equation 3.8) includes the concentration of organic carbon which is orders of magnitude greater than the concentration of ammonium used in the nitrification equation (Table 3.1, equation 3.8). Consequently, the realized rate of nitrate based organic mineralization (denitrification) is far higher than the realized rate of nitrification. However, when $k_{no3}$ is as low as at site 2 (up to 4 orders of magnitude less than at other sites, Table 3.5), rates of nitrification exceed rates of denitrification (Figure 5.11b).

### 5.6.6. Annually integrated rates of mineralization: comparisons with $M_{fit}$

The modeled rates of the different pathways of organic carbon mineralization in the sediments at the 4 sites in the upper Gt. Ouse are shown in Figure 5.19. The rate of each pathway varied over the season at each site. This had the effect of changing the relative proportion of mineralization due to oxic, suboxic and anoxic pathways for each month at each site. Overall, these proportions were similar to those derived for the annually

Figure 5.19. Modeled seasonal rates of oxic, suboxic and anoxic mineralization at 4 sites in the upper Gt. Ouse

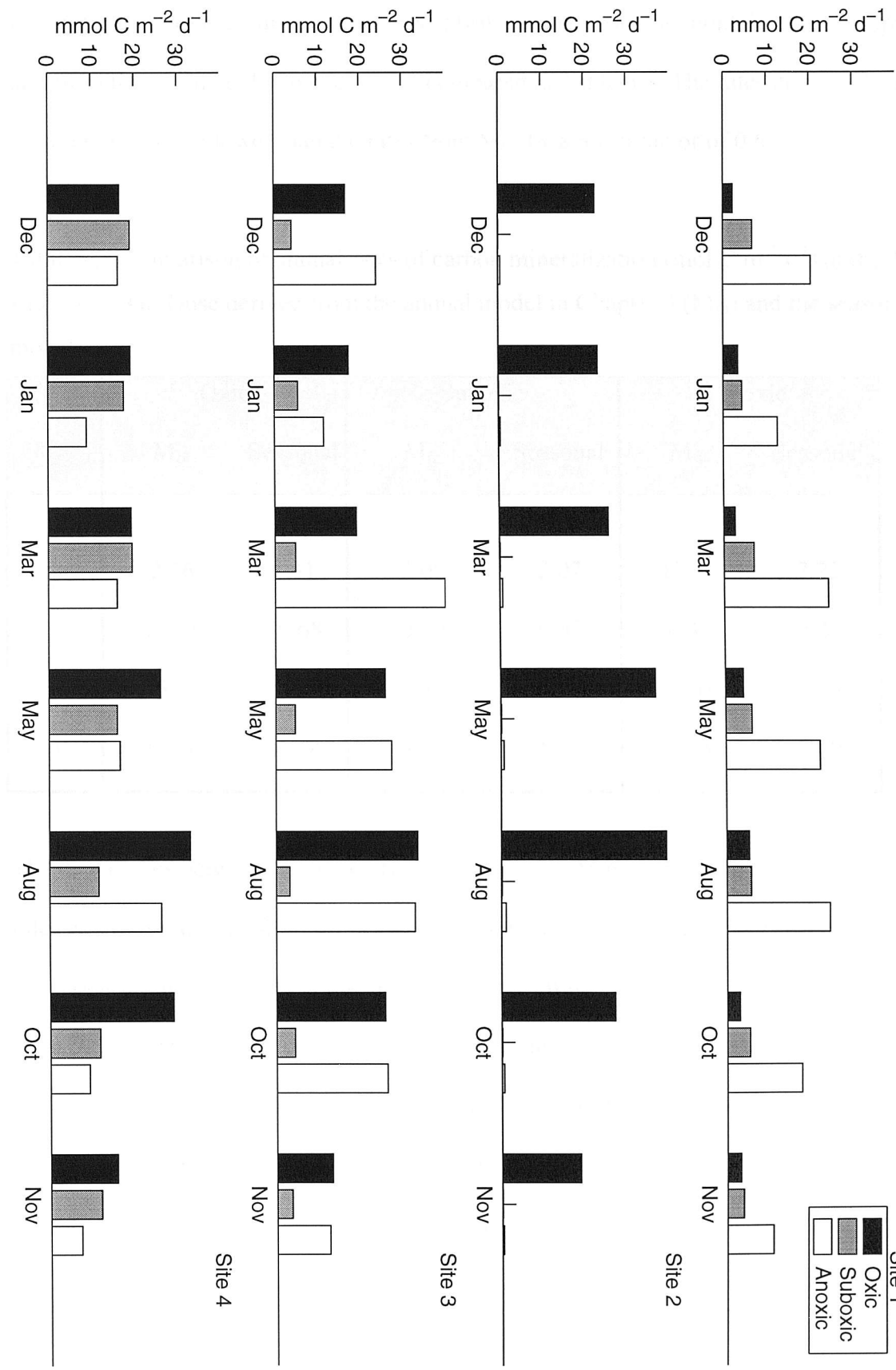

integrated data at each site (Table 2.2). Hence, sulphate reduction dominated at site 1 while oxic mineralization mostly dominated at the remaining sites. The annually integrated rates of each mineralization pathway derived from the monthly model output and from the $M_{fit}$ model (Chapter 3) are compared in Table 5.3. The rates derived from the monthly output are lower than the rates from $M_{fit}$ by a mean factor of 0.67.

Table 5.3 Comparison of annual rates of carbon mineralization (mol C $m^{-2} y^{-1}$) at the 4 sites in the Gt. Ouse derived from the annual model in Chapter 3 ($M_{fit}$) and the seasonal model

| Site | Oxic | | Suboxic | | Anoxic | |
|---|---|---|---|---|---|---|
| | $M_{fit}$ | Seasonal | $M_{fit}$ | Seasonal | $M_{fit}$ | Seasonal |
| 1 | 2.16 | 1.31 | 3.09 | 2.07 | 10.62 | 7.25 |
| 2 | 15.28 | 10.68 | 0.00 | 0.05 | 0.32 | 0.23 |
| 3 | 15.57 | 8.45 | 2.42 | 1.56 | 12.10 | 9.75 |
| 4 | 15.96 | 8.74 | 8.33 | 5.53 | 7.38 | 5.60 |

The differences between the annually integrated rates derived from the modeled monthly rates and those derived from $M_{fit}$ (Table 5.3) are due to the use of the temperature dependency equation (5.2). A test run (not shown) in which equation 5.2 was removed from the diagenetic equations revealed annually integrated rates of organic carbon mineralization similar to those derived in Chapter 3. Deriving the model parameters by calibration against the annually integrated data (Chapter 3) took no account of the effect of temperature on these parameters. Temperatures in the Gt. Ouse sediments ranged between 2°C and 18°C which meant that the $Q_{10}$ temperature factor (equation 5.2) was in the range 0.28-0.87. Consequently, diagenetic rates in the seasonal model were always multiplied by

factors <1. In contrast, the results from $M_{fit}$ did not account for temperature effects. This explains the lower annually integrated rates in the seasonal model compared to $M_{fit}$.

## 5.7. Conclusions

The success of the model in reproducing the seasonal observations in the upper Gt. Ouse sediments is variable. Porewater profiles of oxygen, nitrate and ammonium were well modeled in terms of both visual and statistical comparisons. Sulphate was poorly represented in the model for unknown reasons. Comparisons of modeled and observed fluxes of oxygen, nitrate and ammonium across the SWI were more variable. The seasonality of modeled and measured oxygen fluxes were the same at two sites (1 and 2) but different at the remaining sites. The seasonal oxygen fluxes in the model were controlled by temperature and overlying sulphate concentrations.The model did not represent the observed and irregular seasonality in nitrate and ammonium fluxes. Modeled nitrate and oxygen fluxes generally underestimated the observations (by factors of 0.2-0.5 and 0.5-0.9, respectively) and modeled ammonium fluxes were within ±50% of the observed ammonium fluxes at most times. The difference between the predicted and measured fluxes may have been due to porewater advection or enhancement of transport by turbulent diffusion induced by the stirring rates in the core incubations. This may also explain the lower oxygen penetration depths in the model compared to the observations at some sites.

Variations in temperature and overlying concentrations of nitrate, ammonium and sulphate were insufficient to explain all of the variability in observed solute fluxes across the SWI. This casts doubt on the assumption that concentrations of organic carbon were in steady state at all sites. It is concluded that the availability of labile organic carbon and its

variability should be accounted for in the model and in the data collection. In the present model, this would be analogous to seasonally varying the values of the first order rate constants for each pathway of organic mineralization. Lack of a clear seasonal cycle in the observed fluxes of nitrate and ammonium (and oxygen in the case of two sites) means that there was no reliable predictor for enabling variations in these parameters.

Annual integrals of the seasonal rates of organic carbon mineralization in the model are lower than the annual integrals derived from the observed data and the model in Chapter 3. This is due to the use of the temperature dependency equation (5.2) which lowers the diagenetic rates in the model compared to the model in Chapter 3. The difference between the two estimates (33%) provides a possible range in error for annually integrated rates.

# 6. Pathways of dissimilatory nitrate reduction in the lower Gt. Ouse: a diagenetic model discriminating denitrification and dissimilatory nitrate reduction to ammonium on the basis of temperature

## 6.1. Introduction

Less than half of the nitrate flux into the sediments of the lower Gt. Ouse was denitrified, the remainder ending up as ammonium (Trimmer *et al.*, 1998). In section 1.9.1 an outline of the factors controlling the proportioning of nitrate reduction into denitrification and DNRA was given (Table 1.3). In this Chapter, temperature is used to implement DNRA into a diagenetic model for the first time. The central hypothesis is that temperature controls the proportioning of nitrate reduction into denitrification and DNRA in the lower Gt. Ouse sediments. This work builds on the diagenetic model developed in Chapters 3 and 5.

## 6.2. Model description, equations and assumptions

A full description of the basic model is given in Chapters 3 and 5. The difference here is that nitrate reduction has been extended (see below) to account for DNRA and is the main subject of this Chapter. Model assumptions are also identical to those in Chapter 3 (section 3.4.1). Note that in Chapter 5, it was concluded that changes in the availability of organic carbon were needed to simulate the observed seasonality in the upper Gt. Ouse. However, as the model is applied to the lower Gt. Ouse where no measurements of TOC concentrations were made, and the emphasis is on modelling nitrate reduction, the same assumptions as those in Chapter 3 are applied as a starting point.

### 6.3. Boundary conditions, initialisation and imposed data

In the absence of porewater data, a zero flux bottom boundary condition is imposed for all model variables (note the difference for ammonium in the upper Gt. Ouse sediments where the bottom boundary condition was fixed by measurements, see Table 3.3). This assumes that all reactive organic carbon has been respired at the depth of the model domain. Top boundary values at the sediment-water interface (SWI) for oxygen, nitrate and ammonium are the mean (triplicates) core incubation concentrations in the water column during the incubation period. For all model runs, free sulphide levels are set to zero in the water column. Sulphate concentrations in the water column are calculated from salinity assuming conservative mixing from an end-member concentration of 28.23mM$SO_4^{=}$ (Wilson, 1975) at 35 salinity. At sites 5 to 9 the salinity range of 25 to 29 yields sulphate concentrations of 20.17 to 23.39 m$MSO_4^{=}$, respectively. As the model is insensitive to this range in sulphate concentrations a mean sulphate concentration of 21.78 m$MSO_4^{=}$ is used as the top boundary condition at sites 5 to 9. At low tide, salinity at site 4 was always approximately 1. Consequently, the sulphate top boundary concentration is calculated as 0.81 mM at site 4. Measured TOC concentrations (Table 2.1b) are imposed in each model box and assumed to be evenly distributed with depth. No porewater measurements were made in these sediments and so initial concentrations of each model variable ($O_2$, $NO_3^-$, $NH_4^+$, $SO_4^{=}$ and $S^{=}$) are set to the same value in each model box (i.e. uniform concentrations with depth). Preliminary runs (not shown) show that the model outcome was not sensitive to the initial conditions of these solutes.

## 6.4. Temperature and proportioning of nitrate reduction into denitrification and DNRA

For the purposes of the analysis that follows, nitrate reduction, denitrification and DNRA refer to the components of these processes which are fuelled by nitrate from the overlying water column. Consequently, to avoid confusion, the terms $NR_w$ (nitrate reduction fuelled by nitrate from the overlying water), $D_w$ and $DNRA_w$ will be used from hereon. All other references to nitrate reduction, denitrification and DNRA are for total rates (i.e. the sum of rates fuelled by nitrification and by incoming nitrate from the overlying water column). Hence, it is assumed that the flux of nitrate to the sediment is equivalent to the rate of $NR_w$, where $NR_w = D_w + DNRA_w$. This assumption is justified by the findings (Trimmer *et al.*, 1998) that at all sites, the nitrate fluxes (90% of which were directed into the sediment) were significantly correlated ($p<0.05$) with both the rates of $D_w$ and the ammonium effluxes ($r=0.47$), the strongest correlation being at site 7 ($r=0.78$). Rates of nitrification can therefore be assumed to be negligible or in constant proportion with nitrate reduction. Furthermore, as nitrification is inhibited by the acetylene blockage technique used here, the effect of nitrification on the following calculations is, at best, minimal.

Linking the measurement of $D_w$ with the contemporaneously measured nitrate flux, enables a description of the partitioning of $NR_w$ into $DNRA_w$ and $D_w$. Dividing $D_w$ by the nitrate flux gives the proportion ($P_D$) of $NR_w$ due to $D_w$. It follows that the remaining proportion ($P_{DNRA}$) is due to $DNRA_w$. Thus,

$$P_D = D_w \div \text{Nitrate flux to the sediment} \qquad 6.1$$

and

$$P_{DNRA} = 1 - P_D \qquad 6.2$$

Table 6.1. Rates of uncoupled denitrification ($D_w$), fluxes of nitrate($N_f$) across the sediment water interface and values for $P_D$ (=$D_w$ / $N_f$, see text) at the six sites in the lower Gt. Ouse.(cnp=calculation not possible; nm =not measured;units =μmol N $m^{-2}$ $h^{-1}$; negative value =flux to sediment)

| Temp | Month | Site 4 | | | Site 5 | | | Site 6 | | | Site 7 | | | Site 8 | | | Site 9 | | |
|---|---|---|---|---|---|---|---|---|---|---|---|---|---|---|---|---|---|---|---|
| °C | | $N_f$ | $D_w$ | $P_D$ | $N_f$ | $D_w$ | $P_D$ | $N_f$ | $D_w$ | $P_D$ | $N_f$ | $D_w$ | $P_D$ | $N_f$ | $D_w$ | $P_D$ | $N_f$ | $D_w$ | $P_D$ |
| 5 | Jan 95 | 432.95 | 21 | cnp | nm | nm | cnp | nm | nm | cnp | -227.24 | 30 | 0.13 | nm | nm | cnp | -115.65 | 9 | 0.08 |
| 7 | Apr 94 | -154.61 | 18 | 0.12 | -8.55 | 47 | 5.50 | 161.20 | 42 | cnp | -1149.58 | 50 | 0.04 | -1081.12 | 91 | 0.08 | -27.75 | 15 | 0.54 |
| 9 | Nov 94 | -251.08 | 81 | 0.32 | -399.37 | 60 | 0.15 | 575.00 | 19 | cnp | -1070.64 | 84 | 0.08 | 383.77 | 40 | cnp | -211.83 | 8 | 0.04 |
| 14 | May 94 | -184.20 | 158 | 0.86 | -300.09 | 176 | 0.59 | -327.13 | 174 | 0.53 | -433.21 | 228 | 0.53 | -474.86 | 121 | 0.25 | -121.30 | 88 | 0.73 |
| 17 | Aug 94 | -165.08 | 131 | 0.79 | nm | nm | cnp | nm | nm | cnp | -68.68 | 63 | 0.92 | -343.83 | 32 | 0.09 | nm | nm | cnp |
| 22 | Jul 94 | -288.31 | 106 | 0.37 | -149.90 | 166 | 1.11 | -218.41 | 19 | 0.09 | -290.68 | 60 | 0.21 | -56.41 | 37 | 0.66 | -30.31 | 4 | 0.13 |

Note that this calculation is only valid if the flux of nitrate is directed towards the sediment. As mentioned above, the lower Gt. Ouse sediments, with few exceptions (only 10% of the 112 measurements of nitrate fluxes were directed from the sediment to the water column), were consistent sinks for nitrate. The range of $P_D$ values derived in this way is between 0.04 and 0.92 when all sites are considered (Table 6.1). This large range indicates considerable variation in the proportioning of $NR_w$ into $DNRA_w$ and $D_w$. Figure 6.1 shows the relationship between temperature and $P_D$ at sites 4 to 9. Note that because of either a lack of measurement at a particular temperature and/or a flux of nitrate out of the sediment, not all sites have $P_D$ values at every temperature.

The values of $P_D$ show some variation between sites. However, an overall pattern in the behaviour of $P_D$ with temperature is discernible. Statistical analysis (one-way ANOVA tests) shows that there is no significant difference ($p=0.89$) in the means between sites, but that there is a significant difference ($p=0.04$) between temperatures when sites are grouped together. This suggests a correlative link between temperature and the partitioning of $NR_w$ into $D_w$ and $DNRA_w$. It also suggests that the mean affect of temperature on $NR_w$ partitioning is the same at each site. Note that the lowest mean $P_D$ value ($0.28\pm0.16$ (SE) occurs at site 7 which has the highest C:N (19) ratio (Table 2.1b) while the highest mean $P_D$ ($0.49\pm0.14$ (SE)) occurs at site 4 which has the lowest C:N (5) ratio (Table 2.1b). Measurements of total organic carbon and total organic nitrogen at other times in the year were not significantly different (Trimmer, 1997). Consequently it is assumed that there is no correlation between C:N ratio and nitrate reduction partitioning (see discussion). With the exception of site 8, the overall effect of temperature on $P_D$ is to yield highest values at temperatures between 14°C and 17°C and lowest values at the extremes of the observed temperature (5°C and 22°C). On the basis of the aforementioned significant correlations ($p<0.05$) between the nitrate fluxes and both the rates of $D_w$ and

Figure 6.1. Relationship of $P_D$ (temperature selection in nitrate reduction, see text) with temperature at six sites in the lower Gt. Ouse sediments.

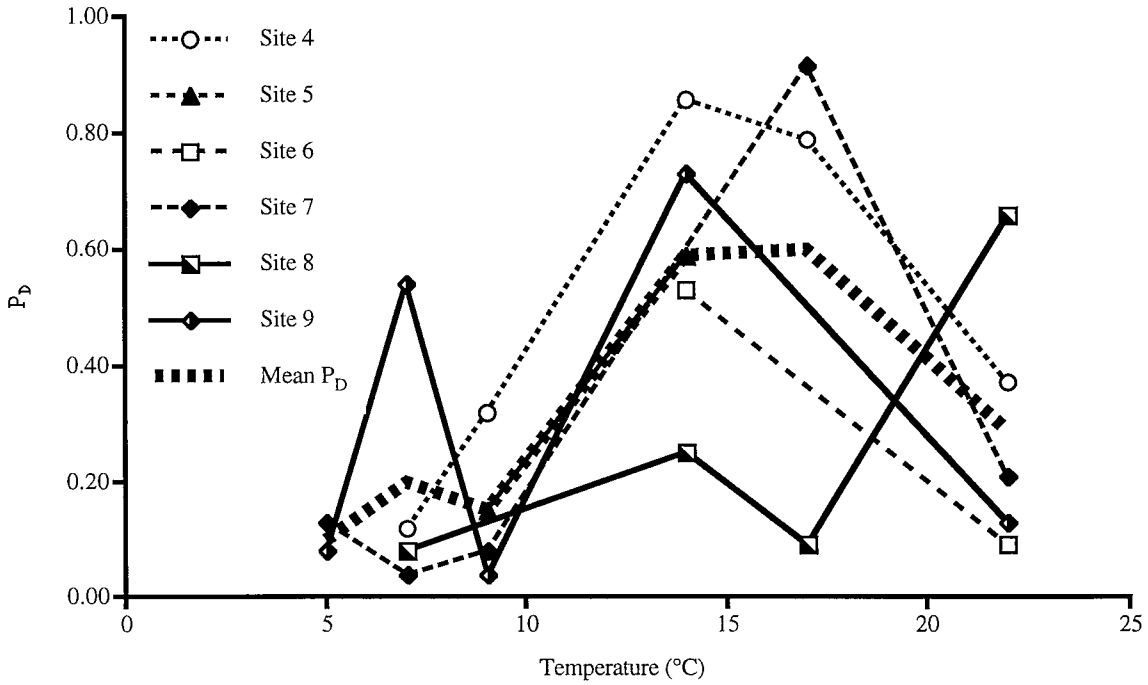


the ammonium effluxes, it is assumed from hereon that this temperature relationship holds for total nitrate reduction (i.e. $D_w$ + coupled nitrification-denitrification, $D_n$, + $DNRA_w$ + coupled nitrification-DNRA, $DNRA_n$). Hence, the function $P_D$ indicates that in the lower Gt. Ouse sediments, colder (<14°C) and warmer (>17°C) temperatures favour DNRA and moderate (14°C-17°C) temperatures favour denitrification. This effect is well illustrated by the variation with temperature of the mean $P_D$, (Figure 6.1). The exceptions to the general behaviour are found at site 9 ($P_D$ = 0.54 at 7°C) and at site 8 ($P_D$ =0.66 at 22°C). These are caused by large values of $D_w$ relative to the nitrate flux. It is not possible to explain why these exceptions exist.

To implement this behaviour into the model, it is necessary to derive a function from this data set. The function requires a form which follows the mean $P_D$ at all sites (Figure 6.1). Fitting yields a slightly right-skewed bell-shaped curve which has the form:

$$\mathrm{FitP_D} = Ae^{-\left(\frac{T_{opt}-T}{\sigma}\right)^2} \qquad 6.3$$

where $T_{opt}$ is the optimum temperature for selection of $D_w$ (i.e. highest $P_D$), $T$ is the temperature, $\sigma$ is the standard deviation of the temperature and $A$ is a coefficient that is derived by fitting equation 6.3 to the pooled data. The mean $P_D$ (Figure 6.1) suggests $T_{opt}$ =16°C. Given $\sigma$=6.09, $A$ is calculated numerically with the statistical software package SYSTAT yielding $A$=0.65. Figure 6.2 shows the fit of equation 6.3 to the pooled data of calculated $P_D$ values for all sites. The fit has the correlation $r^2$=0.42 and closely resembles the mean $P_D$ which is repeated in Figure 6.2 for comparison purposes. Given that there is a significant difference (p=0.04, see above in this section) in the mean $P_D$ between temperatures, there is sufficient reason to have confidence in the use of equation 6.3

## 6.5. Implementation of equation 6.3 into the model

The model equation for carbon oxidation via nitrate (SuboxMin) is

$$\mathrm{SuboxMin} = k_{no3}\left(\frac{1-\phi}{\phi}\right)\mathrm{TOC}\underbrace{\left[\frac{NO_3}{NO_3 + k_{s_{NO3}}}\right]}_{\text{NO3 limitation}}\underbrace{\left[\frac{O_2}{O_2 + k_{sInhO2}}\right]}_{\text{O2 inhibition}}\mathrm{Q10fact} \qquad 6.4$$

where T is temperature, TOC is total organic carbon, $ks_{NO3}$ is the half saturation constant for nitrate limitation, $ks_{inhO2}$ is the half saturation constant for oxygen inhibition, $k_{no3}$ is the first order rate constant, Q10fact is the temperature dependency (equation 5.1) and the units are in mmol C $m^{-3}$ $d^{-1}$. All parameter values used in this model (except for $k_{no3}$) and their definitions are shown in Table 3.2. Multiplying equation 6.3 by equation 6.4 yields a

formula that, according to the temperature, determines what proportion of total nitrate reduction follows DNRA and denitrification.

Figure 6.2. Plot of $FitP_D$ and mean $P_D$ (from Figure 6.1) versus temperature

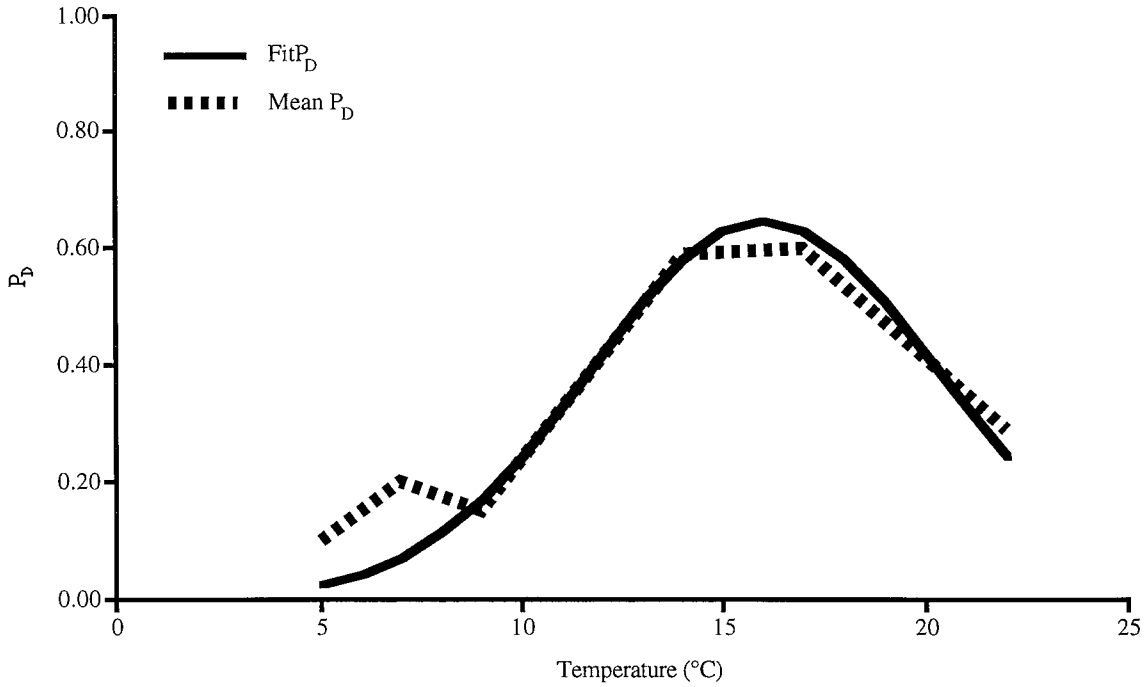


However, equation 6.4 needed modification to account for the stoichiometric conversion of TOC to either dinitrogen gas (denitrification) or to ammonium (DNRA). Using

$$(CH_2O)_{106}\,(NH_3)_{16} + 94.4HNO_3 \rightarrow 106CO_2 + 47.2N_2 + 16NH_3 + 177.2H_2O \qquad 6.5$$

and

$$(CH_2O)_{106}\,(NH_3)_{16} + 53HNO_3 \rightarrow 106CO_2 + 69NH_3 + 53H_2O \qquad 6.6$$

for denitrification and DNRA respectively, yields stoichiometric ratios ($\gamma$) of 0.4 (mole of $N_2$ produced per mole of carbon oxidised via nitrate) and 0.65 (mole of $NH_3$ produced per

mole of carbon oxidised via nitrate and per tomole of nitrate ammonified), respectively. Thus, combining equations 6.3, 6.4 and 6.5 yields for total denitrification:

$$FitP_D \times SuboxMin \times \gamma_{N_2}^{NO_3} \qquad 6.7$$

and combining equations 6.3, 6.4 and 6.6 yields for total DNRA:

$$(1\text{-}FitP_D) \times SuboxMin \times \gamma_{NH_4}^{NO_3} \qquad 6.8$$

Note that the standard formula for nitrate reduction used in the earlier version of this model (equation 3.8, Table 3.1) and in other diagenetic models (e.g. Boudreau, 1996), is an equation similar to 6.7 but without $FitP_D$.

In equations 6.7 and 6.8, it must be assumed that the temperature dependent components, $FitP_D$ and Q10fact are mutually exclusive. In $FitP_D$, it is assumed that temperature is selecting different types of nitrate reducing bacteria (King and Nedwell, 1984; Ogilvie *et al.,* 1997a). In other words, denitrifying bacteria and nitrate ammonifiers have optimally adapted to different temperature ranges. Consequently, the effect of temperature works at the adaptive (genetic) level of the organism. In contrast, Q10fact works on the metabolic (enzymatic) level of the bacteria. Hence, these two temperature components, $FitP_D$ and Q10fact, can be considered as independent effects on nitrate reduction which justifies them being multiplied together in equations 6.7 and 6.8.

Derivation of $k_{no3}$ was achieved by fitting modelled rates of $D_w$ to the peak rates of measured $D_w$ which occurred at 14°C at all sites. The value of $k_{o2}$ and $k_{so4}$ (first order rate constants for oxygen respiration and sulphate reduction, respectively) at each site is taken as the mean value (8.7 $y^{-1}$ and $10y^{-1}$, respectively) from sites 1 to 4 in the Gt. Ouse (Table

3.5). All remaining parameter values have not been changed from their settings in Table 3.2. The advantage of this is a model with only 1 parameter ($k_{no3}$) to fit, yielding a low degrees of freedom.

Finally, to distinguish $D_w$ in the model and thus facilitate comparisons with the measurements, total modelled denitrification ($D_n + D_w$, equation 6.7) is multiplied by the ratio of the nitrate flux to the sediment to the sum of the nitrate flux plus the depth integrated rate of nitrification i.e.

$$D_w = \frac{NO_3^- \text{ flux}}{\left( NO_3^- \text{ flux} + \sum_{z=z_{max}}^{z=z_0} \text{Nitrification} \right)} \text{ x } FitP_D \text{ x SuboxMin x } \gamma_{N_2}^{NO_3} \qquad 6.9$$

where the interval $z_0$ to $z_{max}$ is the total depth (15cm) considered in the model. Note that although nitrification has been assumed to have a negligible effect on the calculation of $P_D$ (because of the use of the acetylene blockage technique), this does not mean that nitrification is not occurring in the lower Gt. Ouse sediments. Hence, nitrification is included in the model.

## 6.6. Results

The model is run for each site and each temperature (i.e. for different months). Differences between model runs at each site are thus caused by temperature and additionally by variations in the water column boundary values for the three measured solutes $O_2$, $NO_3^-$ and $NH_4^+$. Differences between sites are due to differences in TOC concentrations, porosity and top boundary values. Temperature does not vary between sites. Model and measurement derived results (i.e. $D_w$ and $DNRA_w$ rates) are displayed with respect to

temperature. The contribution of DNRA to total ammonium production is also presented as are nutrient and oxygen fluxes across the SWI.

### 6.6.1. Nitrate reduction

Measured and modelled rates of sedimentary $D_w$ are plotted in Figure 6.3 against sediment temperature at the six sites in the lower Gt. Ouse. The general pattern in the observations shows a bell-shaped curve with rates of denitrification peaking at 14°C (May 1994) at all sites. Modelled rates of $D_w$ (which use equation 6.9) show the same relationship with temperature as the observations. From hereon, this model run is referred to as M+Fit$P_D$. The comparison between M+Fit$P_D$ and the measurements is highly significant ($p < 0.001$). For comparison purposes, model output which does not account for temperature based proportioning of nitrate reduction (i.e. equation 6.9 without Fit$P_D$ and henceforth this model run is called M-Fit$P_D$) is also plotted in Figure 6.3.

Table 6.2 Values of the first order rate constant for nitrate reduction used in the model output with (M+Fit$P_D$) and without (M-Fit$P_D$) equations 6.7 and 6.8 (units ; $y^{-1}$; NB $k_{o2}$ = 8.7 $y^{-1}$ ; $k_{so4}$ = 10 $y^{-1}$ ; the latter two parameters are the mean values for the four sites in the Gt. Ouse, Table 3.5)

| Site | M+Fit$P_D$ | M-Fit$P_D$ | Factor difference |
|---|---|---|---|
| 4 | 11.57 | 4.68 | 2.47 |
| 5 | 0.79 | 0.34 | 2.29 |
| 6 | 4.83 | 1.90 | 2.54 |
| 7 | 1.18 | 0.52 | 2.25 |
| 8 | 1.45 | 0.61 | 2.36 |
| 9 | 0.83 | 0.37 | 2.25 |

Figure 6.3. Modeled (M+Fit$P_D$ and M-Fit$P_D$, see text) and observed rates of uncoupled denitrification at 6 sites in the lower Gt. Ouse; error bars =±SE; nitrate in the overlying water is also plotted. Data from Trimmer *et al.*, 1998)

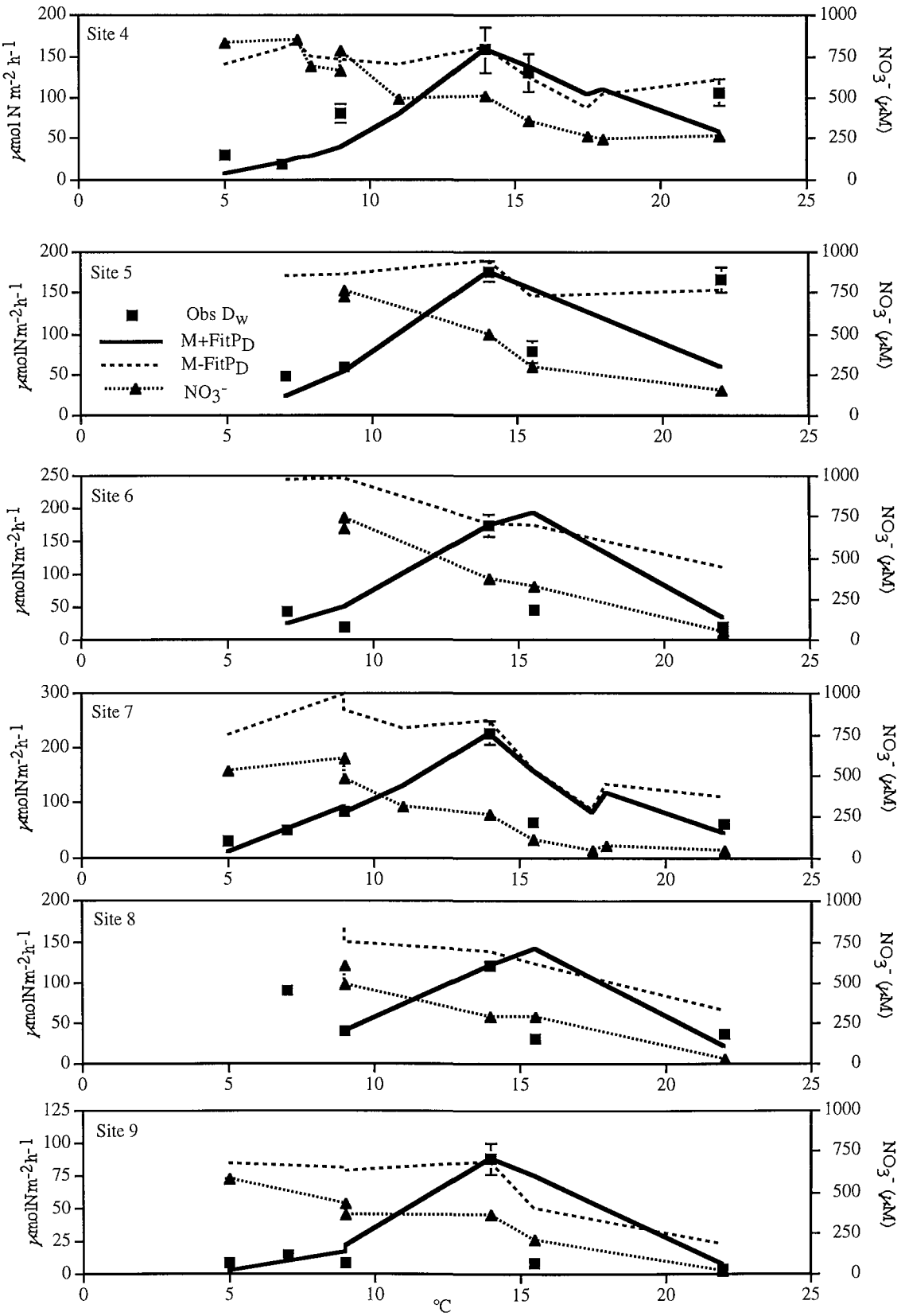

Figure 6.4. Modelled and calculated rates of sedimentary $DNRA_w$ (see text for details) at six sites in the lower Gt. Ouse (calculated rates = measured nitrate flux to sediment - measured rate of denitrification ($D_w$); error bars = ±SE; Data from Trimmer *et al.*, 1998).

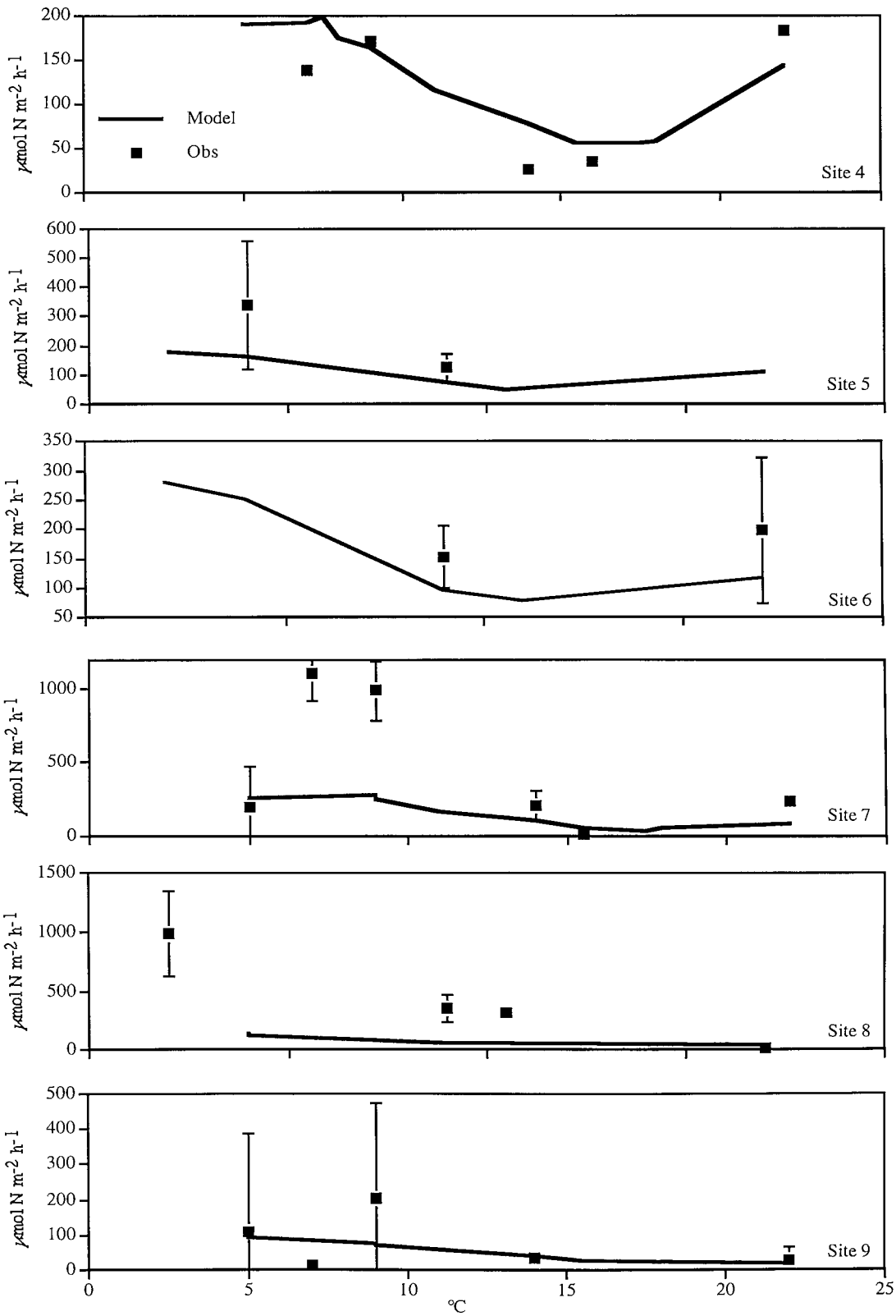

The correlation between M-Fit$P_D$ and the observations is not significant (p=0.18). As with M+Fit$P_D$, M-Fit$P_D$ was derived by fitting the model to rates of $D_w$ measured at 14°C. Fitted values for the first order rate constant $k_{no3}$ derived by M+Fit$P_D$ and M-Fit$P_D$ are shown in Table 6.2. $k_{no3}$ values are higher in M+Fit$P_D$ by a mean factor of 2.36 compared to M-Fit$P_D$.

Rates of $D_w$ in M-Fit$P_D$ overestimate the observations by a mean factor of 6.8 at temperatures less than 14°C compared to a factor of 1.4 for M+Fit$P_D$. For temperatures greater than 14°C, $D_w$ rates in both M-Fit$P_D$ and M+Fit$P_D$ are a mean factor of ~2 higher than the observations. Concentrations of nitrate in the overlying water column are also plotted in Figure 6.3. As expected, nitrate levels decrease with increasing temperature at all sites, reflecting weather induced seasonality (i.e. higher runoff in winter compared to summer). This in part accounts for the decrease in both model and measured $D_w$ at temperatures greater than 14°C (see discussion).

$D_w$ rates in M+Fit$P_D$ are consistently higher than the observations (mean factor = 4) at 16°C. Site 4 is the exception to this. Note that values of Fit$P_D$ are at a maximum (=0.66) at this temperature.

Figure 6.4 compares modelled and calculated rates of $DNRA_w$ at all sites in the lower Gt. Ouse. Calculated rates of $DNRA_w$ were derived as the difference between the measurements of the flux of nitrate into the sediment and the rates of $D_w$. Variability in the calculated rate was determined by adding the variances of both the nitrate fluxes and the $D_w$ rates and then subtracting double the covariance of the two measurements i.e.

$$Var(DNRA_w) = Var(NO_3^- \text{ flux}) + Var(D_w) - 2CoVar(NO_3^- \text{ flux}, D_w)$$

where Var is the variance and CoVar is the covariance. This assumes that the nitrate flux and the rate of $D_w$ are not independent of one another.

In some cases (site 4 at 7°C-March 1995, 9°C-November 1994, 14°C-May 1994 and 15.5°C-September 1994, see Figure 6.4), the standard deviation is larger than the calculated rate of $DNRA_w$. This impossible spread in $DNRA_w$ is caused by the large variation in the nitrate flux (i.e. within the same sample of triplicate measurements both influxes and effluxes of nitrate were measured). However, overall, the modelled rates of $DNRA_w$ compare well with the calculated rates. Linear regression shows a significant correlation ($p<0.0001$) between modelled and calculated $DNRA_w$. In some months (March 1995-7°C, November 1994-9°C at site 7; March 1995-7°C at site 8) calculated rates (~1000 μmol N $m^{-2}$ $h^{-1}$) of $DNRA_w$ are much greater than the modelled rates (~150-300 μmol N $m^{-2}$ $h^{-1}$). Overall, the model underestimates the calculated rates of $DNRA_w$ (regression slope = 0.3).

### 6.6.2. DNRA and total ammonium production

Figure 6.5 shows the percentage contribution of total DNRA to total ammonium production for each temperature at all sites. (DNRA ammonium production consists of ammonium derived from both the nitrate nitrogen and from the nitrogen bound in the organic matter (see equation 6.6)). The remaining percentage is due to the respiration of TOC by oxygen reduction, denitrification and sulphate reduction. Site 4 has the highest percentage contribution of DNRA to the total production of ammonium ( 15-58%, mean=36%), then, in descending contribution order, site 6 (7-47%, mean=24%), site 8 (4-31%, mean=17%), site 7 (2-37%, mean=16%), site 5 (5-31%, mean=16%) and site 9 (1-16%, mean=7%). Each site shows a similar pattern: decreasing percentage contributions to the ammonium pool from total DNRA with increasing temperatures. Sites 5 and 7 show a

slight increase (by 2%) in the percentage contribution between 15.5°C and 22°C and between 18°C and 22°C, respectively. Site 4 percentage contributions increase by a greater amount from 15% to 28% between 18°C and 22°C.

Figure 6.5. Percentage contribution of DNRA to total ammonium production at each temperature at 6 sites in the lower Gt. Ouse sediments. The remaining percentage is due to TOC mineralization.

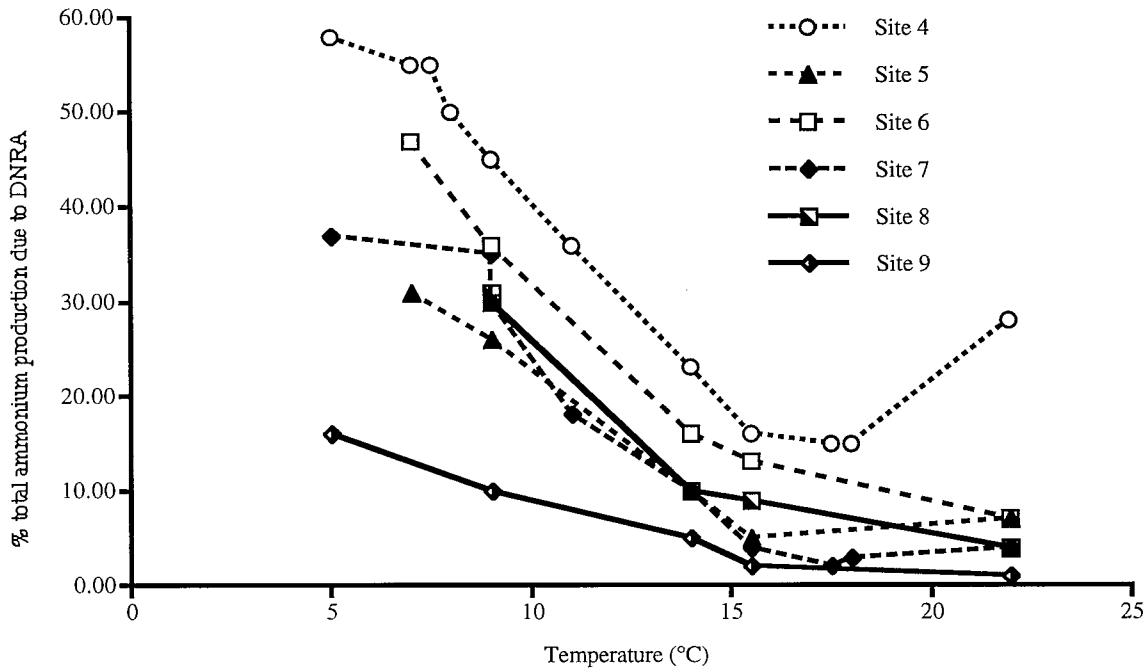


### 6.6.3. SWI Fluxes

The model output described in the following sections refer to model runs with M+Fit$P_D$.

#### 6.6.3.1.Nitrate

Model nitrate fluxes for each site are shown along side the observations in Figure 6.6. The range of model fluxes across the sites is between 30 and 368 μmol $NO_3^-$ $m^{-2}$ $h^{-1}$. This

compares with the observed range of 30 to 1150 μmol $NO_3^-$ $m^{-2}$ $h^{-1}$. The model does not simulate effluxes of nitrate which are apparent in the observations (e.g. site 4 at 17.5°C in August 1994 = 59 μmol $NO_3^-$ $m^{-2}$ $h^{-1}$ and site 6 at 9°C in November 1994 = 575 μmol $NO_3^-$ $m^{-2}$ $h^{-1}$). Many of the observed fluxes have large error bars (±SE) associated with them (e.g. site 4, 7°C-9°C; site 9, 5°C sand 9°C). Consequently, the model fluxes often fall close to or within the range of the observed fluxes. Note the large fluxes of nitrate (>1000 μmol $NO_3^-$ $m^{-2}$ $h^{-1}$) at sites 7 and 8. These cannot be reproduced by the model.

Observed nitrate fluxes do not correlate with either temperature or nitrate concentrations in the water column (Trimmer *et al.*, 1998) which contrasts with the model output. In the latter for all sites, nitrate fluxes increase with temperature up to a maximum at 14°C above which nitrate fluxes decrease. The initial increase is due to the direct effects of temperature (via Q10fact, equations 5.1 and 6.4) on nitrate reduction while the subsequent fall in nitrate uptake by the sediment is related to the decrease in nitrate concentrations in the overlying water.

### 6.6.3.2.Ammonium

Figure 6.7 shows modelled and measured ammonium fluxes plotted against temperature at the six sites in The lower Gt. Ouse sediments. Model effluxes across all sites are in the range 118-324 μmol $NH_4^+$ $m^{-2}$ $h^{-1}$. This compares with the observed effluxes of 5 to 1021 μmol $NH_4^+$ $m^{-2}$ $h^{-1}$. On some occasions (e.g. September 1994, temperature = 15.5°C, site 8) ammonium fluxes are directed into the sediment. The model does not reproduce these fluxes. The best comparison with the observed data is at site 7 (Figure 6.7).

Figure 6.6. Modeled and observed fluxes of nitrate across the SWI at 6 sites in the lower Gt. Ouse (error bars are ±SE from triplicate samples; Trimmer *et al.*, 1998)

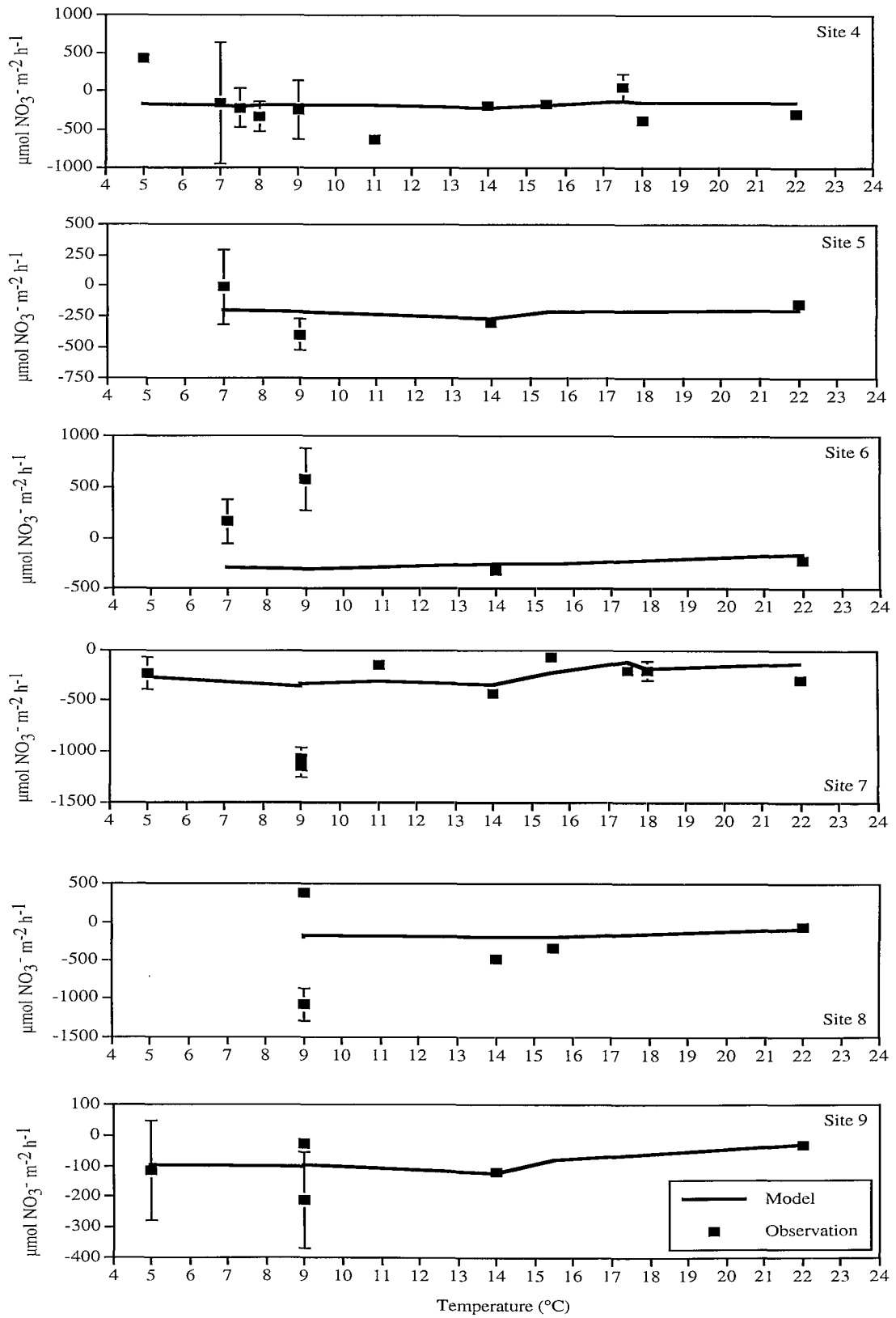

Figure 6.7. Modeled and observed fluxes of ammonium across the SWI at 6 sites in the lower Gt. Ouse (error bars are ±SE from triplicate samples; Trimmer *et al.*, 1998)

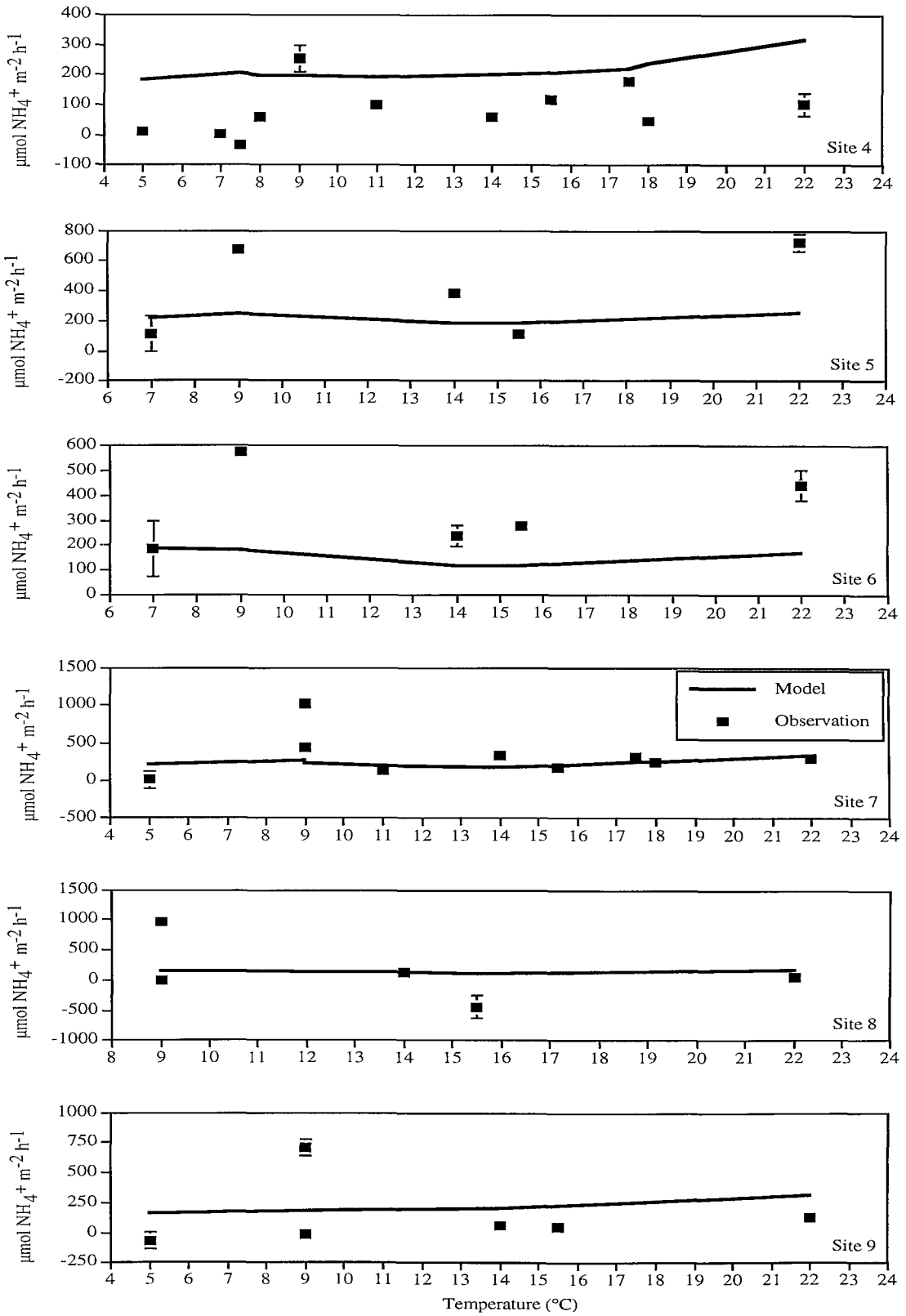

Figure 6.8. Modeled and observed fluxes of oxygen across the SWI at sites 4 and 7 in the lower Gt. Ouse (error bars are ±SE from triplicate samples; Trimmer *et al.*, 1998)

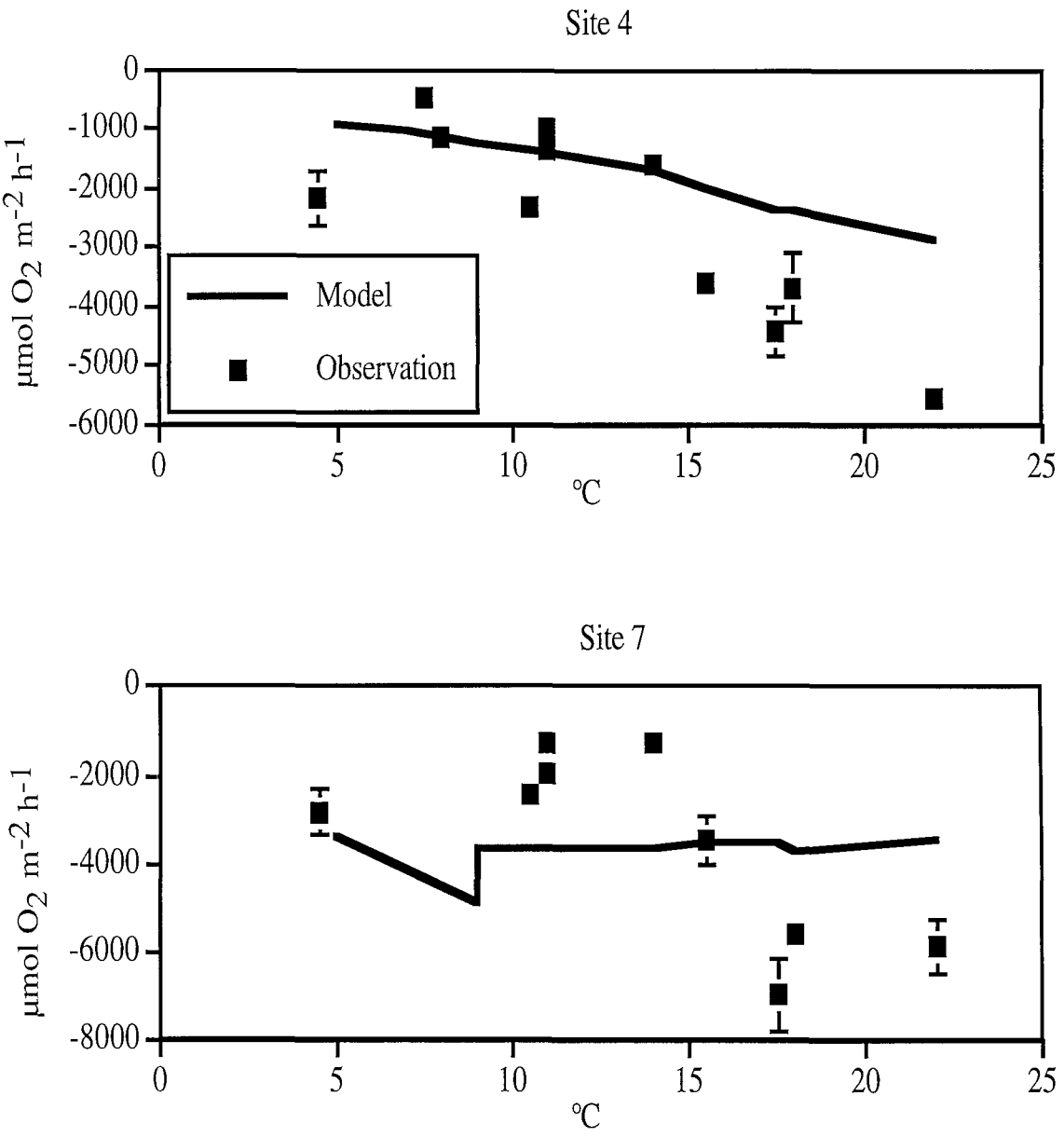


### 6.6.3.3.Oxygen

Figure 6.8 plots modelled and observed fluxes of oxygen across the sediment-water interface at sites 4 and 7 in The Wash. Modelled fluxes range between 931 and 4932 µmol $O_2$ $m^{-2}$ $h^{-1}$ which compares with the observed range of 458 to 6965 µmol $O_2$ $m^{-2}$ $h^{-1}$. At site 4 modelled fluxes increase with temperature as do the measurements. This contrasts with

the model output at site 7 in which model fluxes remain constant (3471-3740 μmol $O_2$ $m^{-2}$ $h^{-1}$) for temperatures >9°C. Observed fluxes at site 7 decrease with temperature. Model fluxes at temperatures greater than 14°C are lower than the observed fluxes at site 4. The invariance in the model fluxes at site 7 (except at 9°C) mean that observed fluxes are underestimated at temperatures less than 15°C and overestimated at temperatures greater than 15°C.

## 6.7. Discussion

### 6.7.1. Nitrate reduction

The range of values of $FitP_D$ (0.07-0.66) suggests that $NR_w$ (and by assumption, total nitrate reduction) in the lower Gt. Ouse sediments is always made up of contributions from both DNRA and denitrification. One process never fully dominates the other suggesting considerable overlap of denitrifying and nitrate ammonifying activity.

The $P_D$ values also show that $DNRA_w$ (and by assumption, total DNRA) is the more significant process. This is in line with many coastal studies of nitrate reduction from different parts of the world (Table 1.3). For a number of east coast UK estuaries, Herbert and Nedwell (1990) showed that fermentative bacteria were numerically dominant and potentially the most active nitrate reducing bacteria in the sediments. Similar bacterial findings have been reported for a wide range of sediment types in the north west European shelf region (Cole and Brown, 1980).

According to the temperature relationship ($FitP_D$, equation 6.3) derived from this data both $D_w$ and $DNRA_w$ occur to varying degrees, at all temperatures. However, both colder (<14°C) and warmer (>17°C) temperatures favour $DNRA_w$ over $D_w$ while $D_w$ is the favoured pathway in $NR_w$ at moderate temperatures (14°C-17°C). Given the

significant correlations ($p<0.05$) between nitrate fluxes and ammonium effluxes in these sediments, it is likely that this temperature effect is also true for total nitrate reduction.

The relationship of $P_D$ to temperature may be explained by observations which suggest that nitrate ammonifying bacteria and denitrifiers are adapted to different temperatures (King and Nedwell, 1984; Ogilvie *et al.,* 1997a). However, plotting the King and Nedwell (1984) results alongside $FitP_D$ (Figure 6.9) shows differences in the relationship between the proportioning of nitrate reduction and temperature.

Figure 6.9. Comparison of $FitP_D$ and data from King and Nedwell (1984) vs temperature. (King and Nedwell data calculated from their Figure 4).

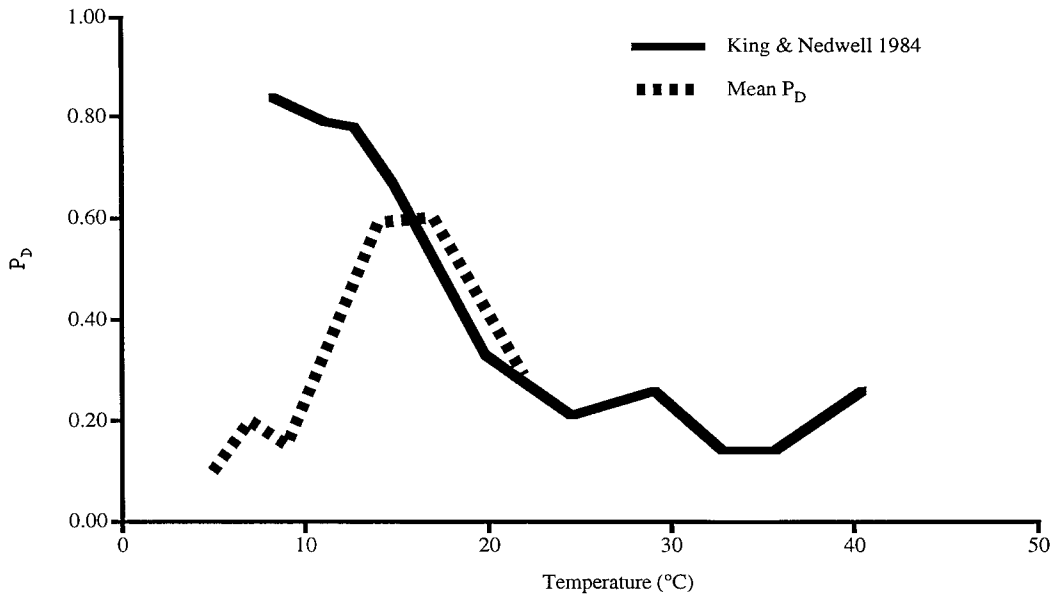


King and Nedwell (1984) show, using anoxic estuarine sediment slurries and chemostat experiments, that colder temperatures favour denitrification while warmer temperatures are preferred by nitrate ammonifying bacteria, leading to the idea that denitrifiers are psychrophilic and that nitrate ammonifiers are mesophilic. Their results have subsequently been supported by fieldwork (Ogilvie *et al.,* 1997b) from the same estuary (the Colne, UK east coast, a high nitrate, temperate estuary). These two quoted studies suggest that $FitP_D$,

derived from the lower Gt. Ouse data, does not reflect a causal relationship between sediment temperature and the pathway selected in nitrate reduction. The 'cold' response of $NR_w$ favouring $DNRA_w$ may be an artefact of $FitP_D$. That is, the assumption that the nitrate flux to the sediment is equivalent to dissimilatory $NR_w$ may not be true. This is difficult to check without measurements of DNRA and this assumption has been warned against in previous studies (Jørgensen, 1989). However, this warning is concerned with sediment populated by either heterotrophic bacteria, which carry out assimilatory nitrate reduction to meet nutritional requirements, and/or benthic algae. Assimilatory nitrate reduction is known to be inhibited in the presence of ammonium (Cole and Brown, 1980) and can therefore be ignored in this data. It has already been mentioned that the effects of benthic algae were removed by dark incubations. Although it has been shown that nutrient assimilation can continue after the onset of darkness (Rysgaard *et al.,* 1993), seasonal measurements of both light and dark nutrient exchange and of chlorophyll a (consistently $<3\mu g\ g^{-1}$ dry sediment) showed that light had no significant effect on the nutrient flux (Trimmer *et al.,* 1998). In contrast to the latter, where chlorophyll concentrations are much higher ( e.g.$>26\mu g\ g^{-1}$ dry sediment, Dong *et al.,* 2000), it has been shown that light makes a significant difference to nutrient fluxes compared to dark incubations.

The preferred selection for $DNRA_w$ at the colder temperature range indicated by $FitP_D$ is caused by the high winter nitrate fluxes relative to the low rates of $D_w$. The latter are likely to be caused by cold temperatures slowing down bacterial metabolic activity. A major cause of high solute fluxes can be the activity of macrofauna (Aller and Aller, 1998). However, the lack of benthic animals (a consistent finding during a total of 4 years study in which hundreds of cores were sifted, Trimmer, 1997) in the lower Gt. Ouse sediments excludes this factor. Diffusive enhancement by turbulence across the SWI may cause increased solute fluxes (Lohse *et al.,* 1996) but the core incubations used to derive

the data in Trimmer *et al.* (1998) removes this effect. It is concluded that the high nitrate fluxes observed in the colder months (e.g. site 7, November 1994, March 1995, temperature = 9°C and 7°C, respectively, Table 6.1) is due to high nitrate ammonifying activity.

Alternative explanations for the dominance of $DNRA_w$ in summer may be due to the fact that (i) sediments become increasingly reduced environments (Jørgensen, 1989 ) or that (ii) labile carbon to nitrate ratios (Herbert and Nedwell, 1990) are high relative to those in winter. These factors cannot be excluded from this work and it is likely that the dominance of DNRA in summer is caused by a combination of temperature, labile carbon:nitrate ratios and pH. However, the temperature relationship with $NR_w$ (Figure 6.2) suggests an important controlling effect. This implies that in the lower Gt. Ouse sediments nitrate ammonifying bacteria are best adapted to both colder and warmer temperatures, while denitrifiers only outcompete them over a small intermediate temperature range. This runs counter to the findings from laboratory based work (King and Nedwell, 1987; Herbert and Nedwell, 1990) which show that high nitrate concentrations (as found in winter) favour denitrification. However, plotting $FitP_D$ against overlying nitrate concentrations in the lower Gt. Ouse (not shown) shows no relationship between high nitrate concentrations (shown to be proportional to the nitrate concentration in the top 1cm of sediment in the Gt. Ouse sediments, Nedwell and Trimmer, 1996) and $FitP_D$. Consequently, for the lower Gt. Ouse sediments, it is proposed that temperature is a dominant controlling factor in determining the end products (N-gases or ammonium) of total nitrate reduction.

It is possible that the temperature range favouring denitrification is wider than is suggested by the calculations of $P_D$. There is a 5°C gap between 9°C and 14°C and between 17°C and 22°C for which there is no data for $P_D$ (Table 6.1). If true, seasonal

denitrification may be of a longer duration compared with DNRA. However, this does not change the main conclusions of this work (see below) although the overall annual balance of the two nitrate competing processes may favour the production of N-gases over ammonium. Note that Trimmer *et al.* (1998) calculated that 46% of the nitrate flux into these sediments was converted to N-gases, the remainder ending up as ammonium.

Attempts to model $D_w$ in the lower Gt. Ouse sediments without partitioning nitrate reduction (M-Fit$P_D$) were not successful across the full range (5°C-22°C) of observed temperatures. Measured rates of $D_w$ could not be reproduced by the model (M-Fit$P_D$) at the lower temperatures (<14°C). In contrast, for temperatures $\geq$ 14°C the effect of decreasing nitrate concentrations in the overlying water column on $D_w$ (M-Fit$P_D$) was similar to that with the run of M+Fit$P_D$. A test run was carried out to determine whether the decrease in $D_w$ for temperatures $\geq$ 14°C is due to i) lowering nitrate concentrations in the water column, ii) the effects of temperature selection favouring $DNRA_w$ or iii) both i) and ii). The test run (not shown) used M+Fit$P_D$ with a constant top boundary value for nitrate (the mean across all sites was used = 406 μM) for all temperatures at all sites. As before, the model was calibrated to rates of $D_w$ at 14°C. Modelled $D_w$ rates for temperatures >14°C were higher than the standard run (i.e. M+Fit$P_D$ with observed boundary values) by a mean factor of 2.3. This suggests that lowering nitrate concentrations are needed to better represent the observed rates of $D_w$ in summer. Hence, both temperature selection and changing nitrate concentrations are needed in the model.

It is possible that the variability in $P_D$ may be caused by the variable efficiency of the acetylene blockage technique (Seitzinger *et al.,* 1993). However, these latter authors added acetylene to only the overlying water to measure sediment denitrification. In the denitrification data collected by Trimmer *et al.* (1998), acetylene was injected into the sediments and in this way the method has been shown to give reliable estimates (Koike

and Sørenson, 1988, Knowles, 1990, van Raaphorst *et al.,* 1992) as argued by Ogilvie *et al.* (1997b). Furthermore, rates of $D_w$ are well correlated (r=0.83) with seasonal variations in overlying nitrate concentrations (Trimmer *et al.,* 1998) which has been shown in other studies (Ogilvie *et al.,* 1997b, Dong *et al.,* 2000).

Nitrification is inhibited by the acetylene blockage technique and consequently has little effect on the calculation of $P_D$. This does not mean that nitrification is absent in these sediments. Only 10% of the nitrate fluxes are directed out of the sediment (Table 6.1) indicating, in these situations, that nitrification is greater than total nitrate reduction. However, the large majority (90%) of the measured nitrate fluxes are directed into the sediment (Table 6.1) and more importantly, they are significantly ($p<0.05$) correlated to both rates of $D_w$ and ammonium effluxes. This suggests that total nitrate reduction, not just $NR_w$, is correlated to the nitrate flux which supports the assumption that the relationship between $P_D$ and temperature can be extended to total nitrate reduction in these sediments. Consequently, for these sediments, nitrification is i) negligible and invariant with temperature or ii) in constant proportion to nitrate reduction.

### 6.7.2. DNRA and total ammonium production

The percentage contribution of total DNRA to total ammonium production in the lower Gt. Ouse sediments (Figure 6.5) varies between 1% and 58% across all temperatures and sites. This is a large variation fuelled by the range (21-830 μM $NO_3^-$) in overlying nitrate concentrations since most (>70% for all sites) of the ammonium nitrogen produced by DNRA derives from the nitrate nitrogen rather than the nitrogen bound in the organic matter. This is not surprising given the stoichiometry of equation 6.6 which yields 1 mole of ammonium for every mole of nitrate reduced and 0.15 (16/106) mole of ammonium for every mole of TOC mineralised via nitrate. Consequently, variations in concentrations of

nitrate in the water column have a considerable effect on the production of ammonium from DNRA. This helps to explain the significant ($p<0.05$) correlations found between the measured nitrate fluxes and the ammonium effluxes in the lower Gt. Ouse sediments (Trimmer *et al.,* 1998). The increase in the percentage ammonium production from DNRA at sites 4, 5 and 7 (Figure 6.5) is caused by increases in the nitrate concentration in the overlying water between 15.5°C and 22°C. This effect also explains the increases in modelled $DNRA_w$ rates at the same sites and temperatures (Figure 6.4).

The differences between the sites (Figure 6.5) is related to differences in both the first order rate constant ($k_{no3}$) for nitrate reduction and the nitrate concentrations in the overlying water (Figure 6.3). A comparison between the mean percentage contribution of DNRA to total ammonium production at each site with both the mean nitrate concentration in the water column and the $k_{no3}$ value at each site is shown in Table 6.3. High $k_{no3}$ values coincide with high percentage contributions of DNRA to total ammonium production (sites 4, 6,7 and 8). The order of the percentage contribution of DNRA to ammonium production in the last two sites in Table 6.3 does not match the order of the $k_{no3}$ values. This is because the mean nitrate concentration is greater at site 5 (484 μM

Table 6.3 Comparison of the mean percentage contribution of DNRA to total ammonium production (%DNRA⇒$NH_4^+$) with both $k_{no3}$ values and the mean nitrate concentration in the water column at 6 sites in the lower Gt. Ouse.

| Site | %DNRA⇒$NH_4^+$ | $k_{no3}$ ($y^{-1}$) | $NO_3^-$ (μM) |
|---|---|---|---|
| 4 | 36 | 11.57 | 540 |
| 5 | 16 | 0.79 | 484 |
| 6 | 24 | 4.83 | 432 |
| 7 | 16 | 1.18 | 271 |
| 8 | 17 | 1.45 | 340 |
| 9 | 7 | 0.83 | 330 |

$NO_3^-$) than at site 9 (330 μM $NO_3^-$) even though the two sites have similar $k_{no3}$ values (0.79 $y^{-1}$ and 0.83 $y^{-1}$, respectively). A similar argument explains why sites 5 and 7 have the same percentage: the higher $k_{no3}$ value by a factor of 1.49 at site 7 compared to site 5 compensates for the lower mean nitrate concentration at site 7 compared to site 5.

### 6.7.3. First order rate constants

The range (0.79-11.57 $y^{-1}$) of fitted values of the first order rate constants, $k_{no3}$,) for nitrate reduction fall within the published range of first order rate constants for TOC degradation (e.g. 0.1-4.8 $y^{-1}$; McNichol *et al.,* 1984; 0.005-53 $y^{-1}$, Andersen, 1996; 0.2-7 $y^{-1}$ ; Middelburg *et al.,* 1996b). The larger values in model run M+Fit$P_D$ compared to M-Fit$P_D$ are caused by the presence of Fit$P_D$. That is, only a fraction of the nitrate reduction in M+Fit$P_D$ can follow the denitrification pathway, compared to 100% in M-Fit$P_D$. Thus, higher $k_{no3}$ values are needed in M+Fit$P_D$ to fit rates of denitrification to the observed rates at 14°C.

### 6.7.4. SWI Fluxes

#### 6.7.4.1.Nitrate

Observed fluxes are reasonably well represented by the model (Figure 6.6). That is, model fluxes often fall within or close to (within less than a factor of 1) the standard errors of the data (e.g. site 4, 7°C≤temperature<11°C and temperatures between 14°C and 17.5°C). However, some model comparisons with the data show considerable differences. For instance, at site 7 in November and March (temperature = 9°C) the observed fluxes are

more than a factor of 3 greater than the modelled fluxes and in contrast at site 9 in November (temperature=9°C) and July (temperature=22°C) the model flux is ~100 times greater than the observations. Fluxes at some sites (e.g. sites 4, 5 and 9) are better modelled than at others (e.g. site 8). Better, here, is defined as model output that is within the limits of the standard errors. The model does not reproduce any of the effluxes of nitrate observed at some of the sites (Figure 6.6 e.g. January 1995, temperature = 5°C, site 4; November 1994, temperature = 9°C, site 6). The latter point indicates that the process of nitrification and its balance with denitrification must be modelled in a more complete way (ie not just as a 1 step process). However, the direction of the model nitrate fluxes support the idea that the lower Gt. Ousesediments are a sink for nitrate.

The large (~1000 μmol $NO_3^- m^{-2} h^{-1}$) fluxes of nitrate measured in November (sites 7 and 8) and March (site 7) cannot be accounted for by changes in temperature or overlying nitrate concentrations. Instead it is possible that these fluxes were caused by a deposition of labile organic matter, by bio-irrigation or by microphytobenthic activity. Support for the deposition event can be seen in the maximum effluxes of ammonium recorded during these months at all sites (Figure 6.7). However, this is not reflected in the oxygen fluxes at either of the sites (4 and 7) where measurements were made (Figure 6.8). This may mean that sulphate reduction or an alternative oxidation pathway, may have become more important as a result of the increased supply of organic matter from the overlying water. Macrofaunal activity has been reported to affect nutrient fluxes across the SWI (Aller and Aller, 1998). However, benthic animals were never encountered or observed by sieving in the lower Gt. Ouse sediments (M. Trimmer, pers. comm.). Although microphytobenthos can strongly influence nutrient exchange across the SWI (Rysgaard *et al.,* 1999), core incubations were kept in the dark to exclude their effects (Trimmer *et al.,* 1998). It is concluded that these large fluxes in the non-summer months

may have been caused by an allochthonous input of organic carbon. As the model does not account for the flux of TOC (instead the concentration is imposed in the sediment), this represents a limitation of the model. Note also that in Chapter 5 the possibility of porewater advection induced by the stirring in the core incubations was raised as a factor explaining the discrepancy between modeled and observed fluxes (section 4.6.3).

#### 6.7.4.2.Ammonium

There is no consistent pattern in the output of the model between sites (Figure 6.7). At some sites (e.g. sites 5 and 6) model ammonium fluxes underestimate the observations and at others (e.g. sites 4 and 9) the model overestimates them. In the core incubations used to measure ammonium fluxes (which contained no macrofauna or benthic algae), the ammonium flux will be determined by the concentration difference between the water column and the sediment. The concentration of ammonium in the sediment will result from a balance between production from organic oxidation and removal by nitrification. In both the model and the data, except for nitrate based carbon respiration, the relative importance of the mineralisation pathways is unknown. Trimmer *et al.* (1998) were not able to distinguish between sulphate and oxygen based organic degradation because sulphur based processes and determinands were not measured. Consequently, they describe the data in terms of nitrate based- and the sum of oxygen plus sulphate (the unknown quantity) based- mineralisation. Although sulphate based respiration is explicitly modelled, the rate cannot be validated due to this lack of data. Consequently, the first order rate constant for sulphate reduction cannot be derived from the model and so its value is the mean of sites 1-4 in the upper Gt. Ouse (Table 3.5). It is therefore possible that some of the variability in the ammonium fluxes, not captured in the model, is due to

variations in the rate of sulphate reduction, which is controlled by the magnitude of the flux of organic carbon (higher fluxes mean both higher rates and increasing proportion of the total organic mineralisation).

#### 6.7.4.3.Oxygen

Figure 6.8 shows that at site 4 the model mostly underestimates the observed fluxes while at site 7, the model both underestimates and overestimates the observed fluxes. The variability in oxygen fluxes at each site in the model is caused by changes in both temperature and the boundary values for sulphate (section 5.6.2.1, Table 5.2). Although observed oxygen fluxes increase with temperature, this increase is not linear. This is especially evident at site 7 (Figure 6.8) where oxygen fluxes decrease between 4.5°C and 14°C and then increase. This suggests that other factors such as the changing availability of labile organic matter and/or stirring induced porewater advection may be the cause of the variability in observed oxygen fluxes (section 4.6.3). This casts doubt on the assumption of steady state in the model. However, this assumption arises from the observations in both the upper Great Ouse (Nedwell and Trimmer, 1996) and in the lower Gt. Ouse (Trimmer *et al.*, 1998). It is concluded that for oxygen fluxes, variability within sites cannot be accounted for by differences in boundary values or temperature. This points to the need for future work to include modelling of the flux of organic matter to and its incorporation in the sediment.

## 6.8. Conclusions

In the lower Gt. Ouse sediments, temperature selection in dissimilatory $NR_w$ can be used to model both $D_w$ and $DNRA_w$. It is assumed from the significant correlations ($p<0.05$) between nitrate fluxes and both the rates of $D_w$ and the ammonium effluxes that this temperature effect can be applied to the partitioning of total nitrate reduction.

Use of equation 6.9 in the diagenetic model has been shown to be an effective way to simulate observed rates of $D_w$. The same equation can be used to model rates of $DNRA_w$ which compare well to calculated rates. This represents a first attempt to simulate DNRA in a diagenetic model. Future models will need to rely on more mechanistic equations (which require more detailed work on the underlying microbiology and kinetics) to describe the proportioning of nitrate reduction into denitrification and DNRA. Until such detailed experimental work is done, the work presented here shows that a simple model can be used to interpret field observations. Furthermore, the simplicity of this modelling approach is highlighted in the fact that only 1 free parameter ($k_{no3}$) needs to be fitted.

It is concluded that over the measured temperature range (5°C-22°C) in the lower Gt. Ouse sediments, temperature is an important control in partitioning nitrate reduction into denitrification and DNRA. The narrowness of the temperature range suggests that there is an overlap in the two pathways which is indicated by the fact that $P_D$ is never equal to 1 or 0. Thus, both pathways occur to varying degrees at all temperatures in the lower Gt. Ouse sediments.

Overall, the implication is that during an extended warm summer in temperate estuaries receiving high nitrate inputs, nitrate reduction may contribute to, rather than counteract a eutrophication event. The conversion of nitrate to the more biologically preferred form of the nitrogen nutrient, ammonium, means that nitrate reduction has

considerable fertilising potential. This implication acts as a caveat for studies which concentrate solely on one aspect of nitrate reduction (i.e. denitrification) with respect to nitrogen inputs. The search for similar relationships from other data sets must be continued before general conclusions about the response of nitrate reduction to temperature (and other environmental factors) can be made.

The variable success of the model in reproducing the observed fluxes of nitrate, ammonium and oxygen across the SWI indicates the need for improvements in the way in which TOC is modelled. Interpretations of the results suggests that some of the variability in the observed fluxes may be due to variations in the quantity and quality of the TOC arriving at the sediment throughout the year. This could be incorporated by using equations from models that are capable of accounting for TOC variability (e.g. Boudreau, 1996; Soetaert *et al.,* 1996).

Finally, it is concluded that diagenetic models of the nitrogen cycle should and can include DNRA.

## 7. Summaries and final conclusions

### 7.1. Summary

A reaction-diffusion model of early diagenesis was developed for the first time for temperate estuarine sediments (the Gt. Ouse, North Sea, UK coast) exposed to globally

Figure 7.1. Biogeochemical reactions of the diagenetic model(TOC = total organic carbon)

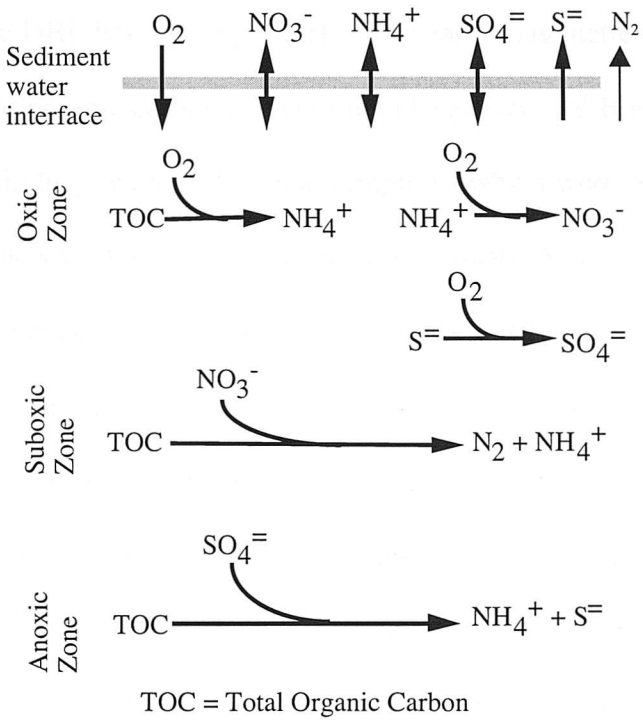


high concentrations of nitrate in the overlying water (265 - 1240 μM). Five variables ($O_2$, $NO_3^-$, $NH_4^+$, $SO_4^=$ and $S^=$) were modeled from steady state concentrations of total organic carbon which was evenly distributed with sediment depth (Figure 7.1). Organic carbon mineralisation was mediated via oxygen, nitrate and sulphate, with each pathway producing ammonium (and free sulphide in the case of sulphate reduction). Other processes included sulphide oxidation and nitrification, both of which consumed oxygen.

In the first science Chapter (Chapter 3), different representations of the first order rate constant for organic decay, $k$, were tested by calibration against observed data. A parameter sensitivity analysis (PSA) was also undertaken in this Chapter with the aim of understanding both qualitatively and quantitatively, the internal dynamics of the model processes. In Chapter 4, the effect of different thicknesses (0.0001 - 0.1cm) of the diffusive boundary layer (DBL) on the different model processes (e.g. mineralization rates and solute fluxes across the sediment water interface, SWI) was assessed. Previous work suggested that the DBL has a negligible effect on early diagenetic processes, especially oxygen fluxes and organic carbon preservation (Jørgensen and Boudreau, 2001). However, those findings were based on assumptions which were not globally applicable to coastal/estuarine sediments. The aim here was to quantify the significance of not accounting for the presence of a DBL during core incubation flux measurements. In the fifth Chapter, the calibrated model from Chapter 3 was used to investigate the causes of the intra-annual changes in the measurements. This tested both the assumption of steady state (which was based on observations of organic carbon concentrations) and the ability of the fitted values of $k$ to simulate the observed seasonality. In the final science Chapter (Chapter 6), dissimilatory nitrate reduction to ammonium (DNRA) was incorporated into the model. The need to include this process arose from model results in Chapter 3 and from analysis of the observations (Trimmer *et al.*, 1998).

A common interpretational feature throughout Chapters 3 to 5 was the relevance of 1) the variability in the relative contributions of the different pathways of organic carbon oxidation across the sites in the Gt. Ouse; 2) the magnitude of the oxygen consumption rates and 3) the oxygen penetration depth.

## 7.2. Conclusions

Calibration of the model against the observations resulted in two main findings. 1) The model could only reproduce the observed data by fitting separate first order rate constants to individual pathways of mineralisation (other common representations of $k$ were inadequate). This yielded high degrees of freedom which casts doubt on the ability of diagenetic models for estuaries with high nitrate loads to be universally applicable. 2) Pathways of nitrate reduction other than denitrification were active in these sediments. This led, for the first time, to the inclusion of DNRA into an early diagenetic model.

DNRA was implemented into the model via an empirically derived temperature function. This function partitioned dissimilatory nitrate reduction into denitrification and DNRA. Both denitrification and DNRA occurred at all temperatures (5°C-22°C). Colder (<14°C) and warmer (>17°C) temperatures favoured DNRA while denitrification was the preferred pathway in nitrate reduction at moderate temperatures (14°C-17°C). The implication is that during an extended warm summer in temperate estuaries receiving high nitrate inputs, nitrate reduction may contribute to, rather than counteract a eutrophication event. Implementing the temperature function into the model meant that measured seasonal rates of denitrification were realistically simulated as were calculated rates of DNRA. It was concluded that temperature is an important control in partitioning nitrate reduction into denitrification and DNRA in the lower Gt. Ouse sediments. Future development should focus on implementing mechanistic equations (currently unavailable) that predict the proportioning of nitrate reduction into denitrification and DNRA. Until then, the work presented here shows that a simple model, requiring only 1 free parameter ($k_{no3}$) to be fitted, can be used to interpret field observations.

A literature review indicated that DNRA may be globally significant in terms of its contribution to nitrate reduction. Consequently, it is recommended that diagenetic models of the nitrogen cycle should and can include DNRA.

The parameter sensitivity analysis (PSA) revealed complex, non-linear relationships between model quantities (fluxes, rates) and parameters. Furthermore, the results of the PSA were not uniform across the sites. The differences among the sites were related to the relative contributions of oxic, suboxic and anoxic mineralization to total organic carbon mineralization and to the rate of oxygen consumption (and the oxygen penetration depth). For instance, a reduction in the free solution diffusion coefficient for oxygen ($D_{o2}^{0}$) caused the highest reduction, relative to all other adjusted parameters, in the oxygen flux to the sediment at the site where oxygen demand was greatest and where oxygen penetration was least (site 3). Consequently at site 3, limitation by oxygen on oxic mineralization was greatest, yielding a high sensitivity of oxygen respiration (56% reduction) to a reduction in $D_{o2}^{0}$ relative to the other sites (1-13%). This reduction in oxic mineralization reduced total organic carbon mineralization by the greatest amount (22%) at site 3 where organic carbon oxidation via oxygen was the dominant carbon degradation process. Organic carbon mineralization rates were most sensitive to porosity and diffusion related parameters ($D_{O2}^{0}$, $D_{SO4}^{0}$ and $D_C$, equation 2.3). In addition, use of the literature range of values of the half saturation constants for nitrate inhibition in sulphate reduction ($k_{sAnoxInhNO3}$) and for sulphate limitation in sulphate reduction ($k_{sSO4}$), showed that these parameters are also important. These latter two parameters influence the rate of sulphate reduction and so the largest percentage changes in organic carbon oxidation rates (24% and 29%,respectively) occurred at the site where sulphate reduction dominated organic carbon mineralization rates (site 1). This highlights the importance of considering a range of sediment environments with different organic carbon mineralization budgets when

carrying out PSA. Furthermore, these examples of parameter changes suggest that it is unwise to consider parameters as universally constant in space. Consequently, when undertaking PSA as part of diagenetic model development, all parameters should be included in the exercise before model robustness can be assessed

The model results suggest that is important to take account of the DBL. For the range in measured thicknesses of the DBL, solute fluxes obtained from core incubation experiments may not represent *in situ* fluxes. Fluxes of oxygen and ammonium decreased by up to 61% and 38%, respectively for DBL thicknesses of 0.1cm while fluxes of nitrate and sulphate increased by up to 20% and 980%, respectively. In other words, neglecting the presence of the DBL in core incubations may result in higher oxygen and ammonium fluxes and lower nitrate and sulphate fluxes than might be occurring *in situ*. The lower the oxygen penetration the greater the sensitivity of oxygen consumption rates to changes in the diffusive sublayer. This is because lower oxygen penetration means that a higher proportion of the oxygen concentration gradient is contained in the DBL. The largest percentage change in rates of total organic matter mineralization (42%) occurred where oxygen penetration was least and where oxic respiration was the dominant mineralization pathway. This lowering of organic mineralization rates with increased DBL thicknesses caused the reduction in the ammonium effluxes which could limit rates of primary production in areas where phytoplankton growth is fuelled by nitrogen regenerated in the sediments.

The model also suggests that the effect of the DBL on oxygen fluxes may influence organic carbon preservation in shallow coastal sediments. This is in contrast to the findings of Jørgensen and Boudreau (2001) which were based on the assumption that oxygen demand in coastal sediments is fuelled only by the oxidation of reduced substances (e.g. sulphide). The observations in the Gt. Ouse conflict with this assumption

in that oxygen consumption at some locations was mostly accounted for by oxic mineralization. Consequently, it is recommended that the use of high stirring rates in core incubations of shallow sediments should only be considered if supported by measurements showing high near-bed current speeds which are known to inhibit the formation of a DBL.

Variations in temperature and overlying concentrations of nitrate, ammonium and sulphate were insufficient to explain all of the variability in the intra-annual changes in the observed solute fluxes across the SWI. This casts doubt on the assumption that concentrations of organic carbon were in steady state at all sites. It is concluded that this model limitation may be overcome by dynamic modelling of organic carbon as done by others (e.g. Soetaert et al., 1996). In conjunction with such a development it would be beneficial to have measured indicators of labile organic carbon (e.g. chlorophyll).

Differences in magnitude between the predicted and measured fluxes of oxygen and nitrate across the SWI, highlighted another possible limitation of the model. The higher measured fluxes may have been due to porewater advection or enhancement of transport by turbulent diffusion induced by the stirring rates in the core incubations. Inclusion of such transport processes is a recommended area for future work.

**Appendix A. The finite difference form of the diffusion term in equation 3.1**

Direct differencing of the diffusion term yields

$$\frac{1}{\phi}\frac{\partial}{\partial z}\left(D_{c_j}\phi_j\left.\frac{\partial C}{\partial z}\right|_j\right) = -D_{c_j}\phi_j\frac{C_i - C_{i-1}}{\phi_i dz^2} + D_{c_{j+1}}\phi_{j+1}\frac{C_{i+1} - C_i}{\phi_i dz^2} \qquad \text{A1}$$

Note that the i and j indices refer to the numerical grid scheme shown in Figure 3.1. The fully discretised form of the diagenetic reaction-diffusion equation (3.1) is

$$\text{Rate of change} = -D_{c_j}\phi_j\frac{C_i - C_{i-1}}{\phi_i dz^2} + D_{c_{j+1}}\phi_{j+1}\frac{C_{i+1} - C_i}{\phi_i dz^2} + \Sigma R_i \qquad \text{A2}$$

where $R_i$ for each grid cell is defined in equations 3.7-3.11 (Table 3.1). Note that the porosity parameter ($\phi_i$) in the reaction term (R) is to the found in equations 3.7-3.11.

# Appendix B. Tables B2.1 - B2.4

Table B2.1a. Parameter sensitivity analysis at site 1 (each parameter decreased by 50%; values represent rate/flux (unit mol $m^{-2}$ $y^{-1}$) associated with each variable; swi=SWI flux; o2r= oxygen respiration; nit= nitrification; s-ox= sulphide oxidation; nr= nitrate reduction; bf lx= bottom boundary flux; oxamm= oxic ammonification; subamm= suboxic ammonification; anamm= anoxic ammonification; totamm= total ammonification; sr= sulphate reduction; ox, sub,an= oxic, suboxic, anoxic mineralization; parameters defined in Table 2.2)

| Parameter | Oxygen | | | | Nitrate | | | Ammonium | | | | | | | Sulphate | | | Sulphide | | | Carbon | | | |
|---|---|---|---|---|---|---|---|---|---|---|---|---|---|---|---|---|---|---|---|---|---|---|---|---|
| | swi | o2r | nit | s-ox | swi | nit | nr | swi | bflx | $ox_{amm}$ | $sub_{amm}$ | $an_{amm}$ | $tot_{amm}$ | nit | swi | sr | s-ox | swi | sr | s-ox | ox | sub | an | total |
| $M_{in}$ run | -12.4316 | 2.1623 | 0.1982 | 10.0711 | -2.3820 | 0.0991 | 2.4811 | 0.2752 | 0.0555 | 0.0370 | 0.0530 | 0.1751 | 0.2652 | 0.0455 | -0.0842 | 5.1198 | 5.0356 | 0.0842 | -5.1198 | -5.0356 | 2.1623 | 3.1014 | 10.2396 | 15.5032 |
| $D_{O2}^{0}$ | -11.7607 | 2.1456 | 0.1929 | 9.4223 | -2.3882 | 0.0965 | 2.4846 | 0.2665 | 0.0558 | 0.0367 | 0.0531 | 0.1651 | 0.2549 | 0.0442 | -0.1158 | 4.8269 | 4.7111 | 0.1158 | -4.8269 | -4.7111 | 2.1456 | 3.1058 | 9.6538 | 14.9052 |
| $D_{NO3}^{0}$ | -13.0018 | 2.1605 | 0.1974 | 10.6439 | -1.8356 | 0.0987 | 1.9343 | 0.2745 | 0.0562 | 0.0370 | 0.0414 | 0.1853 | 0.2636 | 0.0453 | -0.0954 | 5.4174 | 5.3220 | 0.0954 | -5.4174 | -5.3220 | 2.1605 | 2.4178 | 10.8347 | 15.4131 |
| $D_{NH4}^{0}$ | -12.4534 | 2.1622 | 0.2229 | 10.0682 | -2.3701 | 0.1115 | 2.4815 | 0.2469 | 0.0329 | 0.0370 | 0.0531 | 0.1751 | 0.2651 | 0.0511 | -0.0843 | 5.1184 | 5.0341 | 0.0843 | -5.1184 | -5.0341 | 2.1622 | 3.1019 | 10.2368 | 15.5010 |
| $D_{SO4}^{0}$ | -10.5336 | 2.1711 | 0.1955 | 8.1670 | -2.3824 | 0.0977 | 2.4802 | 0.2435 | 0.0569 | 0.0371 | 0.0530 | 0.1413 | 0.2315 | 0.0448 | -0.0472 | 4.1307 | 4.0835 | 0.0472 | -4.1307 | -4.0835 | 2.1711 | 3.1002 | 8.2613 | 13.5327 |
| $D_{S}^{0}$ | -12.4946 | 2.1596 | 0.1964 | 10.1386 | -2.3829 | 0.0982 | 2.4811 | 0.2756 | 0.0555 | 0.0369 | 0.0531 | 0.1752 | 0.2652 | 0.0451 | -0.0517 | 5.1209 | 5.0693 | 0.0517 | -5.1209 | -5.0693 | 2.1596 | 3.1014 | 10.2419 | 15.5029 |
| $D_{O2}^{const}$ | -12.1805 | 2.1577 | 0.1960 | 9.8268 | -2.3838 | 0.0980 | 2.4818 | 0.2720 | 0.0556 | 0.0369 | 0.0531 | 0.1714 | 0.2613 | 0.0450 | -0.0959 | 5.0093 | 4.9134 | 0.0959 | -5.0093 | -4.9134 | 2.1577 | 3.1023 | 10.0187 | 15.2787 |
| $D_{NO3}^{const}$ | -12.5982 | 2.1618 | 0.1978 | 10.2386 | -2.1959 | 0.0989 | 2.2948 | 0.2745 | 0.0558 | 0.0370 | 0.0491 | 0.1781 | 0.2641 | 0.0454 | -0.0875 | 5.2068 | 5.1193 | 0.0875 | -5.2068 | -5.1193 | 2.1618 | 2.8685 | 10.4136 | 15.4439 |
| $D_{NH4}^{const}$ | -12.4375 | 2.1623 | 0.2049 | 10.0703 | -2.3787 | 0.1025 | 2.4812 | 0.2654 | 0.0473 | 0.0370 | 0.0531 | 0.1751 | 0.2652 | 0.0470 | -0.0842 | 5.1194 | 5.0352 | 0.0842 | -5.1194 | -5.0352 | 2.1623 | 3.1015 | 10.2388 | 15.5026 |
| $D_{SO4}^{const}$ | -11.6962 | 2.1650 | 0.1967 | 9.3345 | -2.3824 | 0.0984 | 2.4807 | 0.2631 | 0.0561 | 0.0370 | 0.0530 | 0.1620 | 0.2521 | 0.0451 | -0.0699 | 4.7371 | 4.6672 | 0.0699 | -4.7371 | -4.6672 | 2.1650 | 3.1009 | 9.4742 | 14.7401 |
| $D_{S}^{const}$ | -12.4481 | 2.1616 | 0.1977 | 10.0888 | -2.3822 | 0.0989 | 2.4811 | 0.2753 | 0.0555 | 0.0370 | 0.0530 | 0.1751 | 0.2652 | 0.0454 | -0.0757 | 5.1201 | 5.0444 | 0.0757 | -5.1201 | -5.0444 | 2.1616 | 3.1014 | 10.2402 | 15.5031 |
| $K_{nit}$ | -12.3446 | 2.1625 | 0.1014 | 10.0807 | -2.4289 | 0.0507 | 2.4796 | 0.2975 | 0.0555 | 0.0370 | 0.0530 | 0.1753 | 0.2653 | 0.0233 | -0.0840 | 5.1244 | 5.0404 | 0.0840 | -5.1244 | -5.0404 | 2.1625 | 3.0995 | 10.2488 | 15.5107 |
| $K_{nox}$ | -12.2804 | 2.1692 | 0.2027 | 9.9086 | -2.3796 | 0.1013 | 2.4810 | 0.2742 | 0.0555 | 0.0371 | 0.0530 | 0.1750 | 0.2652 | 0.0465 | -0.1625 | 5.1168 | 4.9543 | 0.1625 | -5.1168 | -4.9543 | 2.1692 | 3.1012 | 10.2336 | 15.5040 |
| $k_{aLimO2}$ | -12.4341 | 2.1623 | 0.2029 | 10.0689 | -2.3800 | 0.1015 | 2.4814 | 0.2741 | 0.0555 | 0.0370 | 0.0531 | 0.1751 | 0.2651 | 0.0466 | -0.0843 | 5.1187 | 5.0345 | 0.0843 | -5.1187 | -5.0345 | 2.1623 | 3.1018 | 10.2374 | 15.5015 |
| $k_{aInhNO3}$ | -12.4311 | 2.1623 | 0.1982 | 10.0706 | -2.3773 | 0.0991 | 2.4764 | 0.2751 | 0.0555 | 0.0370 | 0.0529 | 0.1751 | 0.2650 | 0.0455 | -0.0842 | 5.1195 | 5.0353 | 0.0842 | -5.1195 | -5.0353 | 2.1623 | 3.0955 | 10.2390 | 15.4969 |
| $k_{aAnoxInhO2}$ | -12.4072 | 2.1623 | 0.1981 | 10.0468 | -2.3820 | 0.0991 | 2.4811 | 0.2748 | 0.0555 | 0.0370 | 0.0530 | 0.1747 | 0.2647 | 0.0454 | -0.0838 | 5.1071 | 5.0234 | 0.0838 | -5.1071 | -5.0234 | 2.1623 | 3.1013 | 10.2143 | 15.4779 |
| $k_{aAnoxInhNO3}$ | -10.5634 | 2.1708 | 0.1951 | 8.1974 | -2.3826 | 0.0976 | 2.4802 | 0.2427 | 0.0555 | 0.0371 | 0.0530 | 0.1418 | 0.2320 | 0.0448 | -0.0478 | 4.1465 | 4.0987 | 0.0478 | -4.1465 | -4.0987 | 2.1708 | 3.1002 | 8.2930 | 13.5640 |
| $k_{xO2}$ | -12.4502 | 2.1835 | 0.1982 | 10.0684 | -2.3820 | 0.0991 | 2.4811 | 0.2755 | 0.0555 | 0.0374 | 0.0530 | 0.1751 | 0.2655 | 0.0455 | -0.0844 | 5.1186 | 5.0342 | 0.0844 | -5.1186 | -5.0342 | 2.1835 | 3.1014 | 10.2371 | 15.5220 |
| $k_{xNO3}$ | -12.5371 | 2.1619 | 0.1988 | 10.1764 | -2.4637 | 0.0994 | 2.5631 | 0.2787 | 0.0555 | 0.0370 | 0.0548 | 0.1770 | 0.2688 | 0.0456 | -0.0863 | 5.1745 | 5.0882 | 0.0863 | -5.1745 | -5.0882 | 2.1619 | 3.2039 | 10.3489 | 15.7148 |
| $k_{xSO4}$ | -13.8469 | 2.1581 | 0.2019 | 11.4869 | -2.3809 | 0.1009 | 2.4818 | 0.2995 | 0.0555 | 0.0369 | 0.0531 | 0.2003 | 0.2903 | 0.0463 | -0.1119 | 5.8553 | 5.7435 | 0.1119 | -5.8553 | -5.7435 | 2.1581 | 3.1023 | 11.7107 | 16.9711 |
| $k_{xSox}$ | -12.4293 | 2.1590 | 0.1960 | 10.0743 | -2.3831 | 0.0980 | 2.4811 | 0.2757 | 0.0555 | 0.0369 | 0.0530 | 0.1752 | 0.2652 | 0.0450 | -0.0840 | 5.1211 | 5.0372 | 0.0840 | -5.1211 | -5.0372 | 2.1590 | 3.1014 | 10.2423 | 15.5027 |
| $\phi$ | -11.1063 | 3.4510 | 0.1510 | 7.5043 | -1.8264 | 0.0755 | 1.9019 | 0.2195 | 0.0225 | 0.0590 | 0.0407 | 0.1319 | 0.2316 | 0.0346 | -0.1050 | 3.8572 | 3.7522 | 0.1050 | -3.8572 | -3.7522 | 3.4510 | 2.3774 | 7.7144 | 13.5428 |

Table B2.1b. Parameter sensitivity analysis at site 1 (each parameter increased by 50%; values represent rate/flux (unit mol $m^{-2}$ $y^{-1}$) associated with each variable; swi=SWI flux; o2r= oxygen respiration; nit= nitrification; s-ox= sulphide oxidation; nr= nitrate reduction; bf lx= bottom boundary flux; oxamm= oxic ammonification; subamm= suboxic ammonification; anamm= anoxic ammonification; totamm= total ammonification; sr= sulphate reduction; ox, sub,an= oxic, suboxic, anoxic mineralization; parameters defined in Table 2.2)

| Parameter | Oxygen | | | | Nitrate | | | Ammonium | | | | | | | Sulphate | | | Sulphide | | | Carbon | | | |
|---|---|---|---|---|---|---|---|---|---|---|---|---|---|---|---|---|---|---|---|---|---|---|---|---|
| | swi | o2r | nit | s-ox | swi | nit | nr | swi | bflx | $ox_{amm}$ | $sub_{amm}$ | $an_{amm}$ | $tot_{amm}$ | nit | swi | sr | s-ox | swi | sr | s-ox | ox | sub | an | totul |
| $M_{st}$ run | -12.4316 | 2.1623 | 0.1982 | 10.0711 | -2.3820 | 0.0991 | 2.4811 | 0.2752 | 0.0555 | 0.0370 | 0.0530 | 0.1751 | 0.2652 | 0.0455 | -0.0842 | 5.1198 | 5.0356 | 0.0842 | -5.1198 | -5.0356 | 2.1623 | 3.1014 | 10.2396 | 15.5032 |
| $D_{O2}^{0}$ | -13.1036 | 2.1756 | 0.2070 | 10.7209 | -2.3765 | 0.1035 | 2.4800 | 0.2832 | 0.0552 | 0.0372 | 0.0530 | 0.1852 | 0.2754 | 0.0475 | -0.0530 | 5.4135 | 5.3605 | 0.0530 | -5.4135 | -5.3605 | 2.1756 | 3.1000 | 10.8270 | 16.1026 |
| $D_{NO3}^{0}$ | -12.1082 | 2.1634 | 0.1993 | 9.7455 | -2.8351 | 0.0997 | 2.9347 | 0.2782 | 0.0549 | 0.0370 | 0.0627 | 0.1694 | 0.2691 | 0.0457 | -0.0779 | 4.9506 | 4.8728 | 0.0779 | -4.9506 | -4.8728 | 2.1634 | 3.6684 | 9.9013 | 15.7331 |
| $D_{NH4}^{0}$ | -12.4211 | 2.1623 | 0.1863 | 10.0725 | -2.3877 | 0.0931 | 2.4809 | 0.3006 | 0.0782 | 0.0370 | 0.0530 | 0.1752 | 0.2652 | 0.0427 | -0.0842 | 5.1204 | 5.0362 | 0.0842 | -5.1204 | -5.0362 | 2.1623 | 3.1011 | 10.2409 | 15.5043 |
| $D_{SO4}^{0}$ | -14.1834 | 2.1572 | 0.2025 | 11.8236 | -2.3807 | 0.1013 | 2.4820 | 0.3039 | 0.0542 | 0.0369 | 0.0531 | 0.2063 | 0.2962 | 0.0465 | -0.1185 | 6.0303 | 5.9118 | 0.1185 | -6.0303 | -5.9118 | 2.1572 | 3.1025 | 12.0605 | 17.3202 |
| $D_{S}^{0}$ | -12.3705 | 2.1650 | 0.2000 | 10.0055 | -2.3811 | 0.1000 | 2.4810 | 0.2748 | 0.0555 | 0.0370 | 0.0530 | 0.1751 | 0.2652 | 0.0459 | -0.1159 | 5.1186 | 5.0027 | 0.1159 | -5.1186 | -5.0027 | 2.1650 | 3.1013 | 10.2372 | 15.5035 |
| $D_{O2}^{const}$ | -12.6826 | 2.1667 | 0.2008 | 10.3151 | -2.3802 | 0.1004 | 2.4806 | 0.2784 | 0.0554 | 0.0371 | 0.0530 | 0.1789 | 0.2690 | 0.0461 | -0.0726 | 5.2301 | 5.1576 | 0.0726 | -5.2301 | -5.1576 | 2.1667 | 3.1007 | 10.4602 | 15.7276 |
| $D_{NO3}^{const}$ | -12.2953 | 2.1627 | 0.1986 | 9.9339 | -2.5560 | 0.0993 | 2.6553 | 0.2762 | 0.0553 | 0.0370 | 0.0568 | 0.1727 | 0.2665 | 0.0456 | -0.0816 | 5.0485 | 4.9670 | 0.0816 | -5.0485 | -4.9670 | 2.1627 | 3.3192 | 10.0970 | 15.5789 |
| $D_{NH4}^{const}$ | -12.4270 | 2.1623 | 0.1930 | 10.0717 | -2.3845 | 0.0965 | 2.4810 | 0.2847 | 0.0638 | 0.0370 | 0.0530 | 0.1751 | 0.2652 | 0.0443 | -0.0842 | 5.1201 | 5.0359 | 0.0842 | -5.1201 | -5.0359 | 2.1623 | 3.1012 | 10.2401 | 15.5037 |
| $D_{SO4}^{const}$ | -13.1441 | 2.1601 | 0.1999 | 10.7841 | -2.3815 | 0.0999 | 2.4814 | 0.2869 | 0.0550 | 0.0370 | 0.0531 | 0.1878 | 0.2778 | 0.0458 | -0.0981 | 5.4902 | 5.3921 | 0.0981 | -5.4902 | -5.3921 | 2.1601 | 3.1018 | 10.9804 | 16.2423 |
| $D_{S}^{const}$ | -12.4153 | 2.1630 | 0.1987 | 10.0536 | -2.3817 | 0.0993 | 2.4811 | 0.2751 | 0.0555 | 0.0370 | 0.0530 | 0.1751 | 0.2652 | 0.0456 | -0.0927 | 5.1195 | 5.0268 | 0.0927 | -5.1195 | -5.0268 | 2.1630 | 3.1013 | 10.2389 | 15.5033 |
| $K_{nit}$ | -12.5148 | 2.1621 | 0.2907 | 10.0619 | -2.3372 | 0.1454 | 2.4825 | 0.2539 | 0.0555 | 0.0370 | 0.0531 | 0.1750 | 0.2650 | 0.0667 | -0.0844 | 5.1154 | 5.0310 | 0.0844 | -5.1154 | -5.0310 | 2.1621 | 3.1032 | 10.2308 | 15.4960 |
| $K_{sox}$ | -12.4846 | 2.1600 | 0.1967 | 10.1278 | -2.3828 | 0.0984 | 2.4811 | 0.2756 | 0.0555 | 0.0369 | 0.0530 | 0.1752 | 0.2652 | 0.0451 | -0.0568 | 5.1208 | 5.0639 | 0.0568 | -5.1208 | -5.0639 | 2.1600 | 3.1014 | 10.2415 | 15.5029 |
| $k_{sLimO2}$ | -12.4305 | 2.1623 | 0.1963 | 10.0719 | -2.3828 | 0.0982 | 2.4810 | 0.2757 | 0.0555 | 0.0370 | 0.0530 | 0.1751 | 0.2652 | 0.0450 | -0.0842 | 5.1202 | 5.0359 | 0.0842 | -5.1202 | -5.0359 | 2.1623 | 3.1012 | 10.2403 | 15.5038 |
| $k_{sInhNO3}$ | -12.4320 | 2.1623 | 0.1982 | 10.0715 | -2.3863 | 0.0991 | 2.4854 | 0.2753 | 0.0555 | 0.0370 | 0.0531 | 0.1751 | 0.2653 | 0.0455 | -0.0842 | 5.1200 | 5.0357 | 0.0842 | -5.1200 | -5.0357 | 2.1623 | 3.1067 | 10.2399 | 15.5089 |
| $k_{sAnoxInhO2}$ | -12.4543 | 2.1622 | 0.1983 | 10.0938 | -2.3820 | 0.0991 | 2.4811 | 0.2756 | 0.0555 | 0.0370 | 0.0530 | 0.1755 | 0.2656 | 0.0455 | -0.0847 | 5.1316 | 5.0469 | 0.0847 | -5.1316 | -5.0469 | 2.1622 | 3.1014 | 10.2632 | 15.5268 |
| $k_{sAnoxInhNO3}$ | -13.7337 | 2.1585 | 0.2016 | 11.3737 | -2.3810 | 0.1008 | 2.4818 | 0.2976 | 0.0555 | 0.0369 | 0.0531 | 0.1983 | 0.2883 | 0.0462 | -0.1097 | 5.7965 | 5.6868 | 0.1097 | -5.7965 | -5.6868 | 2.1585 | 3.1022 | 11.5930 | 16.8536 |
| $k_{sO2}$ | -12.4163 | 2.1456 | 0.1982 | 10.0725 | -2.3820 | 0.0991 | 2.4811 | 0.2750 | 0.0555 | 0.0367 | 0.0530 | 0.1752 | 0.2649 | 0.0455 | -0.0842 | 5.1204 | 5.0363 | 0.0842 | -5.1204 | -5.0363 | 2.1456 | 3.1014 | 10.2408 | 15.4878 |
| $k_{sNO3}$ | -12.3491 | 2.1626 | 0.1977 | 9.9888 | -2.3149 | 0.0989 | 2.4137 | 0.2724 | 0.0555 | 0.0370 | 0.0516 | 0.1737 | 0.2623 | 0.0454 | -0.0826 | 5.0770 | 4.9944 | 0.0826 | -5.0770 | -4.9944 | 2.1626 | 3.0172 | 10.1540 | 15.3338 |
| $k_{sSO4}$ | -11.5641 | 2.1655 | 0.1964 | 9.2022 | -2.3825 | 0.0982 | 2.4807 | 0.2602 | 0.0555 | 0.0370 | 0.0530 | 0.1597 | 0.2498 | 0.0450 | -0.0673 | 4.6684 | 4.6011 | 0.0673 | -4.6684 | -4.6011 | 2.1655 | 3.1008 | 9.3368 | 14.6031 |
| $k_{sSox}$ | -12.4338 | 2.1655 | 0.2004 | 10.0679 | -2.3809 | 0.1002 | 2.4811 | 0.2747 | 0.0555 | 0.0370 | 0.0530 | 0.1751 | 0.2652 | 0.0460 | -0.0845 | 5.1184 | 5.0340 | 0.0845 | -5.1184 | -5.0340 | 2.1655 | 3.1013 | 10.2369 | 15.5037 |
| $\phi$ | -10.1560 | 1.1684 | 0.4927 | 8.4949 | -1.8267 | 0.2463 | 2.0730 | 0.1911 | 0.0945 | 0.0200 | 0.0443 | 0.1454 | 0.2097 | 0.1130 | -0.0022 | 4.2497 | 4.2475 | 0.0022 | -4.2497 | -4.2475 | 1.1684 | 2.5913 | 8.4994 | 12.2591 |

Table B2.2a. Parameter sensitivity analysis at site 2 (each parameter decreased by 50%; values represent rate/flux (unit mol $m^{-2}$ $y^{-1}$) associated with each variable; swi=SWI flux; o2r= oxygen respiration; nit= nitrification; s-ox= sulphide oxidation; nr= nitrate reduction; bf lx= bottom boundary flux; oxamm= oxic ammonification; subamm= suboxic ammonification; anamm= anoxic ammonification; totamm= total ammonification; sr= sulphate reduction; ox, sub,an= oxic, suboxic, anoxic mineralization; parameters defined in Table 2.2)

| Parameter | Oxygen | | | | Nitrate | | | Ammonium | | | | | | | Sulphate | | | Sulphide | | | Carbon | | | |
|---|---|---|---|---|---|---|---|---|---|---|---|---|---|---|---|---|---|---|---|---|---|---|---|---|
| | swi | o2r | nit | s-ox | swi | nit | nr | swi | bflx | $ox_{amm}$ | $sub_{amm}$ | $an_{amm}$ | $tot_{amm}$ | nit | swi | sr | s-ox | swi | sr | s-ox | ox | sub | an | total |
| $M_R$ run | -15.7796 | 15.3173 | 0.1686 | 0.2938 | 0.0109 | 0.0843 | 0.0734 | 0.0974 | 0.0063 | 0.1266 | 0.0008 | 0.0024 | 0.1298 | 0.0387 | -0.0001 | 0.1470 | 0.1469 | 0.0001 | -0.1470 | -0.1469 | 15.3173 | 0.0918 | 0.2939 | 15.7031 |
| $D_{O2}^{0}$ | -13.8319 | 13.4013 | 0.1366 | 0.2939 | -0.0051 | 0.0683 | 0.0735 | 0.0890 | 0.0063 | 0.1108 | 0.0008 | 0.0024 | 0.1140 | 0.0313 | -0.0002 | 0.1472 | 0.1470 | 0.0002 | -0.1472 | -0.1470 | 13.4013 | 0.0918 | 0.2944 | 13.7875 |
| $D_{NO3}^{0}$ | -15.7806 | 15.2793 | 0.1680 | 0.3332 | 0.0143 | 0.0840 | 0.0698 | 0.0974 | 0.0061 | 0.1263 | 0.0007 | 0.0028 | 0.1298 | 0.0385 | -0.0001 | 0.1667 | 0.1666 | 0.0001 | -0.1667 | -0.1666 | 15.2793 | 0.0872 | 0.3334 | 15.6999 |
| $D_{NH4}^{0}$ | -15.7871 | 15.3099 | 0.1835 | 0.2937 | 0.0183 | 0.0918 | 0.0734 | 0.0910 | 0.0034 | 0.1265 | 0.0008 | 0.0024 | 0.1297 | 0.0421 | -0.0001 | 0.1469 | 0.1468 | 0.0001 | -0.1469 | -0.1468 | 15.3099 | 0.0918 | 0.2938 | 15.6956 |
| $D_{SO4}^{0}$ | -15.7783 | 15.3724 | 0.1693 | 0.2366 | 0.0113 | 0.0847 | 0.0734 | 0.0975 | 0.0066 | 0.1271 | 0.0008 | 0.0020 | 0.1298 | 0.0388 | -0.0001 | 0.1184 | 0.1183 | 0.0001 | -0.1184 | -0.1183 | 15.3724 | 0.0918 | 0.2367 | 15.7009 |
| $D_{S}^{0}$ | -15.7778 | 15.3154 | 0.1685 | 0.2939 | 0.0108 | 0.0843 | 0.0734 | 0.0974 | 0.0063 | 0.1266 | 0.0008 | 0.0024 | 0.1298 | 0.0387 | 0.0000 | 0.1470 | 0.1470 | 0.0000 | -0.1470 | -0.1470 | 15.3154 | 0.0918 | 0.2940 | 15.7012 |
| $D_{O2}^{const}$ | -15.0840 | 14.6327 | 0.1574 | 0.2939 | 0.0053 | 0.0787 | 0.0734 | 0.0943 | 0.0063 | 0.1209 | 0.0008 | 0.0024 | 0.1241 | 0.0361 | -0.0001 | 0.1470 | 0.1469 | 0.0001 | -0.1470 | -0.1469 | 14.6327 | 0.0918 | 0.2941 | 15.0186 |
| $D_{NO3}^{const}$ | -15.7799 | 15.3071 | 0.1684 | 0.3044 | 0.0115 | 0.0842 | 0.0727 | 0.0974 | 0.0062 | 0.1265 | 0.0008 | 0.0025 | 0.1298 | 0.0386 | -0.0001 | 0.1523 | 0.1522 | 0.0001 | -0.1523 | -0.1522 | 15.3071 | 0.0909 | 0.3046 | 15.7026 |
| $D_{NH4}^{const}$ | -15.7816 | 15.3153 | 0.1726 | 0.2937 | 0.0129 | 0.0863 | 0.0734 | 0.0954 | 0.0052 | 0.1266 | 0.0008 | 0.0024 | 0.1298 | 0.0396 | -0.0001 | 0.1470 | 0.1469 | 0.0001 | -0.1470 | -0.1469 | 15.3153 | 0.0918 | 0.2939 | 15.7010 |
| $D_{SO4}^{const}$ | -15.7792 | 15.3366 | 0.1688 | 0.2738 | 0.0110 | 0.0844 | 0.0734 | 0.0975 | 0.0064 | 0.1268 | 0.0008 | 0.0023 | 0.1298 | 0.0387 | -0.0001 | 0.1370 | 0.1369 | 0.0001 | -0.1370 | -0.1369 | 15.3366 | 0.0918 | 0.2740 | 15.7023 |
| $D_{S}^{const}$ | -15.7792 | 15.3168 | 0.1686 | 0.2938 | 0.0109 | 0.0843 | 0.0734 | 0.0974 | 0.0063 | 0.1266 | 0.0008 | 0.0024 | 0.1298 | 0.0387 | -0.0001 | 0.1470 | 0.1469 | 0.0001 | -0.1470 | -0.1469 | 15.3168 | 0.0918 | 0.2940 | 15.7026 |
| $K_{nit}$ | -15.7308 | 15.3482 | 0.0885 | 0.2942 | -0.0292 | 0.0442 | 0.0734 | 0.1160 | 0.0062 | 0.1269 | 0.0008 | 0.0024 | 0.1301 | 0.0203 | -0.0001 | 0.1472 | 0.1471 | 0.0001 | -0.1472 | -0.1471 | 15.3482 | 0.0918 | 0.2944 | 15.7343 |
| $K_{sox}$ | -15.7839 | 15.3221 | 0.1687 | 0.2932 | 0.0109 | 0.0843 | 0.0734 | 0.0974 | 0.0063 | 0.1266 | 0.0008 | 0.0024 | 0.1298 | 0.0387 | -0.0004 | 0.1469 | 0.1466 | 0.0004 | -0.1469 | -0.1466 | 15.3221 | 0.0918 | 0.2939 | 15.7077 |
| $k_{sLimO2}$ | -15.7795 | 15.3029 | 0.1830 | 0.2936 | 0.0181 | 0.0915 | 0.0734 | 0.0940 | 0.0063 | 0.1265 | 0.0008 | 0.0024 | 0.1297 | 0.0420 | -0.0001 | 0.1469 | 0.1468 | 0.0001 | -0.1469 | -0.1468 | 15.3029 | 0.0918 | 0.2938 | 15.6885 |
| $k_{sInhNO3}$ | -15.7796 | 15.3173 | 0.1686 | 0.2938 | 0.0109 | 0.0843 | 0.0734 | 0.0974 | 0.0063 | 0.1266 | 0.0008 | 0.0024 | 0.1298 | 0.0387 | -0.0001 | 0.1470 | 0.1469 | 0.0001 | -0.1470 | -0.1469 | 15.3173 | 0.0917 | 0.2939 | 15.7030 |
| $k_{sAnoxInhO2}$ | -15.7796 | 15.3175 | 0.1686 | 0.2935 | 0.0109 | 0.0843 | 0.0734 | 0.0974 | 0.0063 | 0.1266 | 0.0008 | 0.0024 | 0.1298 | 0.0387 | -0.0001 | 0.1469 | 0.1468 | 0.0001 | -0.1469 | -0.1468 | 15.3175 | 0.0918 | 0.2937 | 15.7030 |
| $k_{sAnoxInhNO3}$ | -15.7774 | 15.4113 | 0.1697 | 0.1963 | 0.0114 | 0.0849 | 0.0734 | 0.0974 | 0.0066 | 0.1274 | 0.0008 | 0.0016 | 0.1298 | 0.0389 | -0.0001 | 0.0982 | 0.0982 | 0.0001 | -0.0982 | -0.0982 | 15.4113 | 0.0918 | 0.1965 | 15.6996 |
| $k_{sO2}$ | -15.8756 | 15.4278 | 0.1539 | 0.2939 | 0.0035 | 0.0770 | 0.0734 | 0.1017 | 0.0063 | 0.1275 | 0.0008 | 0.0024 | 0.1307 | 0.0353 | -0.0002 | 0.1471 | 0.1469 | 0.0002 | -0.1471 | -0.1469 | 15.4278 | 0.0918 | 0.2942 | 15.8138 |
| $k_{sNO3}$ | -15.7797 | 15.3144 | 0.1685 | 0.2968 | 0.0081 | 0.0843 | 0.0762 | 0.0974 | 0.0063 | 0.1266 | 0.0008 | 0.0025 | 0.1298 | 0.0387 | -0.0001 | 0.1485 | 0.1484 | 0.0001 | -0.1485 | -0.1484 | 15.3144 | 0.0952 | 0.2970 | 15.7066 |
| $k_{sSO4}$ | -15.7812 | 15.2529 | 0.1678 | 0.3606 | 0.0105 | 0.0839 | 0.0734 | 0.0974 | 0.0061 | 0.1261 | 0.0008 | 0.0030 | 0.1298 | 0.0385 | -0.0001 | 0.1804 | 0.1803 | 0.0001 | -0.1804 | -0.1803 | 15.2529 | 0.0918 | 0.3608 | 15.7055 |
| $k_{sSox}$ | -15.7784 | 15.3160 | 0.1685 | 0.2938 | 0.0108 | 0.0843 | 0.0734 | 0.0974 | 0.0063 | 0.1266 | 0.0008 | 0.0024 | 0.1298 | 0.0387 | -0.0001 | 0.1470 | 0.1469 | 0.0001 | -0.1470 | -0.1469 | 15.3160 | 0.0918 | 0.2940 | 15.7017 |
| $\phi$ | -18.8823 | 18.5160 | 0.1133 | 0.2530 | -0.0144 | 0.0567 | 0.0711 | 0.1322 | 0.0023 | 0.1530 | 0.0007 | 0.0021 | 0.1559 | 0.0260 | -0.0003 | 0.1268 | 0.1265 | 0.0003 | -0.1268 | -0.1265 | 18.5160 | 0.0888 | 0.2537 | 18.8585 |

Table B2.2b. Parameter sensitivity analysis at site 2 (each parameter increased by 50%; values represent rate/flux (unit mol $m^{-2}$ $y^{-1}$) associated with each variable; swi=SWI flux; o2r= oxygen respiration; nit= nitrification; s-ox= sulphide oxidation; nr= nitrate reduction; bflx= bottom boundary flux; oxamm= oxic ammonification; subamm= suboxic ammonification; anamm= anoxic ammonification; totamm= total ammonification; sr= sulphate reduction; ox, sub,an= oxic, suboxic, anoxic mineralization; parameters defined in Table 2.2)

| Parameter | Oxygen | | | | Nitrate | | | Ammonium | | | | | | Sulphate | | | Sulphide | | | Carbon | | | |
|---|---|---|---|---|---|---|---|---|---|---|---|---|---|---|---|---|---|---|---|---|---|---|---|
| | swi | o2r | nit | s-ox | swi | nit | nr | swi | bflx | $ox_{amm}$ | $sub_{amm}$ | $an_{amm}$ | $tot_{amm}$ | nit | swi | sr | s-ox | swi | sr | s-ox | ox | sub | an | total |
| $M_{B}$ run | -15.7796 | 15.3173 | 0.1686 | 0.2938 | 0.0109 | 0.0843 | 0.0734 | 0.0974 | 0.0063 | 0.1266 | 0.0008 | 0.0024 | 0.1298 | 0.0387 | -0.0001 | 0.1470 | 0.1469 | 0.0001 | -0.1470 | -0.1469 | 15.3173 | 0.0918 | 0.2939 | 15.7031 |
| $D_{O2}^{0}$ | -17.6502 | 17.1593 | 0.1974 | 0.2935 | 0.0253 | 0.0987 | 0.0734 | 0.1060 | 0.0062 | 0.1418 | 0.0008 | 0.0024 | 0.1450 | 0.0453 | -0.0001 | 0.1468 | 0.1467 | 0.0001 | -0.1468 | -0.1467 | 17.1593 | 0.0917 | 0.2936 | 17.5447 |
| $D_{NO3}^{0}$ | -15.7792 | 15.3349 | 0.1688 | 0.2755 | 0.0101 | 0.0844 | 0.0743 | 0.0974 | 0.0064 | 0.1268 | 0.0008 | 0.0023 | 0.1298 | 0.0387 | -0.0001 | 0.1379 | 0.1378 | 0.0001 | -0.1379 | -0.1378 | 15.3349 | 0.0929 | 0.2757 | 15.7035 |
| $D_{NH4}^{0}$ | -15.7760 | 15.3212 | 0.1610 | 0.2938 | 0.0071 | 0.0805 | 0.0734 | 0.1021 | 0.0092 | 0.1266 | 0.0008 | 0.0024 | 0.1298 | 0.0369 | -0.0001 | 0.1470 | 0.1469 | 0.0001 | -0.1470 | -0.1469 | 15.3212 | 0.0918 | 0.2940 | 15.7069 |
| $D_{SO4}^{0}$ | -15.7806 | 15.2779 | 0.1680 | 0.3347 | 0.0106 | 0.0840 | 0.0734 | 0.0973 | 0.0061 | 0.1263 | 0.0008 | 0.0028 | 0.1298 | 0.0385 | -0.0001 | 0.1675 | 0.1673 | 0.0001 | -0.1675 | -0.1673 | 15.2779 | 0.0918 | 0.3349 | 15.7046 |
| $D_{S}^{0}$ | -15.7814 | 15.3192 | 0.1686 | 0.2936 | 0.0109 | 0.0843 | 0.0734 | 0.0974 | 0.0063 | 0.1266 | 0.0008 | 0.0024 | 0.1298 | 0.0387 | -0.0002 | 0.1470 | 0.1468 | 0.0002 | -0.1470 | -0.1468 | 15.3192 | 0.0918 | 0.2939 | 15.7049 |
| $D_{O2}^{const}$ | -16.4677 | 15.9947 | 0.1793 | 0.2936 | 0.0163 | 0.0897 | 0.0734 | 0.1005 | 0.0063 | 0.1322 | 0.0008 | 0.0024 | 0.1354 | 0.0411 | -0.0001 | 0.1469 | 0.1468 | 0.0001 | -0.1469 | -0.1468 | 15.9947 | 0.0918 | 0.2938 | 16.3803 |
| $D_{NO3}^{const}$ | -15.7795 | 15.3251 | 0.1687 | 0.2857 | 0.0105 | 0.0843 | 0.0739 | 0.0974 | 0.0063 | 0.1267 | 0.0008 | 0.0024 | 0.1298 | 0.0387 | -0.0001 | 0.1430 | 0.1429 | 0.0001 | -0.1430 | -0.1429 | 15.3251 | 0.0923 | 0.2859 | 15.7033 |
| $D_{NH4}^{const}$ | -15.7781 | 15.3190 | 0.1654 | 0.2938 | 0.0093 | 0.0827 | 0.0734 | 0.0992 | 0.0073 | 0.1266 | 0.0008 | 0.0024 | 0.1298 | 0.0379 | -0.0001 | 0.1470 | 0.1469 | 0.0001 | -0.1470 | -0.1469 | 15.3190 | 0.0918 | 0.2940 | 15.7047 |
| $D_{SO4}^{const}$ | -15.7800 | 15.3004 | 0.1683 | 0.3113 | 0.0107 | 0.0842 | 0.0734 | 0.0974 | 0.0062 | 0.1265 | 0.0008 | 0.0026 | 0.1298 | 0.0386 | -0.0001 | 0.1557 | 0.1556 | 0.0001 | -0.1557 | -0.1556 | 15.3004 | 0.0918 | 0.3115 | 15.7037 |
| $D_{S}^{const}$ | -15.7801 | 15.3178 | 0.1686 | 0.2937 | 0.0109 | 0.0843 | 0.0734 | 0.0974 | 0.0063 | 0.1266 | 0.0008 | 0.0024 | 0.1298 | 0.0387 | -0.0001 | 0.1470 | 0.1469 | 0.0001 | -0.1470 | -0.1469 | 15.3178 | 0.0918 | 0.2939 | 15.7035 |
| $K_{nit}$ | -15.8258 | 15.2906 | 0.2418 | 0.2934 | 0.0475 | 0.1209 | 0.0734 | 0.0804 | 0.0063 | 0.1264 | 0.0008 | 0.0024 | 0.1296 | 0.0555 | -0.0001 | 0.1468 | 0.1467 | 0.0001 | -0.1468 | -0.1467 | 15.2906 | 0.0918 | 0.2936 | 15.6760 |
| $K_{sox}$ | -15.7781 | 15.3157 | 0.1685 | 0.2939 | 0.0108 | 0.0843 | 0.0734 | 0.0974 | 0.0063 | 0.1266 | 0.0008 | 0.0024 | 0.1298 | 0.0387 | 0.0000 | 0.1470 | 0.1469 | 0.0000 | -0.1470 | -0.1469 | 15.3157 | 0.0918 | 0.2940 | 15.7015 |
| $k_{sLimO2}$ | -15.7796 | 15.3263 | 0.1595 | 0.2939 | 0.0063 | 0.0798 | 0.0734 | 0.0996 | 0.0063 | 0.1267 | 0.0008 | 0.0024 | 0.1299 | 0.0366 | -0.0001 | 0.1470 | 0.1469 | 0.0001 | -0.1470 | -0.1469 | 15.3263 | 0.0918 | 0.2941 | 15.7121 |
| $k_{sInhNO3}$ | -15.7796 | 15.3173 | 0.1686 | 0.2938 | 0.0108 | 0.0843 | 0.0735 | 0.0974 | 0.0063 | 0.1266 | 0.0008 | 0.0024 | 0.1298 | 0.0387 | -0.0001 | 0.1470 | 0.1469 | 0.0001 | -0.1470 | -0.1469 | 15.3173 | 0.0918 | 0.2939 | 15.7031 |
| $k_{sAnoxInhO2}$ | -15.7797 | 15.3173 | 0.1686 | 0.2939 | 0.0109 | 0.0843 | 0.0734 | 0.0974 | 0.0063 | 0.1266 | 0.0008 | 0.0024 | 0.1298 | 0.0387 | -0.0001 | 0.1470 | 0.1469 | 0.0001 | -0.1470 | -0.1469 | 15.3173 | 0.0918 | 0.2941 | 15.7031 |
| $k_{sAnoxInhNO3}$ | -15.7812 | 15.2566 | 0.1679 | 0.3568 | 0.0105 | 0.0839 | 0.0734 | 0.0975 | 0.0062 | 0.1261 | 0.0008 | 0.0030 | 0.1298 | 0.0385 | -0.0001 | 0.1785 | 0.1784 | 0.0001 | -0.1785 | -0.1784 | 15.2566 | 0.0918 | 0.3570 | 15.7053 |
| $k_{sO2}$ | -15.6879 | 15.2172 | 0.1770 | 0.2937 | 0.0151 | 0.0885 | 0.0734 | 0.0947 | 0.0063 | 0.1258 | 0.0008 | 0.0024 | 0.1290 | 0.0406 | -0.0001 | 0.1469 | 0.1468 | 0.0001 | -0.1469 | -0.1468 | 15.2172 | 0.0918 | 0.2938 | 15.6028 |
| $k_{sNO3}$ | -15.7796 | 15.3199 | 0.1686 | 0.2911 | 0.0133 | 0.0843 | 0.0710 | 0.0974 | 0.0063 | 0.1266 | 0.0007 | 0.0024 | 0.1298 | 0.0387 | -0.0001 | 0.1457 | 0.1456 | 0.0001 | -0.1457 | -0.1456 | 15.3199 | 0.0888 | 0.2913 | 15.6999 |
| $k_{sSO4}$ | -15.7786 | 15.3584 | 0.1691 | 0.2512 | 0.0111 | 0.0845 | 0.0734 | 0.0974 | 0.0064 | 0.1269 | 0.0008 | 0.0021 | 0.1298 | 0.0388 | -0.0001 | 0.1257 | 0.1256 | 0.0001 | -0.1257 | -0.1256 | 15.3584 | 0.0918 | 0.2513 | 15.7015 |
| $k_{sSox}$ | -15.7809 | 15.3186 | 0.1686 | 0.2937 | 0.0109 | 0.0843 | 0.0734 | 0.0974 | 0.0063 | 0.1266 | 0.0008 | 0.0024 | 0.1298 | 0.0387 | -0.0001 | 0.1470 | 0.1468 | 0.0001 | -0.1470 | -0.1468 | 15.3186 | 0.0918 | 0.2939 | 15.7043 |
| $\phi$ | -13.2729 | 12.8236 | 0.2660 | 0.1833 | 0.0900 | 0.1330 | 0.0431 | 0.0593 | 0.0123 | 0.1060 | 0.0004 | 0.0015 | 0.1080 | 0.0610 | 0.0000 | 0.0917 | 0.0917 | 0.0000 | -0.0917 | -0.0917 | 12.8236 | 0.0538 | 0.1833 | 13.0607 |

Table B2.3a. Parameter sensitivity analysis at site 3 (each parameter decreased by 50%; values represent rate/flux (unit mol $m^{-2}$ $y^{-1}$) associated with each variable; swi=SWI flux; o2r= oxygen respiration; nit= nitrification; s-ox= sulphide oxidation; nr= nitrate reduction; bf lx= bottom boundary flux; oxamm= oxic ammonification; subamm= suboxic ammonification; anamm= anoxic ammonification; totamm= total ammonification; sr= sulphate reduction; ox, sub,an= oxic, suboxic, anoxic mineralization; parameters defined in Table 2.2)

| Parameter | Oxygen | | | | Nitrate | | | Ammonium | | | | | | | Sulphate | | | Sulphide | | | Carbon | | | |
|---|---|---|---|---|---|---|---|---|---|---|---|---|---|---|---|---|---|---|---|---|---|---|---|---|
| | swi | o2r | nit | s-ox | swi | nit | nr | swi | bflx | $ox_{amm}$ | $sub_{amm}$ | $an_{amm}$ | $tot_{amm}$ | nit | swi | sr | s-ox | swi | sr | s-ox | ox | sub | an | total |
| $M_{st}$ run | -27.5070 | 15.6645 | 0.1396 | 11.7029 | -1.8677 | 0.0698 | 1.9375 | 0.4036 | 0.0559 | 0.1974 | 0.0305 | 0.1519 | 0.3797 | 0.0320 | -0.1758 | 6.0272 | 5.8514 | 0.1758 | -6.0272 | -5.8514 | 15.6645 | 2.4219 | 12.0545 | 30.1409 |
| $D_{O2}^{0}$ | -20.3841 | 6.8680 | 0.0869 | 13.4292 | -2.0128 | 0.0435 | 2.0562 | 0.3322 | 0.0561 | 0.0865 | 0.0324 | 0.1772 | 0.2961 | 0.0199 | -0.3181 | 7.0327 | 6.7146 | 0.3181 | -7.0327 | -6.7146 | 6.8680 | 2.5703 | 14.0653 | 23.5036 |
| $D_{NO3}^{0}$ | -27.8418 | 15.6040 | 0.1391 | 12.0987 | -1.4474 | 0.0696 | 1.5170 | 0.4020 | 0.0564 | 0.1966 | 0.0239 | 0.1571 | 0.3775 | 0.0319 | -0.1837 | 6.2330 | 6.0493 | 0.1837 | -6.2330 | -6.0493 | 15.6040 | 1.8962 | 12.4660 | 29.9663 |
| $D_{NH4}^{0}$ | -27.5374 | 15.6594 | 0.1766 | 11.7015 | -1.8497 | 0.0883 | 1.9380 | 0.3728 | 0.0337 | 0.1973 | 0.0305 | 0.1519 | 0.3797 | 0.0405 | -0.1759 | 6.0266 | 5.8507 | 0.1759 | -6.0266 | -5.8507 | 15.6594 | 2.4225 | 12.0533 | 30.1351 |
| $D_{SO4}^{0}$ | -25.1721 | 15.9408 | 0.1352 | 9.0962 | -1.8641 | 0.0676 | 1.9317 | 0.3748 | 0.0568 | 0.2008 | 0.0304 | 0.1177 | 0.3490 | 0.0310 | -0.1244 | 4.6725 | 4.5481 | 0.1244 | -4.6725 | -4.5481 | 15.9408 | 2.4146 | 9.3449 | 27.7003 |
| $D_{S}^{0}$ | -27.6322 | 15.6408 | 0.1394 | 11.8519 | -1.8683 | 0.0697 | 1.9380 | 0.4035 | 0.0559 | 0.1971 | 0.0305 | 0.1520 | 0.3796 | 0.0320 | -0.1074 | 6.0334 | 5.9260 | 0.1074 | -6.0334 | -5.9260 | 15.6408 | 2.4225 | 12.0667 | 30.1301 |
| $D_{O2}^{const}$ | -26.5391 | 14.4323 | 0.1335 | 11.9733 | -1.8946 | 0.0668 | 1.9614 | 0.3939 | 0.0560 | 0.1818 | 0.0309 | 0.1558 | 0.3685 | 0.0306 | -0.1970 | 6.1837 | 5.9866 | 0.1970 | -6.1837 | -5.9866 | 14.4323 | 2.4517 | 12.3673 | 29.2514 |
| $D_{NO3}^{const}$ | -27.5997 | 15.6485 | 0.1394 | 11.8117 | -1.7312 | 0.0697 | 1.8009 | 0.4029 | 0.0561 | 0.1972 | 0.0284 | 0.1533 | 0.3788 | 0.0320 | -0.1780 | 6.0838 | 5.9059 | 0.1780 | -6.0838 | -5.9059 | 15.6485 | 2.2511 | 12.1677 | 30.0673 |
| $D_{NH4}^{const}$ | -27.5148 | 15.6632 | 0.1491 | 11.7025 | -1.8631 | 0.0746 | 1.9377 | 0.3937 | 0.0482 | 0.1973 | 0.0305 | 0.1519 | 0.3797 | 0.0342 | -0.1758 | 6.0271 | 5.8513 | 0.1758 | -6.0271 | -5.8513 | 15.6632 | 2.4221 | 12.0542 | 30.1394 |
| $D_{SO4}^{const}$ | -26.6689 | 15.7872 | 0.1381 | 10.7436 | -1.8659 | 0.0690 | 1.9350 | 0.3933 | 0.0563 | 0.1989 | 0.0305 | 0.1393 | 0.3687 | 0.0317 | -0.1568 | 5.5286 | 5.3718 | 0.1568 | -5.5286 | -5.3718 | 15.7872 | 2.4187 | 11.0572 | 29.2631 |
| $D_{S}^{const}$ | -27.5383 | 15.6587 | 0.1396 | 11.7401 | -1.8679 | 0.0698 | 1.9377 | 0.4036 | 0.0559 | 0.1973 | 0.0305 | 0.1519 | 0.3797 | 0.0320 | -0.1587 | 6.0288 | 5.8700 | 0.1587 | -6.0288 | -5.8700 | 15.6587 | 2.4221 | 12.0575 | 30.1382 |
| $K_{nit}$ | -27.4508 | 15.6739 | 0.0714 | 11.7055 | -1.9010 | 0.0357 | 1.9367 | 0.4194 | 0.0559 | 0.1975 | 0.0305 | 0.1519 | 0.3799 | 0.0164 | -0.1756 | 6.0284 | 5.8528 | 0.1756 | -6.0284 | -5.8528 | 15.6739 | 2.4209 | 12.0568 | 30.1515 |
| $K_{sox}$ | -27.2090 | 15.7176 | 0.1403 | 11.3512 | -1.8664 | 0.0701 | 1.9365 | 0.4038 | 0.0559 | 0.1980 | 0.0305 | 0.1515 | 0.3800 | 0.0322 | -0.3379 | 6.0135 | 5.6756 | 0.3379 | -6.0135 | -5.6756 | 15.7176 | 2.4207 | 12.0269 | 30.1652 |
| $k_{sLimO2}$ | -27.5082 | 15.6643 | 0.1413 | 11.7026 | -1.8670 | 0.0706 | 1.9376 | 0.4033 | 0.0559 | 0.1974 | 0.0305 | 0.1519 | 0.3797 | 0.0324 | -0.1758 | 6.0271 | 5.8513 | 0.1758 | -6.0271 | -5.8513 | 15.6643 | 2.4220 | 12.0542 | 30.1405 |
| $k_{sInhNO3}$ | -27.5063 | 15.6646 | 0.1396 | 11.7021 | -1.8585 | 0.0698 | 1.9283 | 0.4035 | 0.0559 | 0.1974 | 0.0304 | 0.1519 | 0.3796 | 0.0320 | -0.1758 | 6.0268 | 5.8510 | 0.1758 | -6.0268 | -5.8510 | 15.6646 | 2.4104 | 12.0537 | 30.1287 |
| $k_{sAnoxInhO2}$ | -27.3329 | 15.6929 | 0.1393 | 11.5007 | -1.8673 | 0.0697 | 1.9369 | 0.4014 | 0.0559 | 0.1977 | 0.0305 | 0.1492 | 0.3774 | 0.0320 | -0.1718 | 5.9221 | 5.7503 | 0.1718 | -5.9221 | -5.7503 | 15.6929 | 2.4212 | 11.8442 | 29.9584 |
| $k_{sAnoxInhNO3}$ | -25.1950 | 15.9387 | 0.1350 | 9.1213 | -1.8643 | 0.0675 | 1.9318 | 0.3742 | 0.0559 | 0.2008 | 0.0304 | 0.1181 | 0.3493 | 0.0310 | -0.1249 | 4.6855 | 4.5607 | 0.1249 | -4.6855 | -4.5607 | 15.9387 | 2.4147 | 9.3710 | 27.7244 |
| $k_{sO2}$ | -27.9043 | 16.0579 | 0.1403 | 11.7061 | -1.8689 | 0.0702 | 1.9391 | 0.4085 | 0.0559 | 0.2023 | 0.0305 | 0.1520 | 0.3848 | 0.0322 | -0.1776 | 6.0306 | 5.8530 | 0.1776 | -6.0306 | -5.8530 | 16.0579 | 2.4238 | 12.0612 | 30.5429 |
| $k_{sNO3}$ | -27.5543 | 15.6564 | 0.1399 | 11.7580 | -1.9269 | 0.0700 | 1.9968 | 0.4051 | 0.0559 | 0.1973 | 0.0315 | 0.1526 | 0.3813 | 0.0321 | -0.1769 | 6.0559 | 5.8790 | 0.1769 | -6.0559 | -5.8790 | 15.6564 | 2.4960 | 12.1118 | 30.2643 |
| $k_{sSO4}$ | -29.1768 | 15.2514 | 0.1424 | 13.7831 | -1.8748 | 0.0712 | 1.9460 | 0.4252 | 0.0559 | 0.1922 | 0.0307 | 0.1791 | 0.4019 | 0.0327 | -0.2177 | 7.1092 | 6.8915 | 0.2177 | -7.1092 | -6.8915 | 15.2514 | 2.4324 | 14.2184 | 31.9022 |
| $k_{sSox}$ | -27.5085 | 15.6617 | 0.1394 | 11.7074 | -1.8678 | 0.0697 | 1.9375 | 0.4037 | 0.0559 | 0.1973 | 0.0305 | 0.1519 | 0.3797 | 0.0320 | -0.1742 | 6.0279 | 5.8537 | 0.1742 | -6.0279 | -5.8537 | 15.6617 | 2.4219 | 12.0558 | 30.1394 |
| $\phi$ | -30.4976 | 21.5967 | 0.1134 | 8.7875 | -1.4443 | 0.0567 | 1.5010 | 0.4076 | 0.0227 | 0.2721 | 0.0236 | 0.1151 | 0.4109 | 0.0260 | -0.1752 | 4.5690 | 4.3937 | 0.1752 | -4.5690 | -4.3937 | 21.5967 | 1.8762 | 9.1379 | 32.6109 |

Table B2.3b. Parameter sensitivity analysis at site 3 (each parameter increased by 50%; values represent rate/flux (unit mol $m^{-2}$ $y^{-1}$) associated with each variable; swi=SWI flux; o2r= oxygen respiration; nit= nitrification; s-ox= sulphide oxidation; nr= nitrate reduction; bf lx= bottom boundary flux; oxamm= oxic ammonification; subamm= suboxic ammonification; anamm= anoxic ammonification; totamm= total ammonification; sr= sulphate reduction; ox, sub,an= oxic, suboxic, anoxic mineralization; parameters defined in Table 2.2)

| Parameter | Oxygen | | | | Nitrate | | | Ammonium | | | | | | | Sulphate | | | Sulphide | | | Carbon | | | |
|---|---|---|---|---|---|---|---|---|---|---|---|---|---|---|---|---|---|---|---|---|---|---|---|---|
| | swi | o2r | nit | s-ox | swi | nit | nr | swi | bflx | $ox_{amm}$ | $sub_{amm}$ | $an_{amm}$ | $tot_{amm}$ | nit | swi | sr | s-ox | swi | sr | s-ox | ox | sub | an | total |
| $M_{a}$ run | -27.5070 | 15.6645 | 0.1396 | 11.7029 | -1.8677 | 0.0698 | 1.9375 | 0.4036 | 0.0559 | 0.1974 | 0.0305 | 0.1519 | 0.3797 | 0.0320 | -0.1758 | 6.0272 | 5.8514 | 0.1758 | -6.0272 | -5.8514 | 15.6645 | 2.4219 | 12.0545 | 30.1409 |
| $D_{O2}^{0}$ | -28.5433 | 16.1700 | 0.1444 | 12.2289 | -1.8548 | 0.0722 | 1.9270 | 0.4144 | 0.0557 | 0.2037 | 0.0304 | 0.1578 | 0.3918 | 0.0331 | -0.1461 | 6.2606 | 6.1145 | 0.1461 | -6.2606 | -6.1145 | 16.1700 | 2.4087 | 12.5212 | 31.0999 |
| $D_{NO3}^{0}$ | -27.3187 | 15.6953 | 0.1402 | 11.4831 | -2.2156 | 0.0701 | 2.2857 | 0.4060 | 0.0554 | 0.1977 | 0.0360 | 0.1490 | 0.3827 | 0.0322 | -0.1714 | 5.9130 | 5.7416 | 0.1714 | -5.9130 | -5.7416 | 15.6953 | 2.8571 | 11.8260 | 30.3784 |
| $D_{NH4}^{0}$ | -27.4925 | 15.6669 | 0.1221 | 11.7036 | -1.8763 | 0.0610 | 1.9373 | 0.4299 | 0.0782 | 0.1974 | 0.0305 | 0.1519 | 0.3798 | 0.0280 | -0.1758 | 6.0275 | 5.8518 | 0.1758 | -6.0275 | -5.8518 | 15.6669 | 2.4216 | 12.0551 | 30.1436 |
| $D_{SO4}^{0}$ | -29.4215 | 15.1562 | 0.1425 | 14.1228 | -1.8766 | 0.0712 | 1.9478 | 0.4275 | 0.0550 | 0.1910 | 0.0307 | 0.1836 | 0.4052 | 0.0327 | -0.2246 | 7.2860 | 7.0614 | 0.2246 | -7.2860 | -7.0614 | 15.1562 | 2.4348 | 14.5720 | 32.1630 |
| $D_{S}^{0}$ | -27.3855 | 15.6867 | 0.1399 | 11.5589 | -1.8672 | 0.0699 | 1.9371 | 0.4037 | 0.0559 | 0.1976 | 0.0305 | 0.1517 | 0.3799 | 0.0321 | -0.2420 | 6.0215 | 5.7795 | 0.2420 | -6.0215 | -5.7795 | 15.6867 | 2.4214 | 12.0430 | 30.1511 |
| $D_{O2}^{const}$ | -27.9448 | 15.9759 | 0.1418 | 11.8271 | -1.8601 | 0.0709 | 1.9310 | 0.4081 | 0.0559 | 0.2013 | 0.0304 | 0.1531 | 0.3848 | 0.0325 | -0.1638 | 6.0774 | 5.9136 | 0.1638 | -6.0774 | -5.9136 | 15.9759 | 2.4138 | 12.1548 | 30.5444 |
| $D_{NO3}^{const}$ | -27.4307 | 15.6772 | 0.1398 | 11.6136 | -1.9958 | 0.0699 | 2.0657 | 0.4044 | 0.0558 | 0.1975 | 0.0325 | 0.1507 | 0.3807 | 0.0321 | -0.1740 | 5.9808 | 5.8068 | 0.1740 | -5.9808 | -5.8068 | 15.6772 | 2.5821 | 11.9617 | 30.2210 |
| $D_{NH4}^{const}$ | -27.5009 | 15.6655 | 0.1322 | 11.7032 | -1.8713 | 0.0661 | 1.9374 | 0.4131 | 0.0637 | 0.1974 | 0.0305 | 0.1519 | 0.3797 | 0.0303 | -0.1758 | 6.0274 | 5.8516 | 0.1758 | -6.0274 | -5.8516 | 15.6655 | 2.4218 | 12.0547 | 30.1421 |
| $D_{SO4}^{const}$ | -28.2864 | 15.5098 | 0.1410 | 12.6357 | -1.8703 | 0.0705 | 1.9407 | 0.4133 | 0.0556 | 0.1954 | 0.0306 | 0.1641 | 0.3901 | 0.0323 | -0.1944 | 6.5123 | 6.3178 | 0.1944 | -6.5123 | -6.3178 | 15.5098 | 2.4259 | 13.0246 | 30.9603 |
| $D_{S}^{const}$ | -27.4760 | 15.6702 | 0.1397 | 11.6660 | -1.8676 | 0.0699 | 1.9374 | 0.4036 | 0.0559 | 0.1974 | 0.0305 | 0.1518 | 0.3798 | 0.0320 | -0.1928 | 6.0258 | 5.8330 | 0.1928 | -6.0258 | -5.8330 | 15.6702 | 2.4218 | 12.0515 | 30.1435 |
| $K_{nit}$ | -27.5608 | 15.6553 | 0.2050 | 11.7004 | -1.8359 | 0.1025 | 1.9384 | 0.3885 | 0.0559 | 0.1972 | 0.0305 | 0.1518 | 0.3796 | 0.0470 | -0.1760 | 6.0262 | 5.8502 | 0.1760 | -6.0262 | -5.8502 | 15.6553 | 2.4230 | 12.0524 | 30.1307 |
| $K_{aox}$ | -27.6113 | 15.6449 | 0.1394 | 11.8270 | -1.8682 | 0.0697 | 1.9379 | 0.4036 | 0.0559 | 0.1971 | 0.0305 | 0.1520 | 0.3796 | 0.0320 | -0.1188 | 6.0323 | 5.9135 | 0.1188 | -6.0323 | -5.9135 | 15.6449 | 2.4224 | 12.0647 | 30.1319 |
| $k_{sLimO2}$ | -27.5060 | 15.6647 | 0.1383 | 11.7030 | -1.8684 | 0.0692 | 1.9375 | 0.4039 | 0.0559 | 0.1974 | 0.0305 | 0.1519 | 0.3797 | 0.0317 | -0.1758 | 6.0273 | 5.8515 | 0.1758 | -6.0273 | -5.8515 | 15.6647 | 2.4219 | 12.0546 | 30.1412 |
| $k_{sInhNO3}$ | -27.5076 | 15.6644 | 0.1397 | 11.7036 | -1.8760 | 0.0698 | 1.9458 | 0.4038 | 0.0559 | 0.1974 | 0.0306 | 0.1519 | 0.3799 | 0.0320 | -0.1758 | 6.0276 | 5.8518 | 0.1758 | -6.0276 | -5.8518 | 15.6644 | 2.4323 | 12.0552 | 30.1519 |
| $k_{sAnoxInhO2}$ | -27.6667 | 15.6367 | 0.1399 | 11.8900 | -1.8682 | 0.0700 | 1.9381 | 0.4057 | 0.0559 | 0.1970 | 0.0305 | 0.1543 | 0.3818 | 0.0321 | -0.1795 | 6.1245 | 5.9450 | 0.1795 | -6.1245 | -5.9450 | 15.6367 | 2.4227 | 12.2491 | 30.3085 |
| $k_{sAnoxInhNO3}$ | -29.1007 | 15.2784 | 0.1423 | 13.6800 | -1.8743 | 0.0711 | 1.9454 | 0.4242 | 0.0559 | 0.1925 | 0.0306 | 0.1778 | 0.4009 | 0.0326 | -0.2156 | 7.0556 | 6.8400 | 0.2156 | -7.0556 | -6.8400 | 15.2784 | 2.4318 | 14.1111 | 31.8213 |
| $k_{sO2}$ | -27.1745 | 15.3327 | 0.1390 | 11.7028 | -1.8669 | 0.0695 | 1.9364 | 0.3995 | 0.0559 | 0.1932 | 0.0305 | 0.1518 | 0.3755 | 0.0319 | -0.1745 | 6.0258 | 5.8514 | 0.1745 | -6.0258 | -5.8514 | 15.3327 | 2.4205 | 12.0517 | 29.8049 |
| $k_{sNO3}$ | -27.4686 | 15.6710 | 0.1394 | 11.6582 | -1.8187 | 0.0697 | 1.8885 | 0.4024 | 0.0559 | 0.1974 | 0.0297 | 0.1513 | 0.3785 | 0.0320 | -0.1749 | 6.0040 | 5.8291 | 0.1749 | -6.0040 | -5.8291 | 15.6710 | 2.3606 | 12.0080 | 30.0395 |
| $k_{sSO4}$ | -26.4673 | 15.8119 | 0.1376 | 10.5178 | -1.8656 | 0.0688 | 1.9344 | 0.3904 | 0.0559 | 0.1992 | 0.0305 | 0.1364 | 0.3660 | 0.0316 | -0.1523 | 5.4112 | 5.2589 | 0.1523 | -5.4112 | -5.2589 | 15.8119 | 2.4181 | 10.8225 | 29.0524 |
| $k_{sSox}$ | -27.5056 | 15.6673 | 0.1398 | 11.6984 | -1.8676 | 0.0699 | 1.9375 | 0.4036 | 0.0559 | 0.1974 | 0.0305 | 0.1519 | 0.3798 | 0.0321 | -0.1774 | 6.0266 | 5.8492 | 0.1774 | -6.0266 | -5.8492 | 15.6673 | 2.4219 | 12.0532 | 30.1424 |
| $\phi$ | -20.1594 | 8.2619 | 0.1533 | 11.7442 | -1.7343 | 0.0767 | 1.8109 | 0.3426 | 0.0946 | 0.1041 | 0.0285 | 0.1506 | 0.2832 | 0.0352 | -0.1040 | 5.9761 | 5.8721 | 0.1040 | -5.9761 | -5.8721 | 8.2619 | 2.2637 | 11.9522 | 22.4778 |

Table B2.4a. Parameter sensitivity analysis at site 4 (each parameter decreased by 50%; values represent rate/flux (unit mol $m^{-2}$ $y^{-1}$) associated with each variable; swi=SWI flux; o2r= oxygen respiration; nit= nitrification; s-ox= sulphide oxidation; nr= nitrate reduction; bf lx= bottom boundary flux; oxamm= oxic ammonification; subamm= suboxic ammonification; anamm= anoxic ammonification; totamm= total ammonification; sr= sulphate reduction; ox, sub,an= oxic, suboxic, anoxic mineralization; parameters defined in Table 2.2)

| Parameter | Oxygen | | | | Nitrate | | | Ammonium | | | | | | | Sulphate | | | Sulphide | | | Carbon | | | |
|---|---|---|---|---|---|---|---|---|---|---|---|---|---|---|---|---|---|---|---|---|---|---|---|---|
| | swi | o2r | nit | s-ox | swi | nit | nr | swi | bflx | $ox_{amm}$ | $sub_{amm}$ | $an_{amm}$ | $tot_{amm}$ | nit | swi | sr | s-ox | swi | sr | s-ox | ox | sub | an | total |
| $M_{a}$run | -23.2706 | 15.7410 | 0.3767 | 7.1529 | -6.3890 | 0.1884 | 6.5774 | 0.4741 | 0.0909 | 0.2363 | 0.1234 | 0.1099 | 0.4696 | 0.0864 | -0.0847 | 3.6612 | 3.5765 | 0.0847 | -3.6612 | -3.5765 | 15.7410 | 8.2217 | 7.3224 | 31.2851 |
| $D_{O2}^{0}$ | -19.8866 | 12.6308 | 0.3414 | 6.9144 | -7.3621 | 0.1707 | 7.5328 | 0.4511 | 0.0911 | 0.1896 | 0.1413 | 0.1074 | 0.4383 | 0.0783 | -0.1191 | 3.5763 | 3.4572 | 0.1191 | -3.5763 | -3.4572 | 12.6308 | 9.4160 | 7.1526 | 29.1994 |
| $D_{NO3}^{0}$ | -23.6238 | 15.7204 | 0.3713 | 7.5321 | -4.6917 | 0.1856 | 4.8773 | 0.4496 | 0.0914 | 0.2360 | 0.0915 | 0.1158 | 0.4433 | 0.0852 | -0.0921 | 3.8582 | 3.7661 | 0.0921 | -3.8582 | -3.7661 | 15.7204 | 6.0967 | 7.7163 | 29.5334 |
| $D_{NH4}^{0}$ | -23.3085 | 15.7390 | 0.4183 | 7.1513 | -6.3707 | 0.2091 | 6.5799 | 0.4283 | 0.0547 | 0.2363 | 0.1235 | 0.1099 | 0.4696 | 0.0959 | -0.0849 | 3.6605 | 3.5757 | 0.0849 | -3.6605 | -3.5757 | 15.7390 | 8.2248 | 7.3210 | 31.2848 |
| $D_{SO4}^{0}$ | -21.7360 | 15.8233 | 0.3747 | 5.5380 | -6.3647 | 0.1873 | 6.5521 | 0.4520 | 0.0927 | 0.2375 | 0.1229 | 0.0847 | 0.4452 | 0.0859 | -0.0535 | 2.8225 | 2.7690 | 0.0535 | -2.8225 | -2.7690 | 15.8233 | 8.1901 | 5.6450 | 29.6584 |
| $D_{S}^{0}$ | -23.3269 | 15.7305 | 0.3757 | 7.2206 | -6.3907 | 0.1879 | 6.5786 | 0.4742 | 0.0909 | 0.2361 | 0.1234 | 0.1099 | 0.4695 | 0.0862 | -0.0516 | 3.6619 | 3.6103 | 0.0516 | -3.6619 | -3.6103 | 15.7305 | 8.2232 | 7.3239 | 31.2776 |
| $D_{O2}^{const}$ | -22.9091 | 15.4990 | 0.3731 | 7.0371 | -6.4761 | 0.1865 | 6.6626 | 0.4716 | 0.0910 | 0.2327 | 0.1250 | 0.1085 | 0.4662 | 0.0856 | -0.0966 | 3.6151 | 3.5185 | 0.0966 | -3.6151 | -3.5185 | 15.4990 | 8.3283 | 7.2302 | 31.0575 |
| $D_{NO3}^{const}$ | -23.3815 | 15.7347 | 0.3749 | 7.2719 | -5.8357 | 0.1875 | 6.0231 | 0.4660 | 0.0911 | 0.2362 | 0.1130 | 0.1118 | 0.4610 | 0.0860 | -0.0870 | 3.7230 | 3.6360 | 0.0870 | -3.7230 | -3.6360 | 15.7347 | 7.5289 | 7.4460 | 30.7095 |
| $D_{NH4}^{const}$ | -23.2804 | 15.7405 | 0.3874 | 7.1525 | -6.3843 | 0.1937 | 6.5780 | 0.4590 | 0.0782 | 0.2363 | 0.1234 | 0.1099 | 0.4696 | 0.0889 | -0.0848 | 3.6610 | 3.5763 | 0.0848 | -3.6610 | -3.5763 | 15.7405 | 8.2225 | 7.3220 | 31.2850 |
| $D_{SO4}^{const}$ | -22.7183 | 15.7714 | 0.3758 | 6.5710 | -6.3795 | 0.1879 | 6.5674 | 0.4662 | 0.0916 | 0.2367 | 0.1232 | 0.1008 | 0.4608 | 0.0862 | -0.0735 | 3.3590 | 3.2855 | 0.0735 | -3.3590 | -3.2855 | 15.7714 | 8.2093 | 6.7179 | 30.6987 |
| $D_{S}^{const}$ | -23.2847 | 15.7384 | 0.3764 | 7.1699 | -6.3894 | 0.1882 | 6.5777 | 0.4741 | 0.0909 | 0.2362 | 0.1234 | 0.1099 | 0.4696 | 0.0863 | -0.0765 | 3.6614 | 3.5849 | 0.0765 | -3.6614 | -3.5849 | 15.7384 | 8.2221 | 7.3228 | 31.2832 |
| $K_{nit}$ | -23.1022 | 15.7498 | 0.1926 | 7.1598 | -6.4704 | 0.0963 | 6.5667 | 0.5163 | 0.0909 | 0.2364 | 0.1232 | 0.1100 | 0.4696 | 0.0442 | -0.0842 | 3.6642 | 3.5799 | 0.0842 | -3.6642 | -3.5799 | 15.7498 | 8.2084 | 7.3283 | 31.2865 |
| $K_{sox}$ | -23.1368 | 15.7668 | 0.3792 | 6.9908 | -6.3849 | 0.1896 | 6.5745 | 0.4738 | 0.0909 | 0.2367 | 0.1234 | 0.1099 | 0.4699 | 0.0870 | -0.1640 | 3.6594 | 3.4954 | 0.1640 | -3.6594 | -3.4954 | 15.7668 | 8.2181 | 7.3188 | 31.3037 |
| $k_{sLimO2}$ | -23.2740 | 15.7408 | 0.3808 | 7.1523 | -6.3876 | 0.1904 | 6.5780 | 0.4731 | 0.0909 | 0.2363 | 0.1234 | 0.1099 | 0.4696 | 0.0874 | -0.0848 | 3.6610 | 3.5762 | 0.0848 | -3.6610 | -3.5762 | 15.7408 | 8.2226 | 7.3219 | 31.2853 |
| $k_{sInhNO3}$ | -23.2686 | 15.7411 | 0.3764 | 7.1511 | -6.2997 | 0.1882 | 6.4879 | 0.4725 | 0.0909 | 0.2363 | 0.1217 | 0.1099 | 0.4679 | 0.0863 | -0.0847 | 3.6602 | 3.5755 | 0.0847 | -3.6602 | -3.5755 | 15.7411 | 8.1099 | 7.3205 | 31.1715 |
| $k_{sAnoxInhO2}$ | -23.2686 | 15.7411 | 0.3767 | 7.1508 | -6.3890 | 0.1883 | 6.5773 | 0.4741 | 0.0909 | 0.2363 | 0.1234 | 0.1099 | 0.4696 | 0.0864 | -0.0847 | 3.6601 | 3.5754 | 0.0847 | -3.6601 | -3.5754 | 15.7411 | 8.2216 | 7.3202 | 31.2829 |
| $k_{sAnoxInhNO3}$ | -23.0010 | 15.7561 | 0.3762 | 6.8687 | -6.3843 | 0.1881 | 6.5724 | 0.4699 | 0.0909 | 0.2365 | 0.1233 | 0.1055 | 0.4653 | 0.0863 | -0.0792 | 3.5136 | 3.4343 | 0.0792 | -3.5136 | -3.4343 | 15.7561 | 8.2155 | 7.0271 | 30.9987 |
| $k_{sO2}$ | -23.5069 | 15.9864 | 0.3772 | 7.1433 | -6.3933 | 0.1886 | 6.5819 | 0.4776 | 0.0909 | 0.2400 | 0.1235 | 0.1098 | 0.4733 | 0.0865 | -0.0857 | 3.6574 | 3.5717 | 0.0857 | -3.6574 | -3.5717 | 15.9864 | 8.2274 | 7.3147 | 31.5285 |
| $k_{sNO3}$ | -23.4308 | 15.7318 | 0.3778 | 7.3212 | -6.6077 | 0.1889 | 6.7966 | 0.4804 | 0.0909 | 0.2361 | 0.1275 | 0.1125 | 0.4762 | 0.0867 | -0.0880 | 3.7486 | 3.6606 | 0.0880 | -3.7486 | -3.6606 | 15.7318 | 8.4957 | 7.4973 | 31.7248 |
| $k_{sSO4}$ | -24.1700 | 15.6862 | 0.3785 | 8.1053 | -6.4068 | 0.1892 | 6.5960 | 0.4881 | 0.0909 | 0.2355 | 0.1238 | 0.1248 | 0.4840 | 0.0868 | -0.1033 | 4.1559 | 4.0527 | 0.1033 | -4.1559 | -4.0527 | 15.6862 | 8.2451 | 8.3119 | 32.2431 |
| $k_{sSox}$ | -23.2631 | 15.7319 | 0.3755 | 7.1557 | -6.3897 | 0.1878 | 6.5774 | 0.4743 | 0.0909 | 0.2361 | 0.1234 | 0.1099 | 0.4695 | 0.0861 | -0.0842 | 3.6620 | 3.5779 | 0.0842 | -3.6620 | -3.5779 | 15.7319 | 8.2218 | 7.3241 | 31.2777 |
| $\phi$ | -28.5367 | 22.8459 | 0.3079 | 5.3829 | -4.5460 | 0.1539 | 4.6999 | 0.4812 | 0.0369 | 0.3429 | 0.0882 | 0.0838 | 0.5149 | 0.0706 | -0.0999 | 2.7914 | 2.6914 | 0.0999 | -2.7914 | -2.6914 | 22.8459 | 5.8749 | 5.5827 | 34.3035 |

Table B2.4b. Parameter sensitivity analysis at site 4 (each parameter increased by 50%; values represent rate/flux (unit mol $m^{-2}$ $y^{-1}$) associated with each variable; swi=SWI flux; o2r= oxygen respiration; nit= nitrification; s-ox= sulphide oxidation; nr= nitrate reduction; bf lx= bottom boundary flux; oxamm= oxic ammonification; subamm= suboxic ammonification; anamm= anoxic ammonification; totamm= total ammonification; sr= sulphate reduction; ox, sub,an= oxic, suboxic, anoxic mineralization; parameters defined in Table 2.2)

| Parameter | Oxygen | | | | Nitrate | | | Ammonium | | | | | | | Sulphate | | | Sulphide | | | Carbon | | | |
|---|---|---|---|---|---|---|---|---|---|---|---|---|---|---|---|---|---|---|---|---|---|---|---|---|
| | swi | o2r | nit | s-ox | swi | nit | nr | swi | bflx | $ox_{amm}$ | $sub_{amm}$ | $an_{amm}$ | $tot_{amm}$ | nit | swi | sr | s-ox | swi | sr | s-ox | ox | sub | an | total |
| $M_{st}$ run | -23.2706 | 15.7410 | 0.3767 | 7.1529 | -6.3890 | 0.1884 | 6.5774 | 0.4741 | 0.0909 | 0.2363 | 0.1234 | 0.1099 | 0.4696 | 0.0864 | -0.0847 | 3.6612 | 3.5765 | 0.0847 | -3.6612 | -3.5765 | 15.7410 | 8.2217 | 7.3224 | 31.2851 |
| $D_{O2}^{0}$ | -23.8474 | 15.9729 | 0.3855 | 7.4889 | -6.3154 | 0.1928 | 6.5081 | 0.4781 | 0.0907 | 0.2398 | 0.1221 | 0.1140 | 0.4758 | 0.0884 | -0.0519 | 3.7964 | 3.7445 | 0.0519 | -3.7964 | -3.7445 | 15.9729 | 8.1351 | 7.5927 | 31.7008 |
| $D_{NO3}^{0}$ | -23.0054 | 15.7559 | 0.3813 | 6.8683 | -7.8027 | 0.1906 | 7.9933 | 0.4949 | 0.0904 | 0.2365 | 0.1500 | 0.1055 | 0.4920 | 0.0875 | -0.0792 | 3.5134 | 3.4341 | 0.0792 | -3.5134 | -3.4341 | 15.7559 | 9.9916 | 7.0267 | 32.7742 |
| $D_{NH4}^{0}$ | -23.2526 | 15.7420 | 0.3569 | 7.1537 | -6.3977 | 0.1784 | 6.5762 | 0.5148 | 0.1271 | 0.2363 | 0.1234 | 0.1099 | 0.4696 | 0.0819 | -0.0847 | 3.6615 | 3.5769 | 0.0847 | -3.6615 | -3.5769 | 15.7420 | 8.2202 | 7.3231 | 31.2852 |
| $D_{SO4}^{0}$ | -24.5765 | 15.6583 | 0.3790 | 8.5393 | -6.4163 | 0.1895 | 6.6058 | 0.4927 | 0.0891 | 0.2350 | 0.1239 | 0.1315 | 0.4905 | 0.0869 | -0.1117 | 4.3814 | 4.2696 | 0.1117 | -4.3814 | -4.2696 | 15.6583 | 8.2572 | 8.7627 | 32.6783 |
| $D_{S}^{0}$ | -23.2161 | 15.7514 | 0.3777 | 7.0870 | -6.3873 | 0.1888 | 6.5762 | 0.4740 | 0.0909 | 0.2364 | 0.1234 | 0.1099 | 0.4697 | 0.0866 | -0.1170 | 3.6605 | 3.5435 | 0.1170 | -3.6605 | -3.5435 | 15.7514 | 8.2202 | 7.3210 | 31.2926 |
| $D_{O2}^{const}$ | -23.5057 | 15.8531 | 0.3795 | 7.2731 | -6.3502 | 0.1898 | 6.5400 | 0.4758 | 0.0908 | 0.2380 | 0.1227 | 0.1114 | 0.4720 | 0.0870 | -0.0729 | 3.7095 | 3.6365 | 0.0729 | -3.7095 | -3.6365 | 15.8531 | 8.1750 | 7.4189 | 31.4470 |
| $D_{NO3}^{const}$ | -23.1704 | 15.7467 | 0.3784 | 7.0453 | -6.9083 | 0.1892 | 7.0974 | 0.4817 | 0.0907 | 0.2364 | 0.1332 | 0.1082 | 0.4778 | 0.0868 | -0.0827 | 3.6053 | 3.5227 | 0.0827 | -3.6053 | -3.5227 | 15.7467 | 8.8718 | 7.2106 | 31.8291 |
| $D_{NH4}^{const}$ | -23.2630 | 15.7414 | 0.3684 | 7.1533 | -6.3927 | 0.1842 | 6.5769 | 0.4887 | 0.1035 | 0.2363 | 0.1234 | 0.1099 | 0.4696 | 0.0845 | -0.0847 | 3.6613 | 3.5766 | 0.0847 | -3.6613 | -3.5766 | 15.7414 | 8.2211 | 7.3227 | 31.2852 |
| $D_{SO4}^{const}$ | -23.7905 | 15.7103 | 0.3776 | 7.7026 | -6.3989 | 0.1888 | 6.5877 | 0.4815 | 0.0902 | 0.2358 | 0.1236 | 0.1185 | 0.4779 | 0.0866 | -0.0954 | 3.9467 | 3.8513 | 0.0954 | -3.9467 | -3.8513 | 15.7103 | 8.2346 | 7.8934 | 31.8384 |
| $D_{S}^{const}$ | -23.2567 | 15.7437 | 0.3769 | 7.1361 | -6.3886 | 0.1885 | 6.5771 | 0.4741 | 0.0909 | 0.2363 | 0.1234 | 0.1099 | 0.4696 | 0.0865 | -0.0930 | 3.6610 | 3.5681 | 0.0930 | -3.6610 | -3.5681 | 15.7437 | 8.2213 | 7.3220 | 31.2870 |
| $K_{nit}$ | -23.4315 | 15.7324 | 0.5528 | 7.1464 | -6.3112 | 0.2764 | 6.5876 | 0.4337 | 0.0909 | 0.2362 | 0.1236 | 0.1098 | 0.4696 | 0.1268 | -0.0852 | 3.6584 | 3.5732 | 0.0852 | -3.6584 | -3.5732 | 15.7324 | 8.2346 | 7.3168 | 31.2837 |
| $K_{sox}$ | -23.3175 | 15.7323 | 0.3759 | 7.2094 | -6.3904 | 0.1879 | 6.5784 | 0.4742 | 0.0909 | 0.2362 | 0.1234 | 0.1099 | 0.4695 | 0.0862 | -0.0571 | 3.6618 | 3.6047 | 0.0571 | -3.6618 | -3.6047 | 15.7323 | 8.2230 | 7.3236 | 31.2788 |
| $k_{sLimO2}$ | -23.2684 | 15.7411 | 0.3741 | 7.1532 | -6.3900 | 0.1871 | 6.5771 | 0.4747 | 0.0909 | 0.2363 | 0.1234 | 0.1099 | 0.4696 | 0.0858 | -0.0847 | 3.6613 | 3.5766 | 0.0847 | -3.6613 | -3.5766 | 15.7411 | 8.2213 | 7.3226 | 31.2851 |
| $k_{sInhNO3}$ | -23.2725 | 15.7409 | 0.3770 | 7.1546 | -6.4726 | 0.1885 | 6.6611 | 0.4756 | 0.0909 | 0.2363 | 0.1250 | 0.1099 | 0.4712 | 0.0865 | -0.0848 | 3.6621 | 3.5773 | 0.0848 | -3.6621 | -3.5773 | 15.7409 | 8.3264 | 7.3241 | 31.3914 |
| $k_{sAnoxInhO2}$ | -23.2725 | 15.7409 | 0.3767 | 7.1549 | -6.3890 | 0.1884 | 6.5774 | 0.4741 | 0.0909 | 0.2363 | 0.1234 | 0.1099 | 0.4696 | 0.0864 | -0.0848 | 3.6622 | 3.5775 | 0.0848 | -3.6622 | -3.5775 | 15.7409 | 8.2217 | 7.3244 | 31.2871 |
| $k_{sAnoxInhNO3}$ | -23.4402 | 15.7313 | 0.3770 | 7.3319 | -6.3921 | 0.1885 | 6.5806 | 0.4767 | 0.0909 | 0.2361 | 0.1235 | 0.1127 | 0.4723 | 0.0865 | -0.0882 | 3.7542 | 3.6660 | 0.0882 | -3.7542 | -3.6660 | 15.7313 | 8.2258 | 7.5083 | 31.4654 |
| $k_{sO2}$ | -23.0591 | 15.5227 | 0.3762 | 7.1601 | -6.3853 | 0.1881 | 6.5735 | 0.4709 | 0.0909 | 0.2330 | 0.1233 | 0.1100 | 0.4663 | 0.0863 | -0.0840 | 3.6641 | 3.5801 | 0.0840 | -3.6641 | -3.5801 | 15.5227 | 8.2168 | 7.3282 | 31.0677 |
| $k_{sNO3}$ | -23.1453 | 15.7481 | 0.3758 | 7.0214 | -6.2148 | 0.1879 | 6.4027 | 0.4691 | 0.0909 | 0.2364 | 0.1201 | 0.1079 | 0.4644 | 0.0862 | -0.0822 | 3.5929 | 3.5107 | 0.0822 | -3.5929 | -3.5107 | 15.7481 | 8.0034 | 7.1858 | 30.9372 |
| $k_{sSO4}$ | -22.6804 | 15.7735 | 0.3756 | 6.5313 | -6.3790 | 0.1878 | 6.5668 | 0.4649 | 0.0909 | 0.2368 | 0.1232 | 0.1002 | 0.4602 | 0.0862 | -0.0727 | 3.3383 | 3.2657 | 0.0727 | -3.3383 | -3.2657 | 15.7735 | 8.2085 | 6.6767 | 30.6586 |
| $k_{sSox}$ | -23.2780 | 15.7500 | 0.3779 | 7.1502 | -6.3884 | 0.1889 | 6.5773 | 0.4739 | 0.0909 | 0.2364 | 0.1234 | 0.1099 | 0.4697 | 0.0867 | -0.0853 | 3.6604 | 3.5751 | 0.0853 | -3.6604 | -3.5751 | 15.7500 | 8.2216 | 7.3208 | 31.2924 |
| $\phi$ | -15.2534 | 8.0146 | 0.4810 | 6.7578 | -6.2274 | 0.2405 | 6.4679 | 0.3870 | 0.1539 | 0.1203 | 0.1214 | 0.1018 | 0.3435 | 0.1103 | -0.0118 | 3.3907 | 3.3789 | 0.0118 | -3.3907 | -3.3789 | 8.0146 | 8.0849 | 6.7814 | 22.8809 |

**References**


Aller, R. C. (1980). Quantifying solute distributions in the bioturbated zone of marine sediments by defining an average microenvironment. *Geochimica et Cosmochimica Acta* **44:** 1955-1965

Aller, R. C. (1982) The effects of macrobenthos on chemical properties of marine sediment and overlying water. In: McCall PL, Tevesz MJS (eds) Animal-Sediment Relations. The biogenic alteration of sediments. Plenum Press, New York, vol. 2, pp. 53-102.

Aller, R. C. (1983). The importance of the diffusive permeability of animal burrow linings in determining marine sediment chemistry. *Journal of Marine Research* **41:** 299-322

Aller, R. C. (1984). The importance of relict burrow structures and burrow irrigation in controlling sedimentary solute distributions. *Geochimica et Cosmochimica Acta* **48:** 1929-1934

Aller, R. C. and Mackin, J. E. (1984). Preservation of reactive organic matter in marine sediments. *Earth and Planetary Science Letters* **70:** 260-266

Aller, R. C. (1990). Bioturbation and manganese cycling in hemipelagic sediments. *Philosophical Transactions of the Royal Society London* **331:** 51-68

Aller, R. C. (1994). The sedimentary Mn cycle in long-island sound - its role as intermediate oxidant and the influence of bioturbation, O2, and c(org) flux on diagenetic reaction balances. *Journal of Marine Research* **52:** 259-295

Aller, R. C. and Aller, J. Y. (1998). The effect of biogenic irrigation intensity and solute exchange on diagenetic reaction rates in marine sediments. *Journal of Marine Research* **56:** 905-936

An, S. and Joye, S. B. (2001). Enhancement of coupled nitrification-denitrification by benthic photosynthesis in shallow estuarine sediments. *Limnology and Oceanography* **46:** 62-74

Andersen, J. M. (1977). Rates of denitrification of undisturbed sediment from six lakes as a function of nitrate concentration, oxygen and temperature. *Arch Hydrobiol* **80:** 147-159

Andersen, F. O. (1996). Fate of organic carbon added asa diatom cells to oxic and anoxic marine sediment microcosms. *Marine Ecology Progress Series* **134:** 225-233

Anon (2001) Nutrient input to the Sea and the Impact on the Marine Ecosystem. Unpublished report. CEFAS, DARDNI, UEA,UEssex, SOC. 179p + i - v.

Antoniou, P., Hamilton, J., Koopman, B., Jain, R., Holloway, B., Lyberatos, G. and Svoronos, S. A. (1990). Effect of temperature and pH on the effective maximum specific growth-rate of nitrifying bacteria. *Water Research* **24:** 97-101

Archer, D., Emerson, S. and Smith, C. R. (1989). Direct measurement of the diffusive sublayer at the deep sea floor using oxygen microelectrodes. *Nature* **340:** 623-626

Asmus, R. M., Sprung, M. and Asmus, H. (2000). Nutrient fluxes in intertidal communities of a South European lagoon (Ria Formosa) - similarities and differences with a northern Wadden Sea bay (Sylt-Romo Bay). *Hydrobiologia* **436:** 217-235

Balls, P. (1994). Nutrient inputs to estuaries from nine Scotiish east coast rivers; influence of estuarine processes on inputs to the North Sea. *Estuarine and Coastal Marine Science* **39:** 329-352

Banta, G. T., Giblin, A. E., Hobbie, J. E. and Tucker, J. (1995). Benthic respiration and nitrogen release in Buzzards Bay, Massachusetts. *Journal of Marine Research* **53:** 107-135

Bates, R. and Jackson, J. (1987). Glossary of Geology. American Geological Institute, Falls Church, pp. 788

Bender, M. L. and Heggie, D. T. (1984). Fate of organic carbon reaching the sea floor : a status report. *Geochimica et Cosmochimica* **48:** 977-986

Benner, R., MacCubbin, A. E. and Hodson, R. E. (1984). Anaerobic degradation of the lignin and polysaccharide components of lignocellulose and synthetic lignin by sediment microflora. *Applied and Environmental Microbiology* **47:** 998-1004

Berner, R. A. (1964). An idealised model of dissolved sulfate distribution in recent sediments. *Geochimica et Cosmochimica Acta* **28:** 1497-1503

Berner, R. A. (1974) Kinetic models for the early diagenesis of nitrogen, sulfur, phosphorus and silicon in anoxic marine sediments. In: Goldberg E (ed) The Sea. Wiley, New York, vol. 5, pp. 427-450.

Berner, R. A. (1976). Inclusion of adsorption in the modelling of early diagenesis. *Earth and Planetary Science Letters* **29:** 333-340

Berner, R. A. (1978). Sulfate reduction and the rate of deposition of marine sediments. *Earth and Planetary Science Letters* **37:** 492-498

Berner, R. A. (1980). Early diagenesis-A theoretical approach. Princeton University Press, Princeton, NJ, p. 241

Berner, E. K. and Berner, R. A. (1987). The global water cycle: geochemistry and environment. Prentice-Hall, New Jersey, pp397

Berounsky, V. and Nixon, S. (1990). Temperature and the annual cycle of nitrification in waters of Narragansett Bay. *Limnology and Oceanography* **35:** 1610-1617

Bianchi, M., Feliatra and Lefevre, D. (1999). Regulation of nitrification in the land-ocean contact area of the Rhone River plume (NW Mediterranean). *Aquatic Microbial Ecology* **18:** 301-312

Billen, G. (1982) Modelling the processes of organic matter degradation and nutrients recycling in sedimentary systems. In: Nedwell DB, Brown CM (eds) Sediment Microbiology. Academic Press, pp. 15-52

Billen, G., Somville, M., de Becker, E. and Servais, P. (1985). A nitrogen budget of the Scheldt hydrographical basin. *Netherlands Journal of Sea Research* **19:** 223-230

Billen, G. (1990) N-budget of the major rivers discharging into the continental coastal zone of the North Sea: the nitrogen paradox. In: Lancelot C, Billen G, Barth H (eds) Eutrophication and algal blooms in North Sea coastal zones, the Baltic and adjacent areas: prediction and assessment of preventive actions. Brussels, pp. 153-171.

Blackburn, T. H. (1979). Method for measuring rates of $NH_4^+$ turnover in anoxic marine sediments using a $^{15}N$-$NH_4^+$ dilution technique. *Applied and Environmental Microbiology* **37:** 760-765

Blackburn, T. H. and Henriksen, K. (1983). Nitrogen cycling in different types of sediment from Danish waters. *Limnology and Oceanography* **28:** 477-493

Blackburn, T. H. (1988) Benthic mineralisation and bacterial production. In: Blackburn TH, Sorensen J (eds) Nitrogen cycling in coastal marine environments. J Wiley & Sons, Chichester, pp. 175-186.

Blackburn, T. H., Blackburn, N. D., Jensen, K. and Risgaardpetersen, N. (1994). Simulation-model of the coupling between nitrification and denitrification in a freshwater sediment. *Applied and Environmental Microbiology* **60:** 3089-3095

Bonin, P., Omnes, P. and Chalamet, A. (1998). Simultaneous occurrence of denitrification and nitrate ammonification in sediments of the French Mediterranean Coast. *Hydrobiologia* **389:** 169-182

Boudreau, B. P. and Guinasso, N. L. (1982) The influence of a diffusive sublayer on accretion, dissolution and diagenesis at the sea floor. In: Fanning KA, Manheim FT (eds) The dynamic environment of the ocean floor. Lexington, pp. 115-145.

Boudreau, B. P. and Westrich, J. T. (1984). The dependence of bacterial sulfate reduction on sulfate concentration in marine sediments. *Geochimica et Cosmochimica Acta* **48:** 2503-2516

Boudreau, B. P. (1986). Mathematics of tracer mixing in sediments: I. Spatially dependent diffusive mixing. *American Journal of Science* **286:** 161-198

Boudreau, B. P. and Taylor, R. J. (1989). A theoretical study of diagenetic concentration fields near manganese nodules at the sediment water interface. *Journal of Geophysical Research* **94:** 2124-2136

Boudreau, B. P. and Ruddick, B. R. (1991). On a reactive continuum representation of organic matter diagenesis. *American Journal of Science* **29:** 507-538

Boudreau, B. P. (1996). A method of lines code for carbon and nutrient diagenesis in aquatic sediments. *Computers and Geosciences* **22:** 479-496

Boudreau, B. P. (1997). Diagenetic models and their implementation. Springer-Verlag, p414

Boudreau, B. P., Mucci, A., Sundby, B., Luther, G. W. and Silverberg, N. (1998). Comparative diagenesis at three sites on the Canadian continental margin. *Journal of Marine Research* **56:** 1259-1284

Bouwman, A. F., Vanderhoek, K. W. and Olivier, J. G. J. (1995). Uncertainties in the global source distribution of nitrous-oxide. *Journal of Geophysical Research-Atmospheres* **100:** 2785-2800

Boynton, W., Kemp, W. and Osborne, C. (1982) Nutrient fluxes across the sediment-water interface in the turbid zone of a coastal plain estuary. In: Kennedy V (eds) Estuarine perspectives. Academic Press, pp. 93-109.

Bralower, T. J. and Thierstein, H. R. (1987) Organic carbon and metal accumulation rates in Holocene and mid-Cretaceous sediments: palaeoceanographic significance. In: Brooks J, Fleet AJ (eds) Marine petroleum source rocks. Blackwell Scientific Publications, Oxford, pp. 345-369.

Cadee, G. (1986). Increased phytoplankton primary production in the Marsdiep area (western Dutch Wadden Sea). *Netherlands Journal of Sea Research* **20:** 285-290

Cadee, G. and Hegeman, J. (1991). Phytoplankton primary production, chlorophyll and species composition, organic carbon and turbidity in the Marsdiep in 1990, compared with foregoing years. *Hydrobiol Bull* **25:** 29-35

Canfield, D. (1989). Sulfate reduction and oxygen respiration in marine sediments: Implications for organic carbon preservation in euxinic environments. *Deep Sea Research* **36:** 121-138

Canfield, D. (1992) Organic matter oxidation in marine sediments. In: Wollast R, Mackenzie FT, Chou L (eds) Interactions of C, N, P and S biogeochemical cycles and global change. Springer-Verlag, Berlin, pp. 333-364

Canfield, D. E., Jorgensen, B. B., Fossing, H., Glud, R., Gundersen, J., Ramsing, N. B., Thamdrup, B., Hansen, J. W., Nielsen, L. P. and Hall, P. O. J. (1993). Pathways of organic-carbon oxidation in 3 Continental-margin sediments. *Marine Geology* **113:** 27-40

Carlucci, A. and Strickland, J. (1968). The isolation, purification and some kinetic studies of marine nitrifying bacteria. *Journal of Experimental Marine Biology and Ecology* **2:** 156-166

Carlucci, A. F., Shimp, S. L. and Craven, D. B. (1987). Bacterial response to labile dissolved organic matter increases associated with marine discontinuities. *FEMS Micobiology Ecology* **45:** 211-220

Christensen, P. and Sorensen, J. (1986). Temporal variation of denitrification activity in plant covered, littoral sediment from lake Hampen, Denmark. *Applied and Environmental Microbiology* **51:** 1174-1179

Christensen, J., Murray, J., Devol, A. and Codispoti, L. (1987). Denitrification in continental shelf sediments has major impact on the oceanic nitrogen budget. *Global Biogeochemical Cycles* **1:** 97-116

Clavero, V., Izquierdo, J. J., Fernandez, J. A. and Niell, F. X. (2000). Seasonal fluxes of phosphate and ammonium across the sediment- water interface in a shallow small estuary (Palmones River, southern Spain). *Marine Ecology-Progress Series* **198:** 51-60

Cole, J. A. and Brown, C. M. (1980). nitrite reduction to ammonia by fermentative bacteria: a short circuit in the biological nitrogen cycle. *FEMS Microbiology Letters* **7:** 65-72

Cole, J. A. (1990) Physiology, biochemistry and genetics of nitrate dissimilation to ammonia. In: Revsbech NP, Sørensen J (eds) Denitrification in soil and sediment. Plenum Press, New York, pp. 57-76.

Cooper, S. (1995). Chesapeake Bay watershed historical land use: Impact on water quality and diatom communities. *Ecol Appl* **5:** 703-723

Cowan, J., Pennock, R. and Boynton, W. (1996). Seasonal and interannual patterns of sediment-water nutrient and oxygen fluxes in Mobile Bay, Alabama (USA): regulating factors and ecological significance. *Marine Ecology Progress Series* **141:** 229-245

Cragg, B., Parkes, R., Fry, J., Herbert, R., Wimpenny, J. and Gotliff, J., Bacterial biomass and activity profiles within deep sediment layers, Suess Eea, Ed., Proceedings of the ODP, Scientific results, College Station , Texas, USA (1990).

Cranston, R. E. and Buckley, D. E. (1990). Redox reactions and carbonate preservation in deep sea sediments. *Marine Geology* **94:** 1-8

Dade, W. B., Hogg, A. J. and Boudreau, B. P. (2001) Physics of flow above the sediment-water interface. In: Boudreau BP, Jorgensen BB (eds) The benthic boundary layer. Transport processes and biogeochemistry. Oxford University Press, New York, p. 4-43

de Haas, H. (1997). Transport, preservation and accumulation of organic carbon in the North Sea. Ph.D., University of Utrecht, Utrech, The Netherlands.

de Haas, H., van Weering, T. C. E. and de Stieger, H. (2002). Organic carbon in shelf seas: sinks or sources, processes and products. *Continental Shelf Research* **22:** 691-717

Delwiche, C. C. (1981). Denitrification, nitrification, and atmospheric nitrous oxide. John Wiley & Sons, New York

Dhakar, S. P. and Burdige, D. J. (1996). A coupled non-linear steady state model for early diagenetic processs in pelagic sediments. *American Journal of Science* **296:** 296-330

Dong, L., Thornton, D., Nedwell, D. and Underwood, G. (2000). Denitrification in sediments of the river Colne estuary, England. *Marine Ecology Progress Series* **203:** 109-122

Dore, J., Popp, B., Karl, D. and Sansone, F. (1998). A large source of atmospheric nitrous oxide from subtropical North Pacific surface waters. *Nature* **396:** 63-66

Duff, J., Triska, F. and Oremland, R. (1984). Denitrification associated with stream periphyton: Chamber estimates from undisrupted communities. *Journal of Environmental Quality* **13:** 514-518

Ehrlich, H. L. (1996). Geomicrobiology, Third Edition, Revised and Expanded. Marcel Dekker, Inc., New York

Emerson, S., Fischer, K., Reimers, C. and Heggies, D. (1985). Organic carbon dynamics and preservation in deep sea sediments. *Deep Sea Research* **32:** 1-21

Emerson, S. and Hedges, J. (1988). Processes controlling the organic carbon content of open ocean sediments. *Paleoceanography* **3:** 621-634

Engel, M. and Alexander, M. (1958). Growth and autotrophic metabolism of *Nitrosomonas Europaea. Journal of Bacteriology* **76:** 217-222

Enoksson, V. and Samuelsson, M. (1987). Nitrification and dissimilatory ammonium production and their effects on the nitrogen flux over the sediment water interface in bioturbated coastal sediments. *Marine Ecology Progress Series* **36**

Fasham, M. J. R., Ducklow, H. W. and McKelvie, S. M. (1990). A nitrogen-based model of plankton dynamics in the oceanic mixed layer. *Journal of Marine Research* **48:** 591-639

Fenchel, T. and Blackburn, T. (1979). Bacteria and mineral cycling. Academic Press, London

Fenchel, T. and Finlay, B. (1995). Ecology and evolution in anoxic worlds. University Press, Oxford

Fenchel , T. and Jorgensen, B. B. (1977). Detritus food chains of aquatic ecosystems; the role of bacteria. *Advances in Microbial Ecology* **1:** 1-58

Fisher, T., Carlson, P. and Barber, R. (1982). Sediment nutrient regeneration in three North Carolina estuaries. *Etuarine and Coastal Shelf Science* **14:** 101-116

Focht, D. and Verstraete, W. (1977). Biochemical ecology of nitrification and denitrification. *Advances in Microbiological Ecology* **I:** 135-214

Forja, J. M., Blasco, J. and Gomezparra, A. (1994). Spatial and seasonal-variation of in-situ benthic fluxes in the Bay of Cadiz (South-West Spain). *Estuarine Coastal and Shelf Science* **39:** 127-141

Froelich, P., Klinkhammer, G., Bender, M., Luedtke, N., Heath, G., Cullen, D., Dauphin, P., Hammond, D., Hartman, B. and Maynard, V. (1979). Early oxidation of organic matter in pelagic sediments of the eastern equatorial Atlantic: suboxic diagenesis. *Geochimica et Cosmochimica Acta* **43:** 1075-1090

Furrer, G. and Wehrli, B. (1996). Microbial reactions, chemical speciation and multicomponent diffusion in porewaters of a eutrophic lake. *Geochimica et Cosmochimica Acta* **60:** 2333-2346

Galloway, J., Schlesinger, W., Levy, H., Michaels, A. and Schnoor, J. (1995). Nitrogen fixation: anthropogenic enhancement-environmental response. *Global Biogeochemical Cycles* **9:** 235-252

Garcia-Ruiz, R., Pattinson, S. N. and Whitton, B. A. (1998). Kinetic parameters of denitrification in a river continuum. *Applied and Environmental Microbiology* **64:** 2533-2538

Gilbert, F., Souchu, P., Bianchi, M. and Bonin, P. (1998). Influence of shell fish farming activities on nitrification, nitrate reduction to amminum and denitrification at the sediment-water interface of the Thau lagoon, France. *Marine Ecology Progress Series* **151:** 143-153

Glud, R. N., Gundersen, J. K., Revsbech, N. P. and Jorgensen, B. B. (1994). Effects on the benthic diffusive boundary-layer imposed by microelectrodes. *Limnology and Oceanography* **39:** 462-467

Glud, R. N., Gundersen, J. K., Revsbech, N. P., Jorgensen, B. B. and Huttel, M. (1995). Calibration and performance of the stirred flux chamber from the benthic lander Elinor. *Deep-Sea Research Part I-Oceanographic Research Papers* **42:** 1029-1042

Glud, R. N., Forster, S. and Huettel, M. (1996). Influence of radial pressure gradients on solute exchange in stirred benthic chambers. *Marine Ecology-Progress Series* **141:** 303-311

Godschalk, G. and Wetzel, R. (1978). Decomposition of aquatic angiosperms, III. Zostera marina L. and a conceptual model of decomposition. *Aquatic Botany* **5:** 329-354

Goeyens, L., Devries, R., Bakker, J. and Helder, W. (1987). An experiment on the relative importance of denitrification, nitrate reduction and ammonification in coastal marine sediment. *Netherlands Journal of Sea Research* **21:** 171- 175

Goloway, F. and Bender, M. (1982). Diagenetic models of interstitial nitrate profiles in deep sea suboxic sediments. *Limnology and Oceanography* **27:** 624-638

Goreau, T., Kaplan, W., Wofsy, S., McElroy, M., Valois, F. and Watson, S. (1980). Production of $NO_2^-$ and $NO_3^-$ by nitrifying bacteria at reduced concentrations of oxygen. *Applied and Environmental Microbiology* **40:** 526-532

Gould, D. J., Dyer, M. F. and Tester, D. J. (1987). Environmental quality and ecology of the Great Ouse estuary. *Water Pollution Control* **86:** 84-103

Graneli, E., Wallstrom, K., Larsson, W., Graneli, W. and Elmgren, R. (1990). Nutrient limitation of primary production in the Baltic Sea area. *Ambio* **19:** 142-151

Greenberg, E. and Becker, G. (1977). Nitrous oxide as end product of denitrification by a strain of fluorescent pseudomonad. *Canadian Journal of Microbiology* **23:** 903-907

Grenz, C., Cloern, J. E., Hager, S. W. and Cole, B. E. (2000). Dynamics of nutrient cycling and related benthic nutrient and oxygen fluxes during a spring phytoplankton bloom in South San Francisco Bay (USA). *Marine Ecology-Progress Series* **197:** 67-80

Grundmanis, V. and Murray, J. (1982). Aerobic respiration in pelagic marine sediments. *Gepchimica et Cosmochimica Acta* **46:** 1101-1120

Gujer, W. and Zehnder, A. (1983). Conversion processes in anaerobic digestion. *Water Science and Technology* **15:** 127-167

Hansen, H. H., Ingvorsen, K. and Jorgensen, J. J. (1978). Mechanisms of hydrogen sulfide release from coastal marine sediments to the atmosphere. *Limnology and Oceanography* **23:** 68-76

Hansen, J. (1980). Potential nitrification in marine sediments. MSc, University of Aarhus, Aarhus, Denmark.

Harding, L. J. (1994). Long term trends in the distribution of phytoplankton in Chesapeake Bay: Roles of light, nutrients and streamflow. *Marine Ecology Progress Series* **104:** 267-291

Hargrave, B. (1969). Similarity of oxygen uptake by benthic communities. *Limnology and Oceanography* **14:** 801-805

Harvey, H. R., Tuttle, J. H. and Bell, J. T. (1995). Kinetics of phytoplankton decay during simulated sedimentation: Changes in biochemical composition and microbial activity under oxic and anoxic conditions. *Geochimica et Cosmochimica Acta* **59:** 3367-3377

Hasan, S. and Hall, J. (1975). The physiological function of nitrate reduction in Clostridium perfringens. *Journal of General Microbiology* **87:** 120-128

Hashimoto, L., Kaplan, W., Wofsy, S. and McElroy, M. (1983). Transformations and fixed nitrogen and $N_2O$ in the Carioco Trench. *Deep Sea Research* **30:** 575-590

Hedges, J. I. and Keil, R. G. (1995). Sedimentary organic-matter preservation - an assessment and speculative synthesis. *Marine Chemistry* **49:** 81-115

Heip, C. H. R., Goosen, N. K., Herman, P. M. J., Kromkamp, J., Middelburg, J. J. and Soetaert, K. (1995). Production and consumption of biological particles in temperate tidal estuaries. *Oceanography and Marine Biology* **33:** 1-149

Helder, W. and de Vries, R. (1983). Estuarine nitrite maxima and nitrifying bacteria (Ems-Dollard Estuary). *Netherlands Journal of Sea Research* **17:** 1-18

Henrichs, S. M. and Reeburgh, W. S. (1987). Anaerobic mineralisation of marine sediment organic matter: Rates and role of anaerobic processes in the oceanic carbon economy. *Journal of Geomicrobiology* **5:** 191-237

Henriksen, K., Hansen, J. and Blackburn, T. (1980). The influence of benthic infauna on exchange rates of inorganic nitrogen between sediment and water. *Ophelia* **:** 249-256

Henriksen, K., Rasmussen, M. and Jensen, A. (1983). Effect of bioturbation on microbial nitrogen transformations in the sediment and fluxes of ammonium and nitrate to the overlying water. *Ecological Bulletin* **35:** 193-205

Henriksen, K. and Kemp, M. (1988) Nitirification in estuarine and coastal marine sediments. In: Blackburn T, Sorensen J (eds) Nitrogen cycling in coastal and marine environments. J Wiley & Sons, Chichester, pp. 207-249.

Herbert, R. A. (1982) Nirate dissimilation in marine and estuarine sediments. In: Nedwell D, Brown C (eds) Sediment Microbiology. Academic Press, London, pp. 53-71.

Herbert, R. A. and Nedwell, D. B. (1990) Role of environmental factors in regulating nitrate respiration in intertidal sediments. In: Revsbech NP, Sorensen J (eds) Denitrification in soil and sediment. Plenum Press, New York, pp. 77-90.

Hill, A. (1983) Nitrate-nitrogen mass balances for two Ontario rivers. In: Fontaine T, Bartell S (eds) Dynamics of lotic ecosystems. Ann Arbor Sci, pp. 457-477.

Hopkinson, C. S., Giblin, A. E., Tucker, J. and Garritt, R. H. (1999). Benthic metabolism and nutrient cycling along an estuarine salinity gradient. *Estuaries* **22:** 863-881

Hopkinson, C. S., Giblin, A. E. and Tucker, J. (2001). Benthic metabolism and nutrient regeneration on the continental shelf of Eastern Massachusetts, USA. *Marine Ecology-Progress Series* **224:** 1-19

Horrigan, S. (1981). Primary production under the Ross Ice Shelf, Antarctica. *Limnology and Oceangraphy* **26:** 378-382

Howarth, R. W., Billen, D., Swaney, D., Townsend, A., Jaworski, N., Lajtha, K., Downing, J. A., Elmgreen, R., Caraco, N., Jordan, T., Berendse, F., Freney, J., Kudeyarov, V., Murdoch, P. and Zhao-Liang, Z. (1996). Regional nitrogen budgets and riverine N & P fluxes for the drainages to the North Atlantic Ocean: Natural and human influences. *Biogeochemistry* **35:** 75-139

Huettel, M. and Gust, G. (1992). Solute release mechanisms from confined sediment cores in stirred benthic chambers and flume flows. *Marine Ecology-Progress Series* **82:** 187-197

Hulth, S., Aller, R. C. and Gilbert, F. (1999). Coupled anoxic nitrification manganese reduction in marine sediments. *Geochimica et Cosmochimica Acta* **63:** 49-66

Hydes, D. and Edmunds, H. (1992). Nutrients in the North Sea, September 1988 to October 1989: use of nutrient ratios and nutrient salinity relationships to identify sources and sinks of nutrients. *Science of the Total Environment* **Supplement 1992:** 1149-1157

Hydes, D., Kelly-Gerreyn, B., Le Gall, A. and Proctor, R. (1999). The balance of supply of nutrients and demands of biological production and denitrification in a temperate latitude shelf sea-a treatment of the southern North Sea as an extended estuary. *Marine Chemistry* **68:** 117-131

Iversen, N. and Jorgensen, B. B. (1993). Diffusion coefficients of sulfate and methane in marine sediments: Influence of porosity. *Geochimica et Cosmochimica Acta* **57:** 571-578

Jahnke, R. A., Emerson, S. R. and Murray, J. W. (1982). A model of oxygen reduction, denitrification and organic matter mineralisation in marine sediments. *Limnology and Oceanography* **27:** 610-623

Jahnke, R. A., Emerson, S. R., Cochran, J. and Hirschberg, D. (1986). Fine scale distributions of porosity and particulate excess $^{210}Pb$, organic carbon and $CaCO_3$ in surface sediments of the deep equatorial Pacific. *Earth and Planetary Science Letters* **77:** 59-69

Jahnke, R. A., Emerson, S. R., Reimers, C. E., Schuffert, J., Ruttenberg, K. and Archer, D. (1989). Benthic recycling of biogenic debris in the Eastern Tropical Atlantic-Ocean. *Geochimica et Cosmochimica Acta* **53:** 2947-2960

Jenkins, M. and Kemp, W. (1984). The coupling of nitrification and denitrification in two estuarine sediments. *Limnology and Oceanography* **29:** 609-619

Jensen, M. H., Andersen, T. K. and Sorensen, J. (1988). Denitrification in coastal bay sediment: regional and seasonal variation in Aarhus Bight, Denmark. *Marine Ecology Progress Series* **48:** 155-162

Jensen, M., Lomstein, E. and Sorensen, J. (1990). Benthic $NH_4^+$ and $NO_3^-$ flux following sedimentation of a spring phytoplankton bloom in Aarhus Bight, Denmark. *Marine Ecology Progress Series* **61:** 87-96

Jetten, M. S. M., Strous, M., van de Pas-Schoonen, K. T., Schalk, J., van Dongen, U., van de Graaf, A. A., Logemann, S., Muyzer, G., van Loosdrecht, M. C. M. and Kuenen, J. G. (1998). The anaerobic oxidation of ammonium. *FEMS Microbiology Reviews* **22:** 421-437

Jorgensen, B. B. (1982). Mineralisation of organic matter in the sea bed. *Nature* **296:** 643-645

Jorgensen, K. S., Jensen, H. B. and Sorensen, J. (1984). Nitrous oxide production from nitrification and denitrification in marine sediment at low oxygen concentrations. *Canadian Journal of Microbiology* **30:** 1073-1078

Jorgensen, B. B. and Revsbeck, N. P. (1985). Diffusive boundary layers and the oxygen uptake of sediments and detritus. *Limnology and Oceanography* **30:** 111-122

Jorgensen, B. B. and Sorensen, J. (1985). Seasonal cycles of $O_2$, $NO_3^-$ and $SO_4^=$ reduction in estuarine sediments; the significance of an $NO_3^-$ reduction maximum in spring. *Marine Ecology Progress Series* **24:** 65-74

Jorgensen, K. S. and Sorensen, J. (1988). Two annual maxima of nitrate reduction and denitrification in estuarine sediment (Norsminde Fjord, Denmark). *Marine Ecology Progress Series* **48:** 147-154

Jorgensen, K. S. (1989). Annual pattern of denitrification and nitrate ammonification in estuarine sediment vacate. *Applied and Environmental Microbiology* **55:** 1841-1847

Jorgensen, B. B. and Marais, D. J. D. (1990). The diffusive boundary-layer of sediments - oxygen microgradients over a microbial mat. *Limnology and Oceanography* **35:** 1343-1355

Jorgensen, B. B. and Boudreau, B. P. (2001) Diagenesis and sediment-water exchange. In: Boudreau BP, Jorgensen BB (eds) The benthic boundary layer. Transport processes and biogeochemistry. Oxford University Press, New York, p. 211-244.

Kaplan, W., Teal, J. and Valiela, I. (1977). Denitrification in salt marsh sediments: evidence for seasonal selection among populations of denitrifiers. *Microbial Ecology* **3:** 193-204

Kaplan, W. (1983) Nitrification. In: Carpenter J, Capone D (eds) Nitrogen in the marine environment. Academic Press, New York, pp. 139-190.

Kaspar, H. (1983). Denitrification, nitrate reduction to ammonium, and inorganic nitrogen pools in intertidal sediments. *Marine Biology* **74**

Kaspar, H., Asher, R. and Boyer, I. (1985). Microbial nitrogen transformations in sediments and inorganic nitrogen fluxes across the sediment / water interface on the south island west coast, New Zealand. *Estuarine and Coastal Shelf Science* **21:** 245-255.

Kelly, J. and Nixon, S. (1984). Experimental studies of the effect of organic deposition on the metabolism of a coastal marine bottom community. *Marine Ecology Progress Series* **17:** 157-169

Kemp, W. M., Sampou, P., Caffrey, J., Mayer, M., Henriksen, K. and Boynton, W. R. (1990). Ammonium recycling versus denitrification in Chesapeake Bay sediments. *Limnology and Oceanography* **35:** 1545-1563

Kieskamp, W. M., Lohse, L., Epping, E. and Helder, W. (1991). Seasonal variation in denitrification rates and nitrous oxide fluxes in intertidal sediments of the western Wadden Sea. *Marine Ecology Progress Series* **72:** 145-151

Killham, K. (1986) Heterotrophic nitrification. In: Prosser JI (eds) Nitrification. IRL Press, pp. 117-126.

Kim, D.-H., Matsuda, O. and Yamamoto, T. (1997). Nitrification, denitrification and nitrate reduction rates in the sediment of Hiroshima Bay, Japan. *Journal of Oceanography* **53:** 317-324

King, D. and Nedwell, D. B. (1987). The adaptation of nitrate-reducing bacterial communities in estuarine sediments in response to overlying nitrate load. *FEMS Microbiology Ecology* **45:** 15-20

King , D. and Nedwell, D. (1984). Changes in nitrate-reducing community of an anaerobic saltmarsh sediment in response to seasonal selection by temperature. *Journal of General Microbiology* **130:** 2935-2941

Klump, J. and Martens, C. (1983) Benthic nitrogen regeneration. In: Carpenter E, Capone D (eds) Nitrogen in the marine environment. Academic Press, New York, pp. 411-457.

Knowles, G., Downing, A. and Barret, M. (1965). Determination of kinetic constants for nitrifying bacteria in mixed culture, with the aid of an electronic computer. *Journal of General Microbiology* **38:** 263-278

Knowles (1990) Acetylene inhibition technique: development, advantages and potential problems. In: Revsbech N, Sorensen J (eds) Denitrification in soil and sediment. Plenum Press, New York, pp. 151-166.

Koch, M., Maltby, E., Oliver, G. and Bakker, S. (1992). Factors controlling denitrification rates of tidal mudflats and fringing salt marshes in south west England. *Estuarine and Coastal Shelf Science* **34:** 471-485

Koike, I. and Hattori, A. (1978). Denitrification and ammonia formation in anaerobic coastal sediments. *Applied and Environmental Micorbiology* **35:** 278-282

Koike, I. and Sorensen, J. (1988) Nitrate reduction and denitrification in marine sediments. In: Blackburn T, Sorensen J (eds) Nitrogen cycling in coastal and marine environments. J Wiley & Sons, Chichester, pp. 251-274

Koike, I. and Terauchi, K. (1996). Fine scale distribution of nitrous oxide in marine sediments. *Marine Chemistry* **52:** 185-193

Kristensen, E. (1988) Benthic fauna and biogeochemical processes in marine sediments: microbial activities and fluxes. In: Blackburn T, Sorensen J (eds) Nitrogen cycling in coastal and marine environments. J Wiley & Sons, Chichester, pp. 275-300

Kristensen, E., Jensen, M. H. and Jensen, K. M. (1997). Temporal variations in microbenthic metabolism and inorganic nitrogen fluxes in sandy and muddy sediments of a tidally dominated bay in the northern Wadden Sea. *Helgolander Meeresuntersuchungen* **51:** 295-320

Kuivila, K., Murray, J., Devol, A., Lidstroml, M. and Reimers, C. (1988). Methane cycling in the sediments of lake Washington. *Limnology and Oceanography* **33:** 571-581

Law, C., Rees, A. and Owens, N. (1991). Temporal variability of denitrification in estuarine sediments. *Estuarine, coastal and shelf science* **33:** 37-56

Lee, C. (1992). Controls on organic carbon preservation: The use of stratified water bodies to compare intrinsic rates of decomposition in oxic and anoxic systems. *Geochimica et Cosmochimica Acta* **56:** 3323-3335

Li, Y.-H. and Gregory, S. (1974). Diffusion of ions in sea water and in deep sea sediments. *Geochimica et Cosmochimica Acta* **38:** 703-714

Lin, S. and Morse, J. (1991). Sulfate reduction and iron sulfide mineral formation in Gulf of Mexico anoxic sediments. *American Journal of Science* **291:** 55-59

Lohse, L., Epping, E., Helder, W. and van Raaphorst, W. (1996). Oxygen porewater profiles in continental shelf sediments of the North Sea: turbulent versus molecular diffusion. *Marine Ecology Progress Series* **145:** 63-75

Luther III, G., Sundby, B., Lewis, B., Brendel, P. and Silverberg, N. (1997). Interactions of manganese with the nitrogen cycle: Alternative pathways to dinitrogen. *Geochimica et Cosmochimica Acta* **61:** 4043-4052

MacFarlane, G. and Herbert, R. (1982). Nitrate dissimilation by Vibrio spp. isolated from estuarine sediments. *Journal of General Microbiology* **128:** 2463-2468

Macfarlane, G. T. and Herbert, R. A. (1985). The use of compound continuous diffusion flow chemostats to study the interaction between nitrifying and nitrate reducting bacteria. *FEMS Microbiology Ecology* **1:** 249-254

Mackin, J. E. and Swider, K. T. (1989). Organic matter decomposition pathways and oxygen consumption in coastal marine sediments. *Journal of Marine Research* **47:** 681-716

Magalhaes, C. M., Bordalo, A. A. and Wiebe, W. J. (2002). Temporal and spatial patterns of intertidal sediment-water nutrient and oxygen fluxes in the Douro River estuary, Portugal. *Marine Ecology-Progress Series* **233:** 55-71

Mancinelli, R., Cronin, S. and Hochstein, L. (1986). The purification and properties of a cd-cytochrome nitrite reductase from Paracoccus denitrificans. *Arch Microbiol* **145:** 202-208

Marnette, E. C. L., Hordijk, C. A., van Breemen, N. and Cappenberg, T. E. (1992). Sulphate reduction and S-oxidation in a moorland pool sediment. *Biogeochemistry* **17:** 123-143

Martin, W. R. and Sayles, F. L. (1994) Seafloor Diagenetic Fluxes. Material Fluxes on the Surface of the Earth. National Academy Press, Washington DC, pp. 143-163.

Marxsen, J. and Witzel, K.-P. (1991) Significance of extracellular enzymes for organic matter degradation and nutrient regeneration in small streams. In: Chrost RJ (eds) Microbial enzymes in aquatic environments. Springer-Verlag, New York, pp. 270-285.

McNichol, A., Lee, C. and Druffel, E. (1988). Carbon cycling in coastal sediments: 1,. A quantitative estimate of the remineralisation of organic carbon in the sediments of Buzzards Bay, Mass. *Geochimica et Cosmochimica Acta* **52:** 1531-1543

Metcalf and Eddy (1979). Wastewater engineering: treatment, disposal, reuse. McGraw-Hill, New York

Meybeck, M. (1982). Carbon, nitrogen and phosphorus transport by world rivers. *American Journal of Science* **282:** 401-450

Meyer-Reil, L.-A. (1987). Seasonal and spatial distribution of extracellular enzymatic activities and microbial incorporation of dissolved organic substrates in marine sediments. *Applied and Environmental Microbiology* **53:** 1748-1755

Meysman, F. (2001). Modelling the influence of ecological interactions on reactive transport processes in sediments. Ph.D., University of Gent, Gent, Belgium.

Middelburg, J. J. (1989). A simple rate model for organic matter decomposition in marine sediments. *Geochimica et Cosmochimica Acta* **53:** 1577-1581

Middelburg, J. J., Klaver, G., Nieuwenhuize, J. and Vlug, T. (1995). Carbon and nitrogen cycling in intertidal sediments near Doel, Scheldt estuary. *Hydrobiologia* **311:** 57-69

Middelburg, J. J., Soetaert, K., Herman, P. M. J. and Heip, C. H. R. (1996a). Denitrification in marine sediments: A model study. *Global Biogeochemical Cycles* **10:** 661-673

Middelburg, J. J., Klaver, G., Nieuwenhuize, J., Wielemaker, A., de Haas, W., Vlug, T. and van der Nat, J. F. W. A. (1996b). Organic mineralisation in intertidal sediments along an estuarine gradient. *Marine Ecology Progress Series* **132:** 157-168

Mitchell, G., Jones, J. and Cole, J. (1986). Distribution and regulation of nitrate and nitrite reduction by Desulfovibrio and Desulfotomaculum species. *Arch Microbiol* **144:** 35-40

Monod, J. (1949). The growth of bacterial cultures. *Annual Review of Microbiology* **3:** 371-394

Morris, A. W. and Howarth, M. J. (1998). Bed stress induced sediment resuspension (SERE 88/89). *Continental Shelf Research* **18:** 1203-1213

Morse, J. (1974). Calculation of diffusive fluxes across the sediment-water interface. *Journal of Geophysical Research* **79:** 5045-5048

Mortimer, R. J. G., Krom, M. D., Harris, S. J., Hayes, P. J., Davies, I. M., Davison, W. and Zhang, H. (2002). Evidence for suboxic nitrification in recent marine sediments. *Marine Ecology-Progress Series* **236:** 31-35

Muller, P. and Mangini, A. (1980). Organic carbon decomposition rates in sediments of the Pacific Manganese Nodule Belt dataed by 230Th and 231Pa. *Earth and Planetary Science Letters* **51:** 94-114

Nedwell, D. B. (1975). Inorganic nitrogen metabolism in a eutrophicated tropical mangrove estuary. *Water Research* **9:** 221

Nedwell, D. B. (1982). Exchange of nitrate and the products of bacterial nitrate reduction between seawater and sediment from a U.K. saltmarsh. *Estuarine, Coastal and Shelf Science* **14:** 557-566

Nedwell, D. B. (1987). Distribution and pool sizes of microbially available carbon in sediment measured by a microbiological assay. *FEMS Microbiological Ecology* **45:** 47-52

Nedwell, D. B. and Trimmer, M. (1996). Nitrogen fluxes through the upper estuary of the Great Ouse, England: the role of the bottom sediments. *Marine Ecology Progress Series* **142:** 273-286

Nishio, T., Koike, I. and Hatori, A. (1983). Estimates of denitrification and nitrification in coastal and estuarine sediments. *Applied and Environmental Microbiology* **45:** 444-450

Nixon, S. W. (1981) Remineralisation and nutrient cycling in coastal marine ecosystems. In: Neilson BJ, Cronin LE (eds) Estuaries and nutrients. Humana Press, Clifton, New Jersey, pp. 111-138.

Nixon, S., Granger, S. and Nowicki, B. (1995). An assessment of the annual mass balance of carbon, nitrogen and phosphorus in Narrangansett Bay. *Biogeochemistry* **31:** 15-61

Nixon, S., Ammerman, J., Atkinson, L., Berounsky, V., Billen, G., Boicourt, W., Boynton, W., Church, T., DiToro, D., Elmgren, R., Garber, J., Giblin, A., Jahnke, R., Owens, N., Pilson, M. and Seitzinger, S. (1996). The fate of nitrogen and phosphorus at the land-sea margin of the North Atlantic Ocean. *Biogeochemistry* **35:** 141-180

Nowicki, B. L. (1994). The effect of temperature, oxygen, salinity and nutrient enrichment on estuarine denitrification rates measured witha modified nitrogen gas flux technique. *Estuarine, Coastal and Shlef Sciences* **38:** 137-156

Officer, C. and Ryther, J. (1980). The possible importance of silicon in marine eutrophication. *Marine Ecology Progress Series* **3:** 83-91

Ogilvie, B., Nedwell, D., Harrison, R., Robinson, A. and Sage, A. (1997a). High nitrate, muddy estuaries as nitrogen sinks: the nitrogen budget of the River Colne estuary (UK). *Marine Ecology Progress Series* **150:** 217-228

Ogilvie, B., Rutter, M. and Nedwell, D. (1997b). Selection by temperature of nitrate reducing bacteria from estuarine sediments: species composition and competition for nitrate. *FEMS Microbiology Ecology* **23:** 11-22

Olson, R. (1981). Differential photoinhibition of marine nitrifying bacteria: a possible mechanism for the formation of primary nitrite maxima. *Journal of Marine Research* **39:** 227-238

Osinga, R., Kop, A. J., Duineveld, G. C. A., Prins, R. A. and VanDuyl, F. C. (1996). Benthic mineralization rates at two locations in the southern North Sea. *Journal of Sea Research* **36:** 181-191

Paavolainen, L. and Smolander, A. (1998). Nitrification and denitrification in soil from: A clear-cut Norway spruce (Picea abies) stand. *Soil Biology & Biochemistry* **30:** 775-781

Painter, H. (1970). A review of the literature on inorganic nitrogen metabolism in microorganisms. *Water Research* **4:** 393-450

Parkes, R. J., Cragg, B. A., Bale, S. J., Getliff, J. M., Goodman, K., Rochelle, P. A., Fry, J. C., Weightman, A. J. and Harvey, S. M. (1994). Deep bacterial biosphere in Pacific-Ocean sediments. *Nature* **371:** 410-413

Patrick, W. and Khalid, R. (1974). Phosphate release and sorption by soils and sediments: effecr of aerobic and anaerobic conditions. *Science* **186:** 53-55

Payne, W. (1973). Reduction of nitrogenous oxides by microorganisms. *Bacteriological Review* **37:** 409-451

Pelet, R. (1987) A model of organic sedimentation on present day continental margins. In: Brooks J, Fleet A (eds) Marine Petroleum Source Rocks. Geological Society of London Sepcial Publication, London, vol. 26, pp. 167-180.

Postma, D. and Jakobsen, R. (1996). Redox zonation: Equilibrium constraints on the Fe(III)/SO4- reduction interface. *Geochimica et Cosmochimica Acta* **60:** 3169-3175

Prakasam, T. and Loehr, R. (1972). Microbial nitrification and denitrification in concentrated wastes. *Water Research* **6:** 859

Press, W., Flannery, B., Teukolsky, S. and Vetterling, W. (1990). Numerical recipes. The art of scientific computing. Cambridge University Press, New York

Prosser, J. I. (1989). Autotrophic nitrification in bacteria. *Advances in Microbial Physiology* **30:** 125-181

Rabouille, C. and Gaillard, J.-F. (1991a). Towards the EDGE: Early diagenetic global explanation. A model depicting the early diagenesis of organic matter, O2, NO3, Mn and PO4. *Geochimica et Cosmochimica Acta* **55**

Rabouille, C. and Gaillard, J.-F. (1991b). A coupled model representing the deep sea organic carbon mineralisation and oxygen consumption in surficial sediments. *Journal of Geophysical Research* **96:** 2761-2776

Radach, G., Berg, J. and Hagmeier, E. (1990). Long term changes on annual cycles of meteorological, hydrographic, nutrient and phytoplankton time series at Helgoland and at LV Elbe1 in the German Bight. *Continental Shelf Research* **10:** 305-328

Rehr, B. and Klemme, J.-H. (1989). Competition for nitrate between denitrifying Pseudomonas stutzeri and nitrate ammonifying enterobacteria. *FEMS Microbiology Ecology* **62:** 51-

Reimers, C., Jahnke, R. A. and Thomsen, L. (2001) In situ sampling in the benthic boundary layer. In: Boudreau BP, Jorgensen BB (eds) The benthic boundary layer. Transport processes and biogeochemistry. Oxford University Press, New York, p. 245-268

Rendell, A. R., Horrobin, T. M., Jickells, T. D., Edmunds, H. M., Brown, J. and Malcolm, S. J. (1997). Nutrient cycling in the Great Ouse estuary and its impact on nutrient fluxes to The Wash, England. *Estuarine, Coastal and Shelf Science* **45:** 653-668

Rhoads, C. R. and Boyer, L. F. (1982) The effects of marine benthos on physical properties of sediments: A successional perspective. In: McCall PL, Tevesz MJS (eds) Animal-sediment relations. Plenum Press, New York, vol. 2, pp. 3-43.

Risgaardpedersen, N., Rysgaard, S., Nielsen, L. P. and Revsbech, N. P. (1994). Diurnal-variation of denitrification and nitrification in sediments colonized by benthic microphytes. *Limnology and Oceanography* **39:** 573-579

Robertsen, L. and Kuenen, J. (1984). Aerobic denitrification: a controversy revisited. *Arch Microbiol* **139:** 351-354

Robertson, L. A. and Kuenen, J. G. (1990) Physiological and ecological aspects of aerobic denitrification, a link with heterotrophic nitrification? In: Revsbech NP, Sørensen J (eds) Denitrification in Soil and sediment. Plenum Press, New York, pp. 91-104.

Rosenberg, R., Elmgren, R., Fleischer, S., Jonsson, P., Person, G. and Dahlin, H. (1990). Marine eutrophication case studies in Sweden. *Ambio* **19:** 102-108

Rosenfeld, J. (1981). Nitrogen diagenesis in Long Island Sound sediments. *American Journal of Science* **281:** 436-462

Roy, H., Huttel, M. and Jorgensen, B. B. (2002). The role of small-scale sediment topography for oxygen flux across the diffusive boundary layer. *Limnology and Oceanography* **47:** 837-847

Rysgaard, S., Risgaard-Petersen, N., Nielsen, L. and Revsbech, N. (1993). Nitrification and denitrification in lake and estuarine sediments measured by the N-15 dilution technique and isotope pairing. *Applied Environmental Microbiology* **59:** 2093-2098

Rysgaard, S., Thastum, P., Dalsgaard, T., Christensen, P. B. and Sloth, N. P. (1999). Effects of salinity on NH4+ adsorption capacity, nitrification, and denitrification in Danish estuarine sediments. *Estuaries* **22:** 21-30

Sagemann, J., Skowronek, F., Dahmke, A. and Schulz, H. D. (1996). Pore water response on seasonal environmental changes in intertidal sediments of the Weser estuary, Germany. *Environmental Geology* **27:** 362-369

Santschi, P. H., Bower, P., Nyffeler, U. P., Azevedo, A. and Broecker, W. S. (1983). Estimates of the resistance to chemical-transport posed by the deep-sea boundary-layer. *Limnology and Oceanography* **28:** 899-912

Santschi, P. H., Anderson, R. F., Fleisher, M. Q. and Bowles, W. (1991). Measurements of diffusive sublayer thicknesses in the ocean by alabaster dissolution, and their implications for the measurements of benthic fluxes. *Journal of Geophysical Research-Oceans* **96:** 10641-10657

Sayles, F. (1979). The composition and diagenesis of interstitial solutions I. Fluxes across the seawater-sediment interface in the Atlantic Ocean. *Geochimica et Cosmochimica Acta* **43:** 526-546

Seitz, H. J. and Cypionka, H. (1986). Chemolithotrophic growth of Desulfovibrio-Desulfuricans with hydrogen coupled to ammonification of nitrate or nitrite. *Archives of Microbiology* **146:** 63-67

Seitzinger, S. P., Nixon, S. W. and Pilson, M. E. Q. (1984). Denitrification and nitrous oxide production in a coastal marine ecosystem. *Limnology and Oceanography* **29:** 73-83

Seitzinger, S. and Nixon, S. W. (1985). Eutrophication and the rate of denitrification and N2O production in coastal marine sediments. *Limnology and Oceanography* **30:** 1332-1339

Seitzinger, S. P. (1987). Nitrogen biogeochemistry in an unpolluted estuary: The importance of benthic denitrification. *Marine Ecology Progress Series* **37:** 65-73

Seitzinger, S. P. (1988). Denitrification in freshwater and coastal marine ecosystems: ecological and geochemical perspectives. *Limnology et Oceanography* **33:** 702-724

Seitzinger, S. P., Nielsen, L. P., Caffrey, J. and Christensen, P. B. (1993). Biogeochemistry. *Denitrification measurements in aquatic sediments - a comparison of 3 method* **23:** 147-167

Seitzinger, S. P. and Kroeze, C. (1998). Global distribution of nitrous oxide production and N inputs in freshwater and coastal marine ecosystems. *Global Biogeochemical Cycles* **12:** 93-113

Sloth, N. P., Blackburn, T. H., Hansen, L. S., Risgaard-Peterson, N. and Lomstein, B. A. (1995). Nitrogen cycling in sediments with different organic loading. *Marine Ecology Progress Series* **116:** 163-170

Soetaert, K., Herman, P. M. J. and Middelburg, J. J. (1996). A model of early diagenetic processes from the shelf to abyssal depths. *Geochimica et Cosmochimica Acta* **60:** 1019-1040

Sorensen, J. (1978). Capacity for denitrification and reduction of nitrate to ammonia in a coastal marine sediment. *Applied Environmental Microbiology* **35:** 301-305

Sorensen, J., Tiedje, M. and Firestone, R. (1980). Inhibition by sulfide of nitric and nitrous oxide reduction by denitrifying Pseudomonas fluorescens. *Applied Environmental Microbiology* **39:** 105-108

Sorensen, J. (1982). Reduction of Ferric Iron in Anaerobic, Marine Sediment and Interaction With Reduction of Nitrate and Sulfate. *Applied and Environmental Microbiology* **43:** 319-324

Sorensen, J. (1987). Nitrate reduction in marine sediment: pathways and interactions with iron and sulfur cycling. *Geomicrobiology Journal* **5:** 401-421

Stewart, W. (1975) Biological cycling of nitrogen in intertidal and sublittoral marine environments. In: Barnes H (eds) Proceedings 9th European Marine Biology Symposium. University Press, Aberdeen, pp. 637-660.

Stouthamer, A. H. (1988) Dissimilatory reduction of oxidised nitrogen compounds. In: Zehnder A (eds) Biology of Anaerobic Microorganisms. J. Wiley & Sons, New York, pp. 245-303

Strauss, E. A. and Lamberti, G. A. (2000). Regulation of nitrification in aquatic sediments by organic carbon. *Limnology and Oceanography* **45:** 1854-1859

Strauss, E. A., Mitchell, N. L. and Lamberti, G. A. (2002). Factors regulating nitrification in aquatic sediments: effects of organic carbon, nitrogen availability, and pH. *Canadian Journal of Fisheries and Aquatic Sciences* **59:** 554-563

Strous, M., Kuenen, J. G., Fuerst, J. A., Wagner, M. and Jetten, M. S. M. (2002). The anammox case - A new experimental manifesto for microbiological eco-physiology. *Antonie Van Leeuwenhoek International Journal of General and Molecular Microbiology* **81:** 693-702

Stumm, W. and Morgan, J. (1970). Aquatic chemistry. Wiley Interscience, New York

Sumi, T. and Koike, I. (1990). Estimation of ammonification and ammonium assimilation in surficial coastal and estuarine sediments. *Limnology and Oceanography* **35:** 270-286

Sun, M.-Y., Lee, C. and Aller, R. C. (1993). Laboratory studies of oxic and anoxic degradation of chlorophyll a in Long Island Sound sediments. *Geochimica et Cosmochimica Acta* **57:** 147-157

Sundby, B., Gobeil, C., Silverberg, N. and Mucci, A. (1992). The phosphorus cycle in coastal marine sediments. *Limnology and Oceanogrpahy* **37:** 1129-1145

Suntharalingam, P. and Sarmiento, J. L. (2000). Factors governing the oceanic nitrous oxide distribution: Simulations with an ocean general circulation model. *Global Biogeochemical Cycles* **14:** 429-454

Suzuki, I., Dular, U. and Kwol, S.-C. (1974). Ammonia or ammonium ion as substrate for oxidation by *Nitrosomonas* cells and extracts. *Journal of Bacteriology* **120:** 556-558

Sweerts, J., Stlouis, V. and Cappenberg, T. E. (1989). Oxygen Concentration Profiles and Exchange in Sediment Cores With Circulated Overlying Water. *Freshwater Biology* **21:** 401-409

Thamdrup, B., Hansen, J. W. and Jorgensen, B. B. (1998). Temperature dependence of aerobic respiration in a coastal sediment. *Fems Microbiology Ecology* **25:** 189-200

Thamdrup, B. and Dalsgaard, T. (2000). The fate of ammonium in anoxic manganese oxide-rich marine sediment. *Geochimica et Cosmochimica Acta* **64:** 4157-4164

Thamdrup, B. and Dalsgaard, T. (2002). Production of N-2 through anaerobic ammonium oxidation coupled to nitrate reduction in marine sediments. *Applied and Environmental Microbiology* **68:** 1312-1318

Thornton, D., Underwood, G. and Nedwell, D. (1999). Effect of illumination and emersion period on the exchange of ammonium across the estuarine sediment-water interface. *Marine Ecology Progress Series* **184:** 11-20

Tiedje, J., Sexstone, A., Myrold, D. and Robinson, J. (1982). Denitrification: ecological niches, competition and survival. *Antonie van Leeuwenhoek J Microbiol Serol* **48:** 569-583

Tiedje, J. (1988) Ecology of denitrification and dissimilatory nitrate reduction to ammonium. In: Zehnder A (eds) Biology of Anaerobic Microorganisms. J. Wiley & Sons, New York, p. 179-241

Toth, D. and Lerman, A. (1977). Organic matter reactivity and sedimentaton rates in the ocean. *American Journal of Science* **277:** 465-485

Trimmer, M., Purdy, K. and Nedwell, D. (1997). Process measurement and phylogenetic analysis of the sulphate reducing bacterial communities of two contrasting benthic sites in the upper estuary of the Great Ouse. *FEMS Microbiological Ecology* **24:** 333-342

Trimmer, M., Nedwell, D. B., Sivyer, D. B. and Malcolm, S. J. (1998). Nitrogen fluxes through the lower estuary of the river Gt. Ouse, England: the role of the bottom sediments. *Marine Ecology Progress Series* **163:** 109-124

Trimmer, M., Nedwell, D. B., Sivyer, D. B. and Malcolm, S. J. (2000). Seasonal benthic organic matter mineralisation measured by oxygen uptake and denitrification along a transect of the inner and outer River Thames estuary, UK. *Marine Ecology-Progress Series* **197:** 103-119

Tromp, T. K., Van Cappellan, P. and Key, R. M. (1995). A global model for the early diagenesis of organic carbon and organic phosphorus in marine sediments. *Geochimica et Cosmochimica Acta* **59:** 1259-1284

Tyson, R. (1995). Sedimentary organic matter. Chapman and Hall, London, p. 615

Ullman, W. J. and Aller, R. C. (1982). Diffusion coefficients in nearshore marine sediments. *Limnology and Oceanography* **27:** 552-556

Upton, A. C., Nedwell, D. B., Parkes, R. J. and Harvey, S. M. (1993). Seasonal benthic microbial activity in the southern North-Sea - oxygen-uptake and sulfate reduction. *Marine Ecology-Progress Series* **101:** 273-281

Usui, T., Koike, I. and Ogura, N. (1998). Vertical profiles of nitrous oxide and dissolved oxygen in marine sediments. *Marine Chemistry* **59:** 253-270

Van Cappellen, P., Gaillard, J. F. and Rabouille, C. (1993) Biogeochemical transformations in sediments: kinetic models of eary diagenesis. In: Wollast R, Mackenzie FT, Chou L (eds) Interactions of C,N,P and S biogeochemical cycles and global change. Springer-Verlag., pp. 401-446.

Van Cappellen, P. and Wang, Y. (1995). Cycling of iron and manganese in surface sediments: A general theory for the coupled transport and reaction of carbon, oxygen, nitrogen, sulfur, iron and manganese. *American Journal of Science* **296:** 197-243

Van de Graaf, A., Mulder, A., de Bruijn, P., Jetten, M., Robertsen, L. and Kuenen, J. (1995). Anaerobic oxidation of ammoniium is a biologically mediated process. *Applied Environmental Microbiology* **61:** 1246-1251

Van der Weijden, C. (1992) Early diagenesis and marine pore water. In: Chilingarian G, Wolf K (eds) Diagenesis, III. Elsevier, Amsterdam, vol. 3, pp. 1-134.

van Luijn, F., Boers, P. C. M. and Lijklema, L. (1998). Anoxic N-2 fluxes from freshwater sediments in the absence of oxidized nitrogen compounds. *Water Research* **32:** 407-409

van Raaphorst, W., Kloosterhuis, H., Berguis, E., Gieles, A., Malschaert, J. and van Noort, G. (1992). Nitrogen cycling in two banks of sediments in the southern North Sea (Frisian Front, Broad Fourteens): field data and mesocosm results. *Netherlands Journal of Sea Research* **28:** 293-316

Vanderborght, J., Wollast, R. and Billen, G. (1975). Kinetic models of diagenesis in disturbed sediments. I. Mass transfer properties and silica diagenesis. *Limnology and Oceanography* **22:** 787-793

Velegrakis, A. (2000) Geology, geomorphology and sediments of the Solent system. In: Collins M, Ansell K (eds) Solent Science - a review. Elsevier Science, Amsterdam, pp. 21-43.

Verstraete, W. (1975). Heterotrophic nitrification in soils and aqueous media. *Izvestija Akademii Nauk SSSR Ser Biol* **4:** 541-558

Vidal, M. (1994). Phosphtate dynamics tied to sediment disturbances in Alfacs Bay (NW Mediterranean). *Marine Ecology Progress Series* **110:** 211-221

Vidal, M., Morgui, J. A., Latasa, M., Romero, J. and Camp, J. (1997). Factors controlling seasonal variability of benthic ammonium release and oxygen uptake in Alfacs bay (Ebro delta, NW Mediterranean). *Hydrobiologia* **350:** 169-178

Wang, Y. and Van Cappellan, P. (1996). A multi-component reactive transport model of early diagenesis: Application to redox cycling in coastal marine sediments. *Geochimica et Cosmochimica Acta* **60:** 2993-3014

Ward, B. B. (1992) Nitrogen cycle of the sea. In: Nierenberg W (ed) Encyclopaedia of Earth System Science. Academic Press Inc, San Diego, vol. 3, pp. 295-306.

Welsh, D. T., Castadelli, G., Bartoli, M., Poli, D., Careri, M., de Wit, R. and Viaroli, P. (2001). Denitrification in an intertidal seagrass meadow, a comparison of N-15-isotope and acetylene-block techniques: dissimilatory nitrate reduction to ammonia as a source of N2O? *Marine Biology* **139:** 1029-1036

Westrich, J. and Berner, R. A. (1984). The role of sedimentary organic matter in bacterial sulfate reduction: The G model tested. *Limnology and Oceanography* **29:** 236-249

Williams, J. J., Humphery, J. D., Hardcastle, P. and Wilson, D. J. (1998). Field observations of hydrodynamic conditions and suspended particulate matter in the southern North Sea. *Continental Shelf Research* **18:** 1215-1233

Wilson, T. (1975) Salinity and major elements of seawater. In: Liley J, Skirrow G (eds) Chemical Oceanography. Academic press, London, vol. 1, pp. 365-413.

Wollast, R. (1983) Interactions in estuaries and coastal waters. In: Bolin B, Cook RB (eds) The major biogeochemical cycles and their interactions. SCOPE report 21. Wiley, New York, pp. 385-407.

Wood, P. (1988) Monooxygenase and free radical mechanisms for biological ammonia oxidation. In: Cole J, Ferguson S (eds) The nitrogen and sulphur cycles. Cambridge University Press, Cambridge, pp. 219-243.

Woods, D. (1938). The reduction of nitrate to ammonia by Clostridium welchii. *Biochemistry Journal* **32:** 2000-2012

Zengler, K., Richnow, H. H., Rossello-Mora, R., Michaelis, W. and Widdel, F. (1999). Methane formation from long-chain alkanes by anaerobic microorganisms. *Nature* **401:** 266-269